National Library of Canada
Canadian Theses Service
Ottawa, Canada
K1A 0N4

Bibliothèque nationale du Canada
Services des thèses canadiennes

CANADIAN THESES

THÈSES CANADIENNES

NOTICE

The quality of this microfiche is heavily dependent upon the quality of the original thesis submitted for microfilming. Every effort has been made to ensure the highest quality of reproduction possible.

If pages are missing, contact the university which granted the degree.

Some pages may have indistinct print especially if the original pages were typed with a poor typewriter ribbon or if the university sent us an inferior photocopy.

Previously copyrighted materials (journal articles, published tests, etc.) are not filmed.

Reproduction in full or in part of this film is governed by the Canadian Copyright Act, R.S.C. 1970, c. C-30. Please read the authorization forms which accompany this thesis.

AVIS

La qualité de cette microfiche dépend grandement de la qualité de la thèse soumise au microfilmage. Nous avons tout fait pour assurer une qualité supérieure de reproduction.

S'il manque des pages, veuillez communiquer avec l'université qui a conféré le grade.

La qualité d'impression de certaines pages peut laisser à désirer, surtout si les pages originales ont été dactylographiées à l'aide d'un ruban usé ou si l'université nous a fait parvenir une photocopie de qualité inférieure.

Les documents qui font déjà l'objet d'un droit d'auteur (articles de revue, examens publiés, etc.) ne sont pas microfilmés.

La reproduction, même partielle, de ce microfilm est soumise à la Loi canadienne sur le droit d'auteur, SRC 1970, c. C-30. Veuillez prendre connaissance des formules d'autorisation qui accompagnent cette thèse.

THIS DISSERTATION HAS BEEN MICROFILMED EXACTLY AS RECEIVED

LA THÈSE A ÉTÉ MICROFILMÉE TELLE QUE NOUS L'AVONS REÇUE

NL 339 (r. 86/01)

Canada

53

0-315-26786-0

National Library of Canada
Bibliothèque nationale du Canada

Canadian Theses Division
Division des thèses canadiennes

Ottawa, Canada
K1A 0N4

PERMISSION TO MICROFILM — AUTORISATION DE MICROFILMER

• Please print or type — Écrire en lettres moulées ou dactylographier

Full Name of Author — Nom complet de l'auteur

Kimm Marie Harty

Date of Birth — Date de naissance

May 6, 1958

Country of Birth — Lieu de naissance

U.S.A.

Permanent Address — Résidence fixe

598 North Country Road
St. James, New York
U.S.A. 11780

Title of Thesis — Titre de la thèse

"The Geomorphic Role of Snow in a Badland Watershed."

University — Université

University of Alberta

Degree for which thesis was presented — Grade pour lequel cette thèse fut présentée

M.Sc. - Geography

Year this degree conferred — Année d'obtention de ce grade

1984

Name of Supervisor — Nom du directeur de thèse

I.A. Campbell

Permission is hereby granted to the NATIONAL LIBRARY OF CANADA to microfilm this thesis and to lend or sell copies of the film.

The author reserves other publication rights, and neither the thesis nor extensive extracts from it may be printed or otherwise reproduced without the author's written permission.

L'autorisation est, par la présente, accordée à la BIBLIOTHÈQUE NATIONALE DU CANADA de microfilmer cette thèse et de prêter ou de vendre des exemplaires du film.

L'auteur se réserve les autres droits de publication; ni la thèse ni de longs extraits de celle-ci ne doivent être imprimés ou autrement reproduits sans l'autorisation écrite de l'auteur.

Date

February 27, 1984

Signature

Kimm M Harty

NL-91 (4/77)

THE UNIVERSITY OF ALBERTA

"The Geomorphic Role of Snow in a Badland Watershed"

by

Kimm Marie Harty

(C)

A THESIS

SUBMITTED TO THE FACULTY OF GRADUATE STUDIES AND RESEARCH

IN PARTIAL FULFILMENT OF THE REQUIREMENTS FOR THE DEGREE

OF MASTER OF SCIENCE

Department of Geography

EDMONTON, ALBERTA

Spring, 1984

THE UNIVERSITY OF ALBERTA

RELEASE FORM

NAME OF AUTHOR Kimm Marie Harty

TITLE OF THESIS "The Geomorphic Role of Snow in a Badland Watershed"

DEGREE FOR WHICH THESIS WAS PRESENTED MASTER OF SCIENCE

YEAR THIS DEGREE GRANTED Spring, 1984

Permission is hereby granted to THE UNIVERSITY OF ALBERTA LIBRARY to reproduce single copies of this thesis and to lend or sell such copies for private, scholarly or scientific research purposes only.

The author reserves other publication rights, and neither the thesis nor extensive extracts from it may be printed or otherwise reproduced without the author's written permission.

(SIGNED) Kimm M Harty

PERMANENT ADDRESS:

598 North Country Rd.
St. James, New York
USA 11780

DATED 31 January 1984

THE UNIVERSITY OF ALBERTA

FACULTY OF GRADUATE STUDIES AND RESEARCH

The undersigned certify that they have read, and recommend to the Faculty of Graduate Studies and Research, for acceptance, a thesis entitled "The Geomorphic Role of Snow in a Badland Watershed" submitted by Kimm Marie Harty in partial fulfilment of the requirements for the degree of MASTER OF SCIENCE.

.....
Supervisor

.....

.....

Date January 31, 1984

ABSTRACT

This study investigates the geomorphological impact of snow and snowmelt in a semiarid badland watershed in southern Alberta, Canada. Field examinations during the 1981-1982 snow season focussed on assessing the nature and significiance of snow accumulation, distribution, and snowmelt. The hydrologic character of infiltration and runoff is compared to that of rainfall, and is also incorporated into a comprehensive view of the geomorphic role of snow in badlands.

High-velocity northwest and southwest winds predominate during winter, effectively redistributing the snowcover. Maximum accumulation zones include depression features (rills, gullies), and lee slope bases oriented north, clockwise to south. These areas generally experience the highest magnitude of degradation in winter, but differential solar radiation receipt modifies the erosion response of some slopes.

Snowmelt episodes are initiated by chinook activity, and often result in significant mid-winter snow depletion and runoff. Subsurface moisture penetration is deeper under snowmelt than rainfall due to prolonged infiltration and sorption processes permitted by slow-melting snowpacks. Runoff efficiency is high, enhanced by increased material impermeability afforded by the formation of solid, frozen ground and surface ice layers, upon refreeze of meltwater in lowland areas.

Results indicate that the pattern of snow distribution in the badlands is repetitive, and leads to the creation of spatial variations in the seasonal runoff and erosion regimes. The concept of partial source areas of runoff and sediment generation is applicable to the badlands in winter, during which time, zones of hydrologic and geomorphic activity become more highly defined than in summer.

ACKNOWLEDGEMENTS

I give my warmest thanks to the following people, who have provided me with valuable help in preparation of this thesis:

Jim Stomp and **Roger Benoit** (successive Wardens of Dinosaur Provincial Park): for authorization to conduct this research.

Lorne Murton and **Dennis Greenling** (A.E.S. - Edmonton): for use of the Murton snow gauges.

Emma Sicoli-Laipneiks (U. of A.) and **Barry Rennick** (D.P.P.): for help in carrying the snow gauges into the badlands during a rainstorm.

Lawrence Harvey and **Liz Lew** (U. of T.): for help in lugging them out during a heat wave.

Peter Hof (U. of A.): for our detailed discussions on anemometers.

George Smith (AHRC - Brooks): for providing recent meteorological records.

Laura Smith (U. of A.): for assistance in locating obscure meteorological data.

Lise Allard (U. of A.): for fun times with the Intergraph computer.

Olaf Niemann (M.Sc.): for use of his overworked camera.

Jack Chesterman and **Randy Pakan** (U. of A.): for PMT map reproduction.

I also extend kind appreciation to my thesis committee members, **Dr. Neil R.M. Seifried** and **Dr. Richard L. Rothwell**, and especially to **Dr. Ian A. Campbell**, my thesis supervisor, for his time, accessability, and valuable advice.

Special thanks to fellow students and good friends **Andrew Gambier**, **Jan Zimmer**, **Christine Schumacher**, and **Karen Grant**, who have made 1983 a year to remember.

Lastly, I am grateful to my family and friends in New York, Florida, and the Virginia environs, for their continued encouragement and support over the past few years.

Funding for this research was provided in part by an NSERC grant awarded to Dr. Campbell.

Table of Contents

Chapter — Page

1. INTRODUCTION AND STUDY AREA DESCRIPTION 1

1.1 Justification, Objectives, and Scope of Study 1

1.2 Location 2

1.3 Geology and Lithology 4

1.4 Geologic History 5

1.5 Topography and Nature of Surface Materials 6

1.6 Climate and Weather 9

1.6.1 Climatic Classification and Precipitation 9

1.6.2 Temperature 11

1.6.3 Wind and Airmasses 14

1.6.3.1 Wind Data 14

1.6.3.2 Air Mass Characteristics 19

1.7 Vegetation 21

2. PREVIOUS RESEARCH AND THEORY 23

2.1 Snow Characteristics: Origin, Accumulation and Distribution 23

2.1.1 Spatial Variability of Snowfall and Snow Accumulation 23

2.1.2 Snow Distribution and Redistribution 26

2.2 Badland Hydrology 34

2.2.1 Infiltration, Material Behaviour, and Runoff on Differing Lithologies under Rainfall 34

2.2.2 Total Watershed Runoff: Volumes and Runoff Ratios 39

2.3 Snow Disappearance and Snowmelt Runoff 44

2.3.1 Snow Disappearance as Influenced by Factors Governing Direct Solar Radiation Receipt 45

2.3.1.1 Albedo 45

2.3.1.2 Aspect 46

2.3.1.3 Vegetation 48

2.3.1.4 Cloud Cover 49

2.3.2 Snow Disappearance as Influenced by Sensible Heat Parameters 50

2.3.2.1 Temperature 50

2.3.2.2 Sublimation and Evaporation 50

2.3.2.3 Ground Heat Flux, Rain-On-Snow Events 53

2.3.3 Snowmelt Runoff 53

2.4 Badland Erosional Mechanisms and the Geomorphic Role of Snow 58

2.4.1 Badland Erosional Processes under Rainfall 58

2.4.2 The Role of Freeze - Thaw 62

2.4.2.1 Frost Heave and Needle Ice Formation 64

2.4.2.2 Frost Shattering 68

2.4.3 Slope Orientation and Snow Distribution Relationships and Their Effects on Badland Erosional Regimes 72

3. RESEARCH METHODS 79

3.1 Sub-basin Characteristics 79

3.1.1 Sub-basin X 80

3.1.2 Sub-basin Z 87

3.1.3 Sub-basin Y 92

3.2 Methods of Monitoring Snow Accumulation 98

3.2.1 Snow Surveys 99

3.2.2 Snow Gauges 100

3.2.3 Methods of Calculating Snow Accumulation and Water Availability 102

3.3 Methods of Investigating Snow Distribution 104

3.3.1 The Role of Wind 104

3.4 Methods of Investigating Snow Disappearance and Snowmelt Runoff 105

3.4.1 Snow Disappearance 105

3.4.2 Inflitration and Runoff 106

3.5 Methods of Investigating Geomorphic Activity 107

3.5.1 Direct Field Measurements 107

3.5.2 Indirect Field Measurements 108

4. RESULTS AND DISCUSSION 111

4.1 Snow Accumulation 111

4.1.1 Snowstorm Frequency, Magnitude, and Total Season Snow Accumulation: AHRC Records 111

4.1.2 Total Season Water Equivalent, Snow Accumulation, and Volumetric Runoff Potential: Snow Gauges and Extrapolated Results 114

4.1.3 Intra-season Snow Accumulation and Runoff Potential: Snow Surveys 124

4.2 Patterns of Snow Distribution 131

4.2.1 Period 1: November 17 to December 31, 1981 131

4.2.2 Period 2: January 1 to January 17, 1982 132

4.2.3 Period 3: January 18 to February 20, 1982 143

4.2.4 Period 4: February 21 to April 8, 1982 149

4.2.5 Summary of 1981-1982 and Long-term Wind and Snow Distribution Patterns 152

4.3 Snowmelt Initiation and Patterns of Snow Disappearance 161

4.3.1 Enumeration of Chinook Days 161

4.3.2 Period 1: November 17 to December 13, 1981 162

4.3.3 Period 2: January 1 to January 17, 1982 166

4.3.4 Period 3: January 18 to February 20, 1982 166

4.3.5 Period 4: February 21 to April 8, 1982 174

4.4 Meltwater Penetration and Runoff During Two Major Chinook Intervals 178

4.4.1 Subsurface Meltwater Penetration 178

4.4.2 Runoff 189

4.5 The Geomorphic Role of Snow, Ice, and Snowmelt 197

4.5.1 Freeze Thaw: Ice Formation, Frost Heave, and Preferential Erosion ... 198

4.5.2 Wind Erosion 205

4.5.3 Basal Slope Erosion, Mass Movement, and Other Forms of Slope Denudation 205

4.5.4 Sediment Erosion and Transport 221

5. SUMMARY OF RESULTS AND CONCLUSIONS 226

5.1 Summary of Results 226

5.1.1 Snow Accumulation 226

5.1.2 Wind and Snow Distribution 226

5.1.3 Snowmelt 227

5.1.4 Infiltration 227

5.1.5 Runoff 228

5.1.6 Geomorphology 228

5.2 Conclusions 230

References 232

Appendix A : Mean Monthly Wind Speeds and Wind Frequency Percentage at Brooks and Brooks AHRC Stations. 245

Appendix B : Slope Angle Values Surveyed in the Sub-basins. 249

Appendix C : Station Names Corresponding to Letter Denotations and Water Equivalent Values of Figure 4.5. 250

Appendix D : 1982 Snow Survey Data. 251

Appendix E : Wind Data for Brooks AHRC : 1981-1982 Winter Season. 254

Appendix F : Weather Map for March 15, 1982. 255

Appendix G : Paired Slope Angle Measurements. 256

List of Tables

Table		Page
1.1.	Precipitation Data For Brooks Stations	10
1.2.	Precipitation Data For Brooks AHRC: 1953-1980	12
1.3.	Temperature Data For Brooks AHRC: 1953-1980	13
1.4.	Mean Annual Wind Frequency Percentage	16
1.5.	Mean Annual Wind Speed	18
2.1.	Variability Of Snowfall Accumulation Among Brooks Stations During Selected Snowstorms Of 1981-1982	25
2.2.	Summary Of Factors Influencing Snowfall Variability And Post-fall Snow Redistibution In The Prairies (Three Spatial Scales)	33
2.3.	Hydrologic Data For Nine Summer Rainstorms Of 1981-1982	40
4.1.	Daily And Monthly Snowfall And Water Equivalent Values (AHRC), Plus Chinook Days Occurring During The 1981-1982 snow season	112
4.2.	Mean Monthly And Mean Annual Snowfall Recorded At The AHRC For Twelve Snow Seasons *Versus* Monthly And Total Snowfall Recorded At The AHRC For The 1981-1982 Snow Season	113
4.3.	Murton Gauge Snow / Water Equivalents And Cumulative Snow / Water Equivalents Of Murton Gauges And The AHRC: December 12, 1981 To March 15, 1982	116
4.4.	Snow Accumulation And Water Availability In The Sub-Basins And Main Watershed For Three Snow Surveys Of 1982	125
4.5.	Wind Direction And Snow Accumulation During 59 Snowfall Periods From November 17, 1981 to March 31, 1982	158
4.6.	Wind Direction And Maximum Speed During All 1981-1982 Snowfalls Of $\geq$ 5.0 cm	159
4.7.	Densities Of Snowpacks Established At Sope Bases Of Varying Aspects, March 12, 1982	177
4.8.	Maximum Moisture Penetration Depths For Various Lithologies Under Average Rainstorms *Versus* Snowmelt	188
4.9.	Flume Stage Height At Various Intervals Within The Last 53 Hours Of Channel Runoff During The February, 1982 Chinook Period	195
4.10.	Results Of Slope Angle Data Analysis	218
4.11.	Comparison Of Suspended Sediment Samples From A Spring Rainstorm *Versus* Snowmelt Runoff	222

List of Figures

Figure — Page

1.1. Study area and sub-basin locations within the main watershed. 3

1.2. Surficial Geology of the main watershed. 7

1.3. Wind rose diagrams for Brooks AHRC: 1955-1966. 15

1.4. Wind rose diagrams for Brooks: 1966-1980. 15

1.5. Percentage range of variation between percentage frequencies at AHRC and Brooks stations. 16

1.6. Percentage range of variation between wind speeds at AHRC and Brooks stations. 18

1.7. Vegetation map of the main watershed. 22

2.1. Mean annual snow accumulation in southern Alberta. (after Longley, 1972). 25

2.2. Precipitation *versus* total discharge for nine summer rainstorms of 1981-1982. 42

2.3. Slope failure on a claystone slope unit. 63

2.4. Relict collapse scar in a sandstone unit of a lithologically-integrated slope. 63

3.1. Sub-basin histograms plotting slope angle against slope frequency. 81

3.2. Relative sub-basin sizes and orientations. 82

3.3. Aerial Photograph of sub-basin X. 83

3.4. Contour map of sub-basin X. 83

3.5. North-northwest view of sub-basin X. 84

3.6. Northeast view of sub-basin X. 85

3.7. Aerial photograph of sub-basin Z. 88

3.8. Contour map of sub-basin Z. 89

3.9. Northeast view of sub-basin Z. 90

3.10. South-southwest view of sub-basin Z. 91

3.11. South view of the relatively flat upper surface of sub-basin Z. 93

3.12. Aerial photograph of sub-basin Y. 95

3.13. Contour map of sub-basin Y. 95

3.14. North-northeast view of sub-basin Y. 96

3.15. Southwest view of sub-basin Y. 97

3.16. Murton snow gauge and alter shield in sub-basin Y..... 101

4.1. Mean monthly snow accumulation at the AHRC for twelve snow seasons (1969-1970 to 1980-1981) *versus* monthly snow accumulation at the AHRC for the 1981-1982 snow season. 115

4.2. Cummulative snow / water equivalents of 1981-1982: Murton gauges (Nov. 16 - Mar. 15) and AHRC (Nov. 16 - May 7). 117

4.3. North view of sub-basin X..... 119

4.4. Southwest view of the main watershed and arrival of the Arctic front..... 119

4.5. Mean annual snow / water equivalents for stations in southeastern Alberta. 122

4.6. East view of the main watershed on March 14, 1982. 128

4.7. East (same) view of the main watershed on March 15, 1982. 128

4.8. Uniformly-distributed shallow snowcover in sub-basin Z..... 133

4.9. Micro-scale, streamlined snow deposits on the northwest sides of claystone aggregates. 134

4.10. Strong west winds of January 13-14, 1982 permit substantial snow deposition to the lee side of this claystone slope in sub-basin X. 136

4.11. Transverse-oriented west winds of January 13-14 remove snow from interfluves of this north-facing claystone slope (sb-Z), while depositing it within adjacent rill channels. 137

4.12. North winds of January 14-15 compact blowing snow into rills of this windward- and north-facing sandstone slope (sb-Y), while removing it from smooth interfluves. 137

4.13. Head basin area of sub-basin Y on January 16, 1982. 139

4.14. Knife-edged crest of a sandstone slope in sub-basin Y on January 16, 1982..... 139

4.15. Hoodoo in sub-basin Y showing maximum snow redistribution on the south-facing flank (January 16, 1982). 140

4.16. Vegetation clumps stabilize blowing snow that would otherwise be removed from this flat, relatively smooth pediment surface (January 16, 1982). 140

4.17. This northwest-trending, flat-floored coulee was a primary source area for snow removal by wind (January 16, 1982). 141

4.18. Footprints entrenched 6.0 to 7.0 cm into a 10.0 cm snowcover on January 14, 1982 were transformed into 3.0 to 4.0 cm raised prints by the action of northwest winds. 141

4.19. Basal region of this south-facing slope forming the northeast rim of sb-X retains approximately 40 cm of snow on January 15, 1982. 142

4.20. Northeast view of the lower basin of sb-X on January 17, 1982. 142

4.21. Southwest winds of January 26, 1982 created a snow cornice in the headwall region of this northeast-facing surface hollow of sub-basin X. 145

4.22. South-facing headwall slope of sub-basin X retains a large snow accumulation despite changes in effective wind velocity. 145

4.23. Cross-section through a northwest-southeast-trending lee snow drift on February 13, 1983. 147

4.24. Sandstone slope in sub-basin X on February 21, 1983. 150

4.25. Oriented snow drifts formed behind clumps of sage and long grass by extremely strong northwest winds of March 11-12, 1982. 150

4.26. Wind rose diagrams for Brooks AHRC: 1981-1982 winter season. 153

4.27. Characteristic seasonal pattern of lee slope snow redistribution under high-velocity Arctic frontal and chinook winds of south-central Alberta. 156

4.28. Ice layer in the main channel near the basin outlet. 163

4.29. Close-up view of a hole excavated into primary channel ice. 163

4.30. North view of sb-X under cloudy conditions at 10:00 a.m., December 12, 1981 164

4.31. North view of sb-X under sunny conditions at 2:30 p.m., December 12, 1981 164

4.32. Preferential solar radiation melt on a south-facing sandstone slope in sb-Y on December 12, 1981. 165

4.33. Radiation melt on a rilled, south-facing 47° compact claystone slope in sb-X. 167

4.34. Mid-winter peripheral radiation melt of a snowpack on a south-facing, aggregate-mantled claystone slope in sb-Z 167

4.35. Snow depletion on south-facing claystone slopes of the lower basin of sb-Z. 169

4.36. West view of sub-basin X showing snow depletion patterns on February 19, 1982 169

4.37. West view of snow depletion patterns in a vegetation-lined gulley of sub-basin Z. 170

4.38. Rill ice on a north-facing, integrated sandstone slope. 171

4.39. Rill ice on an east-facing claystone slope 171

4.40. North-facing, stepped claystone slope retains near-saturated snowpacks on the mid-slope tread and basal region. 173

4.41. Southeast view of snow depletion patterns in sub-basin X on March 14, 1982 175

4.42. West-southwest view of snow depletion patterns in sub-basin X on March 14, 1982 175

4.43. West-southwest view of snow depletion in the lower basin of sb-Z on March 14, 1982 176

4.44. Flat-lying, meltwater-saturated, desiccated claystone pediment on March 14, 1982 180

4.45. Subsurface view of Figure 4.44. 180

4.46. Meltwater penetration in a compact, flat-lying claystone unit in sb-Z. 181

4.47. Surface sealing of an aggregate-mantled claystone slope convexity. 181

4.48. Water from melting rill ice flows over a low-angled claystone slope. 183

4.49. Cross-sectional diagram of meltwater penetration in a rill of a partially-disaggregated claystone slope. 184

4.50. Water from melting rill ice on a north-facing sandstone slope penetrates rill margins to a maximum depth of 1.75 cm. 185

4.51. Melting snowpack saturates the weathering rind of a north-facing sandstone interfluve. 185

4.52. Snowmelt penetration on a grass-covered terrace composed of silty Brown soil. 187

4.53. Meltwater penetrates 9.0 cm into the silty-clay soil of this vegetated gully flank located on an upper prairie surface. 187

4.54. High temperatures towards the end of the major chinook period of February, 1982 facilitate rapid snowmelt. 190

4.55. Meltwater ponding on a low-lying claystone pediment near sb-Z. 190

4.56. Concentrated meltwater flow etched a rill and dendritic micro-rills into this slightly inclined pediment. 192

4.57. Shallow pipeflow at the base of a claystone slope. 192

4.58. Snowmelt runoff flows through the flume at the main channel outlet. 193

4.59. Ice-crystal marks on a compact, desiccated claystone slope. 199

4.60. Oriented ice-crystal marks on a sandstone interfluve in sb-Y. 199

4.61. Mid-winter erosion on a sandstone slope. 200

4.62. Small, subsurface ice lenses form in the frozen, saturated sides of this ice-filled claystone rill. 202

4.63. Melting ice in the head region of a shallow rill atop a slightly-inclined, aggregate-mantled claystone slope crest. 204

4.64. Ice marks are indicative of freeze-thaw loosening in this rill. 204

4.65. Strong southwest chinook winds deposit sediment on the windward-facing flanks of two streamlined snow dunes. 206

4.66. Basal slope oversteepening by fluvial undercutting. 207

4.67. Basal degradation on a west-facing, disaggregated and rilled claystone slope. 209

4.68. Melting of a mid-slope snowpack at the base of an east-facing siltstone unit. 209

4.69. Peripheral melting of a basal snowpack initiates material weakening and detachment on a north-facing claystone slope. 210

4.70. Peripheral melting of a snowpack on the northeast-facing flank of a vegetation-lined gully in sb-Z. 211

4.71. Peripheral melting of a snowpack on an east-facing claystone slope. 212

4.72. Mid- and upper-slope snowpacks on an east-facing claystone slope near sb-Z generate moisture-weakened aggregates. 214

4.73. Snowmelt infiltration into a north-facing vegetation-mantled claystone slope results in the collapse of a section of the moisture-weakened overhang. 215

4.74. Sediment deposition beneath a slip-off slope near the main channel outlet. 223

4.75. Sediment accumulation and ripple formation in a straight reach of the main channel. 223

1. INTRODUCTION AND STUDY AREA DESCRIPTION

1.1 Justification, Objectives, and Scope of Study

Within the last decade, an increasing number of studies have focussed on the geomorphic processes operating in badlands. Improvements in design of instrumentation and advances in research techniques now allow very detailed measurements and analysis of materials, sediment movement, and runoff. As a result, an increased understanding of the nature and relationships between badland hydrology and geomorphology has been gained. However, because rainfall is the dominant agent initiating geomorphic activity in badlands, little attention has been paid to the effects of snow accumulation, distribution, and snowmelt. This lack of knowledge is partly due to the fact that measurement of various snowcover parameters is an arduous task, often complicated by unfavourable weather conditions.

This thesis is an investigation of snowcover and snowmelt characteristics in a badland environment. The major objective of the study is the assessment of the degree to which snow and snowmelt influence the form and geomorphic behaviour of badlands. Some speculative work on the effects of snow and snowmelt suggests these range from profound (Schumm, 1956; Schumm and Lusby, 1963; Schumm, 1964; Campbell, 1974; 1981; Hogg, 1978; Hodges and Bryan, 1982) to virtually nil (Barendregt and Ongley, 1979), but a lack of comprehensive winter and early spring field data has prevented rigorous examination of the processes initiated by snow.

To formulate a theory on the role and importance of snow to badland geomorphology, a number of objectives were developed, and investigated during the 1981-1982 field season. The first, and perhaps most significant consideration involved the estimation of the amount of potential meltwater available to the badlands during winter, and determining if this water was adequate to initiate erosional activity. This was investigated in the field by measuring snow accumulation. Another important emphasis was in defining the location of this potential meltwater, or, the spatial distribution of the snowcover. Additional attention was given to the methods and patterns of snowmelt activity; how it melts, how much melts, and how rapidly potential meltwater is introduced into the system. Finally, inform[illegible] snowmelt infiltration and runoff characteristics

was collected to determine the hydrologic behaviour of meltwater during winter.

Three approaches were followed. Firstly, field observations and measurements were conducted during the 1981-1982 winter season, to collect information on the short-term geomorphic response in the Alberta badlands. For this examination, direct physical measurements of snow accumulation and distribution are supplemented with the use of photographs and field descriptions. The geomorphic implications of mid-winter and spring snowfall and snowmelt episodes occurring during the field season are examined and discussed, and the importance of freeze-thaw processes, material hydration / dehydration sequences, water availability and retention properties of surface materials is investigated. Secondly, these results are compared to long-term meteorological data, to assess the representativeness of field observations, for purposes of theorizing future as well as past geomorphic development. In addition, short-term results are compared to known hydrologic and geomorphic responses in the Alberta badlands which occur under rainfall. Finally, comparisons are made in terms of total water available to the catchment, subsurface infiltration depth, mechanisms involved in sediment entrainment, and, to a lesser extent, erosion and volumetric runoff estimates. Considerations of short-term observations, long-term data analysis, and comparisons between snowfall and rainfall together give a better understanding of winter and early spring hydrologic and geomorphic activity occurring in the Alberta badlands.

1.2 Location

Badland topography, characterized by a sparsely vegetated maze of highly erodible ravines (often called coulees) and gullies comprises a major physiographic unit of approximately 800 km² (Campbell, 1974) along the margins of the Red Deer River in southern Alberta. The study area consists of three small sub-basins contained within a larger, 0.336 km² ephemeral watershed which lies in a natural preserve region in the badlands of Dinosaur Provincial Park (Figure 1.1). The main watershed is located 1 km south of the Red Deer River and is partly accessible by vehicle via a 3.2 km loop road originating near the Park headquarters.

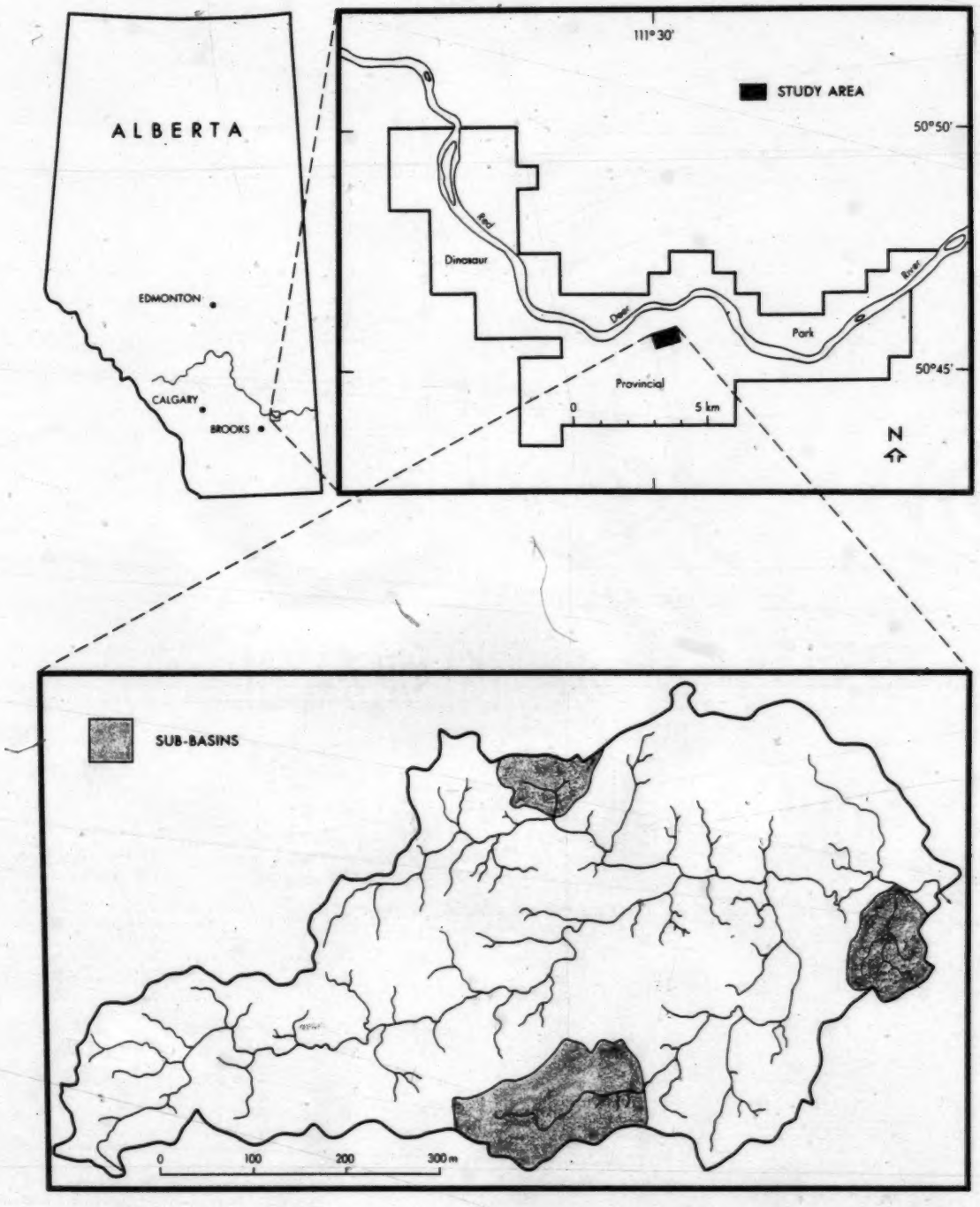

Figure 1.1. Study area and sub-basin locations within the main watershed.

1.3 Geology and Lithology

The Red Deer River badlands are chiefly composed of shales and sandstones of the Upper Cretaceous Belly River Group. Although extensive badlands have formed in the Bearpaw and Oldman Formations of this Group, only the latter outcrops in Dinosaur Park. Here, the Red Deer River is entrenched 100 m below the prairie surface, widely exposing the near-horizontal layers of the Oldman Formation.[1] Shale units vary from pale yellow (5Y8/3 by the Revised Standard Soil Color Chart (1970)) to dark brown (10YR3/3), but are typically light greenish grey (5G7/1 and 7.5GY7/1), and rather soft and non-fissile. They are commonly bentonitic and contain a high montmorillonite clay content which evokes material expansion upon wetting, and contraction upon drying (referred to as the shrink/swell phenomena). Illite and chlorite clay minerals are also present, as is quartz and small calcareous nodules. Because of a general lack of internal structure, Russell and Landes (1940), suggested the term claystone, rather than shale. The classification is appropriate, but should be expanded to include larger grain-sized siltstones, and the slightly indurated argillites also represented in the Formation.

Sandstone units vary in colour from greyish white (N8/10) to dull reddish and greyish brown (7.5R5/3), but are mainly light grey or greyish yellow (7.5Y8/1). While they are often highly indurated and massive in structure, a good portion are lenticular, cross-laminated, cross-bedded, or cross-stratified, and display current and ripple marks (Powers, 1931 ; Russell and Landes, 1940). Most units are lithified with calcium carbonate, but cementation by siderite is also present (Faulkner, 1970), accounting for the reddish brown colour of some layers. Arkosic sandstones are common in the Formation, and likewise display a reddish discolouration. The 'typical' sandstone is fine-grained, often containing silt-size particles and montmorillonite clay. As quartz grains and calcareous cement are major constituents, the designation *argillaceous calcareous-quartz* is proposed as an overall prefixal modifier for the sandstones embodied within the Oldman Formation.

Claystone/sandstone boundaries are ordinarily distinct, but finely interstratified or gradationally obscured in some areas. In addition, sandstone units are often intercallated with thin clay or silt bands, and fossilized dinosaur bones are widely distributed. Massive

---

[1]Also known as the Judith River Formation.

claystones also display silt and sandy-silt layers, as well as foliated selenite crystals and fine bands of amorphous selenite usually less than 1cm in thickness. Both sandstone and claystone units are repeatedly broken by ironstone beds up to 10 cm or more in thickness, which demonstrate blocky fracture. These units are likewise interrupted by ironstone concretions and siderite nodules. Discontinuous coal seams are encountered towards the upper part of the Oldman strata, and add to the colour and complexity of this Formation.

1.4 Geologic History

Age-dating of the Oldman Formation reveals the rocks to be approximately 65 to 70 million years old, and fossil examination confirms a non-marine origin. These terrestrial deposits coincide with the withdrawl of a Late Cretaceous inland sea (Byrne and Favolden, 1959), and orogenic uplift to the west. Lakes, freshwater swamps, and lagoons dominated the landscape, providing a depositional environment now seen in the massive claystone rock exposures. Sandstone sediments, derived from streams and rivers, have internal structures reflecting both overbank and channel deposits (Dodson, 1970). Lying conformably above the Oldman Formation are the younger marine shales of the Bearpaw Formation. As freshwater organisms are found in the above and underlying strata, the Bearpaw is considered a result of a brief, final advance of the brackish sea (Byrne and Favolden, 1959).

Continental sediment accumulation continued for 30 to 35 million years until wide-scale degradational processes commenced 25 million years B.P., due to regional uplifting and tilting of the interior landscape (Beaty, 1976). The Pleistocene Epoch, Wisconsin-Stage glacial advances periodically covered southern Alberta from approximately 70,000 to 12,000 years B.P., leaving behind a thin mantle of till over most of the prairie surface. Along with other major rivers in Alberta, the Red Deer experienced rapid, postglacially-initiated downcutting, exposing the easily eroded Oldman Formation and creating badlands.

1.5 Topography and Nature of Surface Materials

The study area contains a diverse, yet typical display of badland relief features. The contrast of steeply sloping scarps and mesas, flat-lying micro-pediments, and numerous winding dry channels contributes to the intensely dissected appearance of the terrain. Claystone slopes constitute a large portion of the main basin topography, especially near its mouth (Figure 1.2). Longitudinal slope profiles are usually convex towards the upper portion and may grade into a rectilinear form farther downslope. Crests or sub-basin divides are often fairly flat or rounded.

Two primary surface textures are recognized on claystone slopes under dry conditions. The first consists of a compacted regolith, highly broken by desiccation cracks, and more commonly found on the middle to lower sections of steep slopes, or on lower-angled slopes that contain a large percentage of silt and sand-sized particles. The second is a loose and friable regolith of puffy clay aggregates collectively referred to as *popcorn* shale, and is formed by repeated hydration / dehydration sequences interacting with the shrink / swell ability of montmorillonite clay. The regolith varies in thickness, and attains maximum depths of about 20 cm atop flat unvegetated claystone surfaces. Shallow rills are etched into some slopes, but are absent on others. When present, they are spaced between broad, and rounded interfluves.

Sandstone slopes characteristically show concave or rectilinear long profiles, with sharp, knife-edged crests. These slopes are almost always densely and deeply rilled. Massive sandstones develop a surficial weathering rind of a few millimetres in thickness which is loosely adhered in some places, to the unaltered bedrock beneath. Sandstones are found throughout the watershed, but especially towards the north-central and northwestern sections of the basin (Figure 1.2).

Slopes of homogeneous lithology and profile uniformity are rare. When present, they are often seen as low-elevation residual mounds or inselberg-type features. Most macro-slope profiles are interrupted by micro-cliffs, or exhibit micro-faceted or stepped slope faces. These slope disruptions frequently occur on claystone units which possess subtle changes in particle size or mineralogical content (Bryan *et al.*, 1978). Colour variations are also associated with these compositional changes.

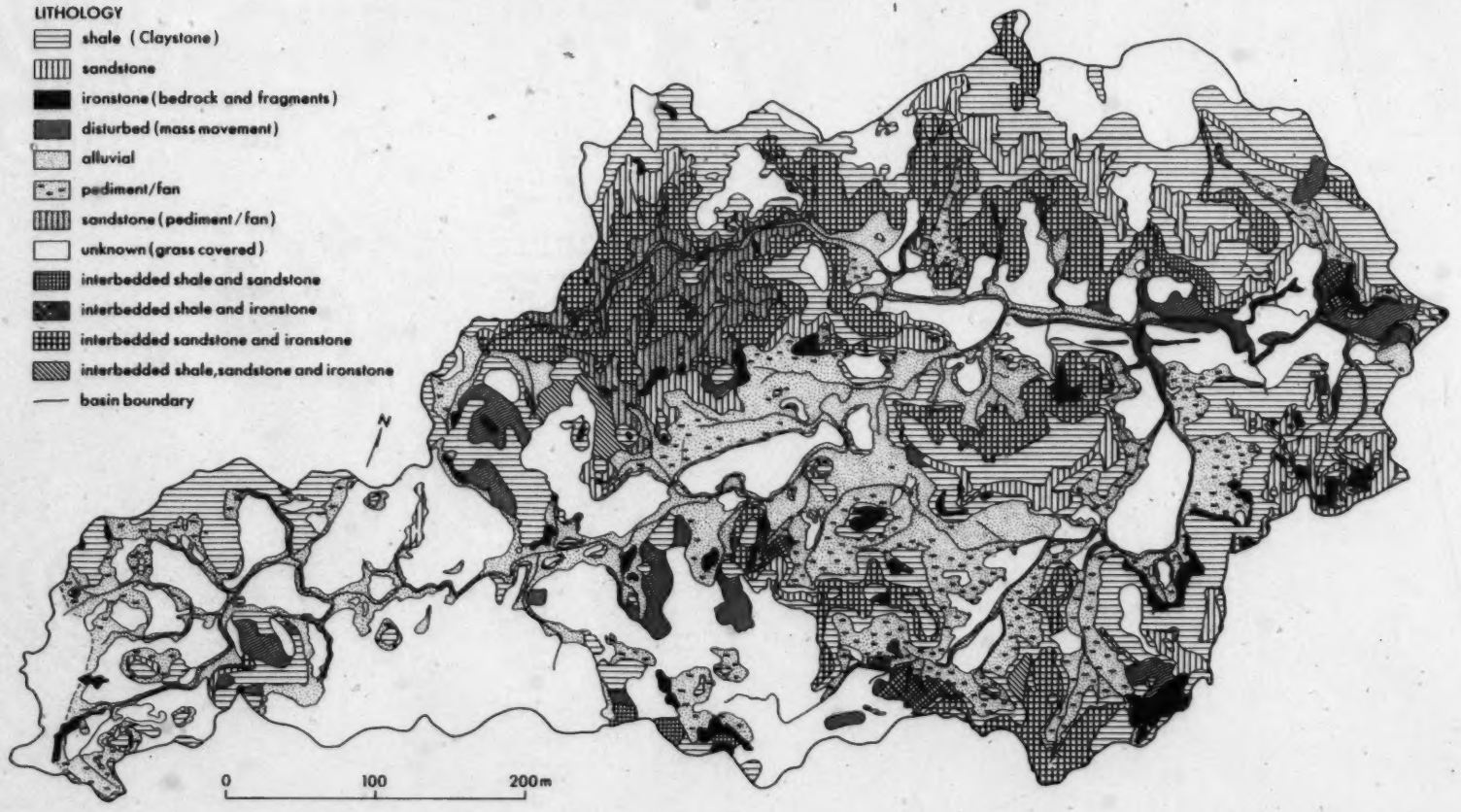

Figure 1.2. Surficial Geology of the main watershed.

Slope 'breaks' are not only encountered on units of similar but slightly varying lithology, but also, at contact planes between differing units. For example, claystone slopes often become oversteepened where overlain by a more resistant material such as sandstone or ironstone (Campbell, 1970), and sharp breaks occur where steep sandstone slopes grade onto the rounded crest of a claystone unit. Hard ironstone beds may produce dramatic slope breaks where the overlying softer materials retreat more rapidly. Although the underlying stratum may also be weak, blocky and spheroidal ironstone fragments can protectively armour these slopes, creating complex slope profiles. Many of these cross-slope ledges serve as natural pathways for animal and human traffic and form ideal areas for preferential snow accumulation.

Evidence of subsurface piping networks is seen surficially in the form of 'blowholes' and pipe outlets that appear on both sandstone and claystone slopes, though more prevalently on the latter. Pipe diameters range in size from a few millimetres to several metres (Bryan *et al*., 1978), and conduits are often partially exposed due to overburden collapse. Although pipe development, network mapping, and runoff characteristics are well described (Rubey, 1928; Buckham and Cockfield, 1950; Fletcher *et al*., 1954; Brown, 1962; Mears, 1963; Parker, 1964; Heede, 1971; Jones, 1971; Atkinson, 1978), comparatively little research has been conducted in the semiarid environment or on pipes developed in bedrock (Gerson, 1971; Bryan *et al*., 1978) [2]

Other topographic features of the study basin include miniature pediments and fine-grained bahadas and alluvial fans, all of which are littered or embedded with mineral, rock, and fossil fragments. Vertical rock pillars or 'hoodoos' are widely distributed and are created where protective cappings overlie weaker material. Cap rocks usually consist of ironstone, but highly indurated sandstones, granite glacial erratics, or fossilized bones are also utilized.

---

[2]A further brief description of the hydrological significance of pipes will be outlined in the *Badland Hydrology* section of Chapter 3.

1.6 Climate and Weather

Essential to the development of a generalized concept relating snowfall to erosional processes of a given region, is a knowledge of the characteristic winter weather patterns. Before this can be done, it is necessary to separate and evaluate the role of individual elements such as precipitation, temperature and wind. This step, which involves the interpretation of long-term meteorological data is important in studies in which actual field observation time is short. This section therefore reviews some of the pertinent average climatic data obtained from nearby meteorological stations and other sources. More detailed discussion on the variable interrelationships will be given in Chapter 2.

1.6.1 Climatic Classification and Precipitation

The study area, along with most of southern Alberta, falls into the semiarid BSk category of the well-known Köppen climatic classification. According to Longley (1968; 1972), the region receives little precipitation with total mean annual values between 300 to 325 mm. However, analysis of figures taken from five locations in the Brooks (35 km southwest of Dinosaur Park) vicinity (Table 1.1) for periods varying between 10 and 27 years, shows a slightly higher combined average annual precipitation (351.8 mm), with all stations recording over 335 mm. Spatial variations in the amount of annual snowfall, rainfall and total precipitation received within southern Alberta are recognized, and are also apparent among the Table 1.1 values of the Brooks stations. In addition, the amount of precipitation recorded by neighbouring stations during individual rain and snowstorms often differs. Reasons for these spatial patterns are numerous, and will be discussed in detail in Chapter 2.

Regardless of these differences in recorded precipitation amounts, the figures are relatively close and provide a good indication of expected precipitation for the study area. The average mean annual rainfall for the five stations is 252.6 mm, and the average mean annual snowfall amounts to 99.2 mm of water (Table 1.1). Comparison of the regional average values reveals that 28.2%, or more than one-fourth of the total annual precipitation falls in the form of snow. Although some potential meltwater losses occur through sublimation and evaporation, this percentage figure indicates a potentially important erosional agent which should not, as it so often is, be casually ignored.

TABLE 1.1. PRECIPITATION DATA FOR BROOKS STATIONS.

Station Name	Brooks AHRC	Brooks	Brooks 1	Brooks North	One Tree	Average
* Code #	1	3	2	3	2	-
Location	50°33'N 111°51'W	50°35'N 111°54'W	50°34'N 111°54'W	50°37'N 111°53'W	50°38'N 111°47'W	-
Elevation (m)	758	755	758	759	737	-
Mean Annual Rainfall (mm)	238.9	265.3	240.8	261.9	256.2	252.6
Mean Annual Snow/Water Equivalent (mm)	96.6	114.2	104.2	87.2	93.9	99.2
Mean Annual Precipitation (mm)	335.5	379.4	345.0	349.1	350.1	351.8
Standard Deviation of Mean Annual Precipitation	83.5	77.8	112.8	86.6	67.8	-

* Codes: 1: Data calculated for 27 years.
2: Data calculated for 15 to 19 years.
3: Data calculated for 10 to 14 years.

Data Source: Canadian Climate Normals: Precipitation 1951-1980. Vol. 3, Environment Canada, 1982.

Because the Alberta Horticultural Research Centre (AHRC) is designated a first-class meteorological station, and has a more adequate set of records than the other Brooks stations, most of the climatic data used is from this station. Mean monthly precipitation values, calculated for the AHRC over a 27-year period (Table 1.2) show that most rain falls between May and September, with peak concentration occurring in June. Monthly snow accumulation is generally erratic, but average maximum quantities are received in December and January, during which 42.3% of the total average annual snowfall is generated. Similar to the combined Brooks station average of 28.2%, the AHRC shows that 28.8% of the total annual precipitation falls as snow.

1.6.2 Temperature

The study region has a mean daily temperature of 3.8°C (Table 1.3). Short, warm summers alternate with long, cold winters, resulting in a high annual temperature range. The mean daily maximum temperature during July, the hottest month, is 26.2°C, and the mean daily minimum temperature during the coldest month, January, is -19.7°C. Hence, an annual average maximum temperature range of close to 46°C is typical of the area. The extreme maximum temperature of 40°C and the extreme minimum temperature of -47.8°C gives a resulting extreme range of 87.8°C. This exemplifies the annual temperature variation which may be experienced in this continental climate.

In conjunction with a large mean annual temperature range, southeastern Alberta also shows the highest daily temperature range in all the prairie provinces. This is mainly attributed to humidity as a function of location, whereby the relatively dry and less cloudy air to the lee side of the Rocky Mountains is more quickly and efficiently heated during the day, and easily cooled at night (Longley, 1972). This condition is certainly observed in the badlands, where light-coloured sandstones and near-white pediments and alluvial fans reflect a high percentage of incoming shortwave radiation, raising daytime air temperatures above those of the surrounding prairie. As a result, summertime peak temperatures over 50°C have been witnessed on occasion within the Dinosaur badlands (personal communication, Park Naturalist, August, 1981).

TABLE 1.2. PRECIPITATION DATA FOR BROOKS AHRC: 1953-1980.

Month	Jan.	Feb.	Mar.	Apr.	May	Jun.	Jul.	Aug.	Sep.	Oct.	Nov.	Dec.	Year
Mean Snow/Water Equivalent (mm)	20.9	13.6	13.5	11.3	0.9	0	0	0	0.6	3.6	12.2	20.0	96.6
Mean Rainfall (mm)	0.9	0.8	2.5	14.8	37.4	65.7	32.2	40.1	32.8	8.3	2.4	1.0	238.9
Total Precipitation (mm)	21.8	14.4	16.0	26.1	38.3	65.7	32.2	40.1	33.4	11.9	14.6	21.0	335.5

Data Source: Canadian Climate Normals: Precipitation 1951-1980, Vol. 3, Environment Canada, 1982.

TABLE 1.3. TEMPERATURE DATA FOR BROOKS AHRC: 1953-1980.

Month	Jan.	Feb.	Mar.	Apr.	May	Jun.	Jul.	Aug.	Sep.	Oct.	Nov.	Dec.	Year
Mean Daily Temp. (°C)	-14.2	- 9.5	- 4.1	4.6	11.1	15.6	18.6	17.3	11.9	6.3	- 3.1	- 9.4	3.8
Mean Daily Min. Temp.	-19.7	-15.1	- 9.8	- 2.2	3.8	8.6	11.0	9.7	4.4	- 1.0	- 9.1	-15.1	- 2.9
Mean Daily Max. Temp.	- 8.6	- 3.8	1.7	11.3	18.4	22.5	26.2	24.9	19.2	13.6	2.9	- 3.7	10.4
Extreme Max. Temp.	17.8	17.2	25.0	31.1	35.6	37.2	40.0	38.9	35.6	31.1	22.2	17.2	40.0
Extreme Min. Temp.	-46.7	-43.9	-37.8	-25.0	-10.0	-2.2	1.7	0.0	-10.6	-24.4	-36.1	-47.2	-47.2

Data Source: Canadian Climate Normals: Temperature 1951-1980. Vol. 2, Environment Canada, 1982

1.6.3 Wind and Airmasses

Wind and its components of direction and velocity are particularly important to this research because they influence the initial sites of snow accumulation and its subsequent redistribution. The seasonal repetition of wind characteristics interacting with surface roughness factors of topography and vegetation determines a reoccurring preferential distribution of snow, and therefore of potential meltwater. A close inspection of regional and smaller-scale wind patterns and their affects will be made, though only regional wind data and airmass characteristics are examined here.

1.6.3.1 Wind Data

Average annual wind directional frequency and mean velocity for the AHRC and Brooks stations are shown on wind rose diagrams (Figure 1.3 and Figure 1.4.). Both sets of diagrams are relevant though differences between the stations are evident. Possible causes for these variations are considered before discussion of observed patterns. Frequency distribution roses (Figures 1.3a and 1.4a) differ most noticeably in north, northwest, and southeast directions, with the latter showing the highest magnitude of variation[3] (52%) (Table 1.4 and Figure 1.5). The most probable explanation is that the wind roses represent average values from successive-year periods (i.e., AHRC from 1955 to 1966; Brooks from 1966 to 1980) as opposed to simultaneous periods. Differences in instrumentation design, calibration, and precision may also partly add to the inter-station variations.

The most obvious difference between the mean annual wind speed diagrams (Figures 1.3b and 1.4b), is that velocities at the AHRC (Figure 1.3b) are generally slightly higher than those of the Brooks station (Figure 1.4b). This is true in five (N, E, SW, W, NW) of the eight directions depicted and is particularly noticeable in the northwest and southwest directions. In addition to the reasons cited above, anemometer height may also be a factor. Both anemometers are located in open, unobstructed areas which exhibit similar surface roughness characteristics, but the AHRC instrument is 3.3 metres higher than that at Brooks (13.4 m *versus* 10.1 m). Wind velocities in lower 300 metres of the atmosphere generally vary logarithmically with increasing altitude (Bagnold, 1941;

---

[3]This value is obtained by dividing the absolute difference between station annual frequency percentages by the mean percentage.

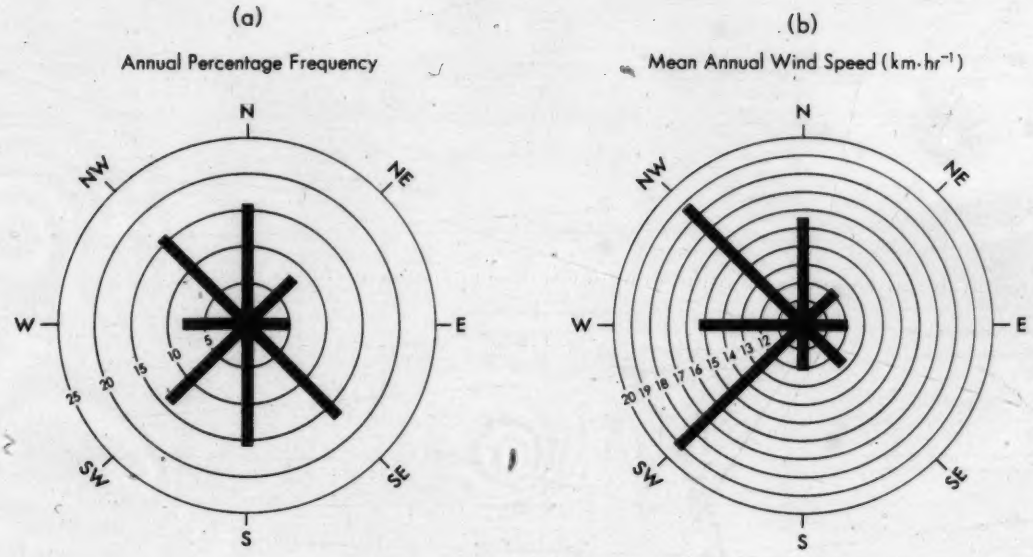

Figure 1.3. Wind rose diagrams for Brooks AHRC: 1955–1966.

Data Source: Canadian Climate Normals: Wind 1955–1972. Vol. 3, Environment Canada, 1975.

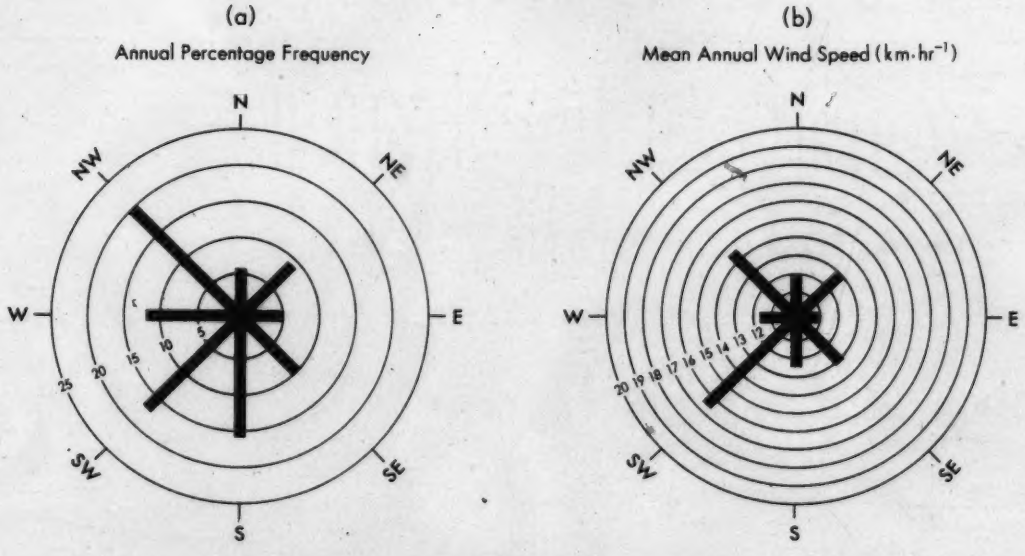

Figure 1.4. Wind rose diagrams for Brooks: 1966–1980.

Data Source: Canadian Climate Normals: Wind 1951–1980. Vol. 5, Environment Canada, 1982.

TABLE 1.4. MEAN ANNUAL WIND FREQUENCY PERCENTAGE.

Wind Direction	Station AHRC: 1955-1966	Brooks: 1966-1980
N	16	11
NE	8	9
E	5	5
SE	17	10
S	16	16
SW	14	17
W	8	12
NW	16	20

Data Sources: Canadian Normals: Wind 1955-1972. Vol. 3, Environment Canada, 1975. Canadian Climate Normals: Wind 1951-1980. Vol. 5, Environment Canada, 1982.

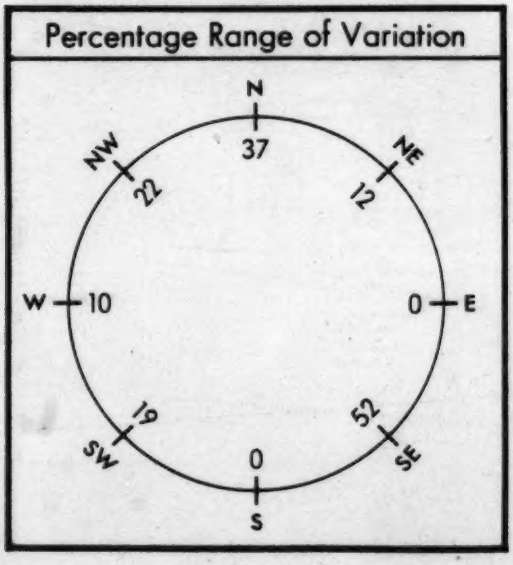

Figure 1.5. Percentage range of variation between percentage frequencies at AHRC and Brooks stations.

Volkovitskaya and Mashkova, 1965; Justus, 1978; and others), thus this relationship may partly account for the higher wind speed recordings at the AHRC. Given the 3.3-metre elevation difference between station anemometers, J-Tec Associates, Inc. (1978) show that there may be as much as a 10% variation between wind velocity recordings. Also, because "...the magnitude of speed fluctuations is proportional to the average or mean speed..." (Kind, 1981, p. 339), relatively stronger winds are likely to show greater variations than lower-velocity winds. Indeed, the stronger winds originating from northern, counterclockwise to southwestern directions vary in percentage range between stations by from 14.5% (southwest) to 26.9% (north), whereas winds from northeastern clockwise to southern vary from a low of 2.4% (south) to a high of 10.4% (east) (Table 1.5 and Figure 1.6). Despite inter-station variations in frequency and wind speed, the differences are relatively small and the data clearly show current wind patterns over the 25 year period (1955 - 1980).

In order that winter wind characteristics be distinguished from yearly averages, wind rose diagrams are considered in conjunction with monthly percentage frequency and wind speed data appearing in Appendix A. Although frequency percentage roses (Figures 1.3a and 1.4a) generally fail to define a prevailing wind direction, analysis of monthly figures yields a more discernable pattern. For example, from October through December, the prevailing direction (highest percentage frequency) recorded by both stations (round bracketed in Appendices A1 and A2) originates from a southerly direction, most often from the south and southwest. From January through April, the dominant wind direction at the AHRC and Brooks station is respectively from the north and northwest. When considering the second highest prevailing wind direction (square bracketed in Appendices A1 and A2) along with the highest, an alternating dominance of primarily southerly and northwest winds is recognized throughout the period extending from late fall to early spring.

Mean annual wind speed roses (Figures 1.3b and 1.4b) show that the strongest winds originate from southwest and northwest. Both stations record the highest annual wind velocity from the southwest (AHRC = 19.2 km hr^{-1}; Brooks = 16.6 km hr^{-1}), and the second highest from the northwest (AHRC = 18.8 km hr^{-1}; Brooks = 14.6 km hr^{-1}). Annual data well reflects monthly velocity averages (Appendices A3 and A4) for the concerned

TABLE 1.5. MEAN ANNUAL WIND SPEED ($km \cdot hr^{-1}$).

Wind Direction	Station AHRC: 1955-1966	Brooks: 1966-1980
N	15.6	11.9
NE	12.2	12.9
E	12.1	10.9
SE	12.7	13.1
S	12.1	12.4
SW	19.2	16.6
W	15.3	11.7
NW	18.8	14.6

Data Sources: Canadian Normals: Wind 1955-1972. Vol. 3, Environment Canada, 1975. Canadian Climate Normals: Wind 1951-1980. Vol. 5, Environment Canada, 1982.

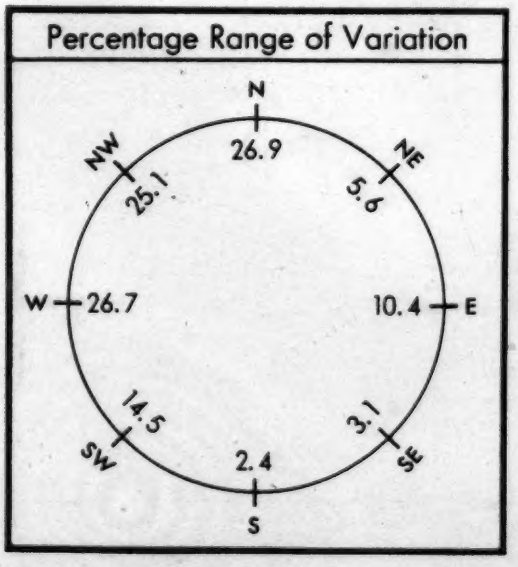

Figure 1.6. Percentage range of variation between wind speeds at AHRC and Brooks stations.

period of October through April. At the AHRC, southwest winds are highest from October through January, then alternate in strength with northwest winds through April (Appendix A3). At Brooks, southwest winds are the most intense, with northwest winds holding the secondary position (Appendix A4). As will be seen, the combination of prevailing and comparatively strong southwest and northwest winds plays a key role in determining seasonally repetitive, preferential snow distribution.

1.6.3.2 Air Mass Characteristics

The interchanging dominance of southwest and northwest winds is closely related to alternations in coverage and magnitude of winter high and low pressure systems, which are characterized respectively as continental polar (cP), and maritime polar (mP) airmasses. High pressures, originating in the arctic region of the Northwest Territories, pump cold air southward during the winter, whereas the lows, forming over the Pacific Ocean, bring relatively warm, dry air to the prairies. The strong west and southwest winds often observed in southern Alberta are largely due to the 'foehn effect' or 'chinook' conditions brought about by the migration of these low pressure centres over the Rocky Mountains. Widespread warming trends may be experienced on the lee side of the mountains as mP airmasses descend and heat by adiabatic compression. High-speed winds are more prominently felt in areas just east of where air is channeled through mountain valleys or passes. These two contrasting air flows (cP and a modified mP) dominate at irregular intervals and their existence is "...more pronounced in winter than any other season" (Longley, 1972, p. 45). The occurrence of chinooks is significant not only because of their effects on snow distribution, but also because they often instigate mid-winter snowmelt.

Given the lack of a strict definition of a 'chinook day', it is difficult to ascertain how many chinook days occur in the field area. Two approaches are taken in defining the chinook (Lester, 1976 ; Golding, 1978); the first describes *dynamic* characteristics or causes, and the second assesses *surface* characteristics or near-ground meteorological effects. Lester (1976) indicates the dynamic approach may be inappropriate in defining the presence of a chinook, as it relies mostly on satisfying preconceived wind and precipitation model requirements. Further, Lester (1976, p.2) states that

The major problem with this definition is that the model may be incorrect or the

> model processes may be operating on a scale which is too small to be resolved by the conventional meteorological data network

Hence, the second approach, using readily available climatic data, is usually followed, though this does unfortunately include meteorological phenomena with similar effects to chinooks but differing causes (Lester, 1976). Although this method is more easily applied to the region in question, the chinook definitions themselves are variable, thus making their application more difficult.

While acknowledging the need for including additional criteria, Longley (1967; 1972) defines a chinook as present when the maximum winter temperature in a given area reaches at least 4.4°C. Using this alone, he shows, through the use of isoline data accumulated over a 35-year span, that the study area normally receives fifteen days of chinook activity each winter. According to Beaty (1975), the area lies well outside the designated 'heavy chinook belt', the boundary of which is loosely based on Longley's (1967) 25-day isoline. Ashwell (1968) outlines three requirements necessary in defining the presence of a chinook; these are wind direction, a minimum rise in temperature over time, and a minimum wind speed. Like Ashwell (1968), Golding (1978) also requires three qualifications including wind speed and direction, and certain temperature criteria.

As the chinook criteria outlined by Lester (1976) are esentially the same as those of Golding (1978), Golding's criteria (along with Longley's (1967) criteria) was chosen for identification of 1981-1982 chinook days[4], based on 27 years of meteorological data from the AHRC. Due to the work involved in compiling daily data over a long time period, the very detailed criteria presented by Lester (1976) and Golding (1978) is only applied and compared to the meteorological records of the AHRC station for the 1981-1982 field season (see Chapter 4). Regardless of the lack of agreement on the definition of a chinook, it will be shown, through the combination of surface melt characteristics and meterological data, that the chinook is present, and, along with strong northwest winds, initiates significant mid-winter geomorphic activity in the badlands.

---

[4]Chinook days could not be calculated according to criteria outlined by Ashwell (1968), as it was impossible to determine from available long-term records one of the three requirements (sharp rise in temperature over a short period of time) necessary to this definition.

1.7 Vegetation

Because of low annual precipitation and other climatic (temperature; slope aspect) and physical ('soil' composition and texture; slope angle) factors, vegetation is limited over most of the watershed. It is however, densely concentrated on surfaces which are both flattish and relatively porous, such as the low-lying alluvial flats and terraces composed of depositional sands and aeolian silts located in the upper part of the watershed (Figure 1.7). It is also abundant on the top of some mesas where runoff is minimized, thus permitting adequate moisture retention for plant colonization and hence shallow brown soil formation.

It is upon the above-mentioned features that the largest variety of vegetation species is located. Flowering xerophytic plants such as the prickly pear (*Opuntia polyacanta*) and cushion cacti (*Mamillaria vivipara*), and the narrow-leaved stone crop (*Sedum stenopetalum*) intermingle among dominating short and mixed prairie grasses. Blue grama (*Boutelova gracilis*) and needle (*Stipa comata*) are the most common and most drought-resistant grasses found in the study region (North, 1976), but western wheat (*Agropyron smithii*), june (*Koeleria cristata*), and Sandberg's blue (*Poa secunda*) also flourish and can dominate in localized areas (Webb *et al.*, 1967). Low shrubs, including hoary sage (*Artemisia cana*) and pasture sage (*Artemisia frigida*), and the perennial herb, moss phlox (*Phlox hoodii*) also prosper on these surfaces.

Vegetation also occurs on the steeply sloping downstream banks of the catchment's primary channel (Figure 1.7), and, to a lesser extent, on the sides of gullies and collapsed piping channels of many claystone and argillite slopes. These areas receive more moisture than most others, due to runoff concentration during rainfall and snowmelt. Plant growth here is usually restricted to some sparse grass, clustering sage bushes, and prickly pear cactus.

Compilation by J. Proudfoot, realization by the Cartographic Division of the University of Alberta Geography Department.

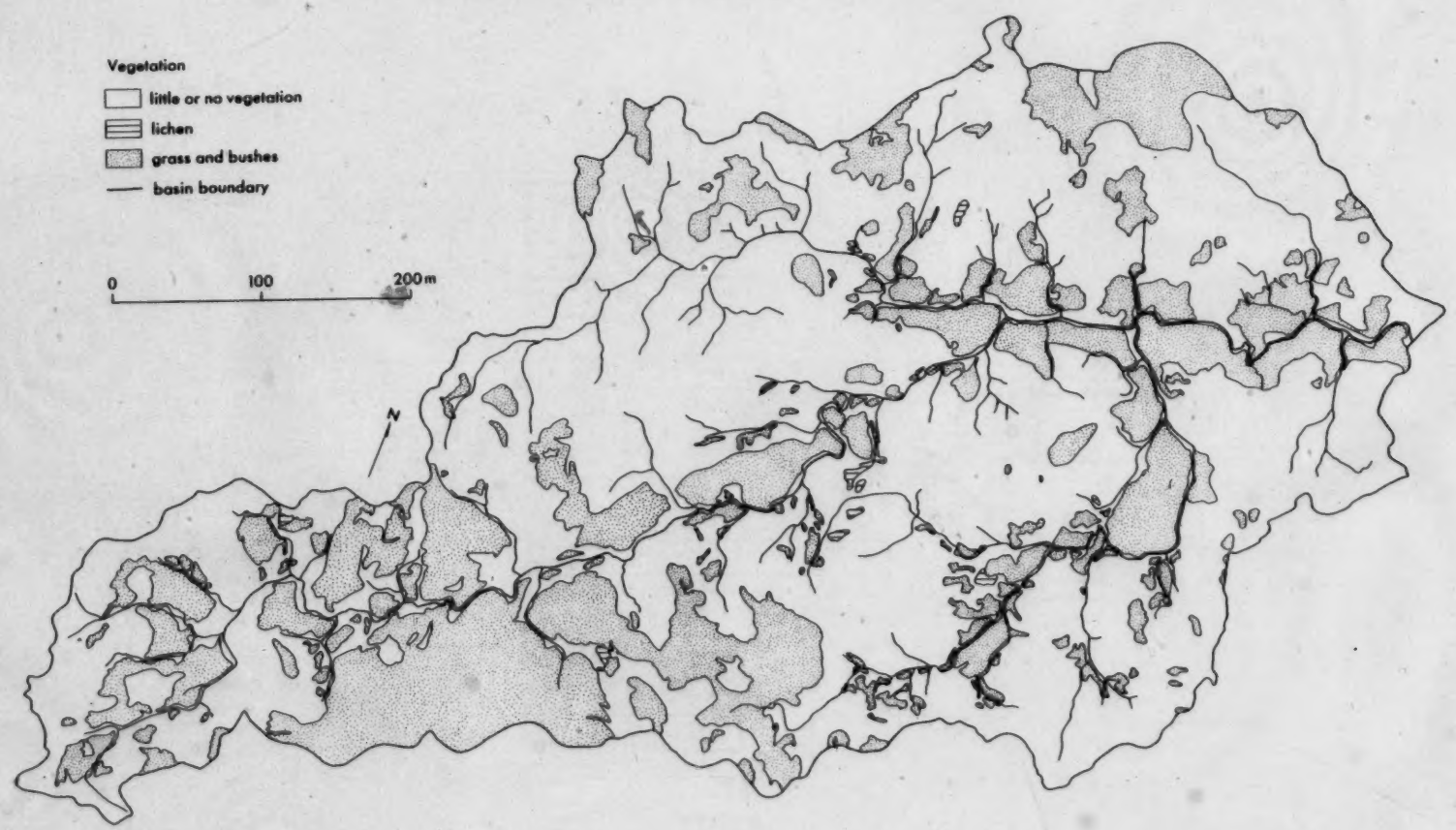

Figure 1.7. Vegetation map of the main watershed.

2. PREVIOUS RESEARCH AND THEORY

2.1 Snow Characteristics: Origin, Accumulation and Distribution

The assessment of snow accumulation is of significant importance to hydrologists and agriculturalists interested in predicting potential snowmelt for purposes of flood forecasting, and determining soil erosion and cropland water availability. Predicting seasonal snowmelt rates and volumes frequently involves the application of multivariate, energy balance equations, or other climatic and physical indices to the snowcover of the area under investigation. However, the accuracy of snowmelt forecasting is often questioned, not only because of the methods employed in its prediction, but also because of the difficulty in measuring snowfall. It is said that this latter problem, that of determining snow accumulation,"...is probably the weakest link in our knowledge of the snow hydrology cycle" (Meiman, 1970, p. 35). The problem is complex due to the initial areal variability of snowfall, the constantly changing characteristics of the snowcover, and, most importantly, to the redistribution of snow by wind. These factors are discussed in terms of their applicability and importance to the study.

2.1.1 Spatial Variability of Snowfall and Snow Accumulation

Because of a differing and changing degree of influence, factors affecting the areal variability of snowfall and the snowcover are typically categorized according to spatial scale. As defined by Gray *et al*. (1978; 1979) and McKay and Gray (1981), these scales are:

1. Macro (Regional):
    a. Areas ranging from 1 to 1 X 10^6 km^2
2. Meso (Local):
    a. Includes linear distances of 10^2 to 10^3 m
3. Micro (Small or Plot Size):
    a. Includes linear distances of 10 to 10^2 m

On the regional scale, snowfall variability is largely controlled by dynamic meteorological effects, including atmospheric circulation, airmass location, and airmass characteristics during precipitation (U.S. Army Corps of Engineers, 1956; Peck, 1972; Gray *et al*.,

1978; 1979; McKay and Gray, 1981). In the prairies, where most snowfall is derived by frontal activity, regional variations in the depth of snowcover may be linked to the position of a front. During winter the arrival of a warm front may produce generous amounts of snow up to 250 km ahead of the front, while depositing very little behind it (Longley, 1972; Gray *et al.*, 1978). In addition, variations in the rate at which snow falls from place to place may be responsible for a non-uniform distribution (Kuz'min, 1960). Thus, snowfall recordings for prairie climate stations may vary considerably in a given snowstorm.

Snowfall variability on the regional scale also results from the combined influence of airmass characteristics and large-scale physiography, including such factors as airmass modification due to orographic uplift, and lake effects (U.S. Army Corps of Engineers, 1956; Peck, 1972; Gray *et al.*, 1978; 1979; McKay and Gray, 1981). The uplift and cooling of moist Pacific air typically produces much more snow in the Rocky Mountains and eastern foothills of Alberta than in the adjacent plains region. Nkemdirim and Benoit (1975) used meterological data from 1941 to 1971 to statistically separate Alberta into two zones of snowfall accumulation extremes. The high intensity zone occurs in the mountains / foothills region, with the hypothetical longitudinal boundary passing through Jasper, Calgary and Lethbridge. Regional snowfall accumulation and variability are seen on Figure 2.1, which depicts mean annual snow accumulation throughout southern Alberta. Spot values show a high variability of snowfall in the mountains, with some areas receiving 500 cm per year or more. A minimum average accumulation value of approximately 102 cm is seen in the southeast, which includes Dinosaur Provincial Park.

On the meso or local scale, variations in snow accumulation are often influenced by topography (obstacle presence and distribution, and slope angle) and vegetative cover (type and density). At the micro scale, surface roughness is the prime determinant of spot accumulation. However, the physical factors influential at these scales present a hindrance to the post-fall measurement of and assessment of snow accumulation, and do not actually cause an areal variability of snowfall. For example, although they may initially receive like quantities of snow, barren slopes, due in part to the effects of wind, usually retain much less snow than those which are heavily vegetated. It is therefore more appropriate to discuss the smaller-scale physical variables in the following section on

TABLE 2.1. VARIABILITY OF SNOWFALL ACCUMULATION (CM) AMONG BROOKS STATIONS DURING SELECTED SNOWSTORMS OF 1981-1982.

Storm Date	Brooks AHRC	Brooks North	Brooks One Tree
Nov. 17-18, 1981	7.5	9.0	m
Dec. 31, 1981 - Jan. 1, 1982	3.9	3.8	3.1
Jan. 11 (AM), 1982	5.5	4.0	3.4
Mar. 1 (AM), 1982	4.3	5.0	3.3

m: Data Missing

Data source: Supplied by Atmospheric Environment Service, Edmonton, Alberta.

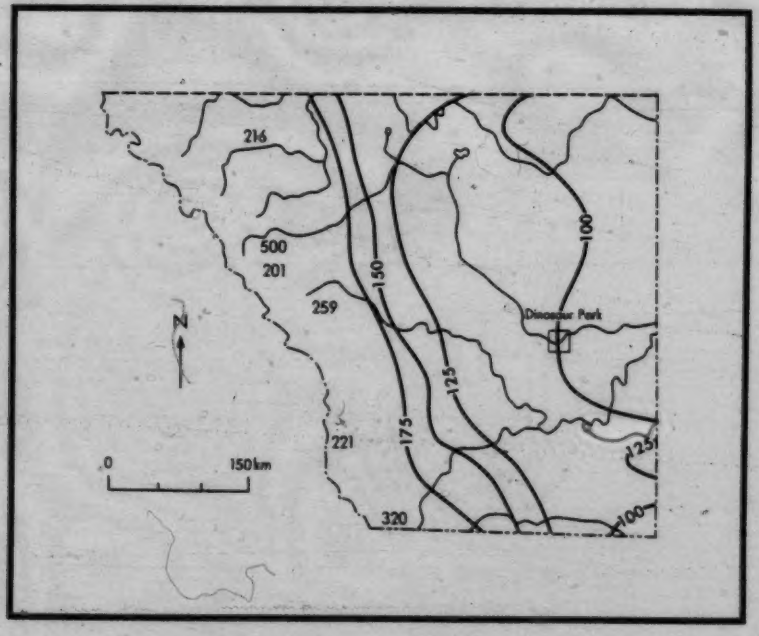

Figure 2.1. Mean annual snow accumulation in southern Alberta (±3 cm). (after Longley, 1972).

snowfall distribution and redistribution, rather than accumulation.

It is maintained that spatial variability of snowfall on local and small scales is not very large though it may appear so as a result of snow deposition under windy conditions (McKay, 1970a). In addition, on the local (as well as regional) scale, initial snowfall tends to be more uniform than rainfall (McKay and Thompson, 1968; McKay and Findlay, 1971). This is most likely due to the differing origins of summer rain and winter snow. That is, frontal precipitation generally covers a larger area than the convective storms responsible for most summer precipitation. Table 2.1 shows snowfall variability among Brooks stations during selected storms of the 1981-1982 snow season. Although there are differences among station values for each particular storm, they are quite small, especially when considering precipitation input in terms of water equivalent. For instance, the 2.1-cm difference in snow depths recorded for the January 11, 1982 storm by the AHRC (5.5 cm) and One Tree (3.4 cm) stations only amounts to a 2.1 mm moisture 'discrepancy', assuming the density of the snow at both stations to be 10%.

Potter (1965, p. 9) contends that the first snowcover (that which lasts a minimum of seven days) in southeastern Alberta appears at the end of November or early December. Using isoline data from McKay and Thompson (1968), McKay (1970b) and Gray (1970) ascertain the mean date of the first snowcover in the study area is day 330 (November 25). Snow accumulation generally reaches an average depth of approximately 10 cm to 13 cm by the end of February (McKay and Thompson, 1968; Longley, 1972; Gray *et al*., 1979), which coincides with the period of maximum seasonal accumulation (Longley, 1972). Median maximum snow depth is 25 cm, and in exceptionally dry winters accumulation may not exceed 10 cm (Potter, 1965).

2.1.2 Snow Distribution and Redistribution

Similar to the discussion of the variability of snowfall, the significance of snow distribution is best considered on different geometric scales. There is unanimity among researchers that wind is the most important factor governing the distribution of the snowcover over a given region. On the prairies (regional scale), Male (1980) contends that blowing snow occurs about 30% of the time during the winter months, provided there is an adequate supply of snow available. This suggests that snow drifting, causing an areal

variation in the depth of post-fall accumulation, is very prominent on the regional scale. However, because of the size of the area, and because the prairies display a relatively homogeneous topography and land cover, a near balance is achieved between the amount of snow drifting in, and that drifting out (Kuz'min, 1960). Therefore, as a unit, the prairies retain about as much snow as they receive, resulting in a fairly uniform pattern of net accumulation.

On the local scale, this balance becomes upset mainly due to the effects of wind as influenced by topography and vegetation. McKay (1964) maintains that open areas in the Canadian plains that are monitored through snow surveys only retain about 65% of the snowfall reported by adjacent climatological stations. Thus, snow redistribution by wind becomes important at this scale, and increases as the size of the area decreases. As the present study concerns local and small scales, concentration focusses on mechanisms responsible for snow transport and deposition, and the significance of distribution at these scales.

Besides the role of surface relief and vegetation, Kuz'min (1960, p. 9) cites two conditions upon which snow transport and deposition depend:

1. the presence of snow particles, derived either from falling snow or an existing snowcover, and
2. a favourable wind direction and speed to dislodge and transport the particles.

Kind (1981, p. 353) cites two mechanisms by which variability in snow depth occurs:

1. the focussing of snowflake trajectories, and
2. non-uniform ground drift.

The first mechanism is caused by a non-uniform wind velocity, and may be responsible for the areal variability in snowfall recognized on the local scale. The magnitude of snow drifts produced by this penecontemporaneous mode of snow distribution is small in comparison to post-fall redistribution. This is attributed to a relatively low frequency of occurrence (during snowstorms only), and to the preferable existence of high obstacles (Kind, 1981). Non-uniform ground drift (mechanism 2) can occur during a snowstorm, but is more frequent after primary deposition has taken place.

Before dealing with the patterns and effects of post-fall snow redistribution, a brief discussion on transport processes acting upon snow particles to cause non-uniform

ground drift is in order. Three transport mechanisms are usually distinguished; snow creep, saltation, and turbulent diffusion (Mellor, 1965; Gray *et al*., 1978). Basically, snow creep is characterized by rolling or 'jumping' of snow particles across the snow surface with a high frequency of surface contact. Saltation is the bounding of particles along the surface in curved trajectories, and turbulent diffusion is the movement of particles in suspension, a good distance above the surface. Of these processes, the latter two are generally considered the most common means of snow transport (Gray *et al*., 1978), but this may be due to a smaller knowledge of the function of snow creep (Mellor, 1965).

For all processes, initial particle detachment from the surface snowcover occurs when surface roughness and shear stresses exerted by the wind are sufficiently strong to overcome some threshold value of particle force resistance. Opposition to movement depends on the size, shape, and weight of snow particles, as well as the extent of inter-particle cohesive forces (Kind, 1981). Increases in the wetness of the snowcover, caused by aging and melting, generally promote an increase of cohesive forces, adding to this resistance. Furthermore, compaction of the snowcover due to wind hardening or partial melt and refreeze (sintering) contributes to the formation of a surface crust or glaze, which may further inhibit snow transport (Kuz'min, 1960; McKay, 1970a; McKay and Gray, 1981; and others).

The wind velocity or shear velocity required to initiate particle movement varies greatly with particle characteristics and the state of the snowcover. For loose, fresh, dry snow, a threshold shear velocity of 4.0 m sec^{-1} (14.4 km hr^{-1}) at ten metres (the standard anemometer height) is suggested to induce movement (Richter, 1945; Kungertsev, 1956; Oura *et al*., 1967; Kobayashi, 1973; Kind, 1976; 1981). McKay (1970a), Mellor (1965), and McKay and Gray (1981) maintain that velocities of approximately 3.0 m sec^{-1} (10.8 km hr^{-1}) may be sufficient. For compact and wind-hardened snow, minimum threshold values ranging from 8.0 m sec^{-1} (28.8 km hr^{-1}) to 10.5 m sec^{-1} (37.8 km hr^{-1}) are suggested (Kungertsev, 1956; Kotlyakov, 1961; Chebotarev, 1962), with speeds exceeding 30.0 m sec^{-1} (108 km hr^{-1}) required in some cases for movement of surface snow that is extremely dense or highly bonded by sintering (Mellor, 1965).

Snow deposition and drift formation fundamentally results from a sufficient decrease in shear velocity. On the small scale, topographic features (e.g., ridges, isolated

slopes, depressions, and vegetation clumps) may cause a decrease in wind shear due to disturbance of air current pathways, thus causing the formation of small eddies and hence snow deposition. The decreased wind shear experienced at the windward bases and leeward zones of obstacles make these areas especially susceptible to preferential snow accumulation. On the regional or local scale, and according to the turbulent diffusion transport process, large eddies may form in the free air stream up to hundreds of metres above the ground surface (Radok, 1977). Furthermore, snow deposition may also result from decreased wind speed within barometric pressure gradients, downslope dissipation of katabatic winds, and particle adherence to wet snow surfaces (Mellor, 1965).

According to Kuz'min (1960, p. 15), snow distribution as influenced by obstacles depends on the number of obstacles, the distance between them, their disposition within an area, their dimensions, and their shape. Hence, he asserts (p. 37) that the more pronounced and frequent the nature of relief features, the greater the variability in distribution and depth of snow deposits. Wind characteristics such as strength, duration and direction are also important to obstacle-induced drift formation, especially in determining a preferential orientation or a seasonally-repetitive occurrence. Kuz'min (1960, p. 34) maintains that the greatest drifts are formed in open, level, steppe regions, and smaller ones where the terrain is highly irregular or covered in vegetation, and larger, more pronounced drifting occurs where sustained, strong winds blow from one prevailing direction (McKay, 1970a; Gray *et al*., 1978; McKay and Gray, 1981). In further support, significant variations in snow distribution were not observed during the winter season on the Russian prairies under winds of varying directions (Kuz'min, 1960). It is important to note here that initial and seasonally-repetitive drift formation depends largely on the *effective* wind direction (i.e., the directional wind strength), rather than simply the prevailing wind direction. Hence, the existence of a prevailing wind is unlikely to produce large or repetitive drifts unless accompanied by strong winds. This view is supported by Odynsky (1958), in his work on sand dune formation and orientation in Alberta.

Besides windward and leeward zones of ridges, slopes, and other obstacles, snow drifts or large deposits are usually found in concavities such as ravines, gullies, ephemeral, perenially-frozen, or intermittant drainage channels, or other more shallow depressions in which eddies form and wind velocity is greatly reduced. The extent of accumulation

within these features, provided there is an adequate supply of blowing snow, also relies on wind characteristics. Largest accumulations are observed when the wind blows transverse to the depression axis. Conversely, less snow is deposited when winds flow parallel or within these features (Kuz'min, 1960). Smaller depressions may become completely snow-filled, thus smoothing the terrain by reducing spatial irregularities. Similarly, small obstacles may become completely buried, with the same results.

Based on comprehensive research of the prairie regions of the USSR, Kuz'min (1960) rated the snow retention abilities of selected landscape features. Accordingly, smallest accumulations appear on ridge crests and steep slopes, especially those exposed to wind. Moderate deposits occupy spaces between ridges as well as flat areas of watersheds. The largest quantities lie in slope lees and surface concavities. Research shows that within a given area, the water equivalent of snowpacks can be correlated fairly well with snowpack depth (Dickinson and Whiteley, 1972; Steppuhn and Dyck, 1974; Storr and Golding, 1974; Adams, 1976). Larger snow accumulations should therefore possess higher water equivalents, and slope lees and depressions should retain much water. This is backed by Kuz'min (1960, pp. 55-58) who cites many examples from Siberian, prairie, and semi-desert snow surveys of the USSR which show that ravines often contain up to 4.5 times more volumetric snow than surrounding flat, relatively open regions. In conjunction, water equivalents in ravines are, on the average, 2 to 4 times greater than in nearby fields.

In some forest steppe areas of western Siberia, where precipitation is low and winds are strong, slopes are often completely snow-barren, with all accumulation drifting into ravines and depressions (Kuz'min, 1960). Beaty (1975) reports the presence and possible geomorphic significance of snow accumulation within aligned coulees of semiarid southern Alberta (details to come). Kuz'min maintains (p. 57) that all else being equal, the total percentage of snow in a given location often depends largely on the percentage area represented by depression features. Anderson (1972, p. 2) contends that "...the distribution of the snowcover becomes very important, as it determines which portions of a watershed are potential contributors to runoff". In conjunction, McKay (1970a) asserts that as gullies and drainageways are major accumulation areas, they also serve as major source areas of runoff. By inference, it is reasonable that these features, as well as other

primary and preferential accumulation areas may also serve as major sediment source areas, as well as foci for winter and early spring geomorphic activity.

The discussion of snow distribution as influenced by the interaction of wind and topography is incomplete without consideration of the extent of vegetation present. The role of landcover is similar to that of terrain in that it too influences surface roughness. It often serves to stabilize snow by decreasing surface wind shear, thereby reducing the ease with which snow may be re-transported. Depending upon the type and density, the presence of a vegetal cover may also favour snowdrift formation. However, the dramatic effects of obstacle-induced snow drifting are generally lessened with an increase in vegetation cover (Goodison, 1978), and densely vegetated landscapes retain larger amounts of snow than open areas, or those with sparser vegetation.

In conjunction with vegetation density, plant *type* is also a consideration. This is demonstrated by Gray *et al*. (1978), using Canadian prairie snow-survey data presented by Steppuhn (1976). The landcover classes studied, arranged by least dense to most dense include: fallow, stubble, pasture, and scrub brush, with the latter class consistently retaining the greatest snow depth. This pattern was also recognized in snow-retention investigations conducted by Goodison (1978) and Fitzgibbon and Dunne (1979). In these studies, it was found that the least dense vegetation class, which also corresponded to that class with the shortest plant height, possessed the lowest snow depths and water equivalents. In both instances, these characteristics are attributed to the relative ease with which snow is removed from these areas by wind. It is noteworthy to mention that in all three studies, snowpacks lying within the least dense, most open vegetation categories also exhibited the highest snow densities because they are more frequently subjected to compaction by wind activity (Goodison, 1978; Fitzgibbon and Dunne, 1979). This conclusion is also reached by McKay and Findlay (1971), in explanation of the typically high snow density values found in both the prairie and tundra regions of Canada.

Most researchers maintain that the combined affects of surface relief and vegetation on snow drifting depend primarily on the degree and type of vegetation cover. In fact, it is argued by Fitzgibbon and Dunne (1979, p. 467) that "topographical influences are only important in open areas of sparse vegetation." This is supported by Steppuhn's (1976) snow depth data which shows, as pointed out by Gray *et al*. (1978), that the most

heavily vegetated class (which is probably considered as sparse by the standards of Fitzgibbon and Dunne) retained the most amount of snow *regardless* of terrain (i.e. slope steepness). This same data also reveals that the average snow depth of all vegetation classes surveyed in *lowland* areas was 101.4 cm, whereas the total class average from *topland* areas was only 27.2 cm. Goodison (1978), working in the Cold Creek watershed in southern Ontario found (p. 39) that "...the effect of terrain on local snowcover depended first on the local land use, which influenced the amount of snow accumulation." He further states (p. 39) that "terrain irregularities, when significant, increased the error of variance of the snowcover properties" (e.g. snow depth and water equivalent). Kuz'min (1960, p. 57) maintains that snow deposition in the semiarid steppe of the Trans-Volga region of the USSR relies on *both* relief and vegetation.

From this discussion, it is apparent that snow distribution and redistribution is indeed dependent, at least on the open prairies, on vegetation *and* topography. It is acknowledged here and by most researchers that topographic relief is less influential in forested areas, where the existence of a tree canopy inhibits wind action. It follows however, that vegetated surface concavities on the prairies may be expected to retain considerable amounts of snow in comparison to either non-vegetated depressions or other vegetated areas that are topographically non-susceptible to snow accumulation.

Table 2.2 summarizes many of the factors governing the spatial variability of snowfall and subsequent redistribution as discussed in this section on snow characteristics. From the table, it is evident that the degree of snowfall variability generally decreases as scale decreases, whereas snow redistribution becomes more highly varied. Thus, it is easy to see how and why accurate snow measurements are frequently difficult to obtain. This is especially true on the local and small scales, where initial input is generally uniform, but redistribution produces measurement difficulties and hence inhibits prediction of runoff and the accurate identification of runoff source areas.

TABLE 2.2. SUMMARY OF FACTORS INFLUENCING SNOWFALL VARIABILITY AND POST-FALL SNOW REDISTRIBUTION IN THE PRAIRIES (THREE SPATIAL SCALES).

	Variability of Snowfall		Variability of Post-fall Snow Accumulation	
Scale	Degree of Variability	Explanation	Degree of Variability	Explanation
Macro (Regional)	High	1) Differing origins of precipitation systems (e.g., orographic; frontal) 2) Differing location (coverage) of precipitating air masses. 3) Differing airmass characteristics (e.g., temperature, humidity, rate of precipitation)	Low	1) Input/output equilibrium of blowing snow
Meso (Local)	Medium to Low	1) Fairly uniform coverage and characteristics of storm systems	Medium to High	1) Depends on degree and type of landcover 2) Depends on spatial frequency of topographic changes
Micro (Small)	Low	1) Uniform coverage and characteristics of storm systems	High	1) High density of surface roughness changes

2.2 Badland Hydrology

Previous research into badland hydrology has emphasized that watershed runoff response is complex, due largely to great variations in slope angle in conjunction with a highly heterogeneous lithology (Bryan *et al*., 1978; Hogg, 1978; Bryan and Campbell, 1980; Campbell, 1981; Hodges and Bryan, 1982). Although the classical Hortonion runoff model of overland flow initiation when precipitation intensity exceeds material infiltration capacity (Horton, 1945) has been considered suitable to the explanation of badland runoff processes (Ward, 1975), recent research shows that the model is only partly satisfactory, and may apply only to specific lithologies (Hodges and Bryan, 1982). Therefore, it appears that a variation of the *partial* or *variable* source area concept, as proposed by workers in humid areas (Betson, 1964; Tennessee Valley Authority, 1964; Hewlett and Hibbert, 1967; Kirkby and Chorley, 1967; Betson and Marius, 1969; Dunne and Black, 1970a; 1970b) is also partly applicable to the interpretation of observed runoff characteristics. However, as stressed by Hodges and Bryan (1982), no single standard runoff concept (such as those outlined in Kirkby, 1978 , and by Bevan and Kirkby, 1979) adequately explains watershed runoff response in the Alberta badlands.

Current badland research is progressing towards the development of a watershed runoff model through knowledge gained from detailed surface plot studies and instrumented monitoring of total basin precipitation and runoff. Through such work, an understanding of runoff properties and geomorphic response under rainfall is gained. It also aids the study of snow by providing a background into many of the mechanisms operating on badland materials during snowmelt. The following sections review pertinent hydrologic information collected from simulated rainfall experiments and instrumented natural rainstorms.

2.2.1 Infiltration, Material Behaviour, and Runoff on Differing Lithologies under Rainfall

Recent hydrologic monitoring has established the study catchment as an extremely efficient runoff producer as compared to humid and other arid land watersheds. This is primarily attributed to low permeability and reduced water transmissibility of materials, caused in part by swelling and sealing of the sodium-rich montmorillonite clay contained in

abundance in claystones and sandstones. It is generally accepted that swelling of montmorillonite, a consequence of hydration (or sorption), stems from the ability of hydration energies of exchangeable cations to overcome electrostatic attraction forces associated with inner layers or particles of the mineral, and to replace or exchange the cations themselves for water (Norrish, 1954a; 1954b; Baver *et al*., 1972). Montmorillonites with high sodium contents possess the greatest swelling ability due to the monovalent nature of the sodium cation, which exhibits an osmotic attraction for water that is twice as high as that of divalent cations of other dominant elements found in clays (Hillel, 1980). As observed by Yair *et al*. (1980), swelling of montmorillonite may be suppressed or restrained by the presence of other prevalent ions, such as calcium in kaolinites distributed in the Zin Valley shale badlands of the Negev desert region in Israel. Material infiltration capacity on these surfaces is much higher, and runoff lower than that observed on claystones in the Alberta badlands (Yair, *et al*., 1980).

Hodges and Bryan (1982) analyzed 21 sandstone units in Dinosaur Park and found an average clay content of 22.6%, with montmorillonite dominating in all but one sample. Infiltration on these surfaces is limited due to a compact structure and rapid surface sealing, and the wetting front rarely reaches depths greater than a few millimetres. Slightly deeper penetration may occur via structural micro-joints in the coherent bedrock below the surface weathering rind (Hogg, 1978), or when there is little erosion of surface sediment (Hodges and Bryan, 1982). In addition, rainsplash, along with possibly aiding in the dispersement of sediment, may also cause a higher degree of surface compaction, the effect of which is to reduce material swelling ability and infiltration capacity (Baver *et al*., 1972; Ward, 1975; Hillel, 1980). Therefore, deeper penetration may also be realized during snowmelt, when the effects of raindrop impact are absent (Hodges and Bryan, 1982).

Simulated rainfall experiments conducted on sandstone plots (Bryan *et al*., 1978; Hodges and Bryan, 1982) and field observations during natural rainstorms reveal a rapid runoff response to precipitation, with flow initiation beginning almost immediately. Threshold precipitation, or that amount required to generate runoff on these surfaces, is usually a few millimetres or less, depending on antecedent moisture conditions (Hodges and Bryan, 1982). Sandstones yield runoff mainly as overland flow, in a manner similar to

that described by Horton (1945). Micro-rivulets form and coalesce on interfluves, and drain downslope and laterally into deeply-incised rill channels. Quasi-laminar sheet flow may occur on interfluves, when material sorption and hence infiltration rates are exceeded by the amount and rate of precipitation input (Hogg, 1978). Wetting depths are usually less in rills than on interfluves, as rill floors are compact and lack a penetrable weathering rind. In addition, they are usually coated with a fine, almost impermeable clay lining, derived from deposition of sediment from previous flow events.

Runoff response on claystone slopes is more variable than on sandstones primarily because of the greater range found in material textures (i.e., degree of compaction and desiccation cracking) and composition (Hodges and Bryan, 1982). As mentioned earlier, many claystones develop a highly desiccated, loose and puffy regolith, while others are more compact and intricately broken by shallow desiccation cracks. Beneath either of these surface layers usually lies a compacted crust which is virtually impermeable except for structural cracks (Hogg, 1978). Below this crust is a thin layer of loose bedrock shards which disintegrate rapidly upon wetting and create a "perfectly impermeable seal" (Bryan *et al*., 1978).

The vertical extent of crust development represents an equilibrium depth whereby the crust / shard interface corresponds to the maximum depth of water penetration by the 'average' rainstorm (Hodges and Bryan, 1982). Since the crust is relatively impermeable, subsurface flow must travel through structural cracks (which may widen into micro-pipes) to the shard layer beneath, where continued downward penetration is negligible. It is at this crust / shard interface that the most elaborate and larger pipe networks are found, where the impermeable wetted shard layer provides a caprock for pipeflow and further pipe development (Bryan *et al*., 1978).

Hogg (1978), Bryan *et al*. (1978), and Hodges and Bryan (1982) studied runoff on claystone units in great detail, and propose similar stages of flow initiation. Runoff on units with a highly disaggregated regolith procedes as follows. Upon initial wetting, clay aggregates (or cells) begin to hydrate and swell. Surface sealing ensues while water penetrates dessication cracks or gaps between aggregates. Slumping and slaking (a process by which compression of entrapped air due to swelling causes cell crumbling and disintegration) of regolith aggregates occurs, and crack, rill, and subsurface pipeflow

follows. Cracks extending from the regolith to the crust layer permit vertical interflow, while sorption processes at this impermeable interface cause basal sealing and closure of cells above. With continued rainfall, surface sealing is complete, and overland flow is sustained from former cracks and rills. Water may penetrate the crust layer through structural cracks to the shard layer, where it may become interflow or pipeflow. Pipeflow is easily sustained due to a thin, impermeable clay layer lining the inside of pipes, similar to that described on sandstone rill floors.

As noted by Hodges and Bryan (1982), all stages of runoff initiation described above are rarely recognized in entirety, and may only occur under prolonged rainstorms of high precipitation, or during snowmelt. For example, it is believed that sustained subsurface flow along either the regolith/crust or crust/shard interfaces requires full saturation of the regolith, a state which may never be reached during (or shortly after) most short-duration, low precipitation summer rainstorms (Hodges and Bryan, 1982). Moreover, full hydration, or 'equilibrium' for most colloidal clays is reached within one to three days, but due to low permeability of sodium montomorillonite, sorption processes may continue for a week or longer (Baver *et al*., 1972; Hillel, 1980a).

Simulated rainfall experiments undertaken in the field by Bryan *et al*. (1978) show that wetting front depths on claystone slopes, under short-duration precipitation inputs are quite shallow. On one stepped and rilled plot, rainfall lasting 20 minutes, with an average intensity of 28.5 mm hr^{-1} yielded a wetting depth of 2 - 3cm, which was confined to the regolith. Although overland flow was observed, no runoff from the dessicated interfluves occurred until the very end of the experiment. On another rilled claystone plot, precipitation administered for 27 minutes at a lower average intensity of 16.5 mm hr^{-1} produced a 4-cm wetting depth on regolith interfluves. On this plot, the crust was only slightly wet along structural cracks, and penetration had not reached the crust/shard interface. On both plots, moisture contents of regolith materials was substantially increased by the end of the experiment, yet remained below average claystone saturation capacities subsequently determined in the laboratory (Hodges and Bryan, 1982).

The varying runoff response on claystones is not only strongly influenced by physical factors mentioned earlier, but also, by antecedent moisture conditions (Bryan and Campbell, 1980; Hodges, 1982; Hodges and Bryan, 1982). In rills and compacted areas

threshold precipitation necessary to induce runoff ranged from 5 to 8 mm on dehydrated surfaces, and from 2 to 6 mm under hydrated conditions. On the highly disaggregated regolith, 12 to 30 mm was required to induce flow on dry material, and from 5 to 12 mm on wet surfaces.

Runoff response on pediment / fan surfaces is similar to that on sandstones in that flow initiation is rapid, threshold precipitation is minimal, and runoff is typically generated as micro-rill and sheet flow. Water penetrates a thin, silty depositional surface to depths of 2 to 3 mm, where it is usually retarded upon reaching a vesicular layer that lies beneath most pediment surfaces (Hodges, 1982; Hodges and Bryan, 1982). This layer may reach a few centimetres in thickness, and its vesiculated nature is probably caused by air entrapment during periods of intense precipitation.

Runoff as overland flow or interflow rarely occurs on vegetated surfaces because of the high porosity and infiltration capacities of sands and brown soils of vegetated alluvial flats and grassed prairie surfaces. For this reason, and because rainfall contribution by individual storms is generally small, it is presumed that runoff threshold precipitation is seldomly reached and that wetting depths may be substantial. It is likely that runoff, if generated at all, probably occurs as throughflow.

Because of the wide range in runoff response exhibited by differing lithologies, a modification of the partial area concept appears applicable to the Alberta badlands (Bryan *et al*., 1978; Hogg, 1978; Bryan and Campbell, 1980; 1982; Hodges and Bryan, 1982; Campbell, 1984). Runoff derived from total surface areas of sandstones, fans, and pediments is generous, and therefore may constitute a very high percentage of total basin runoff. Claystones contribute comparatively little flow, with most emanating from pipes, rills, or compacted zones. Although wet antecedent moisture conditions increase runoff potential on these and other units, the average span between rainstorms is usually sufficient to create dry conditions prior to the onset of most storms (Bryan and Campbell, 1980).

As emphasized by Bryan and Campbell (1980) and Hodges and Bryan (1982), the partial area contribution recognized in the Alberta badlands is mainly governed by spatial variations in lithology, and most runoff, aside from pipeflow, is by overland flow. By contrast, primary contributing areas in humid regions, which are largely vegetated and

usually display well-developed soil profiles, are found in low-lying regions and those adjacent to stream channels. These areas are subject to high saturation levels, controlled in part by throughflow and interflow outlet zones or by proximity to the water table (Hewlett and Hibbert, 1967; Kirkby and Chorley, 1967; Ragan, 1967; Dunne and Black, 1970b). Therefore, the partial area concept, invoked to explain runoff generation in humid lands, becomes modified to include the effects of surficial and subsurface lithologic controls on water flow, in its application to badland hydrologic response.

2.2.2 Total Watershed Runoff: Volumes and Runoff Ratios

As further knowledge of runoff response on various lithologies is gained, so too is an increased understanding of the total basin runoff response. However, because of the spatially-complex lithology, combined with varying influences of climatic and other physical factors, it is difficult to define the degree of importance of a particular parameter as it applies to the total basin runoff hydrograph. Nevertheless, hydrologic field investigations undertaken since 1981 show that the overall basin response under rainfall is one of high efficiency, whereby a large amount of runoff is generated relative to the quantity of precipitation introduced. This information is useful to the present study in that it theoretically permits a comparative assessment of runoff volumes and storage capabilities under rainfall and snowmelt.

Hydrologic data collection in the watershed is currently facilitated by a competent and sophisitcated monitoring system. Rainfall measurements are obtained with the aid of a dense network of standard and automatically-recording rain gauges. Two flumes were recently installed which are gauged both manually and automatically[5]. Thus far, data consisting of volumetric precipitation input and hydrograph runoff volumes for nine rainstorms occurring in 1981 and 1982 (appearing in Bryan and Campbell, 1984) has been used to calculate runoff efficiency and storage within the watershed.

For the nine rainstorms analyzed, for which average precipitation was 17.5 mm, the average percentage of runoff output to volumetric input, or *runoff coefficient* is 35.6% (Table 2.3, column 6). This number signifies that 35.6 units of water escape the watershed for every 100 units entering. Runoff coefficients for individual storms (Table

---

[5]For more details on the equipment used, see Bryan and Campbell, 1982 .

TABLE 2.3 HYDROLOGIC DATA FOR NINE SUMMER RAINSTORMS OF 1981-1982.

1	2	3*	4	5	6
Storm #	Storm Date	Average Precipitation (mm)	Volumetric Input (m^3)	Volumetric Discharge (m^3)	Runoff Coefficient (%)
1	10/6/82	6.1	2055	346	16.8
2	13/7/81	7.6	2560	598	23.4
3	1/7/82	12.2	4109	1563	38.0
4	2/7/82	18.9	6366	3694	58.0
5	13/6/81	20.6	6938	2043	29.4
6	27/6/82	20.8	7006	2394	34.2
7	9/7/82	21.2	7140	2737	38.3
8	25-26/5/82	21.9	7376	2875	39.0
9	1/7/81	28.1	9464	4069	43.0
Average		17.1			35.6

* Values obtained from Bryan and Campbell (1982), and from unpublished measurements.

2.3) were derived by dividing the total volumetric runoff (column 5) by the total basin volumetric precipitation (column 4). A pattern is recognized in that runoff coefficients for seven of the nine storms (numbers 1, 2, and 5 through 9) increase, or approach 100% as precipitation (columns 3 and 4) increases. This pattern well reflects a reduced permeability of materials and thus an increase in runoff ability with increasing precipitation.

Exceptions to the pattern are noted in storms 3 and 4, and are easily explained. The uncharacteristically high runoff coefficients of both storms directly reflect the wet antecedent moisture conditions present prior to both rainstorms. A major storm, followed by daily intermittent showers of a few millimetres occurred four days before storm 3. Although surface materials prior to this storm were only partly hydrated, they retained sufficient moisture to remain in a partially sealed state. Storm 4 occurred the day after storm 3 and yielded the very high runoff coefficient of 58.0% (Table 2.3), indicative of the high runoff efficiency expected under a well-hydrated material state.

Figure 2.2 depicts volumetric runoff (discharge) against precipitation input for the nine storms and may be employed to predict runoff, and hence runoff ratios under both wet and dry antecedent moisture conditions. From the graph, it is ascertained that runoff volumes and coefficients average approximately 1.65 times greater under a moist material state when precipitation input is between 10 mm (3,368 m^3) and 20 mm (6736 m^3). It is important to note that treating consecutively-occurring storms 3 and 4 as one storm of 31.1 mm (10,475 m^3) would yield a dry-state runoff volume of approximately 4,700 m^3, and thus a runoff coefficient of 45%. The *actual* average coefficient of these storms is 48%. The similarity of the two values suggests that the wet and dry antecedent moisture curves (Figure 2.2) probably converge at a precipitation input of just over 30 mm (10,104 m^3). This is significant in that it implies that a wet material state is no longer an important consideration to the study of badland runoff efficiency once the introduction of adequate precipitation enables the dry material to 'catch up' to a fully-hydrated state.

The 30-mm precipitation value also denotes a threshold of maximum, basin-wide storage capacity, after which almost all added precipitation becomes runoff. Although it has been shown that sandstone, fan, and pediment surfaces yield runoff under very low precipitation input, the relatively high 30 mm threshold figure considers the entire catchment, of which approximately 55% is covered by claystones and highly absorbent

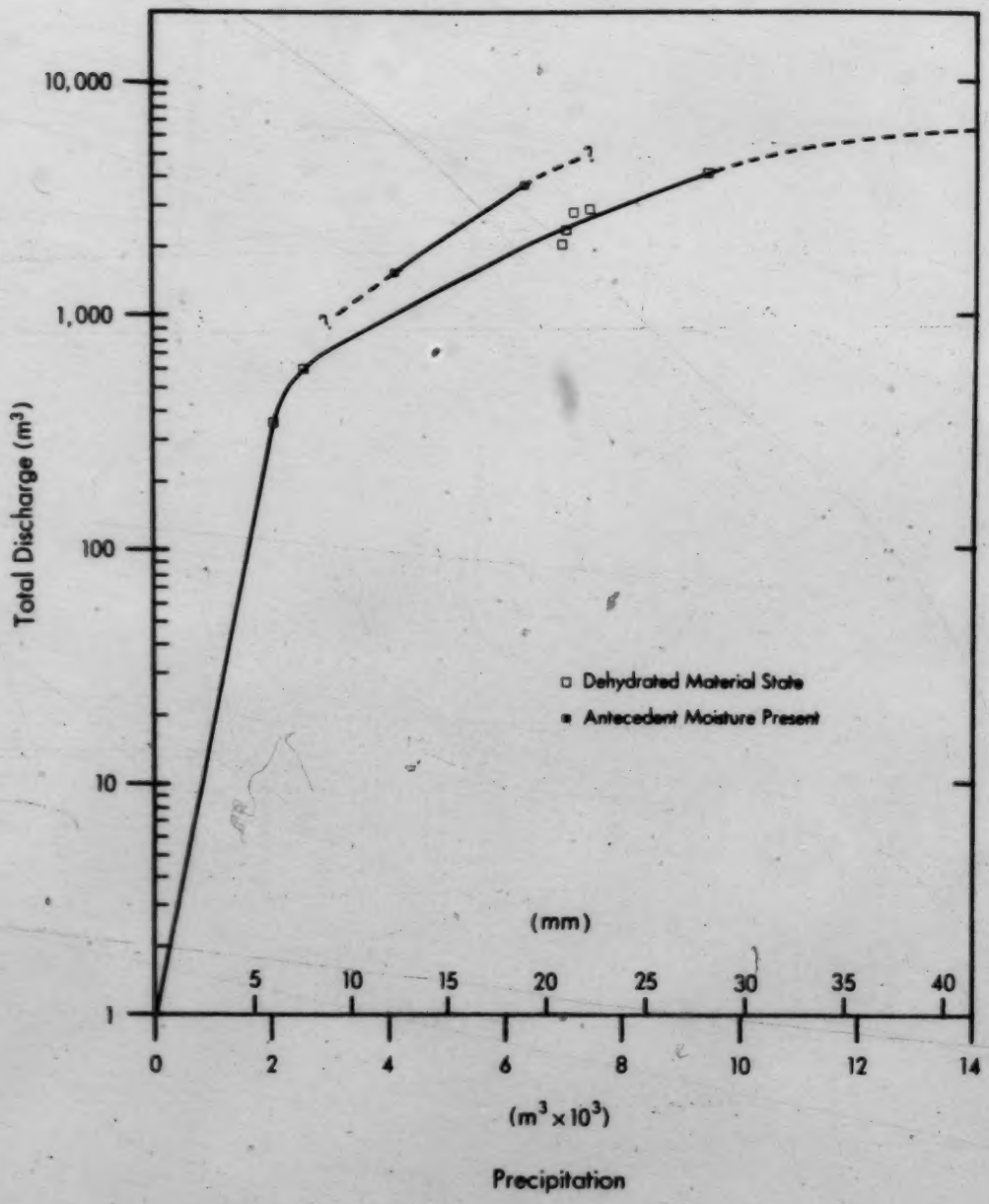

Figure 2.2. Precipitation *versus* total discharge for nine summer rainstorms of 1981–1982.

vegetation flats. The latter surfaces are probably largely responsible for the high threshold figure because, although claystones do not yield runoff in great quantities, they have been shown to generate it during rainstorms, before full hydration (moisture retention capacity) is reached (Hodges and Bryan, 1982). It is stressed that rainstorms of 30 mm or more are not common and occur perhaps once per year. This value therefore lends support to the hypothesis posed by Hodges and Bryan (1982) that full hydration of claystones may only be achieved under prolonged rainstorms or during snowmelt, when saturated conditions are attained beneath snowpacks.

In comparison to other arid and semiarid regions, runoff coefficients derived for the nine storms are similar, but often lower. This is evident despite the large area represented by absorbent claystones and vegetation surfaces, and is a reflection of the high-yielding sandstones, pediments, and fans that comprise the remaining 45% of the catchment's surficial lithology. Campbell (1978) examined runoff characteristics of five summer rainstorms during 1976 in a nearby badland watershed, and suggested a representative runoff coefficient of 8.6%. This value is lower than the average coefficient presented here (35.6%), and may be attributed to the more sophisticated instrumentation now employed in the watershed (Campbell, personal communication). Nevertheless, both sets of average coefficients suggest a very high runoff response for the badlands in comparison to the 1.4% coefficient proposed for the southern prairie region of Alberta (derived by Campbell, 1978 from data presented by Underhill, 1962).

Runoff data obtained during 15 rainstorms by Schumm and Lusby (1963), on the Mancos shale slopes in semiarid western Colorado show that the average runoff coefficient from August to October is 16.1%, or a bit lower than that recently derived for the Alberta badlands. However, seasonal increases in soil infiltration capacity due to mid-winter soil loosening[6] results in springtime (April to June) runoff coefficients that average 1.3% (derived from data presented by Schumm and Lusby, 1963). This seasonally-fluctuating material state has not been recognized in the Alberta badlands, which generate high runoff for the entire rainfall season.

---

[6]The explanation and significance of this process will be discussed in further detail in the last section of this chapter, entitled *Badland Erosional Mechanisms And The Geomorphic Role Of Snow*.

Runoff studies conducted during two rainstorms in a semiarid sub-basin of the Walnut Gulch watershed in southeastern Arizona (Osborn and Renard, 1969; 1970) yield very high runoff coefficients of 45% and 36%. However, these coefficients result from extreme precipitation inputs of 52 mm and 46 mm respectively, and are likely to be much smaller under lower, more representative rainfall amounts. Corresponding precipitation inputs required to obtain similar coefficients in the Alberta badlands are much less, ranging between 20 to 30 mm.

Simulated rainfall experiments carried out on surface plots in the arid Zin Valley badlands of Israel indicate that runoff disposal is less efficient in this region than in other badlands, including those in Alberta (Yair *et al*., 1980). The Zin Valley badlands are developed in the Taqiya Formation, which is composed of homogeneous calcareous shales that exhibit little swelling and retain a high infiltration capacity (Yair *et al*., 1980). Runoff on this material is almost completely confined to rills, pipes, and gullies, with overall plot runoff response similar to that on the claystones of the Dinosaur Park badlands (Yair and Lavee, 1982). Although no volumetric watershed runoff data is available, it seems almost certain that runoff coefficients for these badlands would be substantially lower than those calculated for Alberta.

2.3 Snow Disappearance and Snowmelt Runoff

As concisely expressed by Kuz'min (1960, p. 12), snowmelt, or the "...disappearance of the snow cover is determined by a single decisive factor - the heat balance of the earth's surface". Although this statement is simple, its implications become complex when considering the many and varying interactions of the heat-related parameters leading to inter-seasonal changes in snowcover characteristics (e.g. depth, density, and water equivalent), and to spatial diversity of snowmelt release and runoff. Monitoring of temporally-varying snowcover characteristics is essential to the accurate prediction of the timing and volume of snowmelt runoff. However, measuring the interseasonal changes in the nature of the snowcover is often difficult, particularly when accompanied by a spatial variation in the characteristics themselves, and by spatial variations in snowcover distribution.

As stated earlier, the primary emphasis of this research is placed on assessing the geomorphic impact of snow and snowmelt on badland materials. Although runoff is of concern, it is of secondary importance. For this reason, and for logistical and practical considerations, no snowmelt prediction equations or models are applied to runoff in the study basin. However, a discussion on the factors employed in most energy balance equations, which influence both initial and differential snowmelt is included, to indicate those parameters which are the most influential to snowmelt, runoff, and hence geomorphic response in the badlands.

2.3.1 Snow Disappearance as Influenced by Factors Governing Direct Solar Radiation Receipt

2.3.1.1 Albedo

The albedo or reflectivity property of a snowpack is one of the energy factors which governs the rate at which snow melts. As will be seen, this rate is significant, because it strongly determines whether or not runoff can occur in a given area. The degree to which albedo controls snowmelt is largely a function of the angle or 'height' of the sun, the size, shape, density, and structure of the snow crystals in a snowpack, and the amount of soil or other matter incorporated (McKay, 1970b ; Male and Granger, 1978).

New, fresh, dry snow retains a high coefficient of reflectivity (c. 0.90), whereas aged, moist, or soil-laden snowpacks often possess high radiation absorption capacities, or a low reflectivity ratio of c. 0.40 (U.S. Army Corps of Engineers, 1956 ; Anderson, 1972 ; and others). In general, snowpack albedo tends to diminish as the snow season progresses, especially after the occurrence of the last snowstorm. Accelerated melt usually occurs where dirty snow layers laced with wind-blown soil are exposed, or when patches of bare ground, with their comparatively high radiation absorption properties, allow peripheral melting of the surrounding snowcover (Gray, 1970) In addition, variations in spatial albedo may lead to differential melt of the snowcover. This is particularly evident in areas subject to non-uniform snow accumulation, and is apparently linked to variations in snowcover depth.

The albedo of the underlying ground surface influences the amount of heat energy re-radiated into the snowpack,once the snowcover depth shrinks below some critical value. Kung *et al*. (1964) maintain this value is approximately 12 cm; Gray (1970) proposed a value of 15 cm, which was subsequently altered to 2 to 4 cm after conducting laboratory experiments (O'Neill and Gray, 1972). Gray (1970) suggests snow disappearance on fallow prairie fields is fairly uniform except in gullies and areas conducive to drift formation. These findings imply that reflectivity properties of snowpack and underlying ground surfaces may play a prominent role in the badlands, where gullies and potential drifting areas are plentiful, sediment disturbance by wind commonly occurs, and where there is a wide range of reflective properties exhibited between the light-coloured sandstones, and darker claystones and ironstones.

2.3.1.2 Aspect

Aspect (slope angle and orientation) is generally viewed as a principal factor in determining the amount of direct beam radiation reaching the surface snowcover. According to Meiman (1970), the prime role of aspect is that of influencing snowmelt. The effectiveness of aspect on generating snowmelt depends on the position of the sun as dictated by time of year, and is largely modified by topography, i.e. slope angle and orientation. It is argued that aspect is particularly important in areas where there is variation in surface relief. In fact, it is emphasized by Price and Dunne (1976) and precisely stated by Obled and Harder (1978, p. 200) that during snowmelt, "the main effect of topography is to increase spatial diversity in snowmelt rates resulting in a time staggering of the release of meltwater over the watershed."

Variations in solar radiation receipt as controlled by topography and time of year are easily seen in energy flux data derived by Buffo, *et al*. (1972). This data demonstrates that at 50°N latitude (the field area is 50°46'N), a 30° south-facing slope receives an energy flux of 1268 J cm^{-2} day^{-1} on December 22, whereas a north-facing slope of the same angle receives no direct radiation on this day. On March 8, the identical south-facing slope receives 2562 J cm^{-2} day^{-1}, whereas the north slope is allotted only 159 J cm^{-2} day^{-1}. Moreover, Male and Granger (1978) show that a significant variation in the magnitude of solar radiation receipt is also recognized on gradual slopes. They remark that a 10° south-facing slope at 50°N latitude receives 2.5 times as much direct radiation

as a 10°N slope at the onset of March, but that this figure drops to 1.5 by the first of April.

With such information in mind, it is not surprising to find numerous studies that claim south slopes usually become snow-free before slopes oriented in other directions. This is deemed particularly true in unshaded, non-forested areas, and may be more readily observed in semiarid areas (McKay, 1970a), or in locations where mid-winter thaws are common (Kuz'min, 1960; Meiman, 1970; Gray *et al*., 1978; McKay and Gray, 1981). McKay (1970a) contends that north-facing semiarid hillslopes often retain snow throughout the winter period, whereas south slopes may frequently become snow-barren.

In conjunction with temporal variations in snow disappearance, many studies (e.g. Packer, 1962; Gary and Coltharp, 1967; Landalls and Gill, 1972) show that throughout the winter, snowpack water equivalents on north-facing slopes are generally greater than those of south slopes. This observation is claimed due to less radiation receipt, hence less inter-seasonal melt or evaporation on north-facing slopes. As important as the effects of aspect on snowmelt appear, it is convincingly argued by Male and Granger (1978) and McKay and Gray (1981) that within the prairies aspect is less influential than snow accumulation or snow distribution in determining the rate of snow disappearance. That is, south slopes may not necessarily lose their snowcover before other slopes if they possess larger quantities of snow. This is supported by Hendrick *et al*. (1971, p. 423) who contend that "drift patterns and interception contribute to complex depth patterns which, in turn, lead to a complexity in the growth of bare ground areas during the melt season"

The implications of this discussion indicate that there are a number of varying possibilities as to the effects of aspect on snowmelt response. In the badlands, it seems certain that the highly dissected terrain and accompanying wide range of slope angles and orientations would promote a significant spatial diversity in snowmelt rates. Even though the greatest difference in radiation receipt among slope aspects is realized in December, optimal variations in the spatial disappearance of snow are probably seen during March or April, when the effects of differential radiation may be accelerated by atmospheric heat transfer of warm spring winds. However, as pointed out by Male and Granger (1978) and McKay and Gray (1981), snow distribution patterns may negate the logical progression of

rapid snow depletion on south-facing slopes. By the same token, a pattern of preferential snow accumulation on north slopes would undoubtedly ensure a maximum differentiation in both spatial and temporal rates of snow depletion between north and south slopes.

To date, there has been no research conducted on the relationship between slope aspect and snowmelt progression in badlands. However, a number of workers (Beaty, 1972; 1975; Yair *et al*., 1980; Churchill, 1981; Yair and Lavee, 1982) have considered the possible influences of aspect on slope moisture retention, infiltration, and erosional response on badland materials under rainfall conditions. These studies will be examined under the Badland Erosional Mechanisms And The Geomorphic Role Of Snow section of this chapter.

2.3.1.3 Vegetation

Akin to albedo and aspect, the extent of vegetation present also modifies the amount of incoming solar radiation reaching the snowcover, and hence snowmelt rates. In general, it is accepted that short-wave radiation transmission decreases with an increase in landcover or forest canopy. Thus, it is expected that snowmelt in areas of little vegetation would proceed more rapidly than in zones of dense vegetation. This is acknowledged by Anderson (1972) who cites examples of snowmelt research conducted in two watersheds of differing landcovers.

During the 1968 - 1969 snow season, both the Sleepers Creek watershed in Vermont (Hendrik *et al*., 1971) and the Rock River watershed in Iowa (Paulhus, 1971) received record snow accumulation, yet spring flooding was experienced only in the latter region. This was attributed to the fact that snowmelt in the heavily forested watershed in Vermont continued relatively slowly for a full month, whereas the Iowa catchment, exhibiting no forested areas and a generally flat terrain, experienced a rapid melt period lasting only six days (Anderson, 1972). In the Rock River watershed, the combination of little differential melt as induced by topographic aspect, and lack of a forest cover permitted greater direct radiation penetration to a larger ground surface area, resulting in rapid melt, and severe flooding.

In further testimony to the importance of vegetation in regulating solar radiation, Packer (1962), working in a pine forest in the Columbia River basin (USA), found that snowpack water content increased proportionately with the degree by which canopy

openings were created or expanded. In explanation, Packer cites increased melting activity permitted in these unshaded open areas.

In addition to vegetation influences on insolation, Hendrie and Price (1978) and Price *et al*. (1978) report that a forest cover also reduces the turbulent exchange of water vapour between the atmosphere and snowcover by restricting wind velocity. From this, it may be deduced that snowmelt and evaporation will proceed more slowly in forested areas, where vapour pressure gradients are naturally reduced.

It is apparent from the above discussion that the sparse vegetal cover displayed in the badlands will have a negligible effect on retarding snowmelt rates. It may be that grass-covered alluvial terraces or vegetation-lined gullies retain snow for longer periods due to a slight increase in the shade afforded. However, plant *height* in these areas is generally very short, and thus protection from insolation, and resulting variations in snowmelt lag time between these and unvegetated areas is probably insignificant. Furthermore, it is unlikely that vegetation-induced differential melt (if realized) would have much effect on causing a lag in *runoff* rates, because, like rain, most snow lying upon highly absorbent vegetated flats and upper grassed surfaces becomes lost via infiltration and evaporation, rather than contributing to overland flow or other forms of runoff, *regardless* of its rate of melt.

2.3.1.4 Cloud Cover

A daytime cloud cover serves to inhibit incoming radiation but may also hinder outgoing (long-wave) radiation if present during the night. Cloudcover may therefore produce temporally vacillating effects on snowmelt. Gray (1970) gives a detailed account of the reversing consequences of these temporal variations. As skies in the western prairies are typically cloudless at night because of low humidity, relatively large amounts of long-wave radiation may be lost, possibly resulting in a greater heat escape during the night than that amount gained during the day. This daily net heat loss serves to retain low snowpack temperatures, and may aid in the refreezing of soil or partially melted snow at night (Gray, 1970). Conversely, Gray (1970) contends that during the melt period especially, the occurrence of a nocturnal cloud cover would reduce long-wave radiation losses and encourage continued melting through the evening.

2.3.2 Snow Disappearance as Influenced by Sensible Heat Parameters

Discussion has concentrated on factors which affect a variability of snowmelt in terms of the availability of energy derived through the penetration of *direct* solar radiation. In most cases it is accepted that the factors involved in direct radiation heat exchange are responsible for major snowcover depletion. However, factors included in the transfer of *sensible* heat to the snowcover are also important to the study of snow dissipation.

2.3.2.1 Temperature

Air temperature is a principal factor determining the sensible heat exchange of a snowcover. However, although it may be important, temperature alone is not an adequate indicator of snowmelt or runoff rates (Davar, 1970; Dunne and Black, 1971). In fact, the heat gained from the overlying air surface actually reflects an integration of the effects of temperature (sensible heat transfer) *and* solar radiation (Collins, 1934; U.S. Army Corps of Engineers, 1956; Wisler and Brater, 1959; Østrem, 1964; Dunne and Black, 1971; Ward, 1975; and others). Gray (1970) claims that on the prairies, no appreciable melt occurs as an outcome of a temperature rise until the mean daily temperature is greater than 4.4°C.

2.3.2.2 Sublimation and Evaporation

Sublimation and evaporation of the snowcover also occur mainly through sensible heat transfer, although the significance of these mechanisms is debated in the literature. It is often stated that strong, dry chinook winds create a substantial vapour pressure gradient between the snow surface and overlying air, as well as sufficient atmospheric turbulence, to produce conditions conducive to convective heat transfer and hence snowpack sublimation or evaporation (Louie, 1977; and others). However, it is also claimed (e.g. Hoover, 1948; Diamond, 1953; Linsley *et al*., 1958; Gray, 1970; Williams, 1970; Ward, 1975) that direct sublimation and evaporation losses from the snowcover are very small as compared to the amount of meltwater produced. In other words, heat transferred from warm chinook winds to the snowcover is more likely to result in *snowmelt* rather than sublimation. This is mainly attributed to energy requirements necessary to invoke these respective phase changes; at 0°C, it requires approximately

2826 J g^{-1} to sublimate snow (solid to gaseous phase change), but a heat of fusion of only 335 J g^{-1} to melt snow (solid to liquid phase change).

In addition, Linsley *et al*. (1958) assert that sublimation or evaporation of the snowcover can only occur when the vapour pressure of the overlying air is lower than that of the snow surface, or when the dewpoint is less than the snow temperature. Sublimation halts once the dewpoint temperature reaches 0°C, and melting commences. Therefore, it is argued that the rate of snowmelt far exceeds that of sublimation when temperatures are above freezing as is often the case during chinook winds.

There are two important considerations to add to the above discussion. Firstly, although sublimation is generally regarded as minimal by most researchers (even during cold temperatures), it is possibly facilitated under conditions of blowing snow (Linsey *et al*., 1958; Dyunin, 1967; Schmidt, 1972; Tabler, 1975; Gray *et al*., 1978; Kind, 1981). As a result of laboratory testing, Schmidt (1972) found that during blowing snow, "the sublimation rate nearly doubles for each 10°C rise in ambient temperature in the range between -20°C and 0°C". However, it is questionable whether blowing snow is widespread or common under warmer chinook conditions, when melting of the snowcover may prime the pack with water, increasing cohesive forces and snowpack density, and reducing snow transport capacity.

Secondly, once melting begins, evaporation may proceed more easily, especially from a free water surface such as that created by ponded meltwater (Gray, 1970). Bruce and Clark (1966) found that at an air temperature of 5°C most of the convected sensible heat transferred to the snowpack is used to melt snow, but that at higher temperatures (e.g., 20°C), excess energy may produce both snowmelt and evaporation simultaneously. It is suspected that evaporation losses from meltwater produced at the snow surface under chinook conditions may be minimal as water thus produced may, in some cases, refreeze onto the surface snowpack (Golding, 1978). Also, since the vapour pressure of warm chinook air is lower than that at the air / snow interface, condensation of atmospheric water vapour onto the snowcover may occur, and hence in itself add more water, or generate it through latent heat released. Bruce (1962) supports the notion that the effects of condensation may outweigh snowpack evaporation losses. However, Golding (1978, p. 1651) claims that snowpack condensation is rare during chinooks due

to the need for the combination of high temperatures and high relative humidity, the latter of which is generally not recognized during chinook activity. Working in the Bad Lake research watershed in the prairies of southern Saskatchewan, Granger *et al*. (1977) also found that evaporation usually exceeds condensation (under normal winter conditions), but that condensation dominates when night-time radiation losses are large.

Hutchinson (1966) and Solomon *et al*. (1975) found that evaporation losses during the snowmelt period are substantially higher from exposed soil surfaces than from adjacent snowpacks, during both day and night. This is mainly attributed to the fact that the vapour pressure of melting snowcover is set at a fixed value of 611 Pa, corresponding to 0°C, whereas that of a wet soil is not. Soils generally display a higher albedo thus permitting more energy absorption, higher soil temperatures and greater evaporation (Hutchinson, 1966).

A number of researchers have attempted to estimate snowmelt evaporative losses during chinooks. Employing evaporation equations based on 19 years of data, Louie (1977) calcualted potential evaporation amounts of 71.5 mm and 115.8 mm at Calgary and Lethbridge respectively, for a representative winter period extending from December through March. In the eastern slopes of the Albertan Rocky Mountains, Golding (1978) found during 1975 and 1976, that actual snowmelt evaporation respectively amounted to 50% and 76% of that calculated by Louie (1977). Marsh (1965) noted chinook influences on evaporation but could not estimate quantitative losses. Williams (1970) maintains that an accurate assessment of evaporation is difficult, and that (p. 318) "from a hydrological viewpoint, evaporation losses from a large watershed are likely to be less than the errors in obtaining samples of the total water content of the snowcover". Male and Granger (1978) support this view in stating that predicting losses from a patchy snowcover are especially problematic.

Although the processes of direct snowpack sublimation and evaporation are recognized, they are generally believed to promote only a small percentage of total snow disappearance. Additionally, most evaporation occurs *after* the production of meltwater, from exposed areas surrounding the snowcover. *This* loss may constitute a significant percentage of water disappearance in the badlands. Due to geographic location and thus a lower chinook frequency, however, it is reasonable to assume that losses are likely to be

less than those offered by Louie (1977) and Golding (1978). Evaporation losses may also be reduced by a spatial-temporal factor working in conjunction with impermeable materials and lack of vegetation. That is, runoff, facilitated by an impermeable ground surface and sparse amounts of infiltrating vegetation surfaces, may rapidly travel the relatively short distance to the watershed outlet before significant evaporation can occur.

2.3.2.3 Ground Heat Flux, Rain-On-Snow Events

On the prairies, ground heat flux, or that amount of sensible heat energy conducted from the ground to the overlying snowpack is generally regarded to be very small, having little affect on snowmelt production (U.S. Army Corps of Engineers, 1956; Bruce, 1962; Gray, 1970; O'Neill and Gray, 1971; Smith, 1974; Male, 1980; Male and Gray, 1981). Bruce (1962) contends that like evaporation, condensation may also offset snowmelt generated by this process. Rain-on-snow events, in which raindrops transfer sensible heat to the snowcover may cause considerable melt as well as increases in snowpack water content. However, these events are deemed rare in the southern prairies (Vershuren and Wojtiw, 1980), as most snow is already gone by the onset of the first spring rainstorm. Isoline data prepared by McKay and Thompson (1968) indicates that the mean date of final snow disappearance in the study area lies between the 11th and 21st of March.

The complex interactions of heat-energy parameters, along with initial snowfall variability and snow redistribution cause both temporally and spatially-diverse snowmelt rates and quantities. This in turn complicates the accurate measurement of snowpack characteristics and areal extent, information which is vital to the assessment of potential meltwater availability within a catchment. Nevertheless, previous research and field observations of snow accumulation and distribution patterns, and those factors most influential to snowmelt show the potential impact of meltwater on watershed runoff and geomorphology.

2.3.3 Snowmelt Runoff

Just as there are numerous variables which affect the amount and rates of snowmelt, there are many which influence both the amount and nature of watershed snowmelt runoff. Primary factors, drawn from many studies and descriptions of

snowmelt runoff are: 1. snow / water availability (quantity and location), 2. snowmelt rate (as governed by energy balance parameters), 3. landcover (vegetation extent), 4. topography (slope steepness), 5. ground surface and subsurface porosity and permeability, and 6. ground 'conditions' (frost or frozen soil presence). Since factors 3, 4 and 5 similarly influence the amount and nature of runoff under rainfall as well as snowmelt, the following discussion focuses on the relative importance of the three remaining variables.

Snow availability is obviously a prerequisite for spring runoff in that its presence must be sufficient to survive the effects of winter evaporation as well as the runoff-inhibiting characteristics of the remaining five variables. Even so, and as an extreme example, the combination of slow melt, dense vegetation, flat terrain, high soil porosity and permeability, and lack of frozen ground may easily inhibit appreciable spring runoff despite a seemingly adequate supply of snow. As mentioned earlier, the location of snowpacks or distribution pattern may control runoff source areas, but this also largely depends on the relationship between snowpack location and the other variables governing runoff susceptibility in these areas. For example, Gray *et al*. (1978) maintain that the magnitude of runoff generated from differing land cover classes in the prairies may appear completely opposite to that expected. That is, although considerably more snow may be retained by more densely-vegetated areas, these same areas typically generate much less snowmelt runoff.

The rate at which snow melts during winter and spring is significant to water production, and, as stated by Anderson (1972, p. 3) "...is the most important factor in determining the runoff from a snow cover". This statement is clearly evident in situations where very slow snowmelt allows ample evaporation and infiltration, and hence little runoff. Conversely, rapid melt induced perhaps by chinook conditions may cause infiltration and sorption capacitites of materials to be exceeded. Indeed, Ward (1975) maintains that chinooks may cause quick melt, leading to generous runoff production and streamflow hydrographs with peaks that are very similar to those observed during rainstorms. However, these examples also indicate that the runoff variables which influence material infiltration (i.e. porosity / permeability and ground conditions) are perhaps equally important to runoff production. In fact, Price *et al*. (1978, p. 265) claim:

"by far the most important control on the size and form of basin outflows is exercised by interactions at the soil surface".

Bengtsson (1982) points out the significance of ground conditions in his brief review of the two most widely held theories of snowmelt runoff. In one instance, slow melt leads to sustained infiltration (assuming ground materials are readily permeable), with most runoff derived by groundwater or subsurface flow. In the second case, the presence of frozen soil beneath the snowcover permits runoff as overland flow by restricting the permeability properties of the soil. Popov (1972) claims that previously well-moistened soil becomes virtually impermeable under temperatures of -2°C to -3°C. Bengtsson (1982) astutely remarks that depending on soil characteristics and climatic conditions (i.e. the timing of pre-freeze events), both theories may be correct. Thus, it appears that snowmelt rate, soil porosity / permeability and the thermal state of the near-surface ground at the time of melt are jointly and dependently responsible for controlling basin runoff efficiency during snowmelt.

The significance of ground frost and its affects on snowmelt runoff are increasingly recognized in the literature (Dreibelbis, 1949; Schiff and Dreibelbis, 1949; Gray, 1970; Dunne and Black, 1971; Landalls and Gill, 1972; Popov, 1972; Colbeck, 1974; Beven and Dunne, 1982), but as emphasized by Anderson (1978, p. 338), current snowmelt runoff models do not include considerations of the possible effects of frozen soil.

The presence of frozen soil produces unique effects on runoff patterns, and creates particular partial and variable area runoff patterns and hydrograph responses. In northeastern Vermont, Dunne and Black (1971) noted a widespread presence of 'concrete frost' (formed by mid-winter melt, percolation, and refreezing) to depths of 30 cm in the normally porous and permeable top soil.[1] They found large amounts of surface runoff emanating from a steep, snow-covered south-facing slope where slope angle permitted optimum solar radiation receipt, a favourable gravitational gradient, and concrete frost enhanced runoff by prohibiting infiltration.

Dunne and Black (1971) also found that the spatial extent of frozen soil was sufficient to allow uncharacteristically high quantities of overland flow. In fact, runoff

---

[1] As defined by Glossary of Geology (1980) concrete frost is "an extremely dense structure consisting of many thin ice lenses and small crystals".

data provided yields the extremely efficient runoff coefficient of 47.6%. Furthermore, they ascertained that freshly exposed concrete frost remained in a frozen state for approximately 24 hours, and that "the distribution and pattern of melting of this frost were of great significance in controlling the area that could contribute to surface runoff at any time" (p. 1170). This connection between differential melt and time-dependent, partial-area generation of overland flow is also discussed by Beven and Dunne (1982, p. 278) who also maintain that "the role of frost ....and the level of saturation of the soil are both important in governing the relative amounts of meltwater following fast surface and slow subsurface flow".

This variability in snowmelt escape methods may have a profound affect on the size and shape of the snowmelt hydrograph (Dunne and Black, 1971; Dunne, 1978; Bevan and Dunne, 1982). Through model testing of snowmelt runoff on simulated hillslopes that assumed similar ground conditions as those observed in Vermont by Dunne and Black (1971), Bevan and Dunne (1982) determined that peak discharge occurs very quickly and sharply after peak melt on slopes where frost presence prevents any subsurface flow. On the simulated plot displaying a mixture of ground frost and frost-free or thawed soils, peak runoff was fairly rapid, with smoother, yet distinct diurnal peaks. Similar results were obtained by Bengtsson (1982) through experimentation on simulated impervious plots. He contends that "discharge in a stream in a basin which is dominated by overland flow follows the diurnal snowmelt fluctuation and is high from the first day of snowmelt" (p. 157).

Dunne and Black (1971) also recognized a strong diurnal runoff pattern which closely followed the daily changes in temperature and especially short-wave radiation receipt. However, such rapid and sharply defined hydrograph peaks as those later predicted by the simulated experiments of Beven and Dunne (1982) were not strictly observed in the field due to the slight lag afforded by inter-snowpack water percolation and displacement as mainly determined by snow depth (Dunne and Black, 1971 ; Beven and Dunne, 1982). As seen through the work of these researchers, hydrograph response during snowmelt can often be closely linked to soil-snow interactions, with peak discharge and hydrograph shape altering with variations in flow routes as primarily determined by spatial frost extent and its rate of melt.

In the prairie environment, the relationship between frozen soil conditions and runoff is recognized in some snowmelt studies (Gray, 1970; Male and Granger, 1978), but is generally not considered to be a very important runoff factor. When asked if runoff appears on the prairies as a result of chinook activity, Gray (1970, "discussion") replied that appreciable runoff occurs when soil temperature is low, or when highly moist, frozen soils permit favorable runoff conditions. Male and Granger (1978) contend that melt begins in March or early April in the Bad Lake watershed in southern Saskatchewan, and that soils are typically frozen at this time. However, runoff here appears 3 to 4 days after initial melt begins due to surface ponding activity. Research in the Wascana Creek watershed near Regina, Saskatchewan (Gray *et al*., 1979) reveals a 3- to 4-day difference between peak runoff rates of flatlands *versus* gullies, with the latter areas contributing 36.2% more peak daily runoff than flatlands. The possible influence of frozen soil is not discussed in this study, nor by Gray *et al*. (1978) who stress that landcover is a major determinant of variations in prairie runoff generation. In their investigation of snowmelt recharge on short grass prairies in the U.S., Van Haveren and Striffler (1976) make no mention of frozen soil, and maintain (p. 56) that due to high annual water deficits and evapotranspiration, "runoff from snowmelt is rare, or at best is a very minor component of the hydrologic cycle".

These studies demonstrate that in the prairie environment, landcover (vegetation type and extent) and local topography are primary runoff-inhibiting factors, and that the presence of frozen soil may be of secondary importance. Although frost may preclude initial meltwater infiltration, the levelness displayed by a great portion of the prairie terrain is conducive to surficial meltwater ponding, resulting in slightly delayed and rather slow infiltration as opposed to widespread overland flow or other types of runoff. However, the opposite and virtually anomalous situation may be recognized in the badlands, where sparse vegetation and steep slopes are highly favourable to rapid and generous runoff.

In addition to vegetation and topography, the other primary runoff-determining factors of ground porosity / permeability, ground conditions, and snowmelt rate are highly advantageous to runoff production in the badlands. The impermeable nature of surface materials favours runoff, which may be enhanced further by the presence of frozen ground. Snowmelt rates are likely to be rapid (although spatially variable), during both

mid-winter and spring, due in part to an overall lack of surface shading by vegetation, and to high temperatures accompanying chinooks which accelerate melting by snowpack absorbtion of direct solar radiation.

Although the relationships between these runoff parameters can be complex and variable from one region or watershed to another, there appears to be some uniformity in snowmelt and runoff response from year to year within a particular catchment. This idea is strongly endorsed by Leaf (1971) who, working in three experimental forested basins in central Colorado, found that

> each watershed has a characteristic relationship between snowpack depletion and runoff that apparently does not change appreciably, even though the amount of snowpack and weather conditions which produce runoff each year vary considerably.

This statement is encouraging in that it provides support for the development of a theory on snowmelt runoff response in the badlands based on short-term field observations of snowmelt parameter relationships.

2.4 Badland Erosional Mechanisms and the Geomorphic Role of Snow

Once snow becomes meltwater, its effects on badland materials are, with few exceptions, virtually the same as those of rainfall runoff. Therefore, a review of badland erosional processes operating under rainfall conditions simultaneously illustrates some important aspects of snowmelt erosion. An appraisal of geomorphic processes unique to either rain or snow is also valid, as it may demonstrate a seasonal preference in the spatial application of moisture and hence erosion. In adddition, the *state* of the moisture (i.e. liquid water or solid ice) contained in near-surface materials may lead to seasonal fluctuations in erosion mechanisms and material response. These ideas are considered in accordance with past geomorphic research on the effects of rainfall and snow (and ice) in badlands. Pertinent studies from other regions are also included, as much information regarding the role of snow and ice is lacking in the badlands.

2.4.1 Badland Erosional Processes under Rainfall

Bryan and Campbell (1980) maintain that sediment movement during rainstorms in the Alberta badlands is primarily induced by surface and subsurface wash, rainsplash, rain-induced creep, slumping, and mudflows, though these processes vary according to

lithology. Sandstones are mainly subjected to degradation of the weathering rind by unconcentrated and concentrated surface wash, associated with runoff as overland flow as previously described. Bryan *et al*. (1978) show through the use of dye tracers that raindrop impact is also an effective agent of sediment entrainment. Field study on the role of raindrop impact and sheetwash on Alberta soils (Bryan, 1979) reveals that rainsplash may cause material degradation in areas upslope of those experiencing sheet flow, and that drop impact farther downslope can alter hydraulic flow patterns and reduce sheetflow velocity by creating local turbulence (Yoon and Wenzel, 1971; Bryan, 1979). Due to the highly dissected nature of most sandstones, Bryan *et al*. (1978) logically concluded that most material is removed by flow in rill channels. They also maintain that sediment yield per unit area is less on sandstones than claystones, but that threshold precipitation necessary to entrain sediment is lower (0.37 mm in 1 min. *verses* 4.75 mm in 10 mins.). Thus, sandstones experience a higher rate of surface erosion.

Schumm (1956) explains similar denudation processes operating on the sandstones of the Brule Formation in the White River badlands of South Dakota. He contends that rainwash, by which material is removed by sheets of flowing water, is the main erosional mechanism acting on these slopes. Akin to the findings of Bryan *et al*., 1978), Schumm (1956) surmises that slope erosion occurs twice as rapidly under rainwash than by processes deemed responsible for erosion of shale slopes (to be discussed).

Surface flow erosion is also recognized on claystone units of the Alberta badlands (Bryan *et al*., 1978), along with a variety of other entrainment mechanisms. Rainsplash is likewise considered an active process, and was seen to induce particle detachment by micro-slumping during simulated rainfall experiments (Bryan *et al*., 1978). It is interesting to note, however, that raindrop impact is a fairly inactive erosional agent on the badland shales of Israel (Yair *et al*., 1980). There,

> the high stability of the clay aggregates, which do not disperse easily under the impact of raindrops, contributes also to the low rate of erosion by minimizing the effect of rainsplash which is usually an important agent in both sealing the surface and providing detached particles... (p. 223).

The apparent higher stability or anti-dispersing quality of the clay aggregates of the Taqiya shales *versus* the Oldman claystones is attributed to the strong flocculation properties possessed by the clumps as well as the limited swelling capability described earlier. On shales, most sediment is derived from surface depressions, in which particle

dispersement through water immersion (liquefaction) provides material for removal via channel or mudflows.

As noted by Hodges and Bryan (1982) rainsplash is an erosional mechanism solely recognized during rainfall and its effects are therefore minimal during winter. Quantitative estimates of rainsplash erosion are difficult to obtain however, and compounding this problem is a lack of research (and methodology) dealing with the possible seasonal implications of this time-varying process. In addition, the situation may be further obscured by the presence of a seasonal "counterpart" to rainsplash; that is -- mechanical abrasion or *corrasion* by wind-driven snow particles. Beaty (1975) invokes the idea of corrasion by post-glacial, wind-directed rainfall and snowfall to explain initial formation and alignment of coulees and gullies developed in Late Cretaceous sandstones and shales of southern Alberta. However, it is questionable whether the possible effects of snow particle erosion are comparable in magnitude to rainsplash, or even significant at all in the badlands.

Studies conducted by Heim (1885, in Teichert, 1939) and Bird (1967, in French, 1976) reveal that ice / snow particle hardness attains an approximate value of 6 on the Moh's scale at a temperature of -50°C. Blackwelder (1940) found the same hardness value at -78.5°C, and states "...if....at low temperatures its hardness rises to 5 or 6, ice is then hard enough to abrade limestone, shale, and many other common rocks..." (p. 62). Support of the corrasive powers of snow is given by Teichert (1939) in his discovery of abrasion features on sandstone in Greenland. He attributes their formation to snow corrasion or abrasion by "very small quantities of dust" but not to blowing soil particles due to the absence of land upwind of the prevailing wind direction. French (1976) also backs the effectiveness of snow corrasion by maintaining that most wind erosion occurring in high latitudes is accomplished by snow particles.

However, there is no evidence to suggest that snow abrasion occurs in places other than high latitude regions where temperatures are low, snow particle hardness is at its maximum, and expansive treeless plains permit strong winds throughout typically long winter seasons. Koch and Wegner (1930, in Teichert, 1939) estimate ice hardness at between 2 and 3 at a temperature of -15°C. It seems valid to assume on this basis, and from the above statement made by Blackwelder (1940), that its corrasive ability is

negligible on most rocks at winter temperatures commonly experienced in southern Alberta. Both Embleton and King (1975) and Thorn (1979) maintain that blowing snow is an inert geomorphic process unless accompanied by very low temperatures. Beaty (1975) shows that post-glacial and current prevailing winds in southwestern Alberta were and are from the southwest, as a direct result of chinook activity. It appears highly doubtful that these *warm* winds could permit such low temperatures needed for snow crystals to initiate aligned bedrock furrows, although the action of wind-driven rainfall, as also suggested by Beaty (1975) may be a feasible cause. It should be mentioned that Beaty's proposition of subsequent enlargement of these gullies by runoff from rain and snowmelt from preferentially-distributed snow drifts within these gullies is an acceptable and highly probable means of surface denudation. Snow corrasion however, must be of little significance to winter erosion in the badlands.

In the Alberta badlands, surface slumping and mudflows are considered dominant sediment movement processes and the major causes of slope retreat on claystone units (Bryan *et al*., 1978 ; Bryan and Campbell, 1980). Under simulated rainfall experiments (Bryan *et al*., 1978), active slumping of a convex interfluve was observed, followed by a viscous mudflow. According to Bryan *et al*. (1978), slumping on both gentle and steep claystone slopes results from rainwater percolation through the regolith to the underlying dense crustal layer, where water concentration or lateral flow creates positive pore water pressures, decreased material strength, and finally, a slump, with slip plane located at the junction between the surface material and crust. The slump is often followed by a mudflow, and micro-slumping of the slump scar headwall is also an active process.

Schumm (1956) maintains that creep due to gravity and alternating wet and dry sequences is the dominant erosional process occurring on the shale slope of the Chadron Formation in the South Dakota badlands. Upon applying water to shale slopes with a hand pump, Schumm (1956) observed a downslope sliding and micro-slumping of individual clay aggregates, triggered by swelling and softening activity. A continuous cycle of hydration and dehydration thereby allows aggregates and smaller particles to slowly traverse down an entire slope surface. Schumm also suggests sediment movement by upslope filling of desiccation cracks, rainbeat, as well as slumping activity. Although rain-induced creep is also recognized on claystone slopes in the Alberta badlands, Bryan *et al*. (1978) and Bryan

and Campbell (1980) assert that major sediment contribution is afforded by slumps and mudflows, and that these processes are much more important than either rainsplash or creep, provided a particular threshold value of precipitation is reached.

Apart from rainsplash, all the above-mentioned erosional mechanisms may conceivably operate under snowmelt as well as rainfall, provided there is an adequate moisture supply and it is favourably distributed within the watershed. Another denudational mechanism assumed common to rainfall and snowmelt is the fluvial undermining of slopes by primary channel flows. Essentially, this form of erosion is similar to that operating during concentrated rill flow, with the main difference being one of scale. The creation of erosional niches by fluvial undercutting occurs ephemerally along many higher order (i.e. primary, secondary, and tertiary) drainage channels of the watershed, and quite often leads to mass movement in the form of catastrophic slope collapse. Undermining in itself may lead to slope failure by reducing basal slope support and thereby optimizing the affects of gravity. Or, as witnessed in the field during a November 1981 rain shower, collapse of the undercut slope may be enhanced by the material strength reduction also afforded by rainwater infiltration and sorption processes (Figures 2.3 and 2.4).

2.4.2 The Role of Freeze - Thaw

The most questionable erosional processes operating in the badlands during the cold season are those of freeze-thaw weathering, including creep induced by frost heave and needle ice growth, and frost shattering of rocks. The latter process in particular is in question due in part to the fact that the mechanism(s) involved in material disruption is not clearly understood or agreed upon, and lacks "definitive verification" (Thorn, 1979; 1982). Thorn and Hall (1980) and Thorn (1982) maintain that the failure to design laboratory tests which can isolate and define a specific process rather than multiple processes, and the failure to consider natural conditions also confuses the understanding of freeze-thaw weathering. Compounding this situation is the fact that the role of freeze-thaw in semiarid areas is typically considered through inference and speculation, with limited in-field observation. With these inadequacies in mind, a summary of some of the processes thought to operate under freeze-thaw is nonetheless given, along with theories on its

Figure 2.3. Slope failure on a claystone slope unit. Collapse was triggered by fluvial undermining and material saturation during a November, 1981 rainstorm (photographed one month later).

Figure 2.4. Relict collapse scar in a sandstone unit of a lithologically-integrated slope.

function in the badlands and other semiarid areas.

2.4.2.1 Frost Heave and Needle Ice Formation

According to the Dictionary of Geological Terms (1976), frost heaving is "the lifting of a surface by the internal action of frost". More specifically, Miller (1980, p. 286) states, "if soil expands when it freezes, this volume change is called frost heave". Past experiments have established that water expands by approximately 9% upon freezing to ice, and most researchers readily deploy this axiom to explain soil disturbance observed during cold weather.

It is commonly held that soil disturbance or expansion occurs upon the freezing of water into ice crystals, veins, or lenses, which occupy void spaces between particles or groups of particles. It is said that ice growth occurs not only in pre-existing voids, but aids in the creation of new ones. This assertion is made by Miller (1980) who insists that ice-filled cracks are not simply cracks that have become ice-filled, but rather, cracks created by ice intrusion. Support is given by Hillel (1980) who maintains that expanding ice creates cavities (ice-filled) which are capable of compressing and separating soil aggregates. Miller (1980) further contends that the net heave of a soil represents the volumetric expansion of all the ice forms contained in the soil.

There are several conditions which control the occurrence and extent of soil ice formation and frost heave. Early laboratory experiments conducted by Taber (1929) led to the currently-standing conclusion that subsurface ice growth depends on: 1. the amount of water available, 2. particle grain size, 3. size and percentage of voids present, and 4. rate of cooling. It is a widely held conception that subsurface ice vein and lens formation proceeds as water from below is drawn by capillary flow into a downward-migrating freezing zone (Williams, 1957; Dirksen and Miller, 1966; Baver *et al*., 1972; Miller, 1980; and others). For ice crystal growth, water is drawn from surrounding particles to ice growth centres (Baver, 1956; Baver *et al*., 1972). A limited water supply (requirement #1) necessarily restricts the magnitude of ice growth.

Factors 2 and 3 are especially critical to soil heaving, as they largely determine capillary conductivity and thus the frost susceptibility of a given soil. Baver *et al*. (1972) assert that water flow to the freezing front is facilitated with an increase in capillary conductivity, and that the formation of ice layers is therefore more pronounced in soils

coarser than clays. However, soils which are too coarse, that possess large pore spaces, may preclude capillary flow. Thus Miller (1980; and others) maintains that the heave effects of freezing are fairly minor in gravels and coarse sands. By the same token, very fine-grained soil or rocks with very small voids may also restrict or prevent water migration and may greatly reduce or even prohibit the freezing of water already situated in these voids (Taber, 1929; Hudec, 1973).

If flow and freezing are permitted, colloidal soils often develop networks of ice-filled cracks dispersed among consolidated pockets of ice-free soil (Miller, 1980). However, free ice, in the form of crystals, veins, and lenses may not appear, or may give way to the formation of a homogeneous frozen soil if the soil is below capillary saturation (Beskow, 1935 in Williams, 1957; Schumm, 1964). Support of this view is given by Dirksen and Miller (1966) who found that heaving of frost susceptible soils occurred when the saturation level of soil pores just behind the freezing front reached approximately 90 percent. The consensus among most researchers is adequately summed up by Meentemeyer and Zippin (1981, p. 114) who state that "...soil must be neither too fine to retard the flow of water to the freezing plane nor too coarse to impede capillary [flow]". On this premise, Miller (1980, p. 288) contends that "under favourable conditions, freezing of soils comprised of particles in the size range of silts and coarse (noncolloidal) clay can produce phenomenal heaves".

The rate at which freezing occurs (requirement #4) also largely determines whether or not free ice forms can develop in frost susceptible soils. Baver *et al*. (1972) maintain that large ice crystals can form in tension-free pore spaces of soils when cooling is slow. Likewise, Hillel (1980) comments that the magnitude of ice cavity growth tends to increase with a decrease in cooling speed. Conversely, rapid cooling, like the freezing of unsaturated soils, may preclude the formation of free ice and merely result in the solidification of pore water into a densely-frozen soil mass (Beskow, 1935, in Williams, 1957; Schumm, 1964). Meentemeyer and Zippin (1981) also stress the importance of slow freezing to the growth of needle ice. Called "pipkrake", these small (2 - 6 cm) surface ice pillars require similar growth conditions as other subsurface free ice forms.

The geomorphic impact of frost heaving and needle ice growth varies, depending on the ice content of the soil, and is usually seen after thaw or a number of freeze-thaw

cycles has occurred. Just as soil ice is thought to cause surface upheaval in a direction normal to the original slope profile, needle ice grows in the same direction, and lifts attached soil particles along the crystal stalk and tip. Because of cohesive forces, material or individual particles raised normal to a slope surface are thought, upon thaw, to be redeposited downslope along the line bisecting the angle formed between the vertical drop and the perpendicular path taken above the original slope surface. This essentially, is the slow, almost imperceptible process of frost creep. In alpine, high arctic / periglacial regions, the melt-out of characteristically high contents of ground ice or abundant needle ice often leads to a severe loss of soil strength and ensuing mass wasting by solifluction or more rapidly-moving mudflows.

In areas where soil ice is not widespread or volumetrically large, but where some degree of frost heaving occurs, geomorphic significance is often placed on the slower mechanism of frost creep, as just described. Such is the case in the frost susceptible soils of more arid climates, as illustrated by the work of Schumm and Lusby (1963) and Schumm (1964). These studies report that differences in erosion rates and material response on the Mancos shale slopes of Colorado are largely due to seasonal alternations of effective erosional processes. Whereas summer rainfall causes surface compaction of slope materials by rainbeat and degradation by rainwash and a small degree of rain-induced creep, winter frost heave is believed to aid in surface loosening and the break-up of soil aggregates, as well as downslope soil movement by frost creep.

Although no mid-winter observations were made during the four year study period, small granular ice crystals were seen during late winter within the weathered, silty-clay loam soils overlying the Mancos shale bedrock. Stakes implanted in selected hillslopes generally showed a seasonal fluctuation in the elevation of these surfaces (Schumm and Lusby, 1963; Schumm, 1964). However, there was no detectable net exposure of stakes during the study period, but the placement of small, unanchored markers onto the slopes revealed significant downslope movement, which was mainly attributed to several cycles of freeze-thaw (surface frost creep). Schumm (1964) reports the average rate of creep on a 34° slope to be 1.8 cm yr^{-1}, and 11.3 cm yr^{-1} on a steep, 82° slope. He remarks (p. 231) that these rates are extremely high, surpassing measurements obtained by others in humid regions, and that (p. 235) the results of the

study suggest that a re-evaluation of the role of frost action in arid and semiarid areas should be made.

Plot studies undertaken on claystone and pediments in the Dinosaur badlands led Campbell (1974; 1981) to deduce that frost heave is a dominant winter erosional process in the area. Campbell monitored surface changes over a 10-year period on nine, 1 m^2 plots with the use of a lightweight metal fame and 25 removable erosion pins (see Campbell, 1974 for equipment details). Twice annual measurements (in April or May, and October) during the first 5-year period of study generally showed a seasonal cycle of surface uplift, similar to that described by Schumm (1964). No winter visits to the field were made, nor was surface or subsurface ice observed, but Campbell (1974) concludes from data obtained that this seasonal trend is due to the effects of frost heave. Campbell (1981) maintains that winter frost heave and summer slope wash are the two dominant denudational mechanisms acting on slopes of the Alberta badlands. Together, these processes accounted for a mean annual surface lowering of 3.8 mm yr^{-1} on the seven of nine plots which showed net degradation (Campbell, 1981).

Denudation studies have also been conducted on slopes developed in the Oldman Formation in the One Four badlands of extreme southern Alberta. Although no evidence or elaboration is given, Barendregt and Ongley (1979, p. 228) maintain that these slopes are "affected by freeze-thaw action", and that snowmelt "conditions" (referring presumably to runoff) are limited due to the decrease in effective moisture brought on by chinooks.

An important consideration to the effects of frost heave as surmised by Schumm and Lusby (1963), Schumm (1964), Campbell (1974), and Campbell (1981), is the role it plays in the loosening and subsequent removal of surface materials. Both Schumm (1964) and Campbell (1974) contend that frost heave causes soil/regolith disaggregation. Schumm and Lusby (1963) and Schumm (1964) cite the work of Baver (1956) to explain this loosening process by the transfer of moisture from surrounding soil particles to ice crystal growth centres situated in soil pore spaces. Citing Baver (1956), Schumm and Lusby (1963, p. 3660) and Schumm (1964, p. 222) maintain that "this growth of ice crystals...and the simultaneous drying of adjacent soil causes cracking and loosening of the dry soil". Baver *et al*. (1972) mention that freeze-thaw and wetting/drying act similarly to produce soil disaggregation. In addition, both Hillel (1980) and Miller (1980)

support the view that these processes operate in an analogous manner, as they both involve the transfer of water away from certain areas of the soil. Hence, Schumm's contention that soil loosening due to ice expansion and soil shrinkage through frost-induced dehydration is well founded.

Campbell (1974) does not elaborate on the precise mechanism(s) by which surface loosening during frost heave operates, but goes on to say (p. 135) that material produced is subsequently removed from slopes during the summer rainstorm period. The statement made by Campbell and Honsaker (1982, p. 74) that "...spring runoff from the melting of accumulated winter snow may contribute to a small amount of erosion" appears to lend support to the assumption that frost-disturbed materials are more effectively disposed of during rainstorms. Hogg (1978 , p. 127) asserts that during winter, certain slopes in the Alberta badlands "...may be active due to freeze-thaw activity and shrink-swell phenomena...", and that the primary role of snowmelt may be to "...flush out accumulated debris in the spring causing high sediment yields during the melt season". Schumm and Lusby (1963) and Schumm (1964) also suspect that initial spring rainfalls cause high sediment yields, as a result of the re-establishment of rill channels previously obliterated and clogged with frost-heaved soil aggregates. Although the composition of the Mancos shales and Oldman claystones are not quite alike and are apparently subject to slightly differing summertime erosion and removal processes, there is unanimous agreement that some degree of material disturbance takes place during winter as a result of frost heave in these semiarid regions.

2.4.2.2 Frost Shattering

Other than the process of frost heave, there is little mention of the role that snow may play in the mechanical breakage or frost shattering of badland (or semiarid) rock materials. A consideration of this subject is warranted, as the Alberta badlands display other rock forms (e.g. sandstones, compact claystones, and ironstones) which may not be susceptible to frost heave, but which may be subjected to other forms of freeze-thaw weathering. Although no monitoring of freeze-thaw processes was undertaken in this study, field observations will nonetheless provide useful information to future research on this topic.

Similar to the mechanism of frost heave, it is widely held that frost shattering of rocks occurs as a consequence of ice expansion or ice crystal growth in rock pore spaces. Thorn (1979) and Thorn and Hall (1980) review several theories of frost shattering as proposed by other researchers. Connell and Tombs (1971) maintain that rock disintegration progresses as the growth of oriented crystals exerts pressure in specific places within a rock even though there may be free spaces for potential ice growth left unoccupied. The work of Hudec (1973) lends credibility to the notion that rock shattering may actually be, in some cases, the work of hydration and dehydration rather than freeze-thaw. Supported by White (1976), Hudec (1973) claims that in some 'sorption sensitive' rocks, water filling rock interstices may exert sufficient pressure against side walls to cause expansion of pore spaces. Although drying releases this pressure, these spaces do not respond by contracting, but remain enlarged. Repeated cycles of hydration and dehydration eventually lead to rock breakage due to tensional fatigue. However, Hudec (1973, p. 33) maintains that freeze-thaw shattering is a viable process in many rocks; that is, in those which are not "purely sorption sensitive" or so completely sound that no water may penetrate them. Thorn and Hall (1980 , p. 115) conclude that "domination by one process or the other is primarily dependent upon pore size and its distribution within the bedrock".

For purposes of this review, it is assumed for the moment that rock shattering by any of the ice-related theories described above is a valid process. On this assumption, Thorn and Hall (1980) cite two fundamental controls that limit freeze-thaw weathering and determine the frost heave; the first, and deemed most important, is bedrock porosity, for rocks must be able to absorb water to a certain extent before freeze-thaw can operate. The second control is the location of meltwater as mainly determined by snowpack distribution, as ultimately controlled by winter wind patterns (Thorn and Hall, 1980).

Once a favourable combination of these controls is established in a given area, Thorn and Hall (1980) maintain that the intensity of the freeze-thaw permitted is dependent upon the interplay among the amplitude of bedrock freezing, the degree of heat insulation afforded by the overlying snowpack, and total direct solar radiation reaching the ground. With regard to amplitude, Thorn (1979) and Thorn and Hall (1980) cite several minimum bedrock temperature requirements as suggested by other authors, most of which range

between -4°C and -10°C. It is also mentioned that many researchers (e.g., Tricart, 1956; Wiman, 1963; Martini, 1967; Potts, 1970) also prescribe temperature variation frequency (i.e., number of fluctuations above and below freezing) as well as rate of freezing (e.g. Wiman, 1963) as important determinants of rock shattering, in addition or in place of a minimum amplitude requirement.

Thorn and Hall (1980) compiled a listing of some freeze-thaw requirements and observations as presented in twelve "widely cited research papers". Of these works, five contend that frost weathering is limited beneath snowpacks due to a restriction in temperature amplitudes as caused by insulating effects and lack of solar radiation penetration. Two maintain that frost shattering does occur, and the remaining five make no reference to the question. Thorn and Hall (1980) themselves found that moderate to deep snow accumulation provides sufficient insulation to prohibit or minimize the freezing amplitude of the underlying bedrock. In fact, they found this to be true at both snow patch sites monitored in northern Norway, where diurnal variations in bedrock temperatures below snowpacks were severly restricted.

This leads to the consideration of the role of frost shattering in those areas susceptible to snow accumulation and hence most commonly associated with the process -- slope base headwalls (basal niches) of surface hollows, and areas immediately downslope or around the periphery of snowpacks. Most are familiar with the concept of mechanical freeze-thaw weathering of surface hollows (also called nivation hollows) and cirque headwalls. For the latter feature, it is basically believed that bergschrunds allow meltwater to penetrate the bedrock of the headwall, where the absence of a snow/rock contact also permits a sufficient diurnal temperature variation for freeze-thaw operation. For slope base headwall and basal notch formation, an adequate temperature fluctuation is permitted by the creation of a gap (mini-bergschrund) by means of radiation heating of exposed rock above the contact area (Lewis, 1939), and subsequent melting of the interface snow presumably by heat conduction. There is, however, very little substantiation of this activity, and as noted by Thorn (1979; 1982), actual measurements of diurnal bedrock temperature fluctuations are few.

Gardner (1969) monitored bedrock temperatures at two snowpatch sites near the Lake Louise district of the Canadian Rocky Mountains. Thermisters were placed in the

bedrock headwall, inside a basal notch, just above the snow/rock interface. Among other measurements taken were the number of 'frost alternation days', whereby one crossing above the 0°C base temperature in one 24-hour period was considered one frost alternation day. Over the entire 27-day summer measurement period, 3 frost alternation days were recorded in the headwall bedrock at a north-facing snowpatch site, and only one at the south-facing site. However, Gardner (1969) witnessed, at least on one occasion, the dripping and refreezing of meltwater onto the headwall notch. Despite admittedly little evidence, Gardner maintains that those basal notches formed in limestone and dolomite of the vicinity, that do not have an apparent structural or lithological origin are probably formed by intense frost action, with the possibility of a chemical solution origin.

Thermistor monitoring of bedrock basal niches was also undertaken by Thorn and Hall (1980), who also found that these areas experienced neither a high freezing frequency, nor amplitude, due mainly to the effects of snow insulation. This was discovered despite previous claims that slope breaks or basal niches are subject to optimum freeze-thaw conditions. Based on these results and on the fact that these niche/headwall areas contain an ample supply of moisture upon melt, Thorn and Hall (1980) cautiously but firmly propose that mechanical rock shattering of these features may actually depend on hydration-dehydration cycles or salt weathering rather than freeze-thaw processes. Given this hypothesis, one might assume that the most important aspect of snow with respect to its mechanical erosion capability is merely its locational distribution and reservoir of potential meltwater, with little regard for possible climatic limitations and the varied and detailed requirements associated with freeze-thaw weathering.

All twelve references cited by Thorn and Hall (1980) claim, provided other requirements are met, that freeze-thaw weathering takes its most significant effect around the margins of snowpacks, or, as termed by Lewis (1939), "zones of maximum destruction". In these areas, snowpack insulation is nil, bedrock temperatures are free to fluctuate, and moisture is in adequate supply. However, verification of freeze-thaw shattering in these areas is still inconclusive, due in part to lack of a strict definition of freeze-thaw requirements. This is exemplified by the work of Gardner (1969) who also

monitored bedrock temperatures at snowpatch peripheries. He found that freeze-thaw events occurred more frequently at snowpatch edges than at the headwall sites, but that (p. 120) "although a number of frost alternations occurred in the peripheral zone, the magnitude and rate of freezing did not reach the minimum levels for frost shattering that have been presented in the literature". On the basis of morphological evidence (i.e. the presence of mechanical weathering debris) and snowpack location, Gardner (1969) nonetheless concludes that frost shattering is an active process in the area.

From this discussion on frost shattering, it is evident that its presence and effectiveness is extremely difficult to assess. Therefore, its precise role in the badlands, as in other areas, remains in question. However, field observations of snow patterns and ice formation (to be discussed) will at least assist the understanding of frost shattering in the badlands, from the viewpoint of identifying those areas which should be most susceptible to this process.

2.4.3 Slope Orientation and Snow Distribution Relationships and Their Effects on Badland Erosional Regimes

The significance of slope orientation as related to infiltration, runoff, and erosion is a highly debated topic, and its role has been considered in just about every climatic region. Attempts to isolate the microclimatic importance of slope aspect are widely undertaken in areas where its influence is though to be a key factor in determining differential morphological evolution of a landscape. Arid lands are a prime example because, as pointed out by Churchill (1981, p. 377), "topoclimatic differences may be more pronounced in areas of moisture deficiency where aspect-induced differences in moisture conditions are likely more critical than they would be in areas of abundant moisture". This assertion is likely even more crucial in badlands, where wide variations in slope angle and exposure typically occur with an extremely high spatial frequency.

The relative importance of slope aspect in the Alberta badlands may depend upon two major climatological considerations, both of which may infer the existence of a preferentially-oriented weathering regime. The first consideration is the relationship between solar radiation receipt and slope moisture characteristics under rainfall, from which an understanding of runoff and erosion response can be gained. The second

involves defining these responses as basically influenced by the same relationship, but with the added complexity of considering moisture regime variations as possibly determined by snow distribution and perhaps by wind-induced preferential distribution. As the geomorphic and hydrologic influences of aspect variations are generally regarded to be important in badlands (Yair, *et al*., 1980; Churchill, 1981; Yair and Lavee, 1982), both considerations are explored in this section with reference to past research, and again in Chapter 4 through field observations.

Slope orientation is often invoked to explain local variations in slope form (e.g. the existence of asymmetric valleys) as seen through differential behaviour of slope materials, erosion processes, and erosion rates. The relative importance of aspect is a function of the interrelated factors of insolation receipt, evapotranspiration (or evaporation), and extent of vegetation cover, all of which influence infiltration, soil aggregate and slope stability, and thus erosion susceptibility of a given slope. Although most researchers agree that these factors determine the significance of aspect, they disagree on the eventual effects of these factors. This may be due in part to a differing degree of influence of one variable over another, which is easily recognized between different climatic regions. An example is pointed out by Spence (1972), whereby several researchers (Putnam and Sharp, 1940; Walker, 1948; Melton, 1960) stress the role of vegetation to the maintenance of steep slopes by reducing surface erosion and adding stability to the soil by root growth. In arid areas, however, vegetation growth may still be a factor, but its importance as compared to other aspect variables may be drastically reduced.

As suggested by this example, the most common debate among researchers entails the question of which slope orientation typically displays a steeper slope gradient, and why. Examination of the literature reveals a fair number of advocates for a steeper north-facing slope (e.g., Emery, 1947; Hack and Goodlett, 1960; Hadley, 1961); a steeper south-facing slope (e.g., Russell, 1931; Von Engeln, 1942; Budel, 1953; Spence, 1972; Toy, 1977; Churchill, 1981); and at least one claiming there is no aspect-induced difference (Strahler, 1950). Depending on the degree of influence of a given variable, all theories may be correct, and despite the disparity, there is strong agreement that south-facing slopes in arid areas retain the steepest slope angles (Von Engeln, 1942;

Spence, 1972; Toy, 1977; Churchill, 1981). Support for this claim is given on the basis that south slopes in many parts of the northern hemisphere receive more direct insolation, and hence have higher evaporation rates. These drier surfaces are not as susceptible as north slopes to gradient reduction by such processes as soil creep, slumping, or mudflows (Spence, 1972; Churchill, 1981).

Spence (1972) studied glacial hummocks in semiarid south-central Alberta and found that south slopes are significantly steeper than those facing north. He attributes this to probable soil creep activity on north and west slopes, which, due to an increased vegetation cover, favours high infiltration capacities, moisture retention, and a lower soil strength.

Churchill (1981) examined 45 north- and south-facing shale slopes in the badlands of South Dakota and found that north slopes retain higher moisture levels for longer time periods due to decreased solar radiation receipt. He also discovered these slopes experienced deeper penetration of the wetting front. These observations, plus abundant slump scars, led Churchill (1981) to conclude that saturation of regolith materials occurs more frequently on north slopes, which are thus more susceptible to slope reduction by slumping, mudflows, and fluvial erosion by overland flow. In contrast, Churchill (1981) maintains that steep south-facing slopes are more prone to denudation by small 'rockfalls', initiated by intense desiccation processes associated with hydration-dehydration cycles, as well as perhaps by freeze-thaw activity. Absence of slump scars and the presence of transient debris accumulations at slope bases indirectly attests to this means of degradation (Churchill, 1981).

Churchill (1981) futher maintains that south slopes possess a higher infiltration capacity, but do not retain as much moisture as north slopes because of slope steepness, which reduces rainwater interception and infiltration by enhancing quick runoff disposal via overland flow. However, based on the works of Horton (1945) and Smith and Wischmeier (1957), Churchill (1981) claims that the erosive force exerted by flow on south slopes is not great as compared to that experienced on north slopes, the latter of which in addition to abundant mass movement scars, display a higher degree of rill dissection.

Plot studies undertaken in the Negev desert shale badlands of Israel by Yair and Lavee (1982) reveal similar findings to those of Churchill (1981). On slopes that differ only in orientation, Yair and Lavee (1982) determined that runoff response on north-facing slopes is much quicker than on south slopes. This is also attributed to the differing moisture regimes as affected by insolation receipt, which cause variations in surface material properties and infiltration characteristics (Yair *et al.*, 1980; Yair and Lavee, 1982). It was found that north slopes generally exhibit a thick (20 - 30 cm), broken regolith which, unlike the thin and highly desiccated crust mantling south slopes, displays both a low initial and terminal infiltration rate. Simulated rainfall experiments revealed an 11-minute lag time for south slopes, whereas north slopes yielded runoff in less than half that time (5 minutes). Therefore, Yair and Lavee (1982) conclude that the frequency and magnitude of runoff events is much higher on north slopes than on south slopes. In conjunction, they contend that no runoff contribution should be expected from south slopes during most rainstorms, due to the typically short duration of such storms, and because these slopes display high infiltration rates for extended periods. These results indicate the existence of an aspect-related partial area contribution to runoff (Yair and Lavee, 1982), and, although not specifically mentioned, may imply that sediment removal is more efficient on north slopes.

Toy (1977) compared morphologies of south-facing slopes between several humid and arid areas in the U.S. All 29 slopes examined were developed in marine shales with a structural dip of 3° or less. Toy (1977) concludes that arid land south slopes are steeper, shorter, and that convex segments display a smaller radius of curvature than those in humid regions. Again, this observation is accountable to the extreme lack of moisture on southern slopes of arid regions, as well as the characteristic regional sparseness of the vegetation cover.

As shown, none of the semiarid or arid land studies cited consider the possible geomorphic effects of snow. Moreover, these aspect investigations make no mention of any existing relationship(s) among snowmelt moisture input, solar radiation receipt, and preferential slope steepness. This is to be expected in the Israeli badlands where snow is rare, but is unfortunate in the South Dakota badlands, where winter temperatures are typically low and precipitation is sufficient to permit an estimated annual snowfall

accumulation of approximately 60 cm (estimated by Engelen, 1973).

One possible reason for the omission of commentary by Churchill (1981) on the role of snow in the South Dakota badlands may be linked to the difficulty of separating the degree to which snowfall *versus* rainfall contributes to variations in slope aspect. That is, without the use of meteorological data and in-field observations of snow accumulation and distribution, slope measurements alone (which are *indirect* process measurements) cannot differentiate between the importance of the affects of snowmelt moisture input and that of rainfall on slope form.

Another reason for the lack of elaboration on the relationship between snow and slope form may be due the probable minor role snow plays as a supplier of moisture as compared to rainfall. Although it is acknowledged that water supplied by rainfall is more significant (because of its higher magnitude and frequency) than snowfall to any aspect relationships that may exist in the Alberta badlands, and presumably in those of South Dakota, the role of snow as an additional and perhaps preferential source of moisture should not be ignored or discounted in the overall evaluation of this relationship.

Due to the lack of consideration of the possible geomorphic effects of snow, it is necessary to present some research from other climatic regions which may prove relevant to snow distribution and aspect relations in the badlands. Observations of asymmetric valleys in the Caribou Hills (68°N) periglacial region of the Northwest Territories (Kennedy and Melton, 1972) show that north-facing valley slopes are generally lower-angled relative to south slopes, but that they are steepened in many areas due to basal undercutting by stream action and "nivation" activity instigated by snowpatches which tend to remain at slope basal positions for longer durations (Kennedy and Melton, 1972). It is pertinant to note that creep is considered the dominant erosional mechanism operating on north-facing valley sides in downstream areas, where stream flow and basal undercutting is at a minimum. Thus, these slopes maintain lesser gradients than the south-facing slopes of the same area, which receive more insolation, are drier, and erode primarily through rill wash and gullying (Kennedy and Melton, 1972).

French (1976) describes asymmetric valley formation farther north (74°N), on the Beaufort Plains of Banks Island in the Canadian Arctic. Due to the extreme latitudinal location of the study area, French (1976) stresses that aspect-induced differences in solar

radiation receipt are of minimal significance to geomorphic evolution, and that observed slope variations are caused by preferential snow distribution and the desiccating effects of prevailing summer winds. He noted that west- and southwest-facing stream valley banks are steep and intensely gullied, whereas east and northeast slopes are gentle and shingled by solifluction lobes. It is maintained that prevailing westerly winds deposit snow onto easterly-oriented valley lees, where abundant mositure permits nivation and active solifluction throughout the long summer melt season. In contrast, the windward-oriented west and southwest slopes are swept clear of snow (except within gullies) in winter, and subjected to high, wind-induced evaporation in summer, which aids in maintaining these steeper slopes. Stream undercutting is also deemed an important denudation process, in that it preferentially operates on valley sides which generate the least amount of material, and therefore tends to undercut and further steepen the drier, solifluction-free, windward-facing slopes (French, 1976).

The asymmetric valley hypothesis as described by French (1976) is strikingly similar to theories proposed by Beaty to account for the preferential alignment and location of coulees (1975) and the geographical distribution of post-glacial slumps (1972) along river banks and other topographic features of semiarid southern Alberta. More important than the initiation or preferential axial alignment of coulees and gullies as previously noted, is the contention made by Beaty (1975) that clusters of these features appear almost exclusively on southwest- and west-facing, windward slopes. In conjunction, Beaty (1972) found that 87% of the 124 slumps examined, which are developed primarily in overburden material as well as bedrock shales of the Oldman and Bearpaw Formations, appear on slopes with a north, northeast, east, or southeast exposure. According to Beaty (1972), the tendency towards slumping activity on these slopes is caused by preferential moisture availability afforded by 1. southwesterly and westerly chinook winds which redistribute snow onto northeasterly slopes, and 2. reduced effective insolation receipt and hence decreased evapotranspiration.

Except for Beaty's inclusion of significant solar radiation influences, and French's observations of fluvial undermining activity, geomorphic response on slopes of these two areas is remarkably parallel, and demonstrates the highly significant role of preferential snow distribution. Thorn (1979, p. 227) also stresses the existence of oriented erosional

regimes as determined by preferential snow distribution, and, citing the work conducted by Benedict (1970) in Colorado, contends that "...paleo-winds are known to have had different orientations..., thus reorienting the weathering regime".

Early support for the existence of preferentially-occurring weathering regimes is given by Russell (1931) who examined asymmetrical slope evolution in the humid landscapes of eastern New Jersey and southern Ohio. Russell (1931, p. 484) discards many of the physical factors possibly governing slope asymmetry to conclude that "...the greatest single effect is with reference to snow cover". More specifically, Russell (1931) maintains that slope aspect permits snow to remain on north-facing slopes for longer periods of time, thus protecting these slopes from mid-winter denudation. Upon melt however, the relatively higher available moisture serves to rapidly attack and reduce the gradient of north slopes, thus causing the observed asymmetry.

From this discussion on geomorphic process in badlands, and through relevant research provided from other areas, it appears that winter and early spring erosional response in the Dinosaur badlands likely depends on a complex set of physio-climatic relationships which to date have not been fully explored or explained in any *one* previous research study. In particular, knowledge of freeze-thaw activity is generally lacking in most badland and semiarid regions. In addition, more information on weathering evolution with respect to aspect relationships and snow distribution is needed. Research undertaken by Yair *et al*. (1980), Churchill (1981), and Yair and Lavee (1982) adequately demonstrates the importance of insolation influences on differential slope erosion and runoff on badland slopes. French (1976) shows that preferential patterns of snow distribution can dictate the weathering response of an area. Closer to the badlands, Beaty (1972; 1975) testifies to the importance of both insolation and wind-distributed snow in defining geomorphic behaviour on slopes of the Oldman and Bearpaw Formations of southern Alberta. In combination, this past research and that to be presented in this thesis will undoubtedly add to a more comprehensive understanding of wintertime geomorphic processes operating in the Dinosaur badlands.

3. RESEARCH METHODS

This chapter outlines the objectives of the study, and explains in detail the methods employed. In particular, the research centres on four interrelated aspects of the role of snow in badlands: 1. snow accumulation, 2. snow distribution, 3. snow disappearance and snowmelt runoff, and 4. the geomorphic significance of snow. Eight separate visits to the field area were made during the 1981 - 1982 snow season, each lasting from two to six days. Of these, two early-season trips were made in October and November of 1981, before any snow had fallen, to install snow-measuring equipment. Field observations and measurements began with the first snowfall in November, 1981. Planning of field visits was made in short advance, based largely on weather map analysis and forecasting of snow and chinook activity. Frequent between-visit correspondence with Dinosaur Park personnel aided the planning procedure and additionally helped to keep the author informed of weather and changes in snowcover characteristics.

3.1 Sub-basin Characteristics

Although field measurements and observations were made from the badlands outside the main research watershed, most were taken from within, and these were concentrated in three sub-basins of the watershed. The three sub-basins examined were chosen for their individual diversity as well as their joint representativeness of the main watershed. They were selected on the basis of their variety in size, shape, lithology, slope, and orientation. In addition, each sub-basin (designated X, Y, and Z), is fairly characteristic of its surrounding area within the catchment, which lends credibility to basin-wide extrapolation of results.

Slope surveys were undertaken to determine the mean slope angle and surface area of each sub-basin, and for purposes of explaining patterns of snow accumulation and distribution as perhaps related to slope character and overall basin form. A 48-point square grid was constructed for each basin, and was randomly placed over enlarged sub-basin air photographs. These points were subsequently located in the field and measured with a Brunton compass and 1.0 m x 0.5 m x 2 cm plywood board. Slope angle values (Appendix B) were plotted as histograms, with slope frequency graphed against

angle groups of 5 degrees (Figure 3.1).

3.1.1 Sub-basin X

Sub-basin X (henceforth to be called sb-X) is the smallest of the three catchments, with a total plainimetric area of 4,829 m² (Figure 3.2). The plan area of sb-X, like that of the other two sub-basins was calculated three times from an enlarged aerial photograph (Figure 3.3) by the square counting method. The resulting values were averaged to obtain the final area figure. All three catchment areas were checked against (and closely supported by) planimeter measurements and those calculated with the use of an Intergraph digital computer. Sub-basin X displays a straight-line long axis of 75 m, and, due to its semi-rectangular shape, attains a maximum width of 95 m.

The aerial photograph of sb-X (Figure 3.3) and contour map[1] (Figure 3.4) reveal the semi-flattish nature of the basin floor, which is incised in a forked manner by two primary drainage channels. These dry channels stand out in the air photograph due to the contrasting darkness of the surrounding basin floor, which is extensively mantled by two highly-fractured siderite bands at respective elevations of approximately 0.5 and 1.0 metres above the main channel. These horizontally-continuous layers are more easily seen in the foreground and centre of Figure 3.5, and towards the centre-right foreground of Figure 3.6.

Overall basin relief is generally low, with a 5-metre vertical separation between the head basin boundary and basin outlet. Steep, rilled, predominantly claystone slopes rise from the one- metre high siderite layer of the lower basin floor to meet upper grassed surfaces (visible of Figure 3.3) which make up the southwest, north, and northwest boundaries of the sub-basin. Towards the northeast and east, the lower 1-metre portion of these claystone slopes is actually composed of compact, silty sandstone which is highly rilled and finely intercallated by bands of clayey silt (see extreme right side of Figure 3.5; centre-right of Figure 3.6). This unit appears in all claystone slopes of sb-X, but its position varies within the slope profile in other areas of the basin. In addition, the unit is lightly rilled and frequently obscured by material sloughing on south-facing slopes (see

[1]Due to the small areas involved, there are no adequate, previously constructed contour maps of the sub-basins. Therefore, these maps were prepared from field measurements and detailed ground photographs. All maps display an arbitrary "0" contour at the basin outlet.

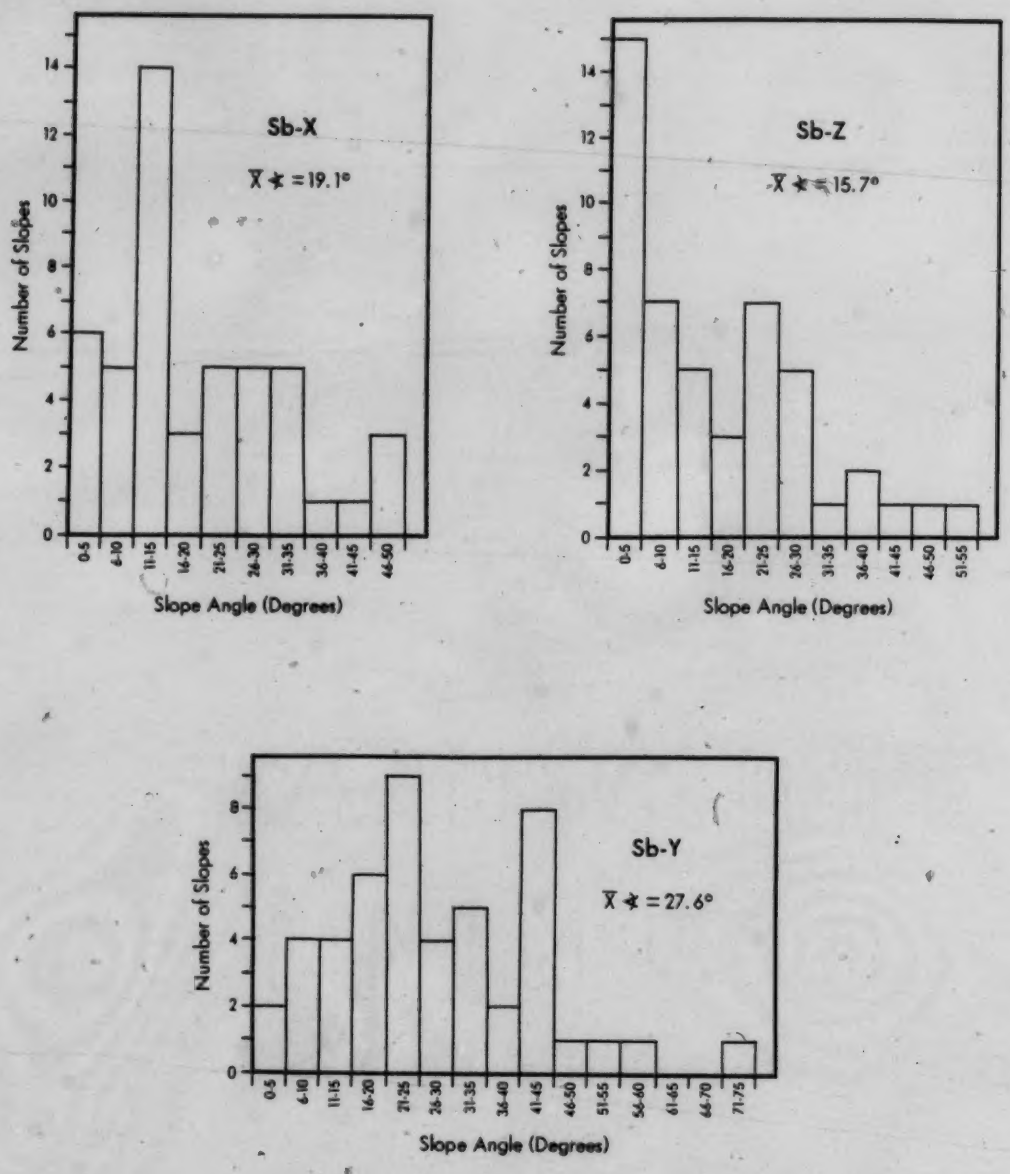

Note: Slope angle class range is 5°; 48 points sampled in each sub-basin.

Figure 3.1. Sub-basin histograms plotting slope angle against slope frequency.

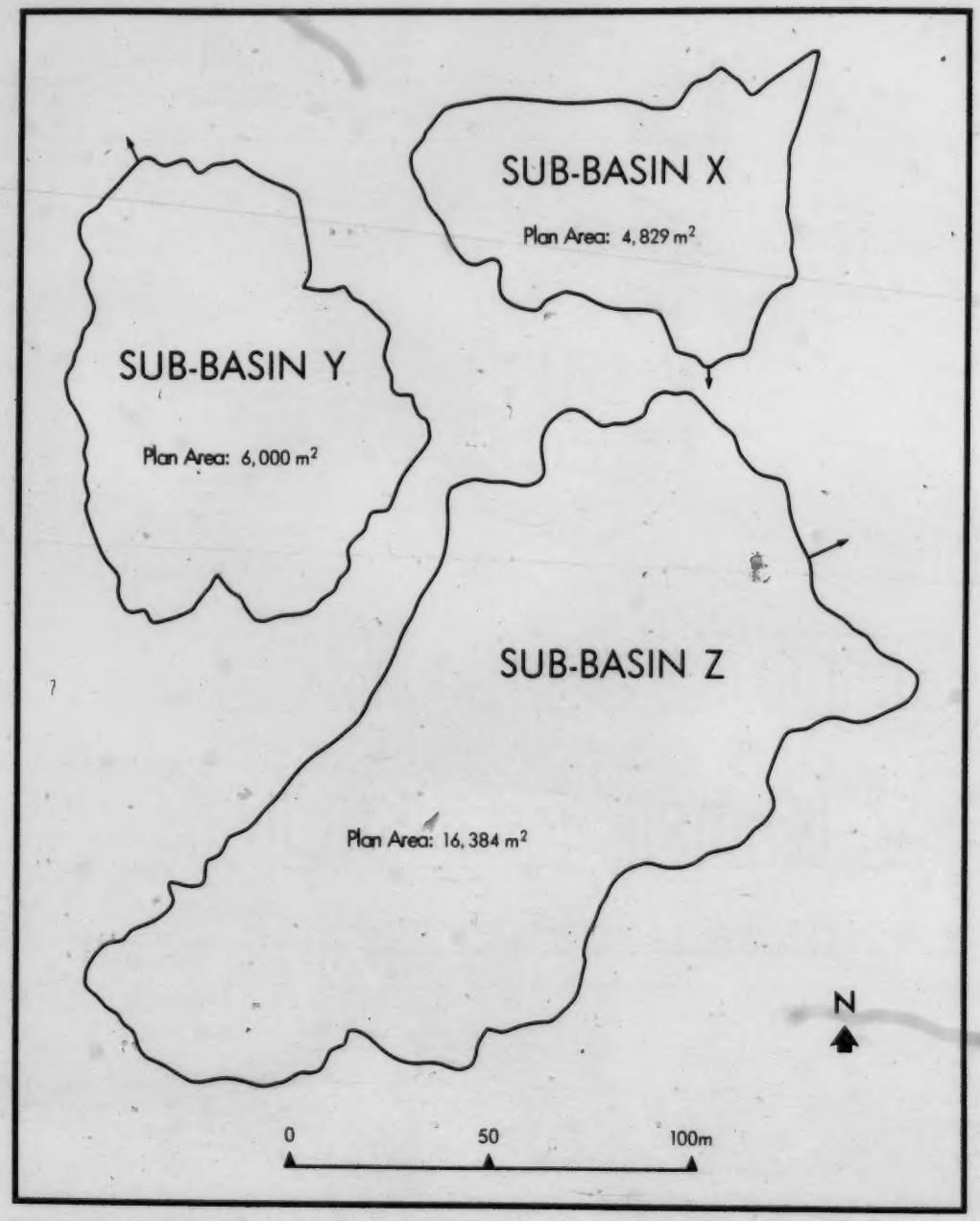

Note: for intrą-basin locations, see Figure 1.1.

Figure 3.2. Relative sub-basin sizes and orientations.

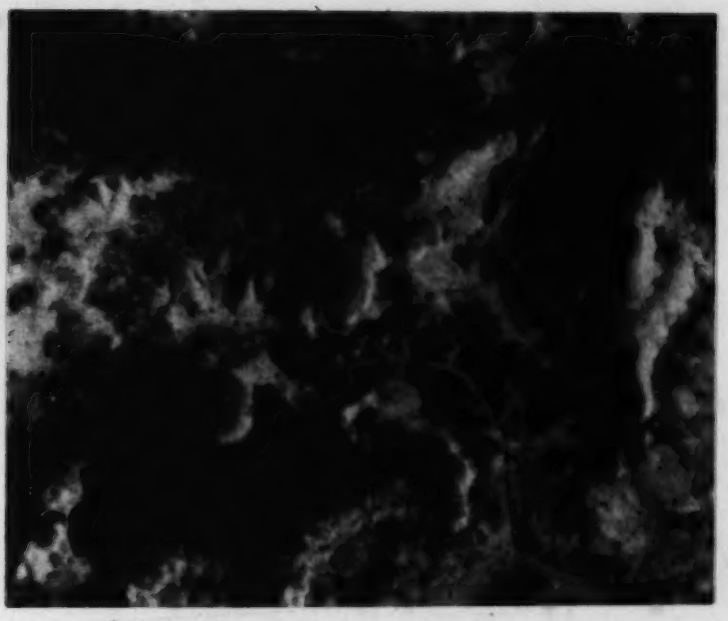

Figure 3.3. Aerial Photograph of sub-basin X.

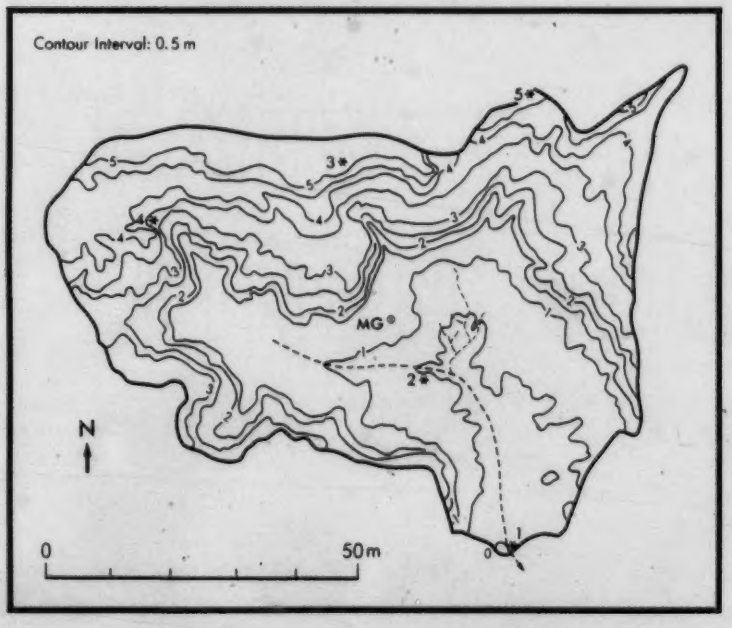

Figure 3.4. Contour map of sub-basin X showing basin boundary, snow survey points (✱), and Murton gauge location (⊗).

Figure 3.5. North-northwest view of sub-basin X. The basin floor is mantled by ironstone fragments derived from two highly fractured beds respectively elevated 0.5 m and 1.0 m above the main channel. A compact, deeply rilled, silty sandstone unit is visible in the extreme right of the photo. Collapsed piping channels, lined with sparse vegetation dissect headslopes of the sub-basin.

Figure 3.6. Northeast view of sub-basin X. Ironstone mantling of the lower basin floor is clearly visible. The compact, silty sandstone layer is distinct, to the right-centre of the photo, on the wsw-facing basin headslopes. Evidence of "rockfalls", and sloughing of aggregate-mantled claystone materials is seen on the south- and southwest-facing slopes towards the left of the photo. An unvegetated portion of the unconsolidated silt unit is visible towards the upper-left of the photo (above the snow gauge). This deposit rests upon the convex segment of the rilled claystone slope lying below. Collapsed, vegetation-lined pipe channels dissect the basin headslopes.

extreme left side of Figure 3.6).

A majority of claystone slopes display a stepped appearance where further overlain by 1- to 1.5-metre deposits of rilled, partly unconsolidated fine silt. Although these units generally exhibit poor internal cohesion, they are able to maintain steep slope profiles (up to about 55°) on south-facing slopes, where solar radiation 'baking' permits the development of a fairly indurated outer crust. These units lie directly below the upper vegetated surface and maintain rectilinear profiles that grade downslope onto the convex upper portions of claystone slopes (see text included with Figure 3.6).

The claystone slopes forming the periphery of the basin floor are dissected in many places by collapsed piping channels (visible in Figures 3.5 and 3.6). Most channels are lined with sparse vegetation consisting of sage or prickly pear. Shallow depressions or hollows are etched into the south, southeast, and northeast basin slopes; some of these drain into the lower basin through collapsed pipes, but those appearing on northeast-facing slopes show evidence of less concentrated surface drainage. Many of these depressions are lined with small bushes and short prairie grass.

The most distinct feature on the histogram prepared for sb-X (Figure 3.1) is the relative high frequency of points (14) appearing in the 11° to 15° slope category. This observation is partly explained by the proportionately large area of the lower basin, which is somewhat undulating in character due to the fairly high density of shallow channel incisions. Also falling into this category are many upper slope convexities and some grassed surfaces of the basin periphery. Most of the six point measurements shown in the 0° to 5° slope range fell upon either the lower basin ironstone flats or upon upper vegetated surfaces. All three of the slopes in the 46° to 50° group represent the steeper claystone or unconsolidated silt slopes in the northern section of the basin. In total, the sb-X point measurements yield a mean slope angle of 19.1°. The ground distance between adjacent measuring points was 11.0 metres. The surface area is 5,110 m^2 and is calculated by dividing the mean slope cosine of 19.1° into the planimetric basin area.

3.1.2 Sub-basin Z

Sub-basin Z is the largest of the three basins, with a planimetric area of over 16,000 m² (Figure 3.2 and Figure 3.7). It is elongated, oriented SW-NE, with a straight-line long axis of approximately 210 m. Sb-Z is similar to sb-X in that it also possesses a large lower basin surrounded by relatively steep slopes (see contour map, Figure 3.8). Like sb-X, the lower basin of sb-Z displays a number of inselberg-like residual mounds that are armoured by ironstone weathering fragments (Figure 3.9). Vegetation tracts are also scattered throughout this area. Unlike sb-X, however, the lower basin of sb-Z possesses a lesser slope gradient, with less-defined stream dissection, and more extensive, flatter-lying fan and pediment regions per unit area (Figure 3.9).

The lower basin narrows in an upchannel direction (visible on the air photo as well as the left-centre of Figure 3.10) and is flanked on all but its eastern side by steep claystone slopes. The south-facing slopes visible in the left-hand section of Figure 3.9 attain a maximum height of approximately 6 m and are generally rectilinear, but convex in the upper portions. These compact slopes are interbedded with a few horizontal siderite layers as well as one highly compact, lighter-coloured claystone unit which is in itself further interbedded by claystone bands of slightly differing composition. A thick regolith cloaks the entire upper surface of these slopes, but thins downslope into a shallow veneer or disappears completely. Evidence of mass wasting in the form of aggregate sloughing scars is visible on some of the steepest upper slopes.

Most of these south-facing slopes are highly rilled and very sparsely vegetated, with only the odd sage bush clinging to the side of a primary rill or to the collapsed pipes which separate these slopes. Most of the other claystone slopes that confine the lower basin retain a bit more vegetation than the south-facing slopes, although the coverage is still sparse. An exception is noted on the north-northeast-oriented headwall slope of the 'upchannel' section of the lower basin. Visible towards the left-centre of Figure 3.10, this slope is densely covered with short grasses and bushes, and exhibits signs of previous mass movement activity by slumping.

Towards the south, where the lower basin begins to narrow, the surrounding slopes rise approximately 7 m to the upper basin, which is generally flat and abundantly covered with long and short prairie grasses. This surface is primarily drained by a large,

Figure 3.7. Aerial photograph of sub-basin Z.

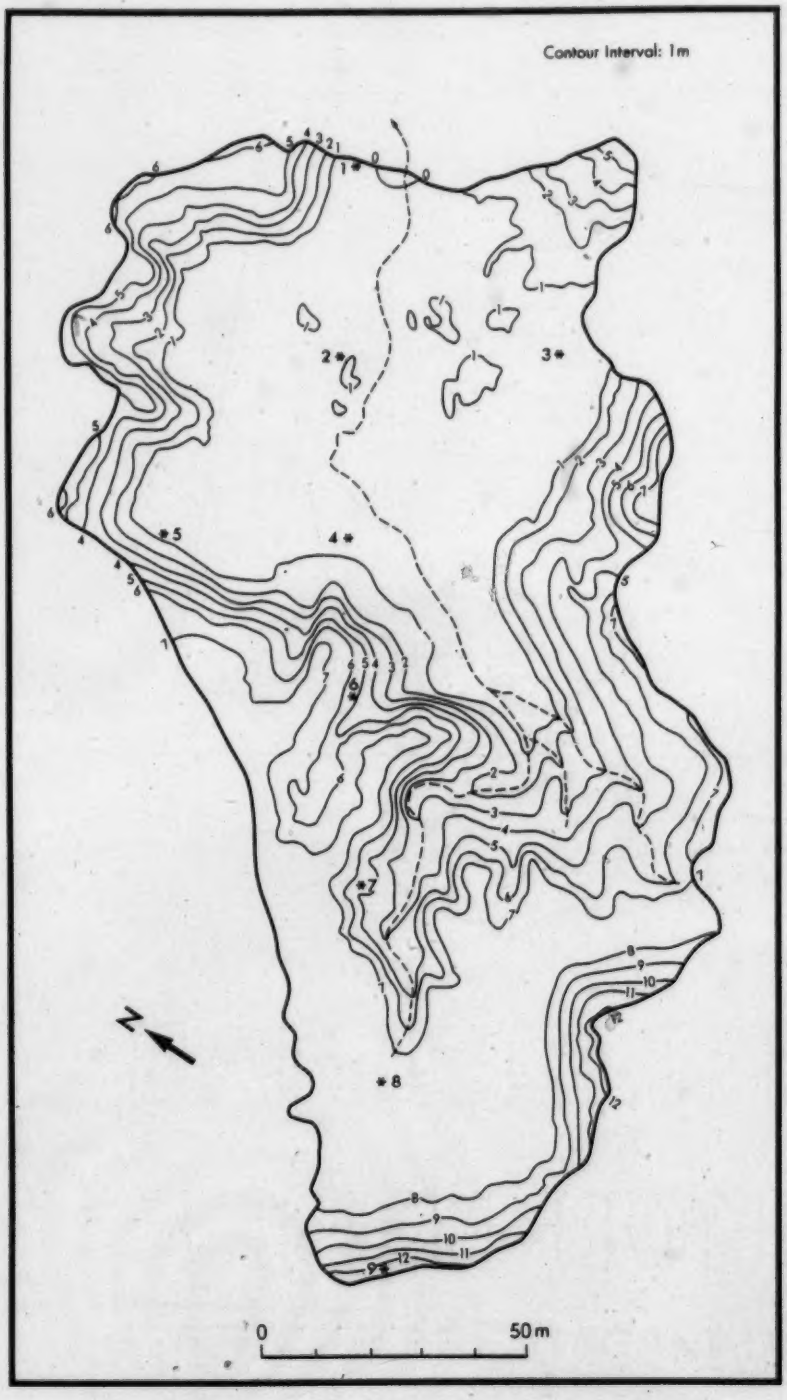

Figure 3.8. Contour map of sub-basin Z showing basin boundary and snow survey points (*).

Figure 3.9. Northeast view of sub-basin Z. Shown is the flat-lying, alluvium-covered floor of the lower basin, upon which ironstone-capped isolated mounds, and vegetation flats are displayed. South-facing, rilled and unvegetated claystone slopes are visible to the left side of the photo.

Figure 3.10. South-southwest view of sub-basin Z. Left-centre of photo shows the upchannel narrowing of the lower basin. The nne-facing headslope of this passage is covered in short grasses and shrubs. Two small buttes project 5 m above the upper basin surface and are visible in the middle and right backgrounds of the photo.

mostly collapsed piping channel which is an extension of the main channel of the lower basin (see aerial photograph, Figure 3.7). Other minor collapsed pipes and surface depressions also incise and drain the upper basin (Figure 3.11). Two large butte-like features make up the south and southwest boundaries of sb-Z (visible on Figures 3.10 and 3.11). They rise 5 m above the upper basin surface and are mainly composed of claystone. Both are flat-topped and protected by a thick cap of resistant ironstone. Denudation of these features has produced a fine-grained, flat-lying alluvial apron in the head region of the upper basin (see air photograph, Figure 3.7 and Figure 3.11).

The slope histogram of sb-Z (Figure 3.1) reveals a high frequency of very low slopes. Of the 15 slopes falling within the 0° to 5° range, 12 represent points surveyed on fan surfaces of either the upper or lower basin. The data shows that 22, or nearly one-half of the total 48 points measured (spaced 17.2 m apart) fell upon slopes of 10° or less. This fact accounts for the relatively low mean slope angle of 15.7° obtained for sb-Z. Although sub-basins X and Z are topographically similar, the latter catchment maintains a larger percentage (per unit area) of level regions, and its lower basin retains a lower slope gradient. Like sb-X, there are few higher-angled point measurements because of the areally limited occurrence of steep slopes. The histogram takes on a bimodal appearance by demonstrating a secondary peak in the combined slope ranges of 21° to 25° and 26° to 30°. One-quarter of the 12 slopes contained in this peak range lie on the vegetated side slopes of collapsed channels. The remainder generally represent claystone slope convexities, residual mounds, and debris-covered portions of lower basin hillslopes. It is worthy to note that both sb-Z and sb-X contain only three measurements in the 18° to 20° slope category. This probably indicates the breakpoint between slope angles maintained by the lower-lying grassed areas, alluvial fans, and ironstone-capped features, and the steeper slopes of most claystones and side areas of depressions and collapsed channels.

3.1.3 Sub-basin Y

The planimetric area of sub-basin Y measures 6,000m ^{2}, placing it between sub-basins X and Z in size (Figure 3.12). The oval-shaped basin trends south-north along a straight-line long axis of approximately 100 m. Unlike the other sub-basins, sb-Y exhibits

Figure 3.11. South view of the relatively flat upper surface of sub-basin Z. Winding, grass-covered gullies and large collapsed pipe channels dissect and drain this surface. The two small buttes form the head basin divide and provide material for the fine-grained, light coloured alluvial apron surrounding the basal regions of these features.

a more incised appearance, with no expansive lower basin area (see aerial photo, Figure 3.12, and contour map, Figure 3.13). Furthermore, the main channel is highly distinct as it is closely paralleled on both sides by steep, fairly high (7 to 10 m) slopes. From the mouth, the first 35 m (the lower one-third) of the channel floor displays a stepped profile due to the presence of two knickpoints, lithologically induced by thin beds of ironstone. The next 35 m of the long profile is fairly level and covered in unconsolidated alluvial deposits (Figure 3.14). The upper one-third of the stream bed transforms into a winding, partially collapsed piping channel. Here, the channel cuts through a maze of aggregate-mantled claystone slopes and rises abruptly at the upper head basin which is flattened and armoured by a thin bed of ironstone fragments (Figure 3.15).

In general, the lithology of sb-Y consists of a vertical succession of three claystone units that are alternately separated by two units of sandstone. As is easily seen in Figure 3.15, the north- and northeast-facing head-basin divides consist of deeply-rilled, sharp-crested sandstones which are capped in places by remnants of the uppermost claystone unit. These sandstone divides are interbedded in places by ironstone bands, and separate the upper basin into a series of bowl-shaped mini-catchments, one of which is easily detected towards the southwest corner of the aerial photograph (Figure 3.12). The southeastern portion of the upper basin divide, as well as the entire eastern basin boundary, is topped by the aggregate-mantled claystone unit which has not yet been eroded to expose the underlying sandstone. Like the head basin, the floor of this section of the upper basin is also partially mantled with broken ironstone fragments (Figure 3.14). Also similar to the head basin region, the coalescing mini-catchments towards the southwest, and the southeastern portion of the upper basin are also respectively emptied by two large, partially collapsed pipes that drain directly opposite of each other into the flat, middle stretch of the main channel (Figure 3.14).

Unlike sub-basins X and Z, sb-Y retains very little vegetation growth in its upper basin region. Aside from a few scattered shrubs, the only vegetation to be found lies along the slope banks of the lower 35 m of the main channel. Short grasses and prickly pear cacti are abundant here.

The slope histogram of sb-Y (Figure 3.1) reveals a very low frequency of lower-angled slopes, reflecting the absence of large areas of flat-lying fans and extensive

Figure 3.12. Aerial photograph of sub-basin Y.

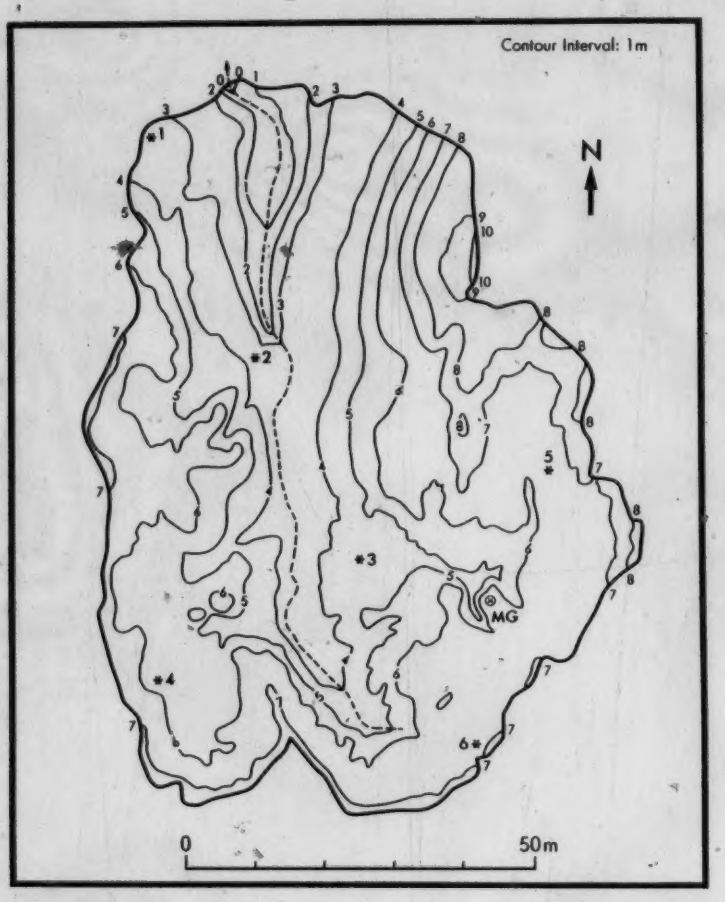

Figure 3.13. Contour map of sub-basin Y showing basin boundary, snow survey points (*), and Murton gauge location (⊗).

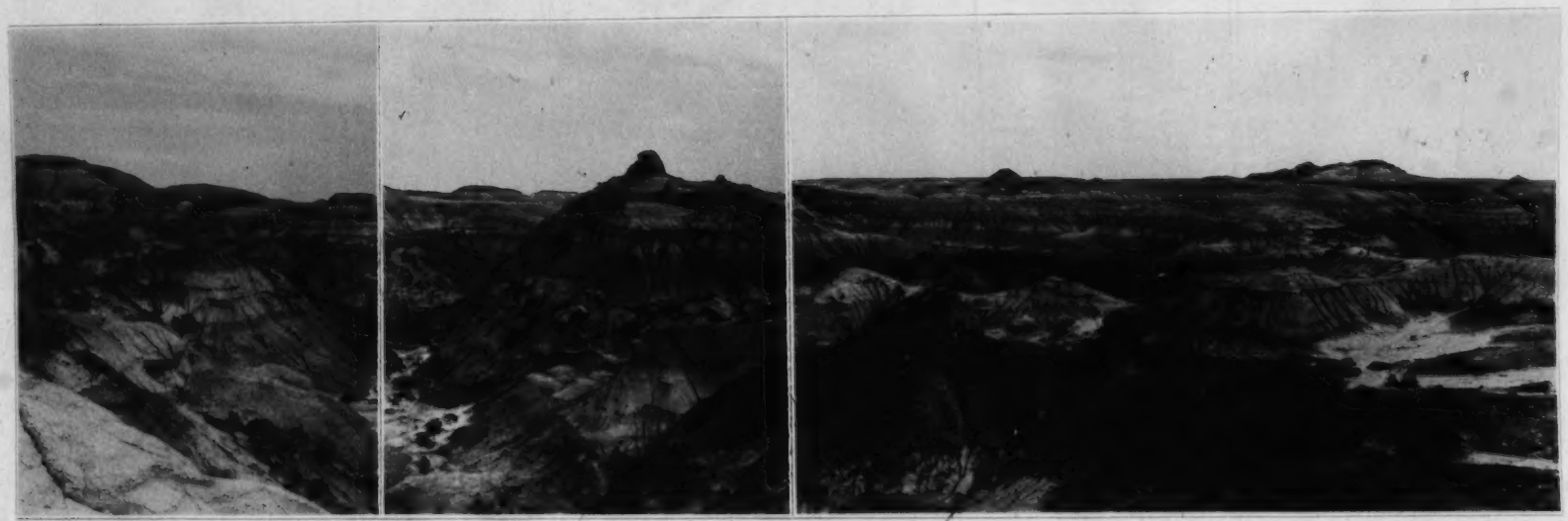

Figure 3.14. North-northeast view of sub-basin Y. The flat-lying, middle one-third of the main channel is visible in the left of the photo. It and the lower third of the channel are paralled on both sides by sharply-rising, interbedded claystone slopes. The snow gauge is visible in the right side of the photo and rests upon the ironstone-mantled floor of the eastern portion of the upper basin. Note one of two opposite-facing pipe outlets which drains into the middle section of the channel from this upper basin area.

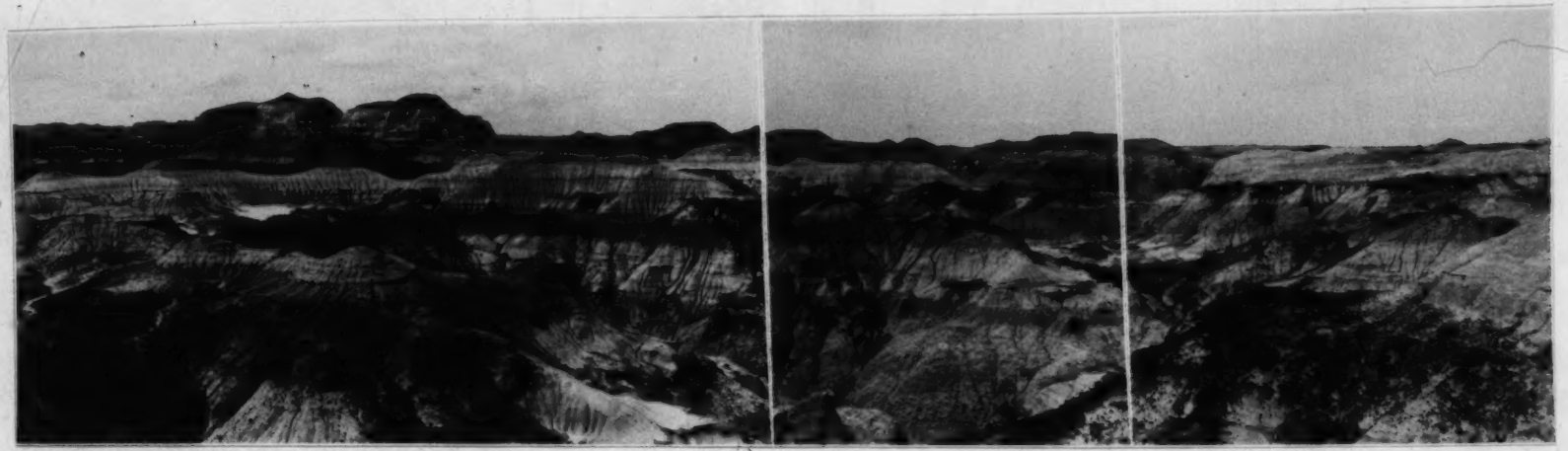

Figure 3.15. Southwest view of sub-basin Y. Clearly visible are sharply-defined vertical alterations of claystone, sandstone, and thin ironstone beds that characterize the slopes of this basin. The upper one-third of the main channel forms a winding, partially-collapsed pipe channel, developed predominantly within the lowest claystone unit. The channel rises abruptly to the head basin, seen in the upper-left of the photo. In the near background, sharp-crested, highly-rilled sandstones traverse the photo (left to right) and form the boundries of most of the north- and northeast-facing slopes of the head basin. These sandstones are capped in places by remnants of a highly-disaggregated claystone unit.

grassed surfaces. The high degree of channel dissection combined with intricate lithologic variations serve to create widespread areas of diverse slope angle characteristics. These field observations are demonstrated on the histogram by the generally lower frequency of slopes contained within any one slope category (as compared to sb-X and sb-Z), as well as by the higher total number of slope categories represented by the sb-Y measurements. These observations account for the higher mean slope angle of 27.6° obtained for this sub-basin. The bimodal nature of the histogram is caused by the eight point measurements (spaced 11.1m apart in the field) contained within the 41° to 45° slope category. Of these, six points fell upon the slightly stepped, but generally rectilinear, west-facing slope that parallels the lower two-thirds of the main channel (visible in Figure 3.14).

In total, the three sub-basins are representative of the main catchment in terms of lithology, basin form / shape, and slope characteristics. The lower one-third of the main watershed is deeply incised and exhibits a high density of steeper slopes. It may therefore be typified by sub-basin Y. The upper two-thirds of the main catchment contains larger areas of grassed flats, pediments, and fans, and is less deeply incised by the main channel; characteristics displayed by sub-basins X and Z. In addition, the sub-basins were collectively chosen such that slopes of every orientation and lithology may be found in at least one of them. These considerations ensure an optimum representation of the morphological character of the main watershed and the sub-basins serve as ideal sites for the study of snowmelt runoff and geomorphic process.

3.2 Methods of Monitoring Snow Accumulation

Snow accumulation, using snow course surveys and snow gauges, was monitored throughout the 1981-1982 field season in an effort to estimate the total water available to the sub-basins as well as the main watershed. This was undertaken to determine the significance of mid-winter and spring runoff in badlands, and to compare the relative volumetric runoff contributions of rainfall and snowmelt.

3.2.1 Snow Surveys

There is no specific geometric layout required for snow survey courses, although a manual of standard surveying procedures compiled by Environment Canada (1973) (and currently followed by the Atmospheric Environment Service (AES) in Alberta) recommends a 10-point survey along a 900 ft (274 m) straight line, with points spaced 100 ft (30 m) apart. Also acceptable is a 5-point setup along a 400 ft (122 m) or 900 ft (274 m) baseline, with points spaced 100 ft (30 m) or 200 ft (61 m) apart. If either of these designs is not possible, the manual suggests course patterns in the shape of a T, Z, L, or +. As well as these standard layouts, other researchers have used random grid sampling techniques (e.g. Hasholt, 1972; Storr and Golding, 1974; Dickison and Daugharty, 1978), circular courses (Gary and Coltharp, 1967), as well as a figure-eight configuration (Ffolliot and Hansen, 1968). The selection of point-spacing distances is also fairly subjective, but most researchers adhere to a 15 to 60 m range between points.

Three snow courses were set up in the watershed in October of 1981; one in each of the sub-basins. A total of 20 sampling points were established -- five in sb-X, six in sb-Y, and nine in sb-Z. Within each sub-basin, sampling points were situated 35 m apart, and marked with wire stakes and flagging tape. The geometric layout of each course was designed to accomodate as many 35-m point spacings as possible, and therefore reflects sub-basin shape, and ensures an adequate spatial representation in each catchment. These designs (shown in Figures 3.4, 3.8, and 3.13) generally follow the pattern guidelines suggested in the snow surveying manual (Environment Canada, 1973).

To maximize the accuracy and statistical apsects of the sampling procedure, Steppuhn and Dyck (1974) maintain that survey points should be randomly selected as well as representative of population variability (i.e. topography, vegetation, and land use). Goodison (1978) also stresses the need for an adequate sampling coverage of differing landscape classes. However. Steppuhn and Dyck (1974) point out that achieving both of these goals simultaneously is difficult, as landscape distribution is seldom random, and (p. 316) "any restriction in basin coverage would limit the representativeness of the survey". Despite these limitations, it is felt that both considerations were sufficiently satisfied within each sub-basin, by random selection alone. That is, after initially plotting the course designs upon enlarged air photos, it was found that the points do reflect the variety of

topographic and land cover characteristics of the sub-basins. For example, of the total 20 points surveyed, eight lie upon fan surfaces, five on vegetated areas, three on claystone slopes, two on flat-lying ironstone beds, one on a sandstone slope, and one on a miniature pediment. In addition, nine points lie in lower basin regions, and eleven lie in upper basin areas. Overall, the survey points accurately reflect the per unit area representation of lithology, slope, and landcover characteristics of the sub-basins.

Three snow surveys were completed during the field season, with the use of a Mount Rose snow sample tube with a 3.77 cm inside diameter. Snow at each survey marker was measured five times at 30 cm radius distances circumscribing the point marker. These values were averaged to attain one depth value.

Snow density and water equivalent at each survey point were calculated once, using the single sample cored at each point. For the first snow survey, the "weighing-in-field" method was used to determine snow density and water equivalent. A spring balance calibrated in centimetres of water equivalent was employed. It was discovered however, that the spring balance was not sufficiently sensitive to give accurate readings from the typically shallow snowpacks encountered in the badlands. Therefore, the 'bulk method' sampling technique was utilized for the two remaining surveys. This procedure involves placing the cored snow sample into an airtight container, and weighing its contents indoors, at a later time. A triple beam balance, accurate to three decimal places was used for these computations.

3.2.2 Snow Gauges

Two non-recording Murton snow gauges were used to monitor total seasonal snow accumulation. One was placed atop a flat-lying ironstone bed in the lower basin of sb-X (for location, see Figure 3.4; also visible in Figures 3.5 and 3.6), and the other[9] on a level claystone surface in the upper basin area of sb-Y (see Figure 3.13; also visible in 3.14). Shown up close in Figure 3.16, the Murton snow gauge consists of a 1.2 metre aluminum catchment cylinder with a 20-cm orifice diameter. This structure was bolted onto the centre of a 1.22 m x 1.22 m x 2 cm plywood baseboard. Also secured to the baseboard were three black iron pipes which support a 1.22 m diameter alter shield. Both

---

[9]A third gauge for placement in sb-Z could not be obtained.

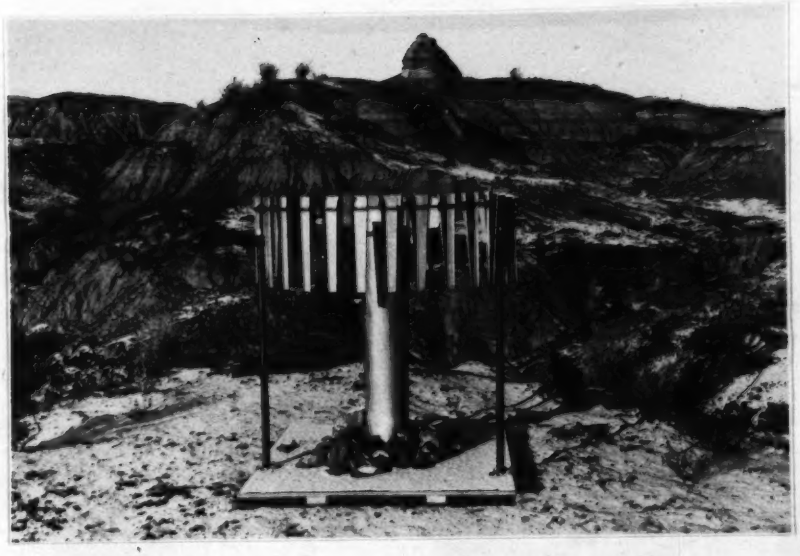

Figure 3.16. Murton snow gauge and alter shield in sub-basin Y.

gauges were anchored with siderite cobbles to prevent possible disturbances by animals or severe winds.

Once erected in the field, the gauges were filled with approximately 2 litres of ethylene glycol -- an anti-freeze agent used to melt incoming snow and to prevent mid-winter freeze of this water. Also added to each gauge was 0.2 litres of a light-weight mineral oil which forms a thin surface film and protects meltwater from evaporation. Cumulative snowmelt trapped in the gauges was measured on twelve occasions (from November, 1981 through March, 1982) with an AES Type 3 snow ruler calibrated in tenths of inches (later converted to millimetres).

3.2.3 Methods of Calculating Snow Accumulation and Water Availability

The snow surveys aided the determination of the volumetric amount of water contained in the sub-basins during various periods throughout the winter. To obtain these figures, the planimetric area of each sub-basin was multiplied by the average depth of snow / water equivalent. For each survey, this latter value was determined by the following known relationship:

$$WE = \rho \times D$$

in which WE = snow / water equivalent, ρ = snowcover density, and D = snow depth. Before this computation is performed, density is calculated by the following formula:

$$\rho = M / (A \times D)$$

in which M = mean mass of the individual snow sample cores, and A = the inside area of the snow sample tube. To estimate the volumetric water potentially available to the total watershed at the time of the snow surveys, the average water equivalent of the three sub-basins was multiplied by the planimetric area of the catchment.

The Murton gauges allowed the calculation of the total meltwater available to the main watershed during the field season. This value was simply attained by measuring and adding successive water gains in the snow gauges, averaging the two final values, and multiplying the resulting figure by the plan area of the main basin.

Because the snow gauges immediately convert incoming snowfall to water, the ruler measurements permit a good estimation of seasonal water equivalent. However, they do not allow direct measurements of snowfall accumulation depth, and thus snow

depth and density are unknown. To estimate snow depth for purposes of comparison to annual accumulation records, the total average water equivalent of the two Murton gauges was divided by the mean density of newly-fallen snow, as calculated for the concerned period from data provided by the Brooks AHRC. To further clarify the procedure, the values of mean monthly snow depth recorded at the AHRC were respectively divided by the mean monthly water equivalent values provided, to obtain mean monthly snow density figures. These numbers were totaled and averaged to obtain the one density value used in the estimation of snow accumulation depth for the field season. It is felt that this method is more accurate than simply employing a general, standardly-accepted fresh snow density value in the calculations.

The means of estimating snow accumulation as just described was carried out for the entire period that Murton gauge measurements were taken. The last measurement was taken at the end of the field season, in mid-March of 1982, after sufficient data and knowledge of snow distribution patterns and erosional processes was obtained. Therefore, a few late-season snowfall events occurring after the last snow gauge measurement were missed. Brooks AHRC snow data was employed to augment the estimated seasonal water availability (total volumetric water equivalent derived from snow) and snow accumulation values obtained up until the termination of the field season. This was accomplished by calculating the percentage of total seasonal snow / water equivalent recorded at the AHRC subsequent to the last measurement taken in the field. This percentage value was applied to the total Murton gauge mean water equivalent figure, to obtain a supplemented, representative total season snow / water equivalent value. This figure was used to calculate the total volumetric amount of water entering the main watershed for the entire snow season. The mean snow density calculated from depth and water equivalent values recorded at the AHRC during these last snowfall events was again used to figure total snow accumulation depth in the watershed.

3.3 Methods of Investigating Snow Distribution

Perhaps the most important question to be answered in this thesis centres upon assessing geomorphological response in the badlands as influenced by the relationship(s) between snow accumulation and the effects of wind. Like rain, snow provides an agent for the initiation of geomorphic process, however its spatial distribution as largely controlled by wind may modify these processes by reducing or enhancing water availability in a given locale.

Although the magnitude and frequency of geomorphic events during winter depends on a number of factors (e.g., snow accumulation, snowmelt rate, and material characteristics among others), it is ultimately controlled by the spatial availability of meltwater, and hence by snow distribution patterns. Therefore, it is important to establish a concept to explain the ways in which variables interact to determine snow distribution in the badlands. These factors, as previously discussed in Chapter 2, include wind characteristics of directional frequency and velocity, as well as the wind-modifying factors of vegetation and topography. This section outlines the methods employed to investigate these factors. The concept relating these variables to snow distribution in the Alberta badlands is presented in the next chapter.

3.3.1 The Role of Wind

The effectiveness of wind velocity and directional approach in initiating snow distribution was most easily determined through repeated visual observations of snow drifting patterns. Time spent in the field permitted sufficient observation of wind characteristics during a number of snowstorms as well as during inter-storm periods. Evidence of between-visit wind activity was often assessed by observing orientation patterns of 'free' snow deposits such as snow ripples. Oriented drifts, formed in the vicinity of single obstacles (e.g. vegetation clumps or small residual hills) were the most obvious indicators of effective wind direction.

While in the field, snow drifting observations were recorded by photography. Wind orientation and prevalency were consistently noted, along with estimates of wind velocity. Radio reports supplemented these notations. Daily anemograph charts were obtained from the Brooks AHRC for the periods concerned, which aided in reconstructing

between-visit activity. These charts supplemented field observations and were particularly useful for comparing effective wind frequencies of varying orientations.

Like the examination of wind characteristics, evidence of the influencing affects of topography and vegetation on wind and snow distribution patterns was also photographically recorded throughout the field season. Visual observations and spot depth measurements from varying terrain features and vegetated surfaces enabled the delineation of areas subject to differing degrees of snow accumulation by wind distribution. Patterns of snow distribution in the sub-basins and main watershed are presented in the following chapter by means of time-sequential photographs and accompanying descriptions of observed distribution patterns.

3.4 Methods of Investigating Snow Disappearance and Snowmelt Runoff

As indicated in the last chapter, the means by which snow disappearance proceeds in a given area is dependent upon the characteristic interactions of many physical and climatic variables. Although it is beyond the scope of this thesis to investigate all these factors in detail, an attempt is made to explain the most significant variable relationships that affect snowmelt rates. This knowledge is applied to that gained through the examination of snow distribution in the badlands, to evaluate observed runoff patterns. These patterns, including the magnitude, frequency and locational characteristics of snowmelt and runoff events are ultimately related to wintertime geomorphic response.

3.4.1 Snow Disappearance

Similar to the determination of snow distribution patterns, spatial snowpack depletion was primarily assessed through field observations of snowmelt events, recorded by photography throughout the season. Meteorological records provided by the Brooks AHRC aided qualitative evaluations of the climatic factors responsible for initiating and maintaining snowmelt activity. These records supplied information on daily temperature (mean and extremes), wind velocity, hourly durations of sunshine receipt, and the amount of snow remaining on the ground at the end of each day.

3.4.2 Infiltration and Runoff

Once converted to water, snowmelt disappearance was determined in a number of ways. Attempts to monitor infiltration depths on a full range of lithologies, vegetated areas, and topographic features within the sub-basins were made by inserting the dye tracer Rhodamine B onto the ground/snow interface beneath 191 mid-winter snowpacks. Rhodamine B was chosen over other flourescent dyes available because of the ease by which it is absorbed by clays. The locations of all dye applications were mapped on air photographs to facilitate their later identification. Snow depth and ground surface lithology for all points were also noted.[10] After completion of a snowmelt event, the points were to be relocated and excavated, so that wetting depths could be recorded by visual examination of the vertical extent of discolouration of subsurface materials.

For the dye application procedure, approximately one gram of crystalline Rhodamine B was sealed inside 2 cm x 2 cm finely-meshed porous bags. The dye was packaged to facilitate its precise placement and to prevent leakage onto the snowpack surface which could falsely lower the natural surface albedo. The packets were set in place by coring a hole in selected snowpacks with the Mount Rose sampler, dropping one packet into the hollow created, and replacing the extracted snow core. This method was designed to create as little disturbance as possible to the surrounding surface snowcover. The use of dye in powdered form *versus* liquid ensured that the dye itself would remain in position until melt-out, and that it would not induce premature melt of the surrounding snow enclosure.

Although the primary reason for administering the dye was to assess the effective subsurface penetration of meltwater, it was also employed as a possible means of tracing overland flow pathways for short distances, until downslope or downstream dilution obscured these trails. Most often, however, surface meltwater routes were visually determined. Piping outlets throughout the main watershed were constantly checked during snowmelt events for evidence of throughflow.

The efficiency of runoff disposal was estimated by observing the duration and magnitude of flows in the primary drainage channel of the watershed. Although the automated runoff-monitoring equipment employed during summer months was not

---

[10]For reasons to be discussed in the next chapter, these notations as well as maps showing application points are not presented.

engaged during winter or early spring, visual recordings of stage height were taken periodically at the flume site near the mouth of the main catchment. Used in conjunction with a pre-designed rating curve, these measurements aided approximations of volumetric discharge. Comparison of basin outflows to water availability values secured from snow surveys yielded an estimation runoff efficiency during snowmelt.

3.5 Methods of Investigating Geomorphic Activity

Field surveillance of water availability (snow accumulation), its spatial location (snow distribution), and its modes of movement (snow disappearance) provided much of the information necessary to formulate a theory on badland geomorphic response during the winter season. In conjunction with the methods described to investigate the behaviour of snow and snowmelt, a number of other direct and indirect field techniques were employed to evaluate the relationship between snowfall and erosion.

3.5.1 Direct Field Measurements

Many small excavation pits were dug on all lithologies throughout the field season to keep track of changes in the physical state and character of subsurface materials. These pits were dug at separate intervals and locations than those excavated at the dyed points, as the latter were useful to assess the effects of only one snowmelt event. Excavations were carried out in both snow-free materials as well as those lying beneath an established snowcover. During periods of below freezing temperatures, emphasis was placed on examining materials for frost presence. Observations and measurements of frost included its spatial distribution, type of ice found, and penetration depth within various materials.

Observations were made in other pits during melt periods, to determine the duration of frost presence and its effects on meltwater infiltration and runoff. After a complete melt of all snow and ice, wetting depths were checked in numerous locations. These were perhaps the most significant subsurface measurements taken, as they provided answers to speculations of the penetration ability and potential of water on badland materials during the naturally extended periods of moisture input afforded by melting snowpacks. Used in conjunction with the spatial snowpack distribution, this

information was vital to defining the locations where, and the degree to which snowmelt permitted material strength reduction and potential mass movement activity.

Seven suspended sediment samples were taken from the main channel outlet at the flume site during a major snowmelt runoff episode. Although the number of samples taken and the sampling frequency was not sufficient to permit estimations of volumetric erosion, they were nonetheless useful for comparison to sediment concentrations calculated for summer rainstorm events. Sampling was carried out manually by dipping plastic bottles into the channel centre at heights approximately halfway between the channel floor and water surface. The samples were oven dried and weighed after recording individual water volumes, and sediment concentrations were calculated in grams per litre. The results were then compared to concentrations obtained at corresponding stage heights during rainfall runoff.

3.5.2 Indirect Field Measurements

To supplement research undertaken during the winter-spring field season, a series of slope angle and orientation measurements was completed during the late summer of 1982. This was done to determine if there is a significant difference among the mean slope angles displayed by slopes of varying aspects. It was also undertaken with the intention of indirectly linking short-term observations of snow distribution, snowmelt, and erosion to long-term geomorphic response and slope evolution.

As shown in chapter 2, the effects of solar radiation on moisture retention and behaviour of slope materials has been investigated in other badland regions (Yair *et al*., 1980; Yair and Lavee, 1982 in Israel; Churchill, 1981 in South Dakota), but not in the Alberta badlands. However, these aspect studies do not consider the role of snow distribution and snowmelt. As mentioned earlier, this may, in part, reflect the difficulty with which the role of rain and snow can be separated when based solely on indirect field measurements. Therefore, separation and evaluation of the long-range evolution of slope characteristics as determined by rain *and* snow must also rely on direct short-term observations.

Analysis of recent meteorological records and field study during winter and early spring must accompany indirect slope measurements. The role of snow as a geomorphic

factor in slope development may then be more distinctly defined to show: 1. if snow distribution is such that there is little preferential distribution and thus its coverage upon melt closely resembles that of rainfall, 2. if snowfall is not sufficient in quantity (even if preferentially redistributed) to be an important factor contributing to preferential slope steepness, or 3. if snow distribution and melt is such that it enhances the effects of differential insolation.

To determine if a preferential slope steepness and thus perhaps a differential runoff or erosion response exists in the Alberta badlands, 220 individual slopes were examined, using methods and criteria similar to that developed by Churchill (1981). Field sampling procedures between the two studies primarily vary in that in Dinosaur Park, sandstone slopes were investigated as well as claystones, a greater number of claystone slopes were examined (110 *versus* 45), and mean slope angle was the sole slope form measurement taken. Like the criteria established by Churchill (1981), only slopes exhibiting orientations within 15° either side of true north or south were considered. Additionally, measurements were consistently taken only from those features (e.g. isolated residual mounds, small buttes, and appendages of major slope systems) exhibiting a pair of north- and south-facing slope components which also met the orientation requirements.

Lithologic criteria was established such that all slopes considered possessed a fairly uniform composition, and minimum interbedding. Slopes of highly diverse lithologies were discarded so as to ensure that vertical changes in material structure or weathering resistancy could not account for differences in slope steepness, and to maintain a distinction between the results found for claystones and sandstones. Although this criteria presented little problem to the measurement of sandstone slopes, extremely subtle changes in composition within some claystones often precludes strict rectilinear slope formation in favour of slightly stepped slope profiles. Because of a high prevalency of slopes of this nature, exclusion of stepped claystones was considered impractical.

The average dip of each slope profile was measured with a Brunton compass lying atop a 1.0 m x 0.5 m board placed on the most representative segment of the slope profile. For stepped claystones, the dip was taken along the imaginary rectilinear profile line defined by connecting the series of miniature tread and riser intersection points. The compass was hand-held for a few measurements where the inclined board could not span

two or more of these points.

Slopes were sampled over a 6 km² area, with most measurements taken from outside the boundaries of the main watershed. It was necessary to expand the sampling area in order to locate a sufficient number or paired slopes meeting the requirements set by slope orientation criteria. As major emphasis was placed on finding such slopes, possible bias towards slope selection according to any pre-conceived notions of steepness relationships was eliminated. Selection bias was also dampened by the practice of not tallying measurements during interim periods. All values were tabulated only after sampling was complete, and results were statistically evaluated using the chi-square (X^2) test.

In addition to the direct and indirect field measurement techniques employed to investigate snow-related geomorphic response, photographically-recorded visual observations of mid-winter erosion activity provided much evidence as to the importance of snow in the badlands. In combination, the methods and procedures used to evaluate snow accumulation, distribution, means of disappearance, and geomorphic response yielded a good basis for development of a snow relationship theory which will augment knowledge gained through rainfall investigations, and the understanding of badland geomorphic evolution.

4. RESULTS AND DISCUSSION

4.1 Snow Accumulation

Meteorological records obtained from the AHRC station for the winter of 1981-1982 provide data on snow accumulation that serves a triple purpose. First, it is used as a comparison to past years, to determine the "normalcy" of snow accumulation during the 1981-1982 season. Secondly, it is compared to and used in support of snow measurements taken within the watershed, and third, it is employed both mathematically and qualitatively in places where field measurements or observations are lacking. In combination, meteorological data and field measurements provided a good estimation of total seasonal snow accumulation, as well as intra-seasonal and total water available (potential runoff) to the catchment.

4.1.1 Snowstorm Frequency, Magnitude, and Total Season Snow Accumulation: AHRC Records

A seven month calendar (Table 4.1) depicts the daily and monthly snow accumulation and snow / water equivalents recorded at the AHRC station during the 1981 / 1982 season. Snow fell on forty-eight days during the season, excluding those days in which trace amounts were recorded. Of these snow days, only eight received amounts equal to or greater than 5.0 cm, and 10.0 cm or more fell during just two 24 hour periods, both in March. Although there was a high frequency of snowfalls, the magnitude of daily accumulation was very small, averaging just 2.9 cm per day for the forty-eight days receiving snow.

Despite the small daily snowfall values, the 1981-1982 season experienced one of the largest accumulations on record in terms of monthly and total annual snow quantities. This is evident in Table 4.2, in which the 1981-1982 monthly and total snow accumulation appear with the mean monthly and mean annual accumulation values of the previous twelve snow seasons. The data (Table 4.2) shows that the total snow accumulation for the 1981-1982 season (141.0 cm) exceeds the previous twelve year mean accumulation (90.3 cm) by the relatively substantial value of 50.7 cm. According to the AHRC records, the 141.0 cm of snow yielded a total of 105.0 mm of water

TABLE 4.1. DAILY AND MONTHLY SNOWFALL AND WATER EQUIVALENT VALUES (AHRC), PLUS CHINOOK DAYS OCCURRING DURING THE 1981-1982 SNOW SEASON.

Month / Year ↓ Day →	1	2	3	4	5	6	7	8	9	10	11	12	13	14	15	16	17	18	19	20	21	22	23	24	25	26	27	28	29	30	31	Monthly Total
November 1981																	1.0 0.8	6.5 5.3		0	+ 0	0						+ 0	+ 0		7.5 6.1
December 1981	+ 0	+ 0	+ 0	+ 0	+ 0	+ 0				+ 0			0.7 0.4	6.3 3.8					+ 0	+ 0	+ 0						2.6 2.1					9.6 6.3
January 1982	3.9 3.2			2.7 2.2	2.0 1.7		0.8 0.4		3.8 2.3	0.6 0.3	5.5 3.5	+ 3.5 2.7	+ T	2.0 1.6		4.5 3.6		2.3 1.7		1.8 1.5	3.0 2.6	T	1.0 0.8	0.5 0.4	+ T	+ 0				T		37.9 28.5
February 1982	2.5 1.7	0.5 0.3			T	+					2.5 2.2	0.5 0.4				+ 0	+ 0	+ 0	+ 0	+ 0	+ 0 T	1.3 0.8	0.5 0.3	2.0 1.2		T	0.7 0.4					10.5 7.3
March 1982	11.3 7.8	4.5 2.9	1.0 0.6	0.5 0.3			T	T	0	T	+ 0 0.4 0.2	+ 0	+ 0	0	0 15.5 10.2	6.9 5.2	2.2 1.6	1.8 1.6	1.5 1.2		0	0	0 4.0 3.6	0.6 0.6			+ 0	0	0	0		50.2 35.8
April 1982	7.0 6.8		3.5 2.2	1.0 0.7	T	6.3 4.9	2.0 1.7											2.0 1.8														21.8 11.3
May 1982				T	1.5 0.9	T	2.0 2.0																									3.5 2.9
																															Total Season	141.0 105.0

T = Trace

+ 0 — Chinook Present According to Lester (1976) and Golding (1978) Criteria.
+ 0 — Chinook Present According to Longley (1967) Criteria.
5.0 — Snow Accumulation (cm)
3.5 — Snow Water Equivalent (mm)

Data Source: AHRC Records

TABLE 4.2. MEAN MONTHLY AND MEAN ANNUAL SNOWFALL RECORDED AT THE AHRC FOR TWELVE SNOW SEASONS VERSES MONTHLY AND TOTAL SNOWFALL RECORDED AT THE AHRC FOR THE 1981-1982 SNOW SEASON.

	AHRC Snowfall (cm)									
Snow Season	Sep.	Oct.	Nov.	Dec.	Jan.	Feb.	Mar.	Apr.	May	Yearly Total
1969 - 1970	0	6.4	3.8	6.4	39.4	3.8	10.7	2.8	T	73.3
1970 - 1971	0	3.8	19.8	15.5	39.9	15.2	10.9	T	0	105.1
1971 - 1972	0	7.6	T	22.9	23.4	24.1	5.1	16.5	0	99.6
1972 - 1973	5.1	1.3	15.2	32.2	T	12.7	3.8	6.9	0	77.2
1973 - 1974	0	T	18.5	16.5	31.8	6.4	16.5	6.4	0	96.1
1974 - 1975	0	0	3.8	20.3	7.6	31.0	27.4	25.7	1.3	115.8
1975 - 1976	0	1.5	22.9	47.5	1.3	11.2	8.6	1.3	0	94.3
1976 - 1977	0	1.0	9.1	7.6	13.5	0	21.6	2.3	T	55.1
1977 - 1978	0	0	12.0	28.4	27.8	11.8	3.8	10.4	0	94.2
1978 - 1979	0	T	24.6	19.5	1.9	15.7	4.5	15.8	5.7	87.7
1979 - 1980	0	5.0	16.0	8.3	17.0	15.0	23.4	T	0	84.7
1980 - 1981	0	6.4	15.2	39.6	8.2	3.3	28.0	T	0	100.7
12 Year Mean	0.4	2.8	13.4	22.1	17.7	12.5	13.7	7.3	0.6	90.3
1981 - 1982	0	0	7.5	12.1	36.9	13.3	52.9	14.8	3.5	141.0
									Snow/Water Equivalent (mm)	105.0

T = Trace Recording (<0.2 cm)

Data Sources: see Figure 4.1.

Note: Monthly snow accumulation values for the 1981-1982 season differ slightly from those appearing in Table 4.1. Snow falling in the early morning hours of the first day of a given month is counted towards the last day of the preceeding month in this Table, in accordance with the AHRC method of recording snowfall, and for purposes of comparison to records of previous years. Values were adjusted to the true day on which snow fell, in Table 4.1.

equivalent (Table 4.1), which, in comparison to the twenty-seven year total mean annual precipitation value of 335.5 mm (Table 1.1 in Chapter 1), represents close to one-third (31%) of the mean annual precipitation normally received in the region. As noted previously in Chapter 1, the mean percentage of water derived from snow is usually close to one-quarter of the total annual precipitation received. Hence, total snow accumulation and snow / water equivalent recorded during the 1981-1982 season was substantially more than in previous years.

Used with Table 4.2, Figure 4.1 illustrates the monthly distribution of snow accumulation recorded at the AHRC during the field season. As shown on the graph (Figure 4.1), monthly snow accumulation during 1981-1982 remained below the previous twelve-year mean until January, at which time it surpassed and sustained greater accumulation values than the twelve-year monthly mean. Especially conspicuous in Figure 4.1 are the accumulation columns for January and March of 1982. Both months show uncharacteristically high snowfall quantities that are much greater than the monthly mean accumulation (refer to Table 4.2). In January, 26% of the total season accumulation fell. March received 38% of the total season snowfall. Together, the two months received 64% of the snow accumulation recorded over the five-month period for which snow fell, and account for the extremely high total season snow accumulation. Table 4.2 and Figure 4.1 also demonstrate the temporally large variability in snowfall from month to month as well as from one year to the next.

4.1.2 Total Season Water Equivalent, Snow Accumulation, and Volumetric Runoff Potential: Snow Gauges and Extrapolated Results

As mentioned in the previous chapter, water availability and snow accumulation in the field region was monitored with Murton snow gauges until March 15, 1982. During this time, twelve separate depth measurements of snow / water equivalent were taken from both gauges. These values plus cumulative water equivalents appear in Table 4.3 and Figure 4.2. For comparative purposes, corresponding water equivalents from the AHRC are also included in Table 4.3 and Figure 4.2. Snow / water equivalents recorded after the last set of Murton gauge readings (noon of March 15) at the AHRC are graphed in Figure 4.2, and the values correspond to actual snowfall dates.

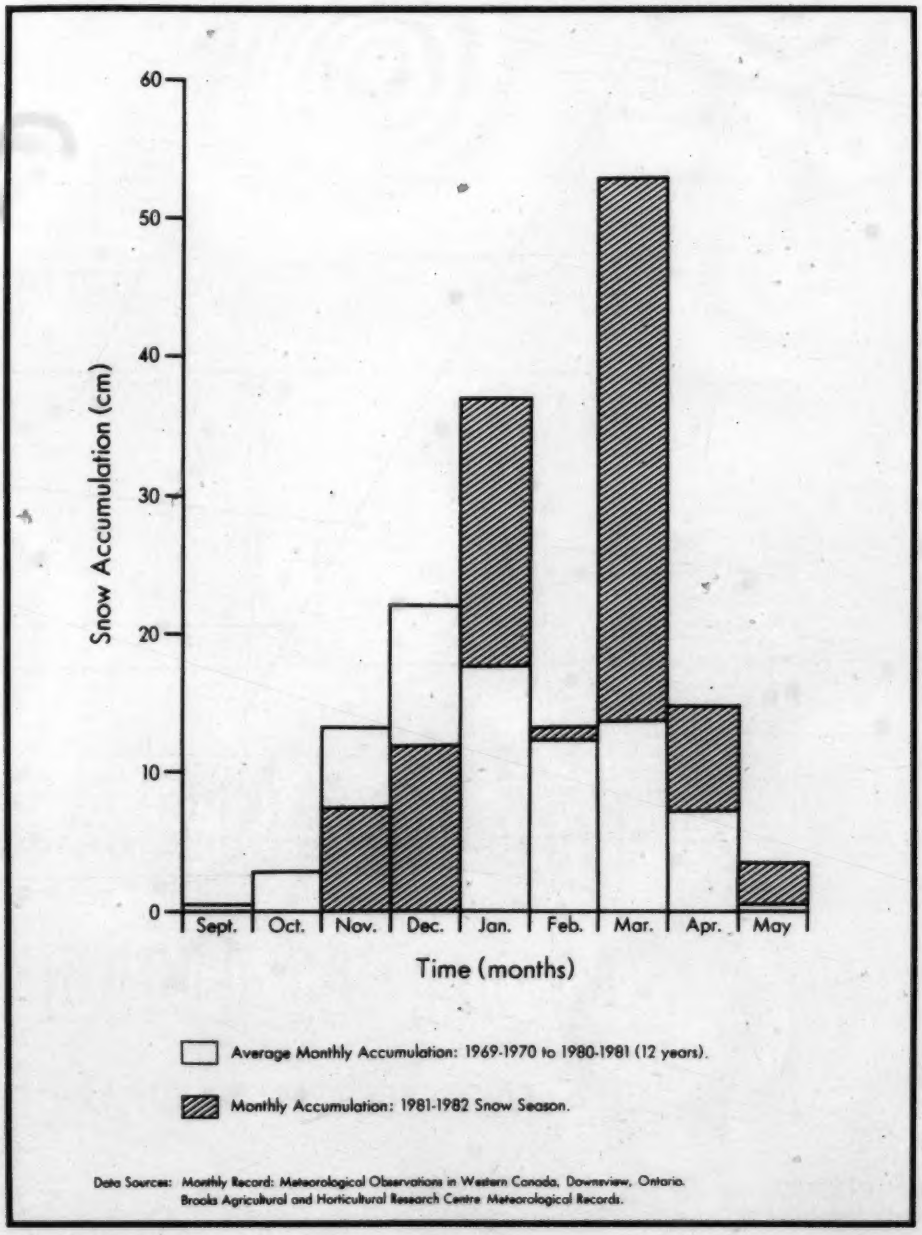

Figure 4.1. Mean monthly snow accumulation at the AHRC for twelve snow seasons (1969–1970 to 1980–1981) *versus* monthly snow accumulation at the AHRC for the 1981–1982 snow season.

TABLE 4.3. MURTON GAUGE SNOW/WATER EQUIVALENTS AND CUMULATIVE SNOW/WATER EQUIVALENTS OF MURTON GAUGES AND THE AHRC: DECEMBER 12, 1981 TO MARCH 15, 1982.

Measurement Dates	Snow/Water Equivalents (mm)			Cumulative Snow/Water Equivalents (mm)		
	Sb-X	Sb-Y	AHRC	Sb-X	Sb-Y	AHRC
14 Nov., 1981	0	0	0	0	0	0
12 Dec., 1981	7.6	7.6	6.1	7.6	7.6	6.1
14 Dec., 1981	1.3	1.3	2.6	8.9	8.9	8.7
14 Jan., 1982	11.4	14.0	20.0	20.3	22.9	28.7
16 Jan., 1982	5.1	1.3	1.6	25.4	24.2	30.3
17 Jan., 1982	1.8	1.3	3.6	27.2	25.5	33.9
6 Feb., 1982	9.7	11.4	9.0	36.9	36.9	42.9
13 Feb., 1982	4.6	1.3	2.6	41.5	38.2	45.5
18 Feb., 1982	1.0	0	0	42.5	38.2	45.5
21 Feb., 1982	2.5	0.5	0(T)	45.0	38.7	45.5
12 Mar., 1982	10.2	8.4	14.5	55.2	47.1	60.0
15 Mar., 1982	8.9	6.4	7.2	64.1	53.5	67.2
Total	64.1	53.5	67.2	64.1	53.5	67.2

(T) = Trace (<0.1 mm)

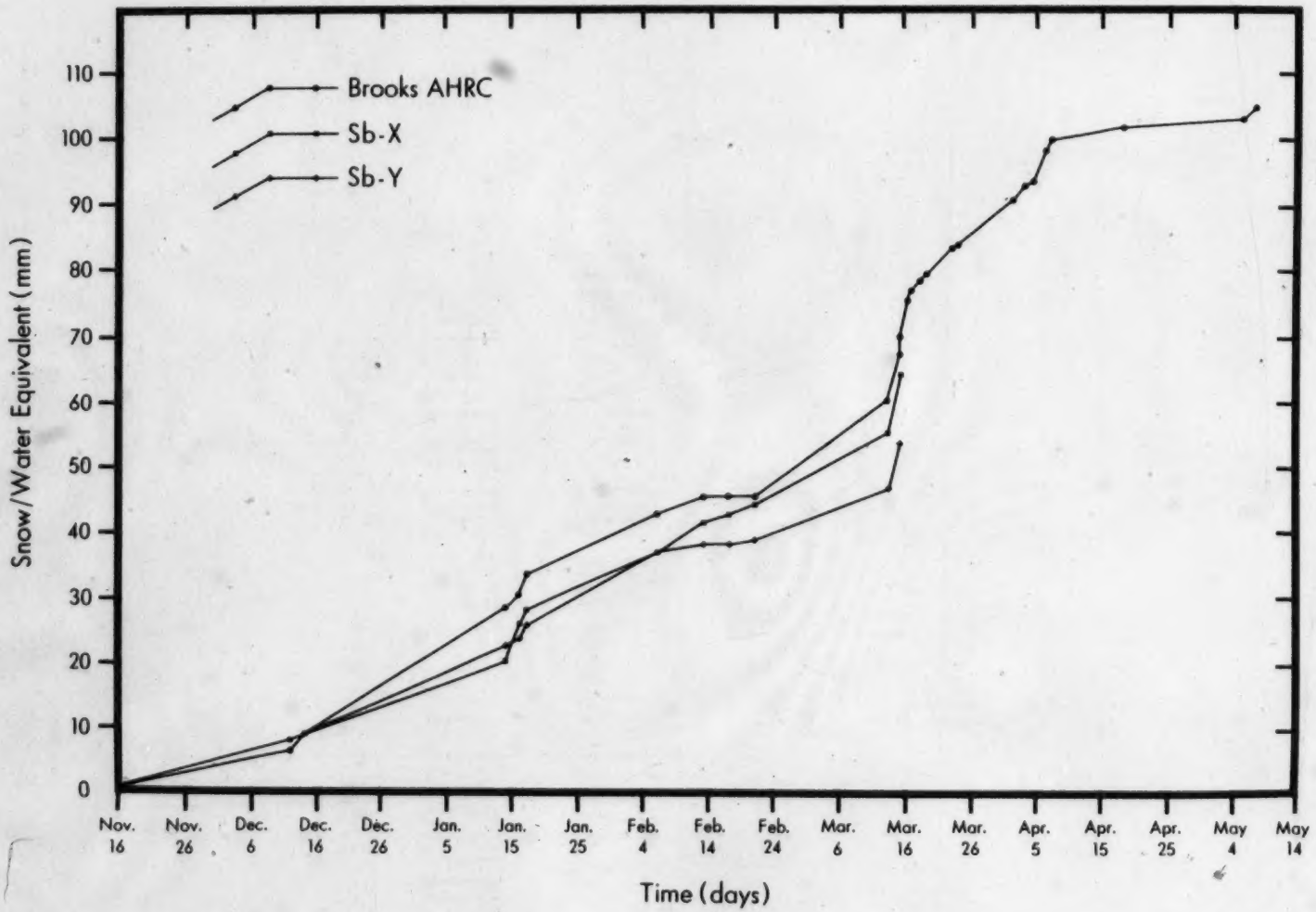

Figure 4.2. Cummulative snow/water equivalents of 1981–1982: Murton gauges (Nov. 16 – Mar. 15) and AHRC (Nov. 16 – May 7).

Table 4.3 shows that water equivalent **(we)** values among the two gauges and the AHRC varies for every measurement period, but that no *one* set of values vary in a consistent manner with respect to the others. There are, however, some conspicuous discrepancies which are easily explained. Between January 14 and 16, the graph (Figure 4.2) depicts a sharp, extended rise in the cumulative **we** line of sb-X, such that it crosses the sb-Y **we** line. Both sb-Y and the AHRC registered small increases in water equivalent during this period (1.3 and 1.6 mm respectively, Table 4.3), yet sb-X recorded more than three times more water (5.1 mm) than either of these places. AHRC snow data (Table 4.1) shows that 2.0 cm of snow fell on January 14th, but that none fell on the 15th. The snowfall of the 16th occurred subsequent to the Murton gauge reading of that day. It is extremely unlikely that 2.0 cm of snow could produce 5.1 mm of water under the meteorological conditions present at the time of snow deposition. Obolenskii (1929, in Chebotarev, 1962) shows that the mean snow density of freshly fallen snow at temperatures below -10°C averages 0.075 g cm^{-3}, with a maximum density of 0.238 g cm^{-3}. The highest temperature recorded in the Park during the January 14 snowfall which began at 5:30 p.m. was -17.5°C. For 2.0 cm of snow, a 5.1 mm water equivalent would produce a snow density of 0.255 g cm^{-3}, which is larger than the theoretical maximum density obtainable at this temperature. This evidence therefore substantiates the notion that the **we** value at sb-X for January 16 is incorrect.

Additional evidence as well as the explanation for the sb-X discrepancy was found through field observations. Shortly before 12:00 noon on January 14, one hour after the snow gauge measurements of this day were taken, an Arctic frontal system with accompanying cold temperatures and strong winds rapidly moved into the field region from the north (see Figures 4.3 and 4.4). Although no snow fell until 5:30 p.m. on this day, fierce winds caused blizzard-like conditions, with snow blowing fiercely for the followng 28 hours. Upon the arrival of the front, snow was observed drifting into the Murton gauge of sub-basin X from the upper grassed surface that comprises the basin's north boundary. Thus, the location of the gauge with respect to both the surrounding physiography and the directional velocity of the wind produced an overcatch of snow, resulting in the excessive **we** value measured two days later, on the morning of January 16.

Figure 4.3. North view of sub-basin X. Seen is the approaching Arctic cold front (dark band on horizon). Photo taken at 11:40 a.m., January 14, 1982. Snow gauge for scale.

Figure 4.4. Southwest view of the main watershed and arrival of the Arctic front. Accompanying fierce north winds and blowing snow (from right to left) begins to obscure the view of distant badlands. Photo taken at 11:50 a.m., January 14, 1982.

The snow gauge located in sb-Y was not subjected to overcatch, as there were no topographic obstacles in the gauge vicinity. That is, the gauge was situated at a higher elevation relative to the main watershed, and was thus much less susceptible to overcatch by far-ranging blowing snow, redistributed from higher topographic features. Therefore, on January 16, it correctly registered only the 1.3 mm of water derived from the 2.0 cm snowfall of January 14.

These qualitative field observations were quantitatively supported by AHRC records and radio reports. AHRC anemograph charts show an abrupt wind change from west to north at 12:00 noon on January 14. The velocity of these north winds averaged 42 km hr^{-1} for the next four hours (12:00 noon to 4:00 p.m.), and averaged 26 km hr^{-1} for the following 24 hour period (4:00 p.m. January 14 to 4:00 p.m. January 15). Radio briefs at 3:00 pm on January 14 (CKBR-Brooks) reported wind gusts of over 60 km hr^{-1}, and a maximum visibility through blowing snow of less than 15 m. In addition, most local highways were closed on the evening of January 14, and not reopened until the morning of January 16. By this time, the Arctic front and strong winds had passed, although the field area remained under the influence of the invading high pressure system and associated cold temperatures (-34°C minimum, -24.5°C maximum during the morning hours of January 16). As shown, these records and field observations adequately explain the variation in gauge catch recognized during this period in mid-January, 1982.

A similar minor discrepancy is seen in Table 4.3 and Figure 4.2 among the **we** values measured on February 18. As illustrated on the graph, the **we** lines of sb-Y and the AHRC remain horizontal (no snow recorded) between the gauge measurements of February 13 and 18, yet that of sb-X rises slightly. Since no snow fell between these days, redistribution of snow must be the cause of the 1 mm **we** measured in the sb-X snow gauge on February 18. AHRC anemograph charts again support this claim, showing fairly strong north winds on the evening of February 13 through the morning of February 14, with a peak average hourly velocity of 24 km hr^{-1}.

The **we** line (Figure 4.2) of the AHRC continues horizontally to the next snow gauge measurement date (February 21), yet both Murton gauges recorded measureable amounts of water. No snow fell between February 18 and 21, except during the morning of February 21. For this day, the AHRC recorded a trace of snow (< 0.1 cm), but a number

of ruler depth readings taken in the field area revealed that approximately 1.0 cm fell in Dinosaur Park. Thus, the discrepancy between the AHRC recording and those of the Murton gauges is partly explained by an areal variability of snowfall.

As implied, spatial differences in snowfall are not entirely responsible, and do not explain the 2.0 mm excess water equivalent measured in the sb-X snow gauge (2.5 mm) *versus* the sb-Y gauge (0.5 mm) on February 21. Between measurements taken on February 18 and 21, very strong southwest winds invaded the field region. However, it is doubtful that these winds caused the small overcatch of the sb-X gauge, because there are no topographic obstructions to the southwest, from which snow could have been blown into the gauge. Anemographs show an abrupt wind change from southwest to northwest at 2:30 a.m. on February 21. These winds continued for the next 11 hours, peaking at 39 km hr^{-1} between 7:00 a.m. and 8:00 a.m. on February 21. It is highly likely that *these* winds caused the overcatching of snow measured in the sb-X gauge later that day.

Water equivalent data in Table 4.3 show that the sb-X gauge overcaught those of sb-Y and the AHRC for seven of the eleven measurement periods. In addition, the AHRC registered larger water equivalents than sb-Y seven times. In general, it may be concluded that the cumulative we of the sb-X gauge as of March 15 (64.1 mm) is larger than that recorded by the sb-Y gauge (53.5 mm) due to the periodic overcatching by the former gauge under strong northerly winds. The generally higher we recordings of the AHRC *versus* sb-Y are most likely due to a naturally-occurring larger snow accumulation at the AHRC station. This notion is best supported upon consideration of the mean annual snow / water equivalents recorded by meteorological stations surrounding the field area, which are depicted on the isohyetal map of Figure 4.5. The map depicts a portion of southeastern Alberta that characteristically receives the least snow accumulation of the province. In the centre of this region lies an anomalous, east-west trending band (shaded pattern, Figure 4.5) of particularly low water equivalents ($\leq$ 90 mm), which varies in width from approximately 25 km to 110 km. As shown, four of the five stations located within a 35-km radius of Dinosaur Park register less than 90 mm of water. The exception is station P, the AHRC, which records 96.6 mm (see Appendix C for station names). From the location of Dinosaur Park with respect to nearby stations, it is clear that the field area should normally receive an annual total season snow / water equivalent of about 85 mm,

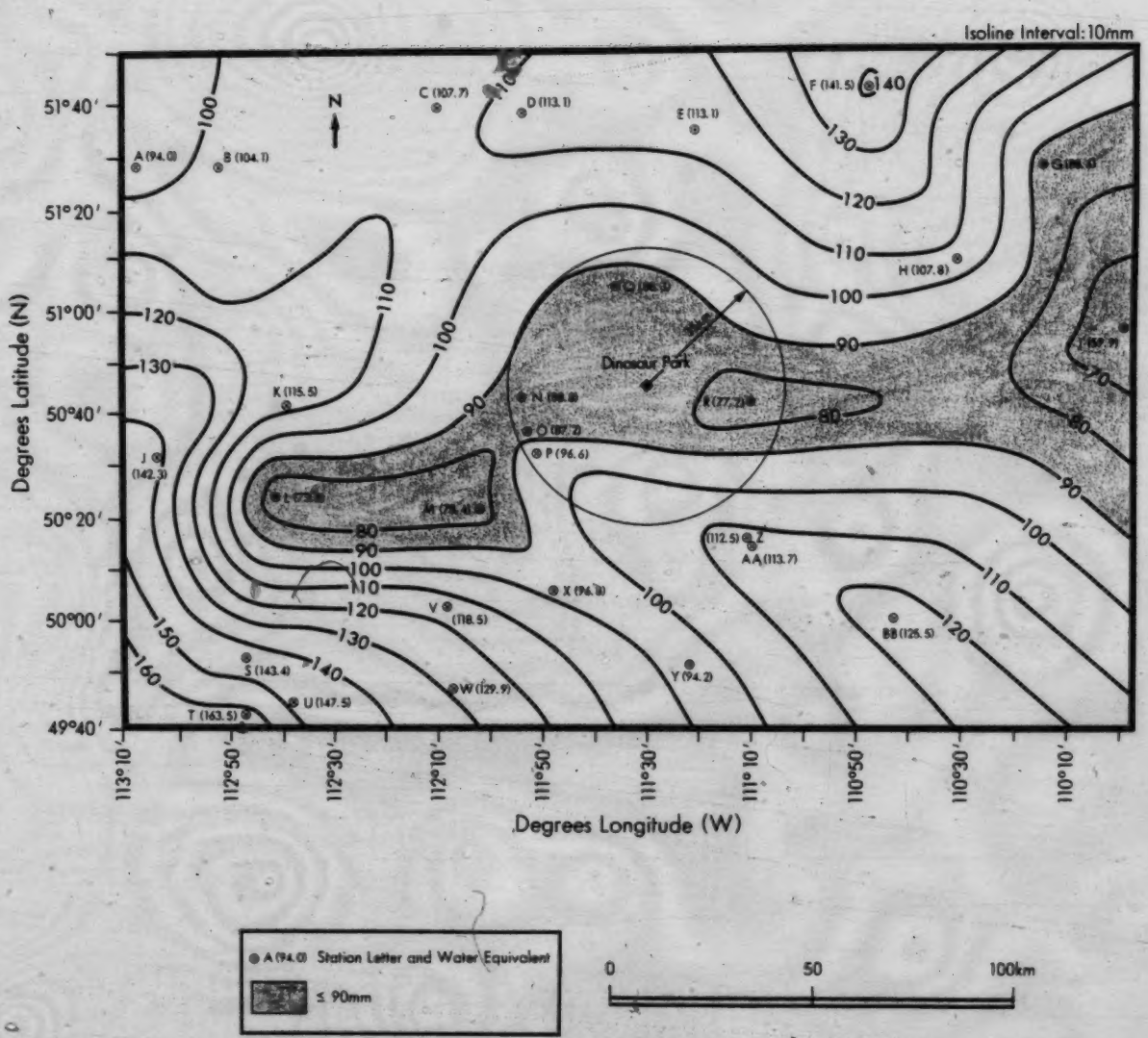

Data Source: Canadian Climate Normals 1951–1980: Temperature and Precipitation – Prairie Provinces. Environment Canada, 1982.

Figure 4.5. Mean annual snow/water equivalents (mm) for stations in southeastern Alberta.

or, in general, approximately 10 mm less **we** per year than the AHRC station. Thus the 13.7 mm less cumulative **we** measured in the sb-Y *versus* the AHRC gauge on March 15 of the 1981-1982 snow season (Table 4.3) is considered the result of a natural spatial decrease in snow accumulation.

As previously noted, the Murton snow gauges register the depth of water derived from snow, but not snow accumulation. Therefore, it was necessary to estimate the depth of accumulation in the field area by dividing the mean snow density of freshly-fallen snow as recorded by the AHRC station (0.071 g cm^{-3} from the first snowfall of November 13, 1981 to March 15, 1982) into the total **we** of the snow gauges. Given that most snow gauges are subject to measurement errors (Weiss and Wilson, 1957; Unesco *et al*., 1970; Larson and Peck, 1974; Goodison and McKay, 1978), due mainly to undercatch caused by wind, it was felt that averaging the two Murton gauge cumulative **we** values would give a better estimate of **we** up to March 15, 1982. That is, the slight overcatch of the sb-X gauge, and the probable slight undercatch of the sb-Y gauge together yield the average **we** of 58.8 mm, which is within general agreement with the 10 mm less water expectancy of the field area *versus* the AHRC (67.2 mm).

Using the average Murton gauge value of 58.8 mm and the AHRC average snow density of 0.071 g cm^{-3}, it is estimated that the badlands received approximately 82.8 cm of snow from November, 1981 to March 15, 1982. Due to its higher **we** value, the AHRC received 94.2 cm during this same period. The latter number is reasonable when compared to the preceding twelve-year total-season mean snow accumulation value of 90.3 cm (Table 4.2). However, as stated earlier, the abnormally large snow accumulation occurring after March 15, 1982 elevated the final AHRC accumulation figure to 141.0 cm.

Since no Murton gauge measurements were taken after midday on March 15, the total season water equivalent and total season snow accumulation values for the field area (November 14, 1981 to May 7, 1982) were extrapolated using AHRC records. For the total season **we**, the partial season (up to March 15) average **we** of the two field gauges (58.8 mm) was proportionately cross-multiplied by the ratio of the partial (67.2 mm) to total season (105.0 mm) water equivalents recorded at the AHRC.[11] This resulted in a total season field **we** value of 91.9 mm (*versus* 105.0 mm for the AHRC). This calculation

---

[11]Similar extrapolation methods are employed between nearby climate stations by Environment Canada to estimate missing meteorological data.

yields a total accumulation depth of 124.2 cm, which is 16.8 cm less snow than that recorded at the AHRC (141.0 cm) for the 1981-1982 season, yet 8.4 cm larger than the highest total snow accumulation recorded at the AHRC (115.8 cm) during the previous twelve seasons (Table 4.2). On this basis, the total season potential snowmelt runoff for the main watershed amounts to 30,953 m^3 of water. Obtained by multiplying total season snow / water equivalent depth (91.9 mm) by basin planimetric area, this figure is considerable, and, as a comparison base, equals the equivalent total precipitation input of slightly more than six 15 mm rainstorms

4.1.3 Intra-season Snow Accumulation and Runoff Potential: Snow Surveys

In this study, data obtained through the monitoring of snowcover characteristics could not be used in a conventional manner as an indication of the seasonal progression of water availabiltity and total runoff potential at the onset of the spring melt period. This is due to the inability to maintain routine snow surveys because of frequent disappearance of snow from survey points as caused by both mid-winter snowmelt episodes and severe snow redistribution by wind. However, data obtained during three mid-winter snow surveys provides information on water availability for specific time periods, which is useful to the evaluation of the nature of snow accumulation within the sub-basins. The data also yields estimations of water available to the entire catchment at the time of the snow surveys. Hence, potential volumetric runoff estimates are similarly compared to the magnitude of water input recognized during rainstorm events.

Average data calculated for the three snow surveys taken in 1982 (January 17, February 5, and March 15) appears in Table 4.4 (individual survey point data is detailed in Appendix D). For the survey of January 17, each average snow density measurement (Table 4.4, column 3) represents the total average density calculated for every snow depth sampling point in all sub-basins, as opposed to densities calculated for each individual sub-basin. This was done because it was found that the spring balance used to weigh snow cores (the weighing-in-field method) was not sufficiently sensitive to give accurate density readings from snow samples of less than about 6.0 cm. Therefore, for this survey only, density measurements were found by sampling points within the sub-basins which contained greater than 6.0 cm of snow depth (Appendix D1, column 2). Due to this

TABLE 4.4. SNOW ACCUMULATION AND WATER AVAILABILITY IN THE SUB-BASINS AND MAIN WATERSHED FOR THREE SNOW SURVEYS OF 1982.

Column #		1	2	3	4 col. (2x3) ÷ 100	5 col. (1x4)
Survey Date	Basin	Basin Area(m^2)	Average Snow Depth (cm)	Average Snow Density ($gr.cm^{-3}$)	Snow/Water Equivalent* (m)	Volumetric Water Available (m^3)
January 17	Sb-X	4,829	6.3	0.15	0.0095	46
	Sb-Y	6,000	8.2	0.15	0.0123	74
	Sb-Z	16,384	5.5	0.15	0.0083	136
	Entire Watershed	336,810	6.7	0.15	0.0101	3,402
February 5	Sb-X		5.4	0.15	0.0081	39
	Sb-Y	same	10.0	0.19	0.0190	114
	Sb-Z	as	5.9	0.16	0.0094	154
	Entire Watershed	above	7.1	0.17	0.0121	4,075
March 15	Sb-X		8.0	0.08	0.0064	31
	Sb-Y	same	6.8	0.105	0.0071	43
	Sb-Z	as	5.8	0.10	0.0058	95
	Entire Watershed	above	6.9	0.10	0.0069	2,324

* Also denotes volumetric water available (m^3) per unit area (1 m^2).

biased sampling scheme, it was felt that the most representative density measurement for each sub-basin should reflect the average density of *all* sampled points (0.15 g cm^{-3}).

The density values of the two remaining snow surveys are taken directly from the *actual* snow course survey points. This was done using the bulk sampling method (described in Chapter 3). For all surveys, density measurements were multiplied by the snow depth measurements taken at the survey course points, to compute snow / water equivalents and thus volumetric water availability.

Table 4.4 shows that for each snow survey, sub-basin Y retains a higher snow / water equivalent value (column 4) than the other two sub-basins, and thus consistently holds more water per unit area. This is true for the survey of January 17 because sb-Y possessed a larger average snow depth than sub-basins X and Z. On February 5, sb-Y displayed not only a higher snow depth, but also a higher average density. Even though sb-Y measured less average snow depth than sb-X on March 15, it retained more water per unit area due to the larger average snow density value.

The higher **we** values recognized in sb-Y for the first two snow surveys are attributed to the larger snow accumulation (average snow depth) present in this basin. This is evident because the same snow densities (0.15 g cm^{-3}) were used in each sub-basin **we** calculation for January 17. Even if sb-Y retained the same, lower average density as sb-X (0.15 g cm^{-3}) on February 5, the larger snow depth would still give a larger per unit area water equivalent.

The larger snow accumulation measured in sb-Y is attributed to snow redistribution as a function of basin form. Both surveys (January 17 and February 5) were conducted after severe snow drifting had taken place, at times when there was minimal freshly-fallen snow on the ground. As discussed earlier, the high-speed north winds occurring on January 14, 1982 had a major influence on snow redistribution in the watershed, which also affected the amount of snow measured during the January 17 survey. Likewise, on January 26, 1982, eight hours of southwest winds with a mean velocity of 43 km hr^{-1} and a peak hourly speed of 50 km hr^{-1} significantly redistributed the snow which fell on each of the previous seven days (Table 4.1). The resulting snow redistribution patterns, which will be examined in more detail in the next section of this chapter, were still evident when the snow survey of February 5 was taken.

The major effect of these two periods of high-velocity winds on the snow surveys was to partially remove the reserves of snow that had originally accumulated in sub-basins X and Z. As shown in Chapter 3, these two sub-basins display similar forms, in that they possess rather expansive, flat-lying lower basin areas which exhibit a generally low surface roughness, with minimum obstacle interference. Thus, these lower basin zones are highly susceptible to snow depletion by wind. In contrast, the deeply-incised nature of sb-Y decreases wind shear velocity within the basin confines, and reduces the amount of snow which may be lifted and removed. These reasons, based on the relationship between basin form and snow redistribution account for the similarity between average snow depths recorded in sb-X and sb-Z on January 17 and February 5 (Table 4.4, column 2), and for the larger amounts of snow measured in sb-Y on these dates.

The variability in snowpack depth, density, and water equivalent values recorded among the sub-basins during the first two snow surveys was generally small for the survey of March 15, 1982. This is due to the fact that this survey was conducted on a newly-derived snowcover which was not subjected to much wind disturbance. Furthermore, the survey took place one day subsequent to the termination of a major snowmelt runoff period, thus there was very little old snow present to cause significant variations in the survey measurements (Figures 4.6 and 4.7) Evidence of the relatively uniform character of this snowfall is seen in that snow densities measured at individual survey points (Appendix D3, column 3) vary little (range difference equals 0.05 g cm^{-3}), reflecting the undisturbed nature of the snowpack. In contrast, density values for the previous two surveys are less similar (range difference equals 0.289 g cm^{-3}), with some points yielding densities of 0.200 g cm^{-3} or more. Such densities indicate the presence of crustal layers within the snowcover, caused by partial melt and refreeze as well as compaction by strong winds. Thus, the lack of high-velocity winds as well as an opportunity for partial melt during this March 15 snowfall did not, at the time of the survey (11:00 a.m. to 12:00 noon), permit a significant depletion of snow from sub-basins X and Z.

A small degree of snow redistribution did occur however, during the morning hours of March 15, but most redistribution took place intra-basinally, in the form of snow

Figure 4.6. East view of the main watershed on March 14, 1982.

Figure 4.7. East (same) view of the main watershed on March 15, 1982.

creep, and thus very little net snow accumulation was lost from any of the sub-basins. The effects of this minor redistribution episode are most easily recognized in sub-basins X and Z, which show a higher range of snow depth values (Appendix D3, column 1) than sub-basin Y. The extreme uniformity of depth values in sb-Y again demonstrates the ineffectiveness with which wind can dislodge snow particles within this basin.

The vegetation cover of both sub-basins also accounts for the slight non-uniformity of the sb-X and sb-Z snowcovers in terms of snow density. Appendix D3 data reveals that the lowest snow densities (column 3) measured on March 15 in sb-X occurred at points 3, 4, and 5, all of which lie on grassed surfaces. Points 6 and 7 in sb-Z, which both have the lowest density values of this basin, are likewise situated on the grassed, upper portion of the basin.

In conjunction with the findings of Goodison (1978), Gray *et al*. (1978), and Fitzgibbon and Dunne (1979), in which the most dense landcover classes surveyed typically retained higher snow depths, it is expected that grassed areas within the study basin, which represent the most dense vegetation class in the watershed, should retain higher snow depths and lower snow densities than the unvegetated survey points. Although snow densities in the grassed areas *are* generally lower for this survey, snow depths are not correspondingly high. This is attributed to the apparent ease with which snow was blown from these grassed areas, which are unobstructed by topographical features in both sub-basins. Furthermore, grass height, especially in sb-X, is extremely short, and offers little protection from snow removal by wind. Hence, for the March 15 snow survey, the generally low average snow density of sb-X (0.08 g cm^{-3} -- Table 4.4, column 3), contributed to the lower water equivalent value obtained for this sub-basin, even though the basin recorded an overall higher accumulation depth than the other sub-basins.

Because of snow drifting, volumetric water availability values calculated for the sub-basins and the entire watershed (Table 4.4, column 5) represent an underestimate of the amount of water present at the time of the snow surveys. This is because most of the snow survey points were located in areas more favourable to snow erosion rather than deposition. Thus, total average snow depth and volumetric water figures generally do not take into account the snow and water equivalent contained in those areas (to be discussed)

susceptible to higher snow accumulation via redistribution.

Volumetric water availability values for the watershed (Table 4.4, column 5) suggest that at the time of each snow survey, the amount of water present was sufficient to potentially generate runoff. This conclusion is based on comparison of these volumetric estimates to those calculated for runoff-producing rainstorms of 1981 and 1982 (see Table 2.3, Chapter 2). The total watershed volumetric snow / water values of 3,402 m^3, 4,075 m^3, and 2,324 m^3 respectively equal water depth inputs of 10.1 mm, 12.1 mm, and 6.9 mm, which are equivalently comparable to inputs derived from lower-precipitation, runoff-producing summer rainstorms (see Table 2.3, column 3).

It should be pointed out that due to partial snow depletion and runoff events occurring between surveys, most of the water recorded on the survey dates represents snow that was newly-generated *between* surveys, rather than simple additions or subtractions to accumulations derived before the surveys. Therefore, volumetric snow / water availability for the survey dates may be considered as individual potential runoff values, in much the same manner as are water potential values of isolated rainstorms. For this reason, volumetric snow / water figures for the three surveys may be justifiably added to obtain an estimate of total water available to the watershed from January 17 to March 15. The results show that close to 10,000 m^3 of water (9,801 m^3) was present during this period, which represents almost one-third of the total season snow / water available in the catchment (30,953 m^3) as determined by the Murton gauge computations.

It is important to state that the 9,801 m^3 figure is a conservative estimate, and does not inclusively reveal the *total* potential runoff present from January 17 to March 15. This is partly due to the fact that the volumetric snow / water values are minimum estimates (snow drifting from survey points), but additionally, because there were some snowfall events and minor melt sequences (in addition to a major melt period) occurring between surveys which could not be measured. Hence, the *actual* total input during this period should be slightly larger than the total amount (9,801 m^3) derived by the addition of watershed snow / water volumes of the three surveys. This assertion was originally made without prior consideration of the Murton gauge data for the corresponding time interval. It was subsequently discovered that from January 17 to March 15, the average cumulative

we value of the gauges measured 32.45 mm. This figure represents a total watershed volumetric snow/water input of 10,929 m^3, which is indeed, for the reasons cited above, slightly greater than that determined through the snow surveys.

Murton gauge and AHRC snow data presented in this section show that the field area received a very large snow accumulation during the 1981-1982 season, equal approximately to one-third of the expected total annual precipitation. However, snow survey results indicate that snow accumulation is affected by wind, resulting in a redistribution and reconcentration of snow and water in certain areas, and by mid-winter melt episodes, resulting in premature partial depletion of snow reserves. The implications of these activities will be discussed in the following sections, to ascertain their importance to the magnitude and frequency of watershed runoff and geomorphic response.

4.2 Patterns of Snow Distribution

Due to the varying nature of snow distribution events, field observations and results obtained throughout the 1981-1982 season are considered and discussed within a framework of four time intervals, each ranging from 2.5 to 6.5 weeks. For each period, wind activity and its influences on snow distribution are outlined. The overall summary of snow distribution patterns for all periods is presented after this series of discussions.

4.2.1 Period 1: November 17 to December 31, 1981

In terms of snow redistribution by wind, this period exemplifies minimal activity. This is due to a relatively small snow accumulation during the period (see Table 4.1), and particularly to the lack of high-velocity winds to permit significant snow drifting. AHRC records show that the first snowfall of the season occurred on November 17, 1981 (1.0 cm) and continued into the next day, dropping a total of 7.0 cm. At the time of deposition, winds were light, shifting from northeast to southeast. Although the author was not present for this snow event, it is probable that snow redistribution was negligible in the absence of sustained, strong wind activity. In addition, the duration of snow on the ground, and thus the duration of susceptibility to wind redistribution was extremely short. AHRC records reveal a total disappearance of this snow by November 23, as the result of chinook activity (to be discussed).

The only observed case of snow drifting during this first period occurred on December 13-14, but even this was minor. Although no snow was recorded at the AHRC station, 0.5 cm fell uniformly over the Park on the evening of December 11, with virtually no wind disturbance. An additional 1.5 cm of light snow was added on the evening of December 13 and morning of December 14. (The AHRC received approximately 5.5 cm more snow accumulation at this time.) As seen in Figure 4.8, this snowfall also coated the field area in a uniform manner, with thinner deposits found on the steepest slope segments. Several sets of snow profile measurements taken along pediment and fan surfaces throughout the watershed revealed a consistent range in depth, varying from 1.5 to 2.0 cm.

For the December 13-14 snow period, AHRC anemographs show a peak wind speed of 13.0 km hr^{-1} (3.6 m s^{-1}) from the southeast. This wind velocity exceeds the threshold shear velocity of 3.0 m sec^{-1} for initial snow particle dislodgment of newly-fallen snow (McKay and Gray, 1981), although it falls short of most other threshold estimates (see section 2.12 -- chapter 2). Field observations showed that the snowcover was removed only in the vicinity of unvegetated, unobstructed hillslope crests or interfluves (of sandstones and claystones) located at high elevations within the catchment. Even so, such crests remained snow-covered, with only those surfaces composed of disaggregated claystone showing evidence of the southeast wind flow, in the form of streamlined snow drifts generated to the lee of micro-scale protuberances (Figure 4.9). In all, no significant snow redistribution or preferential accumulation was recognized during period 1.

4.2.2 Period 2: January 1 to January 17, 1982

During this period, the field area experienced cold temperatures, with an average daily maximum temperature of -22°C, and an average daily minimum temperature of -29°C. Table 4.1 shows numerous small snowfalls were received during the first two weeks of this month. AHRC snowfall data reveals that 24.8 cm of snow fell during this time, and average Murton gauge data indicates an approximate accumulation of 15 cm. A 1 m^2 x 1 m^2 snowboard placed in a flat, open area in the Park measured 10.0 cm of snow between December 15, 1981 and January 12, 1981. This information implies that as

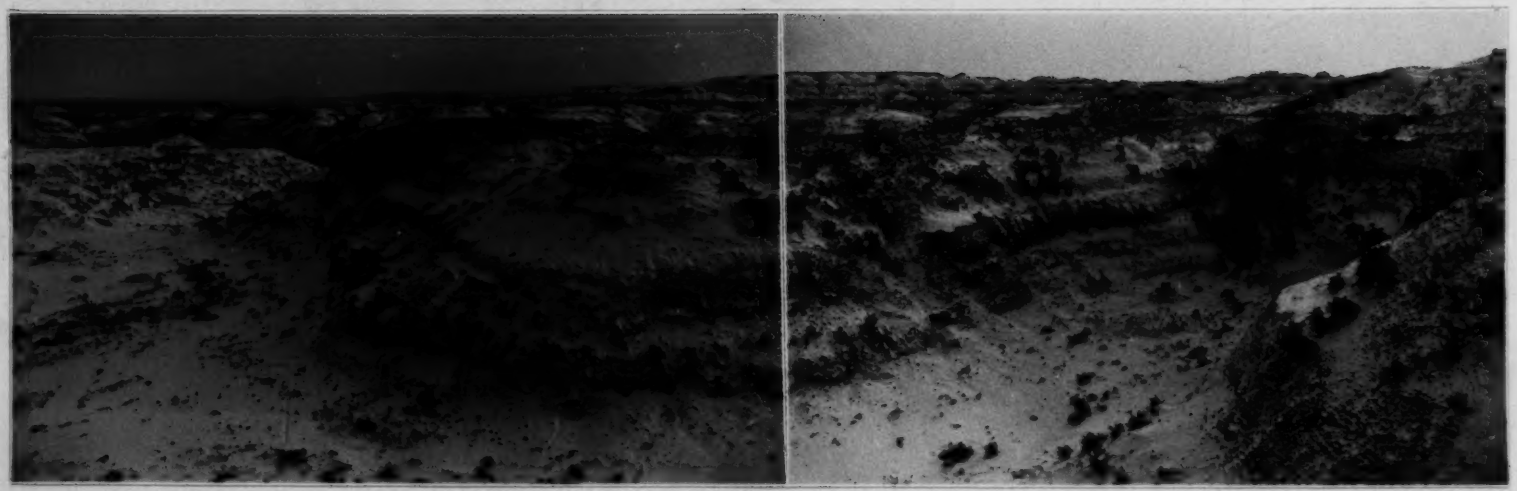

Figure 4.8. Uniformly-distributed shallow snowcover in sub-basin Z. As indicated by the darker bands of claystone, only the steepest slope segments do not retain the 2.0 cm accumulation which fell from December 11 to 14, 1982.

Figure 4.9. Micro-scale, streamlined snow deposits on the northwest sides of claystone aggregates indicate snow drifting under southeast winds of December 13 and 14, 1981.

expected, the field area received less snow than the AHRC. In addition, the 5.0 cm less snow recorded on the snowboard *versus* the the Murton gauge average is mainly attributed to the settling of snow, but also to partial depletion by wind.

AHRC records of January 1 through January 12 show that wind velocity (magnitude and direction) was highly variable, and that snowstorms occurred under generally light, but some strong wind speeds. Although no noticeable preferential snow distribution was observed upon arrival in the field on the afternoon of January 13, 19 hours of strong, alternating southwest and west winds began at 4:30 p.m. of this day, resulting in a significant snow drifting-episode. Wind speeds during the 19 hours averaged 29 km hr^{-1} (8.0 m sec^{-1}), and maintained a peak speed of 39 km hr^{-1} (10.8 m sec^{-1}) from the west between 9:00 and 10:00 a.m. of January 14. As a result of these strong west winds, much snow was blown into gullies, vegetation-filled channels, and other surface depressions. Gullies with long axes trending north-south retained up to 75 cm of snow under transverse wind deposition. East-facing slope lees also retained large deposits, derived from smooth pediment/fan surfaces as well as windward-facing slopes (Figure 4.10).

High-velocity west winds were abruptly replaced at 12:00 noon on January 14 by the strong north winds of the invading Arctic front mentioned earlier in this chapter. Recalling that these north winds maintained an average speed of 42 km hr^{-1} (11.7 m sec^{-1}) for the first 4 hours, and yielded gusts of 60 km hr^{-1} (16.7 m sec^{-1}), it is easily seen that these speeds were more than adequate to cause significant snow movement. In fact, these speeds easily surpass the minimum threshold shear velocities (8.0 m sec^{-1} to 10.5 m sec^{-1}) suggested by Kungertsev (1956) and Kotlyakov (1961) to move moderately compact and wind-hardened snow.

Some important discoveries were made concerning preferential snow distribution under the January 13-14 west winds and January 14-15 north winds. Field observations during this visit (as well as subsequent ones) showed that snow consistently amassed in rill channels and was blown free of slope interfluves *regardless* of wind direction, provided wind speed was of sufficient magnitude to initiate blowing snow. Evidence of this is shown in the photographs of Figures 4.11 and 4.12. Figure 4.11 depicts a north-facing, aggregate-mantled claystone slope subjected to the strong, transverse west winds. As

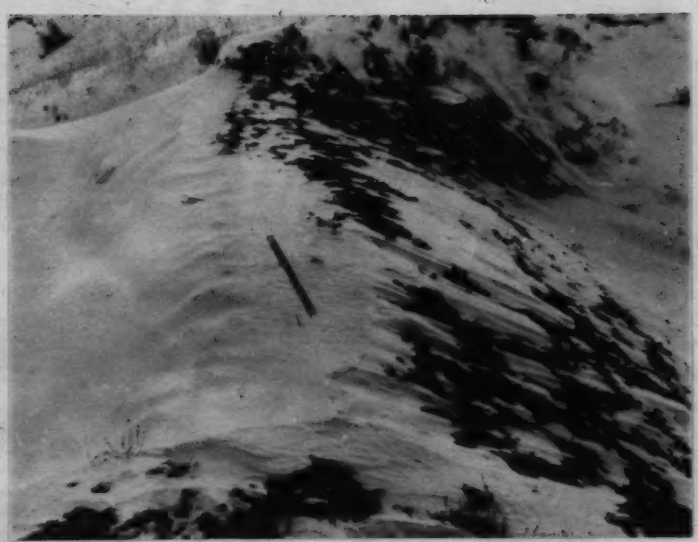

Figure 4.10. Strong west winds of January 13–14, 1982 (wind direction right to left) permit substantial snow deposition to the lee side of this claystone slope in sub–basin X. Metre stick for scale.

Figure 4.11. Transverse-oriented west winds of January 13-14 (blowing left to right in photo) remove snow from interfluves of this north-facing claystone slope (sb-Z), while depositing it within adjacent rill channels.

Figure 4.12. North winds of January 14-15 compact blowing snow into rills of this windward- and north-facing sandstone slope (sb-Y), while removing it from smooth interfluves.

seen, interfluves were exposed, retaining little snow. Figure 4.12 depicts another north-facing slope, composed of sandstone, which also illustrates preferential snow distribution in rills. Strong north winds of January 14-15 compacted snow into these small depressions, while easily removing it from the adjacent interfluve surfaces.

Comparison of Figures 4.11 and 4.12 demonstrates that rilled sandstone slopes exhibit more distinctly-defined accumulation zones than rilled claystones. The latter generally sport a higher micro-scale surface roughness, thereby permitting more snow entrapment and depostion on interfluves. Preferential snow distribution in rill depressions of all slope orientations was observed continuously throughout the field season. The geomorphic implications of this will be outlined in a later section of this chapter.

The north winds of January 14 and 15 caused a number of other significant changes in the location of watershed snow reserves. In addition to the snow retention observed in rills, large quantities of snow were redistributed onto south-facing slopes. Although recognized on south slopes of all lithologies, this was particularly obvious on sandstones, where smooth, north-facing slope interfluves easily permitted snow entrainment and redeposition onto the opposite, south-facing slope faces (Figures 4.13 and 4.14). Significant snow drifts formed at the bases of south slopes, with a gradual upslope thinning. As expected, snow drifts also formed to the leeward side of smaller obstacles (Figure 4.15) and vegetation clumps (Figure 4.16). Larger accumulations were added to many of the already snow-filled incised gullies and collapsed piping channels.

Field observations upon cessation of the January 14-15 redistribution episode revealed that flat-lying surfaces, including pediments, alluvial fans, and areas covered in short grasses were primary source locations for drifted snow. Many near-level surfaces, such as those depicted in Figures 4.17 through 4.20 were rendered almost snow-barren during the windstorm. Slope interfluves, steep slope faces, and slope ridges served as secondary depletion areas in terms of bulk snow removed. In combination, the strong westerly winds of January 13-14, and the north winds of January 14-15 piled largest accumulations into surface depressions and onto slopes of eastern and southern exposures.

Further support for statements made on the locations of snow drifts is gained upon consideration of the depth of accumulation on January 17, at those survey points

Figure 4.13. Head basin area of sub-basin Y on January 16, 1982. Note snow-filled rills and wind-swept interfluves on the north-facing sandstone divide. Opposite, south-facing slope is completely snow covered.

Figure 4.14. Knife-edged crest of a sandstone slope in sub-basin Y on January 16, 1982. North winds of the previous two days redistributed snow from interfluves on the north-facing slope (28° mean slope angle) to the south-facing, wind-sheltered slope (48° mean slope angle).

Figure 4.15. Hoodoo in sub-basin Y showing maximum snow redistribution on the south-facing flank (January 16, 1982).

Figure 4.16. Vegetation clumps stabilize blowing snow that would otherwise be removed from this flat, relatively smooth pediment surface (January 16, 1982).

Figure 4.17. This northwest-trending, flat-floored coulee was a primary source area for snow removal by wind (January 16, 1982). Remaining snow is stabilized by vegetation and the formation of a dense snow crust. Metre stick for scale.

Figure 4.18. Footprints entrenched 6.0 to 7.0 cm into a 10.0 cm snowcover on January 14, 1982 were transformed into 3.0 to 4.0 cm raised prints by the action of northwest winds (photo taken on January 16, 1982).

Figure 4.19. Basal region of this south-facing slope forming the northeast rim of sb-X retains approximately 40 cm of snow on January 15, 1982. North winds of the previous day permitted snow drifting from the short grass region above this slope, thereby adding accumulation to the protected lee slope face. Metre stick for scale.

Figure 4.20. Northeast view of the lower basin of sb-X on January 17, 1982. Note that the 1 m high mini-mesa supporting the Murton gauge retains much snow on its south-facing slope face. Slope breaks and vegetation hollows also retain large accumulations. Snow survey stake #2, bent by persistent northwest winds, is visible in the left foreground of the photo, and is located atop a flat, wind-swept ironstone surface.

which measured the highest snow quantities. In sub-basin X, the largest accumulation was registered at point 1 (21.6 cm), situated on a sandstone pediment, 30 cm from a cluster of snow-trapping sage bushes. Point 6 in sb-Z, located on a south-facing, grass-lined upper wall of an east-west trending collapsed pipe channel retained the highest snow depth (11.6 cm) of this basin. In sb-Y, point 4, situated on an alluvial fan one metre in front of the base of an east-facing sandstone slope measured 19.0 cm of snow. Not only did this point yield the largest snow depth of sb-Y on this first survey date, it also retained the highest value of the six basin points for the remaining two surveys. The snow depth measurements of sb-Z and sb-Y adequately substantiate the higher south- and east-facing slope base snow accumulations recognized after this mid-January snow-drifting episode.

As stated earlier during the discussion on snow accumulation, the majority of snow survey points were not in areas subject to high snow accumulation resulting from wind redistribution. That is, there were few points located at slope bases, within gullies, or very close to other topographic obstacles, which is in compliance with survey design recommendations outlined in the snow surveying guide (Environment Canada, 1972). The 10.0 cm of snow recorded atop the survey board on January 12, added to the 2.0 cm which fell on January 14, and to an additional 2.3 cm which fell in the badlands during the late evening of January 16 ,yielded a total snow depth of 14.3 cm. There was negligible melt between January 12 and the snow survey of January 17, therefore snow drifting must account for the lower average accumulation value of 6.7 cm determined by the January 17 survey. This means that approximately 7.6 cm of the surface snowcover was redistributed to areas other than the survey point locations, and, as stated previously, that the total watershed contained more water equivalent than that estimated through the survey.

4.2.3 Period 3: January 18 to February 20, 1982

From the beginning of period 2 (January 1) to the near end of period 3, the field area experienced a gradual build-up of snow reserves, with a maximum seasonal accumulation realized by February 12, 1982. The large number of small-magnitude snowfalls recognized during period 2 continued throughout the first 3.5 weeks of period 3, during which time the maximum daily temperature rose above 0°C only twice (on

January 26 and 27). One minor and one major snowmelt event occurred during the period, as well as two major snow-drifting episodes. These were of further importance to the determination of the characteristic seasonal snow distribution patterns in the badlands.

Snow accumulation in the field area continued under very cold temperatures and relatively light to moderate wind conditions from January 18 to January 25. On the morning of January 26, however, strong southwest winds, blowing with an average speed of 43 km hr^{-1} for 4.5 hours produced profound effects on snow distribution in the badlands. Although the author was not in field residence at this time, snow distribution patterns induced by these winds remained clearly evident by the following observation period which commenced on February 4. On this day, many of the flat-lying areas outside and within the main watershed displayed transverse snow ripple marks, indicating creation by moderate- to high-speed southwest and west winds. In addition, heavy snow accumulations were found on northeast- and east-facing slope lees and other depressions maintaining a northeast- or east-facing headwall (Figure 4.21).

Although the southwest winds of January 26 redistributed a large quantity of snow and created southwest-northeast oriented drift patterns, many of the drift formations created by the previous west and north winds of January 13 to 15 remained stationary. This is due in part to snowpack stability afforded by the regular formation of a thin surface glaze by means of radiation melt and regelation (even during cold temperatures). However, it is more significantly attributed to the inability of the southwest winds to appreciably deplete snow from those areas previously under the depositional influence of west and north winds. That is, the large snow deposits created earlier upon south-facing slope lees remained in place (Figure 4.22), with the southwest winds of January 26 acting as a reinforcement by windwardly compacting these thick reserves against the slope wall. Although the westerly component of these southwest winds may have caused a slight transverse removal of snow from south slopes, this snow would, theoretically, become redeposited on east-facing slopes, thereby adding even more snow to that deposited earlier in mid-January. It is doubtful, however, that much snow was removed from south slopes, as the stabilizing regelation glaze observed throughout the watershed appeared most prominently on south-facing slopes. These slopes received more direct solar

Figure 4.21. Southwest winds of January 26, 1982 created a snow cornice in the headwall region of this northeast-facing surface hollow of sub-basin X. Southwest wind direction is indicated by the streamlined appearance of the grassed area in the right of the photo. Picture taken on Feb. 5, 1982; mitten for scale.

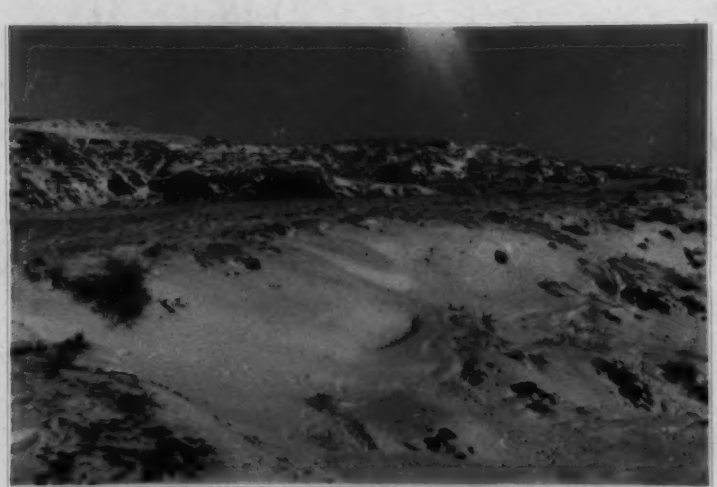

Figure 4.22. South-facing headwall slope of sub-basin X retains a large snow accumulation despite changes in effective wind velocity. (Same slope as that pictured in Figure 4.19). See text for explanation.

radiation during the day, which permitted more melt and thus the formation of a denser surface crust upon refreeze than slopes of other orientations.

The strong southwest winds of January 26 were accompanied by warm temperatures reaching a maximum of 5.5°C on this day and 3.5°C on January 27. This chinook activity induced partial melt of the surface snowcover, resulting in a 5 cm reduction in the depth of snow lying on the ground as recorded by the AHRC (14.0 cm on January 25; 9.0 cm on January 27). Field observations and snow survey results of February 5 suggested however, that this partial melt event served to increase the average snow density of the snowcover rather than initiate a runoff episode. It most importantly served to impart further stability and resistance to wind movement, to preferentially-distributed snowpacks.

The second and last major snow redistribution episode of this period occurred on February 6 and 7. AHRC anemographs show that northwest winds attained a mean maximum speed of 42 km hr^{-1} between 1:00 a.m. and 2:00 a.m., and between noon and 3:00 p.m. on February 6. Radio briefs during this day reported gusting to 70 km hr^{-1}. These winds acted predominantly on the loose snow provided during the light snowfalls of February 1, 2, the evening of February 5 (c. 1.0 cm), and the evening of February 6 (c. 1.3 cm, although not recorded by the AHRC). Once again, these high-velocity northwest winds swept flat-lying areas virtually clean of snow, redistributing it into surface depressions, onto southeast, east, and south slope lees, and behind smaller obstacles. This snow-drifting event further added accumulations to many pre-existing deposits (Figure 4.23).

The last snowfall of period 3 occurred on February 11-12 (see Table 4.1), under slight northeast winds, and a few days prior to a major snow depletion and runoff episode. Therefore, the steady snow accumulation realized from January 1 (period 2) reached a maximum by February 12. On this day, several ruler depth measurements were arbitrarily taken from a variety of relief features, to provide estimates of the relative amounts of snow (thus water) contained within given areas of the watershed. Although accumulation depths were highly variable throughout the catchment, the following three depth categories and accompanying snow accumulation locations were generally found on February 12, 1982:

Figure 4.23. Cross-section through a northwest-southeast-trending lee snow drift on February 13, 1983. Shown is a crust layer (dark band) formed during the chinook of late January, lying below the top 2 cm of snow redistributed on February 6 and 7. The drift was originally created during the north wind redistribution episode of January 14-15, 1982, and shows evidence of lower crust layers which aided in its stabilization throughout repeated windstorms.

1. **0 to 19 cm of snow:**
   a. flat-lying pediments and fans;
   b. flat-lying ironstone mantled surfaces;
   c. grassed areas elevated more than c. 10 m above the floor of the main watershed;
   d. slope faces (except on mid-slope treads).

2. **20 to 49 cm of snow:**
   a. slope bases, especially those facing south and east (includes mid-slope riser bases);
   b. Surface depressions, including shallow source hollows at gully head regions, and larger-scale, partly wind-sheltered basin head regions.

3. **50 to 65 cm of snow:**
   a. linear surface depressions, including collapsed, vegetation-lined pipe channels, and larger incised gullies and ravine floors;
   b. some south-facing slope bases.

The average snow depth of 7.1 cm measured during the snow survey of February 5, added to the approximate 3.0-cm snowfall of February 11-12 (total 10.1 cm), reflects the predominance with which snow survey points were located in areas included in snow depth category (1) above. As mentioned, the flatter-lying, open fan, pediment, and ironstone surfaces, exhibiting low surface roughness characteristics, were often deflated of snow except where crust formation was permitted or where small obstacles anchored deposits. Grassed areas and slope faces usually retained more snow than these areas, but again, they were also subjected to depletion by wind, and, in the case of slope faces, also by gravity. It follows that the water equivalent (which, as stated in Chapter 2 can be correlated closely with snow depth) in areas cited in category (1), which constitute a high percentage of the total watershed area, is low compared to that in snow deposition categories (2) and (3).

Terrain features of categories (2) and (3) often possessed from 2 to 6 times more snow than those of category (1). This observation is in agreement with the results of Siberian prairie snow studies (cited by Kuz'min, 1960) in which it was found that ravines and gullies (category 3) may retain 4.5 times more snow than surrounding open areas (category 1). Vegetation-filled linear depressions lost very little of their redistributed deposits, regardless of whether subsequent winds blew transverse or parallel to the axial orientation of these features. This is due to the combined influence of topography and vegetation. That is, although topography contributed to the intitial receipt of redistributed snow by reducing wind shear velocity, sage bushes, cacti, and grasses inside gullies

ensured that this redeposited snow remained intact. Thus, gullies, plus narrow, unvegetated, but deeply incised collapsed pipe channels (e.g., the upper 35 m of the main channel of sb-Y) received and retained very large snow deposits.

In general, most slope bases contained a bit less snow than gullies. This is due to the fact that whereas incised and vegetation-lined gullies received and retained re-blown snow under strong winds of all directions, the ability to accumulate and maintain snow reserves at slope bases depended largely on the directional strength of snow-redistributing winds. And, since it was shown that winds from more than one direction were able to initiate snow drifting, no one slope of a given orientation received redistributed snow *continuously* throughout the season, as in the case of most gullies. However, consideration of the relative quantities of redistributed snow among slope bases of differing orientations shows that as of February 12, south-facing slope bases were generally in possession of larger deposits. East-facing slope bases also contained significant accumulations. Although north- and west-facing slope bases displayed deposits which also dictated their placement into depth category (2), snow in these areas was generally less than that realized at the basal regions of south- and east-facing slopes. The hydrologic and geomorphic implications of these observations, which became evident during the major melt period of the last week of period 3, will be examined later in this chapter.

4.2.4 Period 4: February 21 to April 8, 1982

During this period, post-fall snow drift formation was effectively patterned by northwest winds. Although very strong southwest winds were influencial in blowing snow on two observed occasions (February 20 and March 11), directional changes to northwest intervened both times, abruptly altering the orientation of drift patterns. However, with regard to slope face and slope base accumulation, directional shifts in strong winds permitted higher accumulations on lee, east-facing slopes, owing to the mutual westerly component of southwest and northwest winds. This is illustrated in Figure 4.24, in which a north-south trending sandstone slope is shown to retain more snow on its east-facing side after sequentially-strong southwest and northwest winds of February 20-21 subsided. As seen in the photograph (Figure 4.24), the quantity of snow affected by these

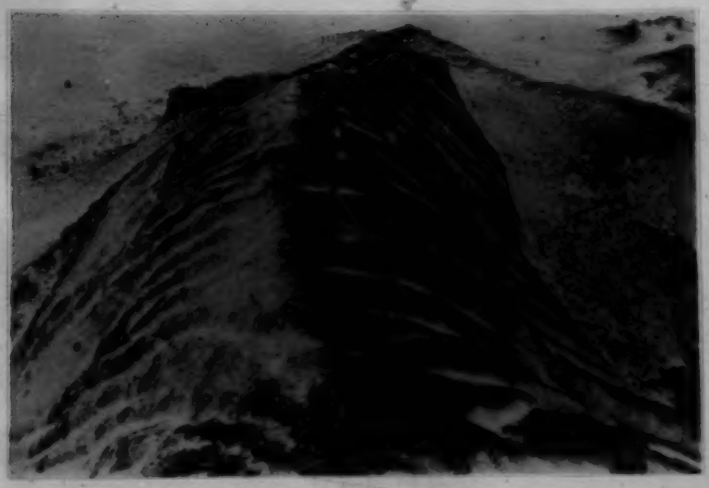

Figure 4.24. Sandstone slope in sub-basin X on February 21, 1983. Snow is redistributed onto the east-facing slope after the cessation of sequentially-occurring, high-velocity southwest and northwest winds. Metre stick for scale.

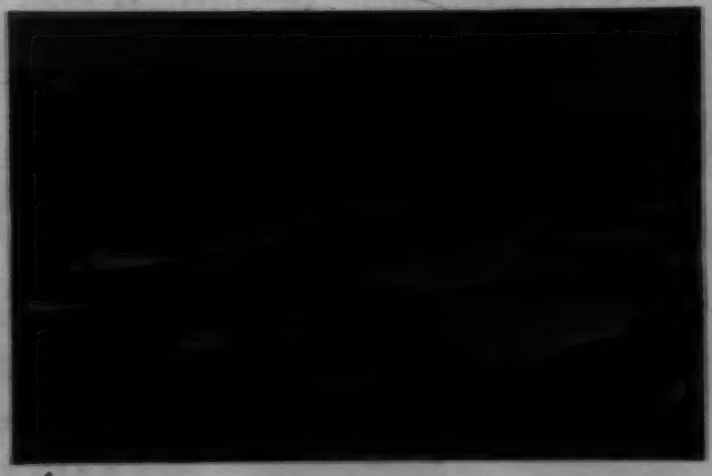

Figure 4.25. Oriented snow drifts formed behind clumps of sage and long grass by extremely strong northwest winds of March 11-12, 1982. Metre stick for scale.

winds was minimal. This is attributed to the lack of fresh snow available (only c. 1.0 cm in depth) at this time.

During the 15 days following this small snow-drifting episode, the field area received steady snowfalls (Table 4.1, February 22 - March 8). Temperatures during these two weeks remained below 0°C, with an average maximum daily temperature of -8°C. A total of 21.8 cm of snow fell in this interim-visit period according to AHRC records. Application of average snow density values (at the AHRC) to Murton gauge water equivalent figures reveals that the field area received approximately 13.3 cm of snow. Anemograph charts show light to moderate wind speeds during this time, with no exceptionally strong or long-duration winds occurring on days receiving snow. On March 7 (a non-snow day) however, 10 hours of north and northeasterly winds with an average speed of 28 km hr^{-1} invaded the region, possibly causing some snow-drifting activity. In addition, prevailing wind directions during snowfalls were highly variable, but generally northerly (especially northeast) in origin. The overall lack of high-velocity winds during this time is reflected in the sub-basin X and Y snow gauge measurements (Table 4.3, March 12), which differ by only 1.8 mm (10.2 and 8.2 mm respectively).

The second major melt episode of period 3 lasted from March 9 to March 14, during which time the maximum daily temperature averaged 6.8°C. Very strong southwest winds were observed on March 11 (8:00 a.m. to 7:00 p.m.), averaging 32 km hr^{-1}, with a peak speed of 43 km hr^{-1}. Although this wind caused noticeable snow drifting, the degree of snowmelt and snowpack priming which had occurred during the two days prior to the onset of this wind episode ensured that only a very small amount of snow was available for redistribution.

As mentioned earlier, southwest-northeast oriented drift patterns were immediately altered by a wind change originating from the northwest. This switch occurred at 7:00 p.m. on March 11, and continued until 10:00 a.m. the following morning. These winds possessed the highest speeds recorded over the entire winter season, averaging 43 km hr^{-1} for the 15-hour duration, with a peak speed of 61 km hr^{-1}.

Approximately 1.0 cm of sleet and snow fell simultaneously at the onset of the northwest winds of March 11, but precise depth measurements were difficult to obtain due to blizzard conditions. One result of this episode is easily seen in Figure 4.25, which

shows the high efficiency with which the winds caused leeward snow accumulation. Snow was also blown onto south- and east-facing slope lees. Although there was again, little snow present on the ground at this time, wind data and snow distribution photographs adequately demonstrate the effectiveness with which southwest and northwest winds continued to influence snow distribution.

As pointed out earlier in the discussion of snow survey results, the approximate 7.0 cm of snow which fell in the field on the morning of March 15 was not subjected to severe wind redistribution while falling. Some degree of drifting may have occurred in days subsequent to this snowfall, but no further field observations were made. By this time, sufficient data on snow drifting, snowmelt, and geomorphic characteristics was obtained, and additional observations were not necessary. However, it should be added that during the last three weeks of period 4 (March 16 to April 8), the field area experienced alternating snowfall and melt episodes, and that maximum daily temperatures exceeded 0°C consistently as of April 8, 1982.

4.2.5 Summary of 1981-1982 and Long-term Wind and Snow Distribution Patterns

This section summarizes wind characteristics and snow-drifting episodes occurring over the four intra-season periods discussed, and presents a generalized concept outlining wind and snow movement in the badlands. As field observations of wind direction and speed were found to closely parallel data recorded by the AHRC station, quantitative wind values taken from the AHRC are used directly in the evaluation of relationships between wind and observed patterns of snow distribution.

Quantitative compilations of 1981-1982 winter wind data are given by means of wind rose diagrams of Figure 4.26, with corresponding numerical data appearing in Appendix E. These diagrams are extremely important, as they substantiate both short-term observations as well as the long-term theory of snow distribution. The frequency percentage rose illustrated in Figure 4.26a gives prevailing wind directions during 404 six-hour intervals over the winter period. As shown, there was no characteristic dominance of a particular wind orientation. This identical observation was made earlier in Chapter 1, while analyzing the ten-year average annual frequency percentage wind rose for the AHRC (Figure 1.3a). In fact, both roses are strikingly similar

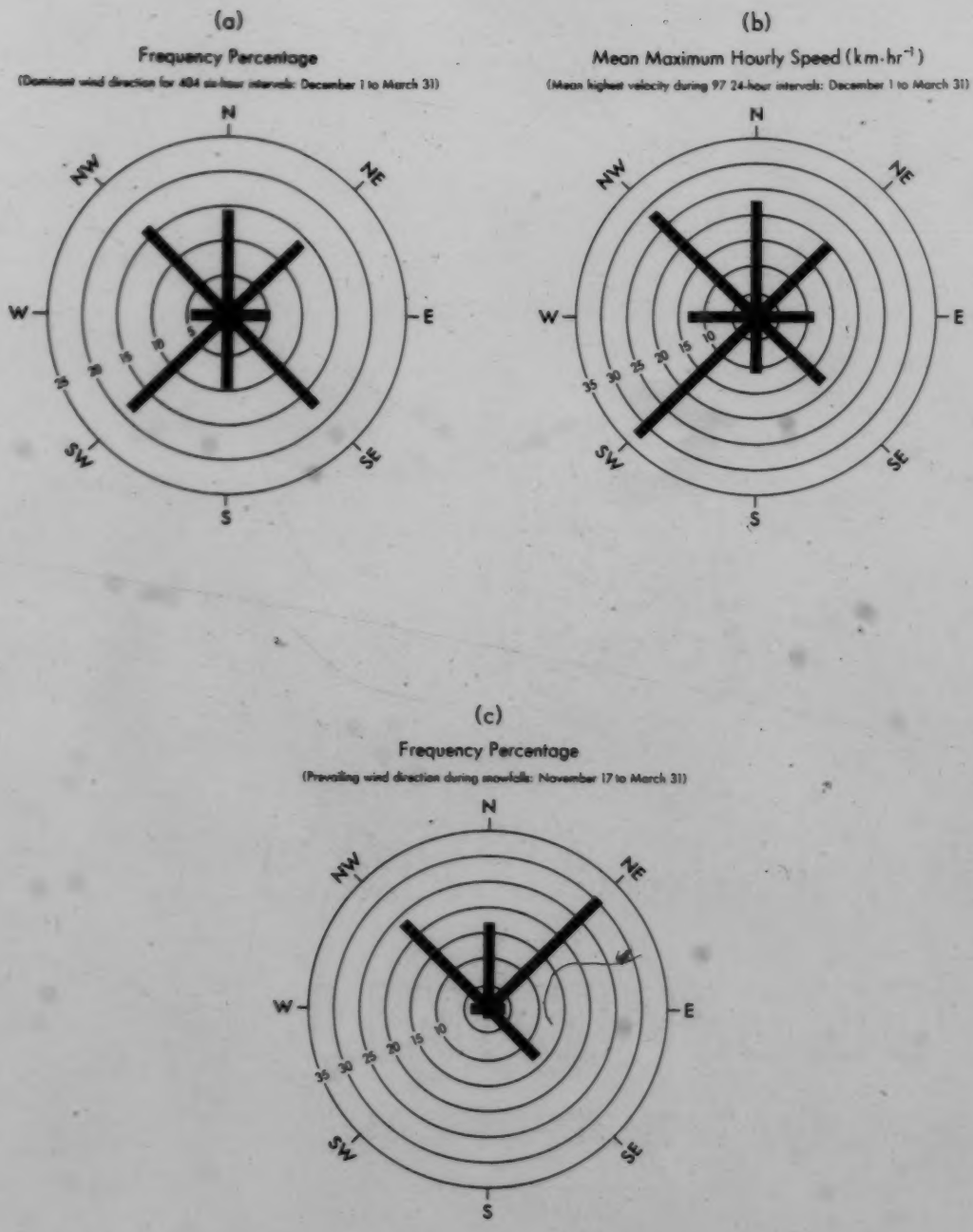

Note: For precise numerical values, see Appendix D.

Figure 4.26. Wind rose diagrams for Brooks AHRC: 1981–1982 winter season.

despite the four-month *versus* ten-year data representations. This implies that the 1981-1982 short-term wind frequency observations (Figure 4.26a) closely reflect those of the long-term (Figure 1.3a), and thus supports the view that the 1981-1982 snow season was 'typical' in terms of wind behaviour.

As it has been established that the direction of the *strongest* winds is the most important consideration to snow movement and seasonally-repetitive redistribution, the velocity rose of Figure 4.26b is instrumental to the determination of such activity. This diagram illustrates the mean velocities of the highest wind velocity recorded during 97 24-hour intervals.[12] It reveals that the strongest daily wind speeds during the winter originated from the southwest, followed in second place by northwest winds, and in third by north winds. Again, this same pattern was found for the ten-year mean annual AHRC wind speeds depicted in the rose diagram of Figure 1.3b (Chapter 1),[13] and also attests to the adherence of short-term wind observations to long-term wind recordings. Most importantly, it enforces the concept of the bimodal nature of effective snow-redistributing southwest and northwest winds as observed throughout the four intra-season periods, and as earlier hypothesized from long-term wind data. It is therefore stated with a good degree of assurance that the observed pattern of alternating northerly and southerly high-velocity winter winds is a seasonally-repetitive characteristic in the Alberta badlands.

As is drawn from the discussion of intra-season snow distribution given earlier, these alternating winds were very efficient in redistributing snow within the field region. Throughout the winter, flat areas within the watershed (and sub-basins) served as supply areas for snow removal activity. Virtually all depressional features received wind-blown snow, regardless of wind direction. Reception areas subject to preferential distribution due to the directional strength of northwest and southwest winds were leeward-facing north, clockwise to south slopes. Surface depressions and lee slopes may therefore both be considered areas of seasonally-repetitive snow accumulation; the former because of

---

[12]For example, if the highest wind speeds recorded on January 1, 2, and 3 were respectively 10, 20, and 30 km hr^{-1}, all originating from the north, the graphed rose value for this direction would be the average of these speeds (20 km hr^{-1}), assuming the highest daily wind speed during the four-month sampling period originated from the north on these three days only.

[13]Wind speeds of Figures 1.3b are of generally lesser magnitude than those of Figure 4.26b due to the comparison of mean *highest* wind speeds to mean *average* wind speeds.

the presence of strong winter winds, and the latter due to the directional components associated with these winds.

The concept of preferential lee slope accumulation is illustrated in Figure 4.27, which depicts a hypothetical, octagonally-shaped isolated hill in which each slope face is directed towards one of the eight major compass orientations. Although all slope orientations received redistributed snow during the field season, it was found that slopes oriented to the lee of the strongest winds generally received more snow than windward slopes. And, as mentioned previously, and also shown in Figure 4.27, the combined influence of strong southwest and northwest winds resulted in large accumulations at the basal portions of east-facing slopes.

These findings differ slightly from those of Beaty (1972), who solely stresses the importance of west and southwest chinook winds to snow redistribution. This is not to say that Beaty (1972) is incorrect, but rather, that the pattern of snow distribution becomes bimodally modified to include the effects of north and northwest winds, as the area under investigation becomes more peripheral (towards the north or west) of the main chinook belt in southwestern Alberta.

This idea is supported by the long-term patterns of effective winds in Alberta, as determined by Odynsky (1958), through his examination of U-shaped sand dune orientations. Odynsky recognized the variation in effective winds (northwest and southwest) in southern Alberta, claiming this variation is greatest in the southeast. According to dune and wind orientation maps prepared, effective winds in the vicinity of Dinosaur Park are from the northwest, with dune orientations averaging 20° south of east. Dune fields located 120 km west of Dinosaur Park also indicate wind orientations from the northwest (32° south of east). South of the Park, effective wind directions are from the southwest, while all mapped dune fields to the north, between the Park and Edmonton, show northwest wind orientations. Odynsky (1958, p. 62) also invokes the theory of uniformitarianism in his contention that "...the probable effective sand-blowing wind directions are in harmony with the present strong wind directions prevalent in Alberta."

There is one last consideration to be made concerning the cause of the observed preferential variation in snow depth in the field region. This deals with whether these variations are primarily attributed to the focussing of snowflake trajectories during

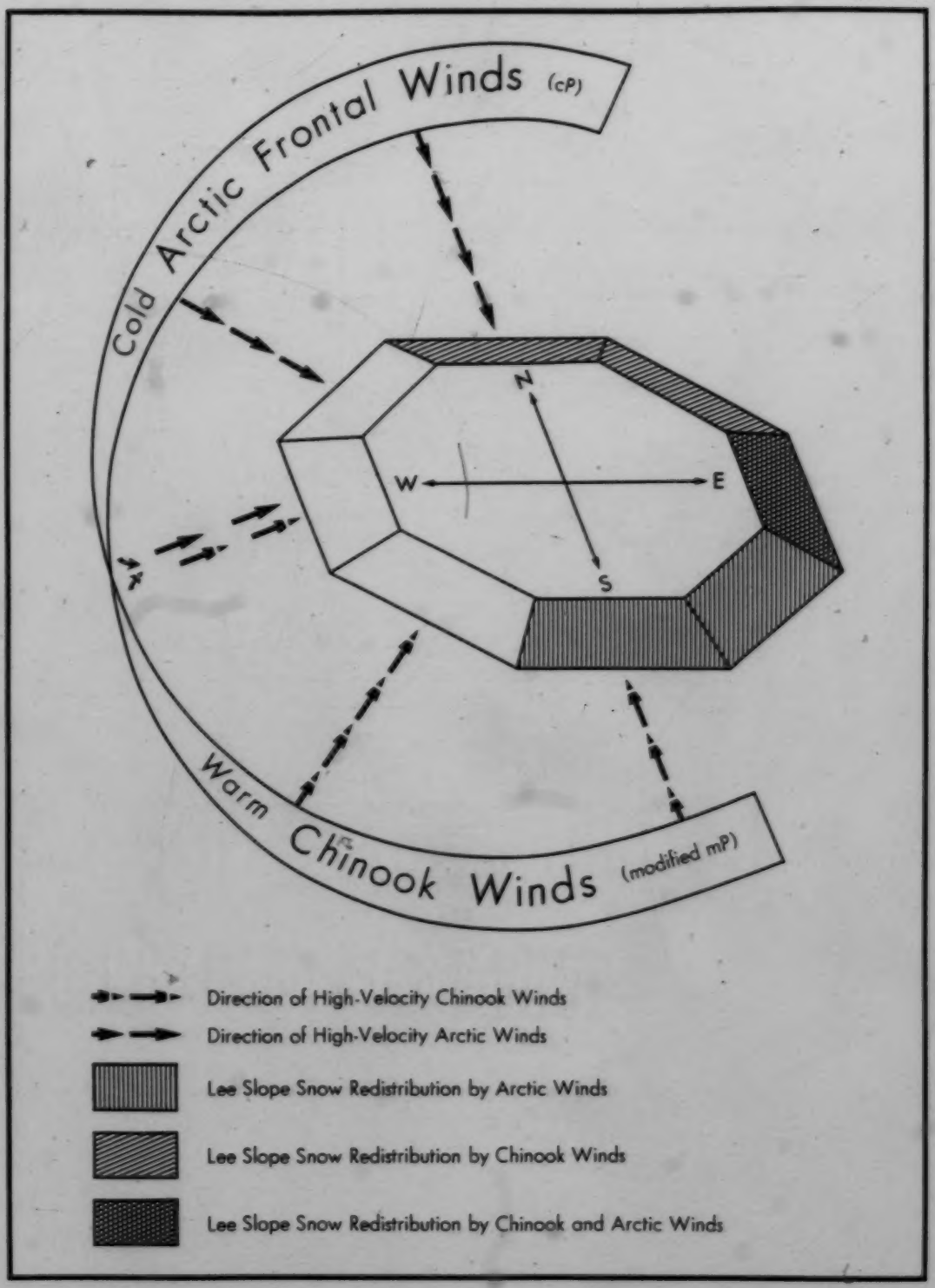
Cold Arctic Frontal Winds (cP)
N
W
E
S
Warm Chinook Winds (modified mP)
Direction of High-Velocity Chinook Winds
Direction of High-Velocity Arctic Winds
Lee Slope Snow Redistribution by Arctic Winds
Lee Slope Snow Redistribution by Chinook Winds
Lee Slope Snow Redistribution by Chinook and Arctic Winds

Figure 4.27. Characteristic seasonal pattern of lee slope snow redistribution under high-velocity Arctic frontal and chinook winds of south-central Alberta.

snowfall, or to non-uniform ground drift by winds after primary deposition has occurred. Although this research has already inferred that significant differences in snow depth were often achieved subsequent to snowfall events, the topic deserves further comment for the following reason. Snow drifting activity occurring simultaneously with snow production may further enhance or obscure the bimodal nature of lee slope accumulation. Its degree of influence should therefore be estimated.

From a qualitative and observational standpoint, and in agreement with assertions made by Kind (1981), it appeared that *most* snow movement in the badlands took place in the form of non-uniform drifting, under high-velocity winds unaccompanied by primary snow deposition. Evidence to support this claim is presented in wind rose diagram (c) of Figure 4.26, which shows the frequency of the prevailing wind direction during 1981-1982 snowfalls. From this diagram and Appendix E numerical values, it is ascertained that 49.2% of snowstorms from November 17, 1981 to March 31, 1982 occurred under winds originating from northeast, east, southeast, or south, directions from which winter winds are known to be light. Furthermore, 6.8% of snowstorms occurred under no discernible wind direction (calm conditions). In total therefore, 56% of snowstorms were unaccompanied by wind directions which are characteristically strong. This general pattern of light winds accompanying snowfall events is also reported by Storr (1973) who found that over 80% of snowfalls occurring in the Marmot Creek watershed (80 km west of Calgary) fell during winds averaging less than 16.2 km hr^{-1}.

No snowstorms progressed concurrently with southwest winds. However, 40.6% of snowstorms occurred under northwest or north winds. Since these directions possess the second and third highest wind speeds, it may be logically concluded that the focussing of snowflake trajectories, if active, should have its highest incidence of occurrence under winds of these directions. This, then, implies that snow which is preferentially distributed during snowstorms would produce higher accumulations on those lee slope bases facing south and southeast, thus enforcing the post-fall redistribution activity recognized under strong north and northwest winds, and supporting the bimodal distribution theory.

In addition to the frequency percentage wind rose diagram presented in Figure 4.26c, Tables 4.5 and 4.6 also provide information useful to defining wind patterns during

TABLE 4.5. WIND DIRECTION AND SNOW ACCUMULATION DURING 59 SNOWFALL PERIODS FROM NOVEMBER 17, 1981 TO MARCH 31, 1982.

Wind Direction	Number of Snow Periods	Total Depth of Snow (cm)	Depth of Average Snowfall (cm)
N	10	13.8	1.4
NE	18	53.4	3.0
E	2	2.1	1.1
SE	8	17.9	2.2
S	1	0.5	2.5
SW	0	0.0	0.0
W	2	2.5	1.3
NW	14	26.1	1.9
no direction (calm)	4	6.5	1.6
Total	59	122.8	-

Data Source: AHRC Records

TABLE 4.6. WIND DIRECTION AND MAXIMUM SPEED DURING ALL 1981-1982 SNOWFALLS OF ≥ 5.0 CM.

Date (1981-1982)	Snowfall (cm)	Prevailing Wind Direction	Maximum Wind Speed ($km \cdot hr^{-1}$)	Average Wind Speed $km \cdot hr^{-1}$	Average Wind Speed $m \cdot sec^{-1}$
November 18	6.3	NE	21	indeterminable	
December 14	6.3	SE	13	8.3	2.3
January 11	5.5	indeterminable due to equipment failure			
March 1	11.3	NE	27	21	5.8
March 15	15.5	NE	21	18	5.0
March 16	6.9	NE	24	16	4.4
April 6	6.3	NE	22.5	indeterminable	

Data Source: AHRC Records

1981-1982 snowfalls. Table 4.5 shows that 53.4 cm, or 43% of the total snow falling between November 17, 1981 and March 31, 1982 fell under winds prevailing from the northeast. The average depth of snow falling under these winds (3.0 cm) is also larger than that of any other direction, indicating that more snow was generated during these winds. This observation becomes more apparent in Table 4.6, which shows that five of the seven largest snowfall episodes of 1981-1982 occurred under the influence of northeast winds.

The larger accumulations received under northeast winds is most likely due to the position of the front between high and low pressure systems, with respect to the field area. That is, during at least two of these snowfall periods (March 15 and 16), a high pressure cell, invading from the northwest, and a low pressure cell migrating slowly eastwards, to the south of the field region, created a frontal position slightly north of the field area.[14] The location and duration of the front was favourable to heavy snow production, accompanied by surface northeast winds created by both clockwise high pressure air flow, and counterclockwise flow around the low pressure cell (see weather map, Appendix F).

Although the largest snowfalls occurred under northeast winds, Table 4.6 shows that these storms were not associated with particularly high average wind speeds. Also, the mean maximum wind speed recorded during the five northeast storms (Table 4.6) amounted to 23.1 km hr^{-1}, which is approximately half the maximum speed usually attained by snow-redistributing winds from the southwest and northwest. Although the concurrence of northeast winds and snowfall events may suggest a high frequency of snowflake focussing and preferential primary accumulation, information given on northeast wind speeds, plus numerous field observations during snowfalls point to the occurrence of significantly more snow movement and preferential accumulation activity subsequent to snowfall events, by non-uniform ground drift under northwest and southwest winds.

---

[14]Meteorological information on frontal, high, and low pressure cell locations supplied through radio reports issued from Brooks and Calgary on March 16, 1982.

4.3 Snowmelt Initiation and Patterns of Snow Disappearance

This section describes the influence of solar radiation and chinooks on patterns of snowmelt during the winter, within the same four time intervals used in the previous discussion on snow distribution. Before this is done however, it is necessary to present the results on the duration of chinook influence, and to explain the intensity, or, degree of effectiveness of the chinook in the field area. Also, because sustained meltwater penetration and runoff occurred twice during the later stages of the field season (periods 3 and 4), and because results of these two separate events complement one another, they are jointly examined in the following section (4.4), after the discussion of intra-season patterns of snow depletion.

4.3.1 Enumeration of Chinook Days

Chinooks were an extremely effective means of initiating mid-winter snowmelt and runoff. As noted in Chapter 1, chinook days were defined according to criteria given by Longley (1967) and Golding (1978), and are shown in the calendar of Table 4.1. The field area received 35 days of winter chinook activity according to Longley (1967), who requires a maximum temperature of at least 4.4°C for a chinook to be present. Application of the Golding (1978) criteria delineates 29 chinook days, most of which coincide with those determined by Longley's criteria.

Because of a lack of detailed meteorological records, the Golding (1978) chinook requirements (Chapter 1) were slightly modified. The directional criterion states that wind must originate from the quadrant encompassing directions from SSW to WNW. Since the AHRC only distinguishes wind orientation from eight compass directions, winds originating from south, clockwise to northwest were used.

Despite the large number of chinook days delineated (Longley and Golding average is 32), it was found that the *effective* chinook days, or those days on which significant snowmelt or runoff occurred, were fewer than those indicated in Table 4.1. For example, five chinook periods, comprising approximately 23 days, caused mid-winter runoff. The remaining 6 to 12 chinook days had either negligible affects on initiating snowmelt, or, allowed only a small degree of melt such that meltwater produced either evaporated or refroze atop or within the snowpack.

4.3.2 Period 1: November 17 to December 13, 1981

Of the five chinook snowmelt periods, the first three occurred early in the winter season, during period 1 (Nov. 20 to 22; Nov. 29 to Dec. 6; Dec 19 to 21, see Table 4.1), when snow reserves were quite small. Of the total season field area accumulation of 124.0 cm of snow, these chinooks, in combination, only affected approximately 14 cm of snow. However, each chinook initiated runoff, and, most importantly, provided water for subsequent refreeze and early formation of ice within every major drainage channel, most minor channels, and some low-lying pediments of the watershed.

The first two chinooks almost completely melted the 10.1 cm (Murton gauge water equivalent conversion) of snow which fell on November 17-18, 1981. Sub-zero temperatures ensued immediately after both chinooks, resulting in a rapid refreeze of meltwater which had not left the watershed. The same sequence of events occurred during and after the third chinook, which depleted most of the 4.0 cm of snow which fell on December 13-14, but did not significantly melt the ice formed during early chinooks.

The third chinook yielded runoff which flowed over pre-existing channel ice, and added to it upon refreezing. Many shallow drainage channels were so completely ice-filled that the expanded ice protruded above the channel confines. The watershed's primary drainage channel contained a vertical succession of solid ice and ice crystal layers which in one borehole, revealed a total solid ice / ice crystal depth of 22 cm (Figures 4.28 and 4.29). Channel ice formed after the first three chinook intervals persisted throughout the remainder of the field season; its hydrologic significance will be explained in part 4.4 of this chapter.

Some early-season indications of the preferential melt effects of direct solar radiation were observed during period 1. Described and depicted in Figures 4.30 through 4.32, shortwave radiation was responsible for differential snowmelt on south-facing slopes of the watershed, under air temperatures below 0°C. Differential melt was most noticeable on December 12, due to the shallow depth of snow (0.5 cm) present at the time, which had fallen on the previous evening (none recorded by the AHRC). Although the effects of this preferential melt, in terms of moisture infiltration were minimum, these sharply-contrasting patterns show that radiation was an active winter snowmelt mechanism.

Figure 4.28. Ice layer in the main channel near the basin outlet. Ice was formed after a succession of runoff-inducing chinooks and refreeze events in November and December, 1981. Hammer for scale.

Figure 4.29. Close-up view of a hole excavated into primary channel ice. Hammer rests atop a 4 cm dirty ice layer. Ice crystals, placed on the 5 cm top layer of solid ice were formed upon the floor of the 13 cm cavity existing between the two layers. Total depth from top ice layer to the channel floor is 22 cm.

Figure 4.30. North view of sb-X under cloudy conditions at 10:00 a.m., December 12, 1981. The sub-basin is uniformly covered by 0.5 cm of snow. Temperature is -8.5°C. Murton gauge for scale.

Figure 4.31. North view of sb-X under sunny conditions at 2:30 p.m., December 12, 1981. South- and west-facing slopes are devoid of snow due to solar radiation melt. Temperature is -9.0°C. Snow remains only on flat-lying treads of stepped slopes (which are receiving three to four times less radiation than south-facing slope risers), on east-facing slopes, and upon the flattest regions of the lower basin. Compare to previous photo.

Figure 4.32. Preferential solar radiation melt on a south-facing sandstone slope in sb-Y on December 12, 1981. Temperature is -9°C.

4.3.3 Period 2: January 1 to January 17, 1982

Snowmelt during this period was limited because of extremely low temperatures, and lack of significant chinook activity. As noted earlier, this period was mainly one of snow accumulation. Table 4.1 shows that two chinook days occurred, however, no runoff ensued. The steadily accumulating snowcover experienced only a small degree of intra-pack percolation, and surface melt and sintering.

Some radiation melt was observed during the period, mainly on south slopes. Melting generally proceeded at snowpack peripheries, and was most efficient on slope faces. On rilled slopes, melting typically commenced at rill / interfluve junctions (Figure 4.33), where snow depth was minimal, thereby permitting radiation penetration into the snowpack to the underlying slope surface. On unrilled slopes, melting ensued outwardly from snow-barren patches (Figure 4.34). As with the minor chinooks of this period, radiation melt caused intra-snowpack percolation of meltwater (visible in Figure 4.33). Micro-scale overland flow occurred to a small extent within troughs created by partial seal of claystone aggregates. Subsurface meltwater penetration was restricted to a few millimetres on sandstone and claystone slopes, where a limited amount of snow was melted by radiation on a given day.

4.3.4 Period 3: January 18 to February 20, 1982

As discussed in connection to snow accumulation and redistribution, this period experienced a continued build-up of snow reserves, disturbed slightly by the minor chinook of January 25-26. Thus, maximum snow accumulation was realized by February 12, the last snowfall day before the onset of a major, six-day chinook on February 16 (see Table 4.1). During this chinook, maximum daily temperatures averaged 6.5°C, with an absolute maximum of 8.5°C on February 20. Southwest winds prevailed throughout the first five of the six chinook days, reaching maximum speeds of 43 km hr^{-1} on February 18, and 42 km hr^{-1} on February 20.

The combined affects of direct solar radiation and sensible heat transfer from warm chinook winds produced widespread snowmelt from surfaces of all orientations and drastically reduced the watershed's storage of snow. Because of continuous radiation melt on south slopes throughout the winter, these slope faces retained less snow

Figure 4.33. Radiation melt on a rilled, south-facing 47° compact claystone slope in sb-X (January 17, 1982). Snow melts quickly from interfluves, which typically retain little snow. Mitten for scale.

Figure 4.34. Mid-winter peripheral radiation melt of a snowpack on a south-facing, aggregate-mantled claystone slope in sb-Z (January 14, 1982). Note partial sealing of clay aggregates by micro-sloughing of particles.

than others by the time the chinook arrived. Therefore, south faces became completely snow-barren more rapidly once the combined melting ability of radiation and atmospheric heat transfer took effect. These observations are in agreement with those made by numerous authors (see chapter 2), that temperature-induced snowmelt is actually caused by the integrated influences of temperature and radiation. However, due to comparatively large snow accumulations at the basal regions of south slopes, many snowpacks in these areas remained throughout the duration of the chinook, though most were greatly primed with meltwater (Figure 4.35).

Of the four major compass directions, snow generally remained on north- and east-facing slopes longest. North slopes were subjected to the least amount of direct solar radiation, thus melting occurred more slowly, primarily by heat transfer. Although east-facing slopes received more radiation than those oriented north, the large snow accumulations on these slopes, caused by preferential snow redistribution, ensured that these snowpacks remained for long durations. West-facing slopes lost their snowcover shortly after south slopes. Although west slopes received virtually the same amount of direct radiation as east slopes, smaller snow reserves permitted more rapid depletion. These observations are illustrated in Figures 4.36 and 4.37.

Snow lying in surface hollows, ravines, gullies, and narrow, collapsed pipe channels was generally retained throughout the chinook period, although much was lost through heat transfer from meltwater flowing beneath snowpacks. On the micro-scale, snow-filled rill channels, especially those on north slopes, experienced diurnal melt, causing snowpack saturation, and ice formation upon night-time refreeze (Figure 4.38). Of the six chinook days, all of which experienced daytime temperatures of 5°C or higher, four had night-time temperatures below 0°C. Rill ice depicted in Figure 4.38 formed during the evening of February 17, under a minimum temperature of -11°C.

Although much of the moisture contributing to the formation of rill ice was derived from pre-existing snow inside rills, daily melting of upslope snowpacks also provided water for nocturnal refreezing (Figure 4.39). Rill ice was observed on all slope aspects, though its lowest incidence was on south slopes. North-facing slopes retained ice day and night throughout the duration of the chinook, with limited melt occurring by slow dripping. Similarly, most east-facing slopes also retained ice through the chinook period.

Figure 4.35. Snow depletion on south-facing claystone slopes of the lower basin of sb-Z (February 20, 1982). Snow remains at the basal slope regions and in depression hollows of upper slopes.

Figure 4.36. West view of sub-basin X showing snow depletion patterns on February 19, 1982. Snow remains on east- and northeast-facing head slopes, in depression hollows of the basin, and on flat surfaces in the lower basin. South-facing slopes visible in the right of the photo are snow-barren except in basal slope areas.

Figure 4.37. West view of snow depletion patterns in a vegetation-lined gulley of sub-basin Z (February 20, 1982). The northeast-facing gully flank is snow-covered. The opposite, southwest-facing flank is barren due to increased radiation melt on slopes with a southerly aspect.

Figure 4.38. Rill ice on a north-facing, integrated sandstone slope (February 18, 1982).

Figure 4.39. Rill ice on an east-facing claystone slope (February 19, 1982).

By the time cold temperatures set in on the evening of February 21, approximately 70% of the watershed snowcover had disappeared through melt, runoff, and evaporation. Most south- and west-facing slope faces were depleted of snow, with some sparse snowpacks lingering at basal slope regions. Partially-depleted snowpacks remained on most north slopes, and some east slopes. In both cases, basal, or mid-slope break accumulations remained, with very little lingering on slope faces (Figure 4.40).

From these observations, it is evident that differential melt, with respect to both location and rate, is common in the badlands. Accelerated melt rates were recognized in all areas during the chinook, due to relatively high temperatures. Non-uniform melt, however, was afforded by differences in the amount of and location of snow, as determined by snow redistribution, and as influenced by differential solar radiation receipt.

In agreement with statements made by Gray (1970), it was found that snow quantity was indeed a factor determining which slope orientations became depleted of snow before others. However, large accumulations redistributed onto south slopes were evidently not sufficient to outlast the melt effects of direct radiation. In these terms, east slopes faired better, for their large deposits survived, aided by reduced radiation receipt. As mentioned, west slopes became almost totally depleted because of smaller accumulations. North slopes, though in possession of less snow than either south or east slopes, were least subjected to direct radiation and thus retained their snow.

These facts indicate that radiation receipt is the most important parameter governing the nature and rate of differential snowmelt in the badlands. Because of rapid depletion of the large snow reserves on south slopes *verses* north slopes, the location of redistributed snow must be considered of secondary importance to slope aspect. This view is supported by the fact that the 1981-1982 winter season received one of the largest accumulations on record, yet did not receive adequate snow (even when preferentially redistributed) to permit long occupation on south slopes.

Figure 4.40. North-facing, stepped claystone slope retains near-saturated snowpacks on the mid-slope tread and basal region (February 20, 1982). Note rill ice which endures temperatures of 8.5°C.

4.3.5 Period 4: February 21 to April 8, 1982

The patterns of snowmelt recognized during this period were nearly identical to those observed during period 3. Again, a major, high temperature chinook in mid-March (Table 4.1) caused rapid, almost complete melt of the preferentially-redistributed snow reserves built-up earlier in the period. Maximum temperatures from March 11 to March 14 exceeded 7°C, peaking at 10°C on the first chinook day (March 11). Shown in Figures 4.41, 4.42, and 4.43, snow reserves were virtually depleted by the fourth chinook day (March 14), except on north, northeast and east slopes.

The effectiveness and rapidity with which differential solar radiation melted snow during the chinook was ascertained through comparison of snow densities obtained from basal snowpacks at varying slope orientations. Table 4.7 gives density values surveyed from randomly-selected slope bases on the second chinook day (March 12). The highest average density, which indicates the highest relative amount of meltwater contained within snowpacks, was found in southerly-oriented basal snowpacks (0.403 g cm^{-3} -- column 3, Table 4.7). Slopes facing west possessed the second highest density values. These results further reflect the faster meltwater production realized on south and west slope orientations. Accordingly, the lower average density value of east slopes (0.313 g cm^{-3}) as compared with west slopes (0.358 g cm^{-3}) is probably due to the less rapid melt of the generally greater amounts of redistributed snow found on east slopes. However, the close similarity of these two values does not provide positive proof of this assertion. North slopes, subjected to the least solar radiation melt, possessed less intra-snowpack meltwater, thus the lowest average density value (0.257 g cm^{-3}). Northeast and east slope-base snowpacks contained less relative meltwater than the faster melting south slopes, yet more than shaded north slopes.

These measurements, and photographic evidence presented for this chinook and the major one occurring at the end of period 3, show a melt rate sequence largely determined by differential radiation receipt. It will be shown, however, that the *combined* affects of snow distribution and aspect-related snowmelt progression permitted preferential and higher-magnitude erosion on some slopes.

Two additional chinook periods occurred towards the end of March 1982 (Table 4.1). Although no field observations were made, it is likely that melt sequences paralleled

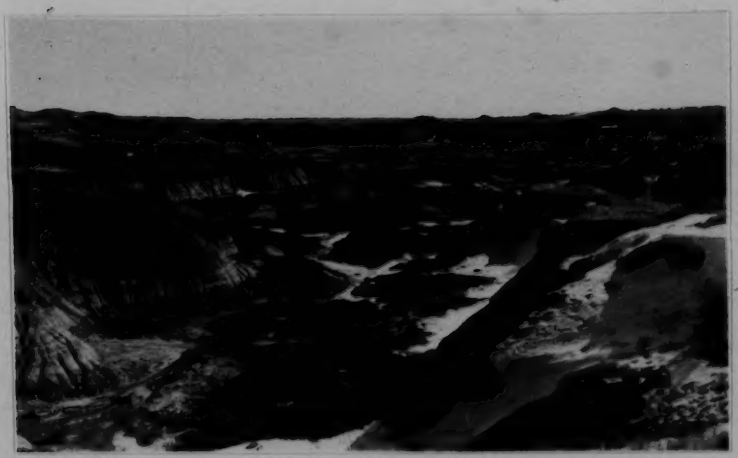

Figure 4.41. Southeast view of snow depletion patterns in sub-basin X on March 14, 1982. South- and west-facing slopes are snow-depleted, while east- and northeast-facing slopes (in right side of photo) retain snow.

Figure 4.42. West-southwest view of snow depletion patterns in sub-basin X on March 14, 1982. Snow and ice remain predominantly in the basin's main drainage channel, and within east- and northeast-oriented head-basin hollows. Murton gauge for scale; compare to Figure 4.36.

Figure 4.43. West-southwest view of snow depletion in the lower basin of sb-Z on March 14, 1982. South-facing slopes (in right of photo) are snow-barren, whereas east and northeast slope faces and basal regions retain snow.

TABLE 4.7. DENSITIES OF SNOWPACKS ESTABLISHED AT SLOPE BASES OF VARYING ASPECTS, MARCH 12, 1982.

column #	1	2	3
Slope Orientation	Snow Depth (cm)	Density ($gr \cdot cm^{-3}$)	Average Density ($gr \cdot cm^{-3}$)
N	11.0	0.229	
N	15.5	0.291	0.257
N	40.0	0.255	
N	21.0	0.251	
NE	15.0	0.360	
NE	14.0	0.262	0.324
NE	17.0	0.349	
E	11.0	0.354	
E	17.5	0.287	0.313
E	24.0	0.282	
E	14.5	0.329	
SE	22.0	0.400	
S	12.5	0.395	0.403
S	10.0	0.414	
W	14.0	0.385	
W	9.0	0.337	0.358
NW	7.0	0.352	
Average	-	0.325	-

the patterns described. The final spring melt, or, the last melt induced by chinook conditions, began on April 8, 1982. However, only 14.0 cm of snow (AHRC records) was present at this time. Therefore, due to mid-winter snow depletion by chinooks, the field area had no significant spring melt during 1982, which is likely a seasonally-repetitive characteristic in the badlands and surrounding region.

4.4 Meltwater Penetration and Runoff During Two Major Chinook Intervals

The two, long-duration mid-winter snowmelt episodes described in the previous section produced sustained runoff over a number of days. In both instances, total snowmelt was halted by the resumption of cold temperatures, accompanied by additional snow accumulation. During these chinook melt periods, observations of the nature and extent of subsurface meltwater penetration and runoff activity were made, to see if significant differences exist between hydrologic responses generated during typically short, summer rainstorms, and sustained snowmelt episodes.

4.4.1 Subsurface Meltwater Penetration

The powdered dye inserted into snowpacks in early February, 1982 proved ineffective as a means of tracing the vertical extent of subsurface meltwater penetration. Although overland flow routes remained visually distinct, the subsurface penetration of the dye was severely restricted and none could be visually detected below a surface depth of 1 mm. The reason for the lack of infiltration of the dye is not known, but it may be due to cohesive binding to surface clay particles. Meltwater penetration was therefore determined by visual observations of subsurface material discolouration (darkening). Some of the pre-seeded dye points had dried by the time of excavation, during the chinook of late February, and moisture depth could therefore not be determined. Many excavations were thus made in areas other than the dyed points; in locations which remained under the influence of melting snowpacks.

In general, water provided by sustained melting of snowpacks reached slightly, but not substantially deeper depths than that of prolonged rainstorms. This points to the importance of material composition and structure (compactness and permeability) in limiting percolation, over the quantity or duration of water available to these materials.

Although snowpacks afforded a generous supply of meltwater, over periods lasting as long as six days (e.g., from March 10 to March 15), extensive vertical penetration of water (other than pipeflow) was not realized on most lithologic units. Instead, surficial ponding of meltwater on flat areas, and overland flow on inclined surfaces proceeded, with infiltration retarded by rapid surface sealing of claystones and sandstones.

Of all lithologies examined (except those covered with vegetation), maximum moisture penetration depths occurred on flat-lying claystone units subject to prolonged input by nearby melting snowpacks. On compact, desiccated claystone units, material saturation was limited to just below the subsurface extent of desiccation cracks, usually no more than a few centimetres. Hydration sealing of these cracks precluded further transmission of meltwater from the surface, but did not interfere with slow percolation of water from the saturated zone to the underlying compact crust (Figures 4.44, 4.45, and 4.46). . However, penetration within the crustal zone was retarded by its indurated structure and low permeability. Maximum wetting depths from the bottom of the saturated zone into the crust generally did not exceed 9 cm, with a total wetting depth of 13 cm. This figure is quite deep when compared to simulated rainfall experiments (Bryan *et al.*, 1978), which yielded maximum penetration depths into claystones of approximately 4.0 cm.

The downward migration of the wetting front within the crust proceeded fairly uniformly, a conclusion based on the observation of visually distinct, horizontal boundries separating the hydrated and dehydrated portions of the crust (visible in Figures 4.45 and 4.46). Meltwater penetration in the upper reaches of the crust therefore occurs by slow percolation, and is not dependent on the presence of micro-joints. However, due to the downwardly-increasing compactness of the crust, further penetration below the "maximum" percolation depth (9 to 10 cm) is probably permitted only through mico-joints, as suggested by Hodges and Bryan (1982).

Relatively deep meltwater penetration was also recognized on flat-lying, aggregate-mantled claystone units. However, due to the often extensive depths of the highly broken regolith, meltwater frequently could not reach the compact crust and instead became completely absorbed by aggregates (Figure 4.47). Nonetheless, maximum wetting depths observed on these surfaces reached approximately 7 cm, which is deeper than

Figure 4.44. Flat-lying, meltwater-saturated, desiccated claystone pediment on March 14, 1982. Ponded water lies within peripheral troughs of sealed polygonal desiccation cracks, which prevents sustained water percolation to the subsurface.

Figure 4.45. Subsurface view of Figure 4.44. Surface material is saturated to depths of 2 to 3 cm, corresponding to lower extents of desiccation cracks. Meltwater infiltrated an additional 9.0 cm into the compact crust below (darkest zone). The lighter portion of the crust towards the bottom of the excavation pit is dry. Total wetting depth varies from 9 to 13 cm.

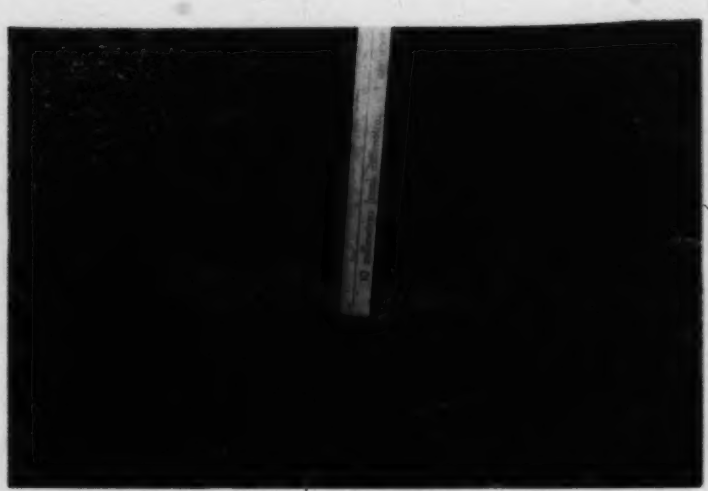

Figure 4.46. Meltwater penetration in a compact, flat-lying claystone unit in sb-Z. The upper 3.0 cm of material is saturated. Moisture penetrated an additional 7.0 cm into the compact crust, for a total wetting depth of 10.0 cm.

Figure 4.47. Surface sealing of an aggregate-mantled claystone slope convexity. Wetting depth below the surface is 7.0 cm.

penetration depths of most natural and simulated rainfalls.

In agreement with results obtained during rainfall experiments (Bryan *et al.*, 1978), wetting depths on claystones during snowmelt were typically greater beneath interfluves than rills, owing to the more compact, less-desiccated nature of rills, and to the impermeable clay lining present within them. However, as a result of snow redistribution, a high proportion of interfluves were snow- or ice-free by the time melt episodes ensued, leaving these features virtually dehydrated throughout melt periods (Figure 4.48). Therefore, unlike during rainfall, when all slope features receive near-uniform amounts of precipitation, micro-scale preferential water penetration and runoff occurs in rills during mid-winter thaw episodes.

Meltwater penetration rarely exceeded 2 to 3 cm beneath rill floors, but typically reached greater extents horizontally, on less compact rill sides or interfluve margins. Figure 4.49 illustrates this frequent observation, and shows that the lower extent of water penetration, as on saturated, flat-lying claystones, generally remained horizontally uniform. In addition, the diagram shows that subsurface maximum penetration into rill sides is reached at points A and B (Figure 4.49), which approximately correspond to the midway depth of rill water or ice. These points are located at subsurface depths which most easily facilitate lateral water flow. Beneath these points, the crust becomes increasingly dense, retarding downward flow. Above the points (especially in the regolith above the rill water / air interface), water transmission occurs against gravity by means of capillary flow. These observations of relatively deep lateral penetration of meltwater into rill sides were made based on visual evidence of moisture zones, and subsurface concrete frost, the latter of which preserved patterns of meltwater penetration from earlier chinook melt episodes.

Meltwater penetration on sandstone slopes reached slightly greater depths under prolonged snowmelt than during most rainstorms. Although wetting depths were typically quite shallow, meltwater frequently penetrated the compact subsurface beneath the weathering rind. As with claystone slopes, the deepest infiltration was on the rill sides (Figure 4.50), which, because of their weathering rind, absorbed more water than compact rill floors. Wetting depths on rill sides of 5.0 mm were common, but slow melt of rill ice on shaded north slopes permitted long-duration infiltration, often resulting in

Figure 4.48. Water from melting rill ice flows over a low-angled claystone slope (left to right). Wetting depth beneath the rill is 2.0 cm; adjacent interfluve (top half of photo) is dry (February 20, 1982).

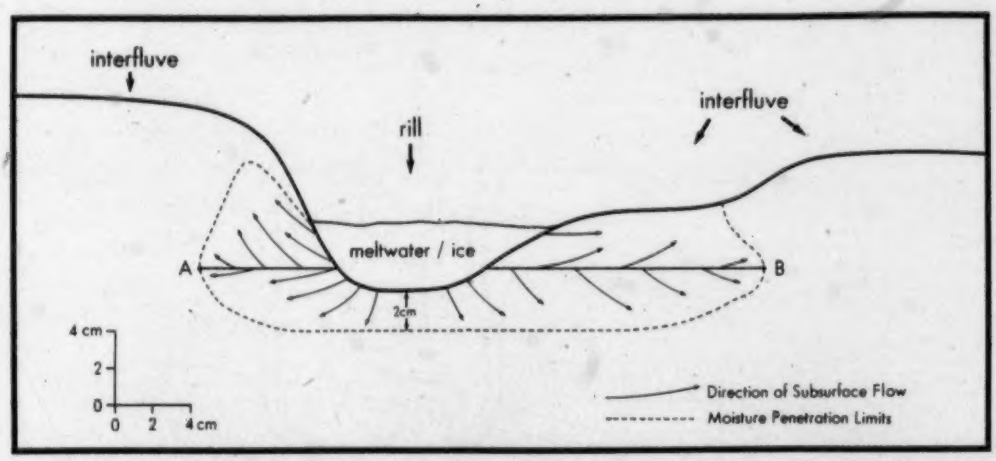

Figure 4.49. Cross-sectional diagram of meltwater penetration in a rill of a partially-disaggregated claystone slope. Drawn from actual measurements; see text for explanation.

Figure 4.50. Water from melting rill ice on a north-facing sandstone slope penetrates rill margins (dark areas) to a maximum depth of 1.75 cm.

Figure 4.51. Melting snowpack saturates the weathering rind of a north-facing sandstone interfluve. The rind is easily scraped away to reveal wetting depths of 5 to 7 mm. Note mico-rilling of interfluve (bottom of photo), indicative of overland travel to rills.

wetting depths three to four times greater (Figure 4.50).

Maximum wetting depths observed on excavated interfluve crests ranged from 5 to 7 mm (Figure 4.51), which are a bit shallower than those on the interfluve margins (or rill sides), due to the smaller amounts of snow found on interfluves. Meltwater penetration on interfluves however, provided adequate snow was available, was also able to penetrate a few millimetres beneath the weathering surface, a state which is not usually recognized during rainfall. In fact, Hogg (1978, p.124) reports that wetting depths on sandstones, after a number of summer rainstorms, typically reached no deeper than 2 to 3 mm, corresponding to the maximum depth of the weathering layer. This deeper penetration may also have been facilitated by the absence of surface compaction by raindrop impact, as suggested by Hodges and Bryan (1982).

Fine-grained alluvial fans and pediments usually exhibited wetting depths similar to those observed during rainfall (by Hodges, 1982; Hodges and Bryan 1982), whereby meltwater penetration halted upon reaching the vesicular layer 2 to 3 mm beneath the surface. In many cases however, where level pediments permitted ponding of meltwater over a period of a few days, or where continuous daily flow ensued over the same pediment area, water entered the vesicular layer to become absorbed in the sponge-like matrix. In these areas, wetting depths frequently reached 2.0 cm, although downwards transmission of water was extremely slow.

Vegetated surfaces, including upper prairie flats, low-lying stabilized alluvial features, and terraces, absorbed meltwater to great depths, seemingly limited only by the amount of meltwater available on the ground surface. Maximum moisture penetration depths just over 30 cm were measured on many low-lying surfaces towards the termination of the chinook melt period in February, 1982 (Figure 4.52). Because of partial snow removal by wind before the onset of the chinook, many of the grassed, upper prairie flats retained less snow, thus shallower meltwater depths (Figure 4.53) than the compositionally-similar, grass-covered features in lower, more sheltered areas within the watershed.

Table 4.8 shows the maximum moisture penetration recognized after a typical summer rainstorm *verses* those measured during later stages of the two major chinook periods (February 16-21; March 10-15) of 1982. As shown, snowmelt exceeds

Figure 4.52. Snowmelt penetration on a grass-covered terrace composed of silty Brown soil. Maximum wetting depth is 30 cm; depth at measuring stick is 25 cm (February 20, 1982).

Figure 4.53. Meltwater penetrates 9.0 cm into the silty-clay soil of this vegetated gully flank located on an upper prairie surface (February 20, 1982).

TABLE 4.8. MAXIMUM MOISTURE PENETRATION DEPTHS FOR VARIOUS LITHOLOGIES UNDER AVERAGE RAINSTORMS VERSES SNOWMELT (CM).

- LITHOLOGIC UNIT -

	Claystone				Sandstone			Fans/Pediments	Vegetated Surfaces	
	Flat-lying, Desiccated, Compact Beneath	Rill Floors	Rill Sides	Inclined, Aggregate-mantled Interfluve	Rill Floors	Rill Sides	Interfluves	———	———	
Rainfall	3.0[a]	2.0	?	4.0[+]	0.4[a]	0.5[a]	0.3[&]	0.3[6]	Limited by Water supply	
Snowmelt	13.0	3.0	15.0	7.0	0.6	2.0	0.7	2.0	Limited by Water supply	
Percentage By Which Snowmelt Penetration Exceeds Rainfall	77	33	?	43	33	75	57	85	———	Ave: 58%

Note: Values do not consider moisture penetration facilitated by deep structural cracks or pipe flow

a Estimate
? Not investigated
+ From Bryan, et al., 1978
& From Hogg, 1978
6 From Hodges and Bryan, 1982

rainwater penetration on all lithologic units examined, by an average of 58%. This is primarily attributed to the longer duration and a slower rate of application (four to five days) with which melting snow and ice supplies moisture, thereby permitting prolonged sorption and infiltration processes to occur in badland materials. Vegetated surfaces are the exception, whereby the quantity of water introduced is generally more important than time. That is, deeper infiltration may be realized under either a snowmelt or rainfall episode, depending on the amount of water available.

4.4.2 Runoff

In theory, the sustained, deeper subsurface moisture penetration recognized during winter snowmelt episodes *verses* summer rainfalls should result in an overall decrease in the relative amount of water escaping the watershed as overland flow. On a smaller scale, this idea may also apply to downslope water movement over a particular slope. However, observations suggest that a seasonally-alternating (i.e., summer *verses* winter) state of partial area runoff exists, which in fact may result in an overall *increase* in the amount of overland flow runoff generated during snowmelt, per unit input of water. In the Alberta badlands, during winter, areas of partial runoff contribution are created by preferential redistribution of snow into rills, gullies, and ravines; areas which are known to generate runoff more efficiently than infiltrating interfluves. Due to rill accumulation, there is less water present on interfluves during snowmelt, whereas during rain, and because of the larger area represented by interfluves, the majority of precipitation falls upon these more absorbent features.

In addition to the reason cited above, the widespread presence of frozen ground and surface ice in many rills, depression features, and drainageways facilitated overland runoff during chinooks, by prohibiting infiltration until melt-out. Channel ice formed in December, 1981 did not melt in entirety by the termination of either of the two major runoff-producing chinooks. Its presence, combined with rapid melt and general material impermeability, induced widespread flooding and overland flow (Figures 4.54 and 4.55).

On the small, plot-size scale, overland flow was observed on slopes of all lithologies, except those covered with prairie grass. Relict dye paths on the surface of sandstone slopes in sub-basins X and Y were visually traced for linear distances up to

Figure 4.54. High temperatures (8.5°C) towards the end of the major chinook period of February, 1982 facilitate rapid snowmelt, creating overbank flooding atop the ice-laden drainage channels in the lower basin of sb-X (February 20).

Figure 4.55. Meltwater ponding on a low-lying claystone pediment near sb-Z. Note the snowpacks still present to the leeward sides (view is towards the north) of isolated sage bushes (February 18, 1982).

10 m before becoming obscured by dilution. Dye inserted on steep, snow-covered sandstone interfluves usually traveled from 5 to 20 cm downslope before diverting into adjacent rill channels and exiting at slope bases onto fans and pediments.

During rainfall, most fans and pediments sustain sheetflow, with nearly the total surface area contributing to runoff. During snowmelt however, there is a high incidence of concentrated rill flow, particularly on fans and pediments swept clear of snow prior to melt (Figure 4.56). It is possible that the absence of raindrop impact also favours concentrated flow, through the lack of creation of micro-diversion channels on rill walls.

Overland flow was also active on rilled claystone slopes during both major chinook intervals, determined by visual observations and by the presence of residual dye paths. In many cases, rill flow could be traced an entire slope length, though its prevalence was not as common as on sandstones due to more efficient infiltration into rill sides. Meltwater flow in both claystone and sandstone rills ensued almost immediately after the initiation of snowmelt, as approximately 60% of rills on all slope aspects contained ice as well as previously-moistened and subsequently refrozen floors.

The presence of frozen ground was also responsible for a delay with which throughflow commenced in the watershed. This is suggested by the fact that for both chinook melt episodes, substantial overland flow was recognized by the second day of each chinook, but pipeflow (except in large pipes with a surface entrance) was not observed until the next-to-last day of both melt periods, when channel runoff was in waning stages. Pipeflow was extremely shallow in depth (Figure 4.57) as compared with that occurring under rainfall, with most pipes issuing meltwater in trickles. This is due to the lack of snow (meltwater) remaining in the watershed by the time of sufficient melt of the throughflow-inhibiting frozen ground.

Runoff in the primary drainage channel took on diurnal characteristics during both chinook periods, with peak flow occurring in late afternoon, and diminished flow during early morning hours. The chinook of mid-February initiated snowmelt on February 16, with concentrated runoff beginning the following day. Snowmelt production and runoff increased each day during the chinook period, and peaked on the late afternoon of February 20 (Figure 4.58).

Figure 4.56. Concentrated meltwater flow etched a rill and dendritic micro-rills into this slightly inclined (4°) pediment (February 19, 1982).

Figure 4.57. Shallow pipeflow at the base of a claystone slope ensues during the second-to-last day (March 14) of the March, 1982 chinook period. Lens cap for scale.

Figure 4.58. Snowmelt runoff flows through the flume at the main channel outlet. Total stage height is 40 cm, including approximately 20 cm of ice at the bottom of the flume (4:00 p.m., February 20, 1982).

During the last two days (53 hours) of this runoff episode, seven measurements of stage height were manually recorded at the flume site at the watershed outlet (Table 4.9), to approximate the volumetric runoff escaping the watershed. These values were plotted as a hydrograph (not shown), from which an additional 46 hourly runoff figures were extrapolated. The total 53 consecutive stage height values were averaged to obtain a 53-hour mean representative stage value of 11.3 cm. Using a pre-designed rating curve for the flume, this value corresponds to a volumetric runoff output of 7,632 m^3 for the 53-hour monitoring period. In terms of uniform water depth over the catchment, this figure represents 22.7 mm of water, and is comparable to the input of a typical convectional rainstorm in the badlands, assuming total runoff. More significantly, the value exceeds the *highest* total discharge figure obtained for a monitored summer rainstorm (4,069 m^3, column 5 of Table 2.3, chapter 2) by nearly 50%, an indication of extremely high runoff efficiency and substantial precipitation input (i.e., build-up of snow reserves).

The discharge figure of 7,632 m^3 is however, a highly conservative estimate of water output during the chinook, as it does not include channel runoff which exited the basin on February 17 and 18, prior to the stage height observation period. In addition, total ice depth within the flume was subtracted from the stage recordings, therefore water flowing between gaps in ice layers could not be determined, and was treated as solid ice depth. Hence, the 53-hour volumetric runoff estimate itself is also underestimated. Nevertheless, it shows that runoff during this mid-winter snowmelt episode was substantial, and indicates that total discharge easily exceeded that derived from any observed, high-intensity or long-duration rainstorm.

A runoff coefficient for this as well as the last major chinook in March, 1982 could not be determined due to the underestimation of precipitation input yielded through snow survey computations. The volumetric water equivalent of snow surveyed on February 5 was added to that which fell in the field from February 5 until the time of the mid-February chinook, for a total input of 5,120 m^3 of water. This figure is incorrect, as it implies that more water exited the basin than entered. The error is largely due to the location of snow survey points in areas subject to snow depletion by wind. It is also attributed to the inability to evaluate, through snow survey measurements or other means, the amount of water contained in the large ice deposits in low areas and drainage channels,

TABLE 4.9. FLUME STAGE HEIGHT AT VARIOUS INTERVALS WITHIN THE LAST 53 HOURS OF CHANNEL RUNOFF DURING THE FEBRUARY, 1982 CHINOOK PERIOD.

Date (1982)	Time	Stage Height (cm)*
February 19	10:00	8.3
	16:00	12.0
February 20	10:00	13.5
	16:00	20.0
	19:00	16.8
February 21	10:00	4,2
	15:00	3.6

* Depth of channel ice subtracted.

just prior to both melt episodes.

Although runoff was not monitored in any of the sub-basins, each contributed substantial diurnal channel flow. During both chinook periods, sub-basin Y appeared to yield more water from its channel outlet than the other sub-basins, exhibiting sustained, deeper channel flow. The larger discharge of sb-Y as compared to sb-X is explained in part by the larger snow reserves held in storage in sub-basin Y. As stated earlier in this chapter, higher snow accumulations in sb-Y are not only attributed to the larger area of this basin, but also, to the lack of a high degree of snow removal by wind, as experienced in other sub-basins.

Although sub-basin Y received less net snow accumulation than sub-basin Z, the latter retains the large, grass-covered upper basin, which greatly inhibited runoff from this area. The largest proportion of runoff from sb-Z was derived from the slope-sheltered head region of the lower basin, which is unvegetated and subject to little snow disturbance by wind. However, runoff emanating from the lower basin of sb-Z still appeared less than that generated by sb-Y. This is likely due to slope gradient; the very flat nature of the lower basin floor of sb-Z permitted meltwater ponding, hence more infiltration, and probably a larger amount of evaporation. By contrast, the steep side slopes and gradient of the first and last 35 m of the main channel of sb-Y greatly facilitated rapid, concentrated runoff.

The larger discharge of sb-Y also reflects the higher drainage density of this basin. Per unit surface area, sb-Y retains a larger percentage of highly-rilled sandstone slopes than sb-X and sb-Z. Since snow accumulation occurred preferentially in rills, sb-Y displayed more snow in areas (rills) and on the lithology (sandstone) most conducive to runoff generation. These results imply that a state of partial area runoff production is evident in the badlands in winter, with variations in sub-basin contribution depending on the factors of snow distribution, drainage density (including the degree of rill dissection), slope gradient, lithology, and spatial extent of a vegetal cover.

Despite the inability to calculate mid-winter runoff coefficients for the main watershed or sub-basins, it is held that runoff is extremely efficient during snowmelt, perhaps even greater than during rainstorms. Of the six factors outlined earlier which influence snowmelt runoff in a given watershed, *all* were favourable to the production of

high runoff yields during the 1981-1982 field season. As noted in chapter 2, watershed runoff parameters of topography, vegetation, and material porosity and permeability are virtually the same under rainfall and snowmelt. Thus, they lend little insight into possible differences in runoff under the two forms of precipitation.

Of the three remaining factors, snow / water availability and ground conditions were both highly conducive to mid-winter runoff production. Early-season preferential snow accumulation and redistribution into rill and gully networks initially provided water for the formation of surface ice and frozen ground within these features, subsequent to the melt by a December, 1981 chinook. Continued depressional snow accumulation led to storage of great water supplies in features exhibiting not only compact, highly impermeable floors, but also, layers of impermeable ice, to facilitate the fast removal of large volumes of runoff. As both these runoff variables (quantity and location of water, and ground conditions) are recognized as being advantageous to badland runoff, and are recognized solely in winter months, their addition to the three runoff variables common to both precipitation forms should heighten the degree of runoff efficiency normally recognized under rainfall.

Snowmelt rate, the final runoff parameter, is conducive to rapid runoff production in the badlands due to the combined influence of solar radiation melt and frequent, intense chinook activity. In comparison to rainfall however, this factor serves as more of a deterrent to runoff, by allowing slow, sustained infiltration and sorption by badlands materials. Nevertheless, snowmelt runoff is maximized through favourable conditions afforded by the five preceeding runoff variables, and appears as efficient, perhaps even more so, than rainfall runoff.

4.5 The Geomorphic Role of Snow, Ice, and Snowmelt

The following discussion on the role of freeze-thaw, wind erosion, slope denudation, and sediment transport shows that snow, ice, and snowmelt are active agents in the initiation of mid-winter geomorphic events. The results of winter and summer field measurements also indicate that there is a seasonal modification in the weathering regime of the Alberta badlands, which is ultimately controlled by snow distribution. The effects of this erosional alteration are not fully described or accounted in previous research most

relevant to snow geomorphology in badlands.

4.5.1 Freeze Thaw: Ice Formation, Frost Heave, and Preferential Erosion

Surface loosening of bedrock materials by freeze-thaw processes was widely recognized in the watershed, and occurred during, as well as between chinook intervals. Visual evidence of freeze-thaw was seen in the widespread creation of ice-crystal marks,[15] on the surfaces of claystones, sandstones, and pediments. These shallow cracks penetrated all lithologies to maximum depths of 5 mm, and often displayed oriented growth patterns (Figures 4.59 and 4.60). The growth of ice crystals took place nocturnally, utilizing water generated by radiation melt during cold periods, and a combination of radiation and atmospheric heat transfer during chinooks.

The ice cracks are distinguished from those formed under ordinary hydration / dehydration sequences by their shape and growth orientation. Whereas the shrink / swell phenomena characteristic of claystones produces jagged, interconnected, and often polygonal crack patterns on compact claystones, ice crystal formation creates clusters of small, individually-separated and elliptically-shaped indentations (see Figure 4.59). On some claystones and most sandstones, ice-crystal marks appeared as elongated, relatively straight cracks, which were easily distinguished from the normally jagged, wider cracks formed in the sandstone weathering rind during summer (see Figure 4.60).

It is probable that persistent night-time growth of ice crystals during winter promotes tensile weakening of surface bedrock materials, assisting the reduction in material strength and cohesiveness caused by hydration / dehydration cracking. The addition of winter-time ice crystal cracking facilitates the erosive capability or sediment removal efficiency of overland runoff during chinooks. On regolith-mantled claystones, ice-crystal marks were etched into individual clay aggregates such that the material crumbled easily into blocky sub-aggregates, upon application of slight pressure. In addition, freeze-thaw processes are likely responsible for a seemingly high incidence of exfoliation weathering on sandstone interfluves (Figure 4.61).

---

[15]According to the Glossary of Geology (1980), an ice-crystal mark is "a crack formed on a sedimentary surface by the sublimation of a crystal of ice".

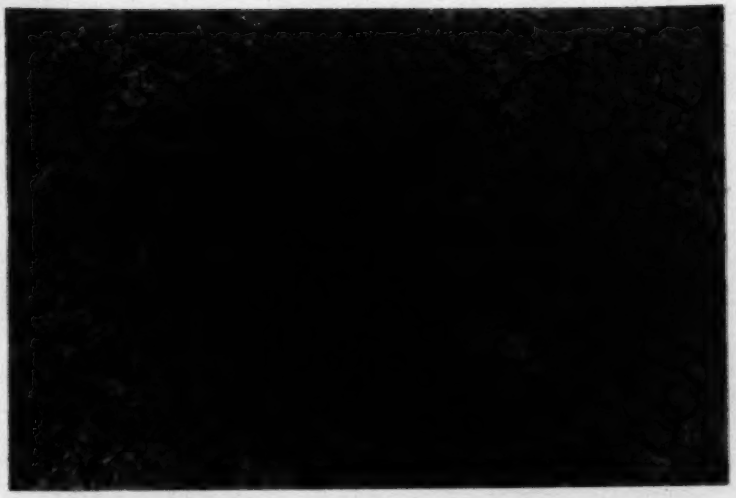

Figure 4.59. Ice-crystal marks on a compact, desiccated claystone slope (February 20, 1982). Note the radiating pattern of cracks in front of the lens cap.

Figure 4.60. Oriented ice-crystal marks on a sandstone interfluve in sb-Y (January 16, 1982).

Figure 4.61. Mid-winter erosion on a sandstone slope. Dark patches on the weathering rind indicate recent removal of material by exfoliation, probably caused by freeze-thaw activity during the chinook of late February, 1982. Note ice in rill. (Photo taken on February 18).

Ice crystal formation was confined to the upper few millimetres of the bedrock or moist channel sediments, with individual crystals always growing along (parallel) to the surface. This is contrary to the perpendicular growth patterns of needle ice, and is mainly due to the high clay content and compactness of badland materials. These characteristics restrict the capillary migration of subsurface water necessary to sustain vertical ice growth. Hence, grain size, material content, and the amount of water available do not favour widespread free ice formation, except in the very near surface of materials.

The restricted frost susceptibility of badland lithologies also applies to the growth of subsurface ice, which, as noted in Chapter 2, requires similar conditions of formation as needle ice. Although present in some claystone units, subsurface free ice formation was rare, encountered only twice during the course of numerous subsurface excavations. Minute ice crystals were found within a subsurface cavity formed in the loosened regolith of a claystone interfluve. On another claystone slope, small ice lenses speckled the frozen material of rill margins (Figure 4.62). Most often however, probably due to grain size, water availability, and the rapidity of refreezing, subsurface materials became frozen into a solid, homogeneous mass, with few free ice inclusions. Such was the case beneath most of the watershed channels that became ice-filled after the December, 1981 chinook melt episode.

These findings raise questions as to the effectiveness of frost heave in badland materials in winter. Relatively low permeability greatly restricts meltwater penetration and little subsurface water is available to act as a resevoir for segregated ice lens formation. As shown earlier, however, claystone units experience the deepest meltwater penetration depths of all badland lithologies. And, the approximate 9% expansion volume gained by water upon freezing suggests that surface heaving occurs in claystones, regardless of whether free ice is formed, or, as observed in many units, the creation of solid, frozen ground dominates.

Support for the heavability of claystones is indirectly provided by seasonal surface height measurements undertaken by Campbell (1974). Of the nine, 1 m^2 plots examined, the three showing the largest net surface rises over four consecutive winter periods (measurements taken in the spring) were all composed of claystone. Two of the plots displayed an aggregate-mantled regolith, while the other was topped by a dense network

Figure 4.62. Small, subsurface ice lenses form in the frozen, saturated sides of this ice-filled claystone rill (March 14, 1982). Due to ice lens inclusions, the frozen rill sides are aptly designated as concrete frost.

of desiccation cracks. It is highly probable that frost heave of frozen ground occurs, and is most profound in claystone units displaying broken surface characteristics, where meltwater may penetrate deeper than in more compact claystones, and sandstones.

Given that surface loosening (caused by repeated frost heaving) and material shrink / swell (caused by meltwater hydration / dehydration) is active in the Alberta badlands, and considering that subsurface ice and frozen ground was found predominantly in rill sides and larger gully channels, it follows that the seasonal accumulation of snow and ice in rills translates into a cycle of preferential material generation in these areas during winter. It also points to a seasonally-varying concentration of sediment *removal* from rill zones, upon melt of these snow reserves. Together, the actions of material production and removal suggests an accelerated winter erosion regime for rills and low areas, or, perhaps more aptly, a 'deceleration' of winter-time degradation in areas (e.g., interfluves) other than these zones. Although measurements of the winter season variations in rates and quantities of rill *versus* interfluve erosion were not undertaken, the fact that snow accumulated preferentially in depression areas supports this claim.

The hypothesis of preferred winter-time widening and deepening of rills is in agreement with Hodges and Bryan (1982), that is, rills are initiated during snowmelt activity. These findings are contrary to those of Schumm and Lusby (1963) and Schumm (1964), who, as noted in Chapter 2, maintain that freeze-thaw loosening of the Mancos shales results in winter season obliteration of rills and re-establishment during spring rainstorms. The disparity is likely due to a lesser magnitude of frost disaggregation and material production around claystone rills of the Oldman Formation in comparison to that occurring in the more frost-susceptible Mancos shales of Colorado. In addition, mid-winter chinook thaws constantly remove accumulated debris and stock piling of disaggregated materials does not occur in rills. No channel obstruction or disappearance was noticed on claystone slopes in the watershed, but rill maintenance and persistance was evident on many slopes (Figures 4.63 and 4.64).

Figure 4.63. Melting ice in the head region of a shallow rill atop a slightly-inclined, aggregate-mantled claystone slope crest (February 19, 1982). Micro-scale liquifaction processes provide the clayey residue on the rill floor, which reduces surface permeability and helps to establish rill permanency.

Figure 4.64. Ice marks are indicative of freeze-thaw loosening in this rill (same as that pictured in the previous photo), but rill obliteration, such as that recognized in the Mancos shales of Colorado is not evident (March 14, 1982).

4.5.2 Wind Erosion

Although frost heaving and material loosening were difficult to ascertain through visual observations, it is extremely likely that the combination of chinook-induced freeze-thaw and hydration / dehydration sequences enhanced geomorphic activity during the winter period. This assertion is also maintained by Hinman and Bisal (1968) and Anderson and Bisal (1969), concerning soil erosion in prairie fields of southwestern Saskatchewan. Repeated thawing, drying, and freezing processes were effective in decreasing soil aggregate particle size and "the soil often becomes highly susceptible to erosion by strong winds which commonly occur throughout the winter period" (Anderson and Bisal, 1969, p. 287).

The effectiveness of wind erosion as facilitated by freeze-thaw and hydration / dehydration was very evident in the badlands during the major chinook period of February, 1982. Towards the latter stages of the chinook, following substantial melt, a resurgence of dry, strong southwest winds removed freshly-desiccated and loosened particles. Much of the deflated material became trapped by the windward-facing surfaces of moist snowpacks (Figure 4.65). While the threshold shear velocity of the wind was sufficient to cause particle dislodgment, it was inadequate to initiate further redistribution of aged, high-density snow deposits.

Although wind erosion occurs throughout the year, it is more easily seen in winter, by means of snowpack discolouration. In fact, wind erosion may be more important in winter than in other seasons, due to the higher winter wind speeds. Both Ives (1950) and Longley (1972) support the idea that chinook winds are capable of dramatic soil drifting activity.

4.5.3 Basal Slope Erosion, Mass Movement, and Other Forms of Slope Denudation

Evidence of differential erosion, in the form of slope oversteepening, occurs on numerous slopes in the watershed, and particularly on claystones. Because many of these oversteepened slopes were not situated adjacent to drainageways, formation by fluvial undercutting (which was also an active erosion process -- see Figure 4.66) was discounted. Uniformly-falling rain could not be considered a cause for preferential basal oversteepening, and cap rock presence was likewise not a factor. Although visually

Figure 4.65. Strong southwest chinook winds deposit sediment on the windward-facing flanks of two streamlined snow dunes (February 18, 1982). Snow redistribution by strong northwest winds created the deposits to the lee of sage bushes. Stabilized by sintering and meltwater percolation induced by radiation melt and warm temperatures, the dunes remained immobile while steady, 60 km hr^{-1} chinook winds transported and deposited loosened sediment throughout the watershed. Sediment accumulation also hastened snowmelt on southwest-facing slopes by decreasing the surface albedo of snowpacks.

Figure 4.66. Basal slope oversteepening by fluvial undercutting (February 19, 1982).

non-detectable, it is probable that many of the oversteepened slope bases and mid-slope breaks were initiated by very subtle changes in lithology (i.e., mineralogical composition or structure).

Once minor slope gradient variations are established, it is highly likely that accelerated differential erosion in basal and slope break zones (shown in Figures 4.67 and 4.68) is facilitated by processes associated with preferential moisture distribution occurring in winter. Bedrock freeze-thaw may account for a small degree of material loosening, but the insulating effects of basal snowpacks, and lack of a substantial freezing amplitude probably restrict this activity to a minimum. It is most likely that the seasonally-repetitive cycle of basal snowpack formation, mid-winter chinook melt, and snowpack replenishment affords a persistent, preferential attack on basal slope materials, by means of meltwater-triggered micro-slumping and liquifaction. Material thus detached is transported across or deposited atop alluvial fans with each chinook-induced meltwater flow. The seasonal pattern of snowpack accumulation ensures a continued, differential weathering regime on lithologically-induced slope breaks and basal zones.

Another, more impressive form of degradation common in the badlands during winter is rapid mass wasting of slope materials by sloughing of small particles, aggregates, and aggregated masses. Observed repeatedly during chinook snowmelt periods, this rapid downslope movement of material occurs on claystone slopes and in the silty-clay soils of vegetation-topped features. The highly compact structure and limited infiltration capacity of sandstone slopes prohibits such activity.

The most intense sloughing occurred during the February, 1982 chinook, between February 18 and 20, when rapid snowpack melting caused material strength reduction by creating positive pore water pressures and decreasing cohesive forces of near-surface particles. Collapsed and sloughed material was largely generated from slope regions, just above dissipating basal snowpacks, where enhanced peripheral melting took place (Figures 4.69 and 4.70). Approximately 80% of all the largest-scale mass movement activity occurred in these upper snowpack zones, near the basal portions of claystone slopes.

On rilled claystone units, aggregate dislodgment by marginal snowpack melting was found more often at rill / interfluve boundaries than on interfluves (Figure 4.71), due to the larger amounts of meltwater available in rills and within rill sides. Additional mass

Figure 4.67. Basal degradation on a west-facing, disaggregated and rilled claystone slope (March 14, 1982). Meltwater paths (left-centre of photo) attest to the recent disappearance of a basal snowpack. Broken metre stick for scale.

Figure 4.68. Melting of a mid-slope snowpack at the base of an east-facing siltstone unit (March 13, 1982). Basal slope oversteepening is apparent. Glove for scale.

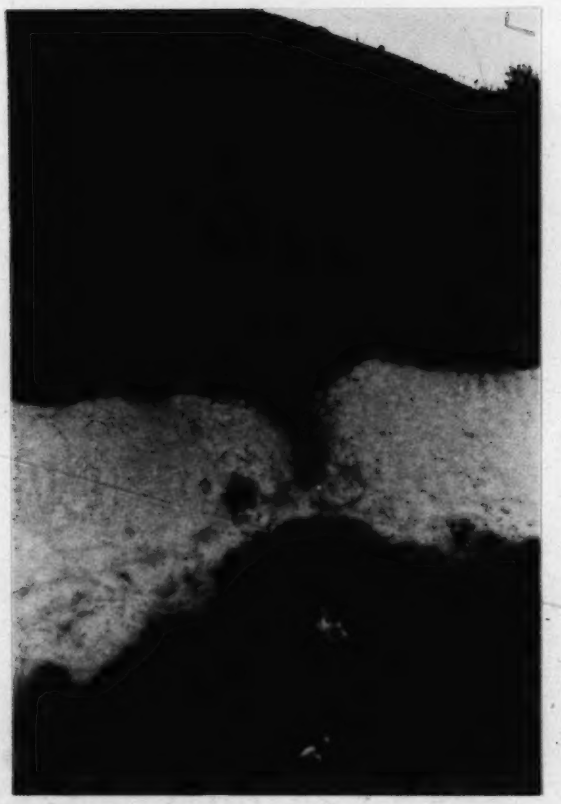

Figure 4.69. Peripheral melting of a basal snowpack initiates material weakening and detachment on a north-facing claystone slope in sb-Z (February 20, 1982). Hammer for scale.

Figure 4.70. Peripheral melting of a snowpack on the northeast-facing flank of a vegetation-lined gully in sb-Z triggers sloughing and sliding of partly unconsolidated silty-clay (February 20, 1982). Sloughing was actively occurring at the time the photo was taken, with individual particles rolling downslope in a procession-like manner. Hammer for scale.

Figure 4.71. Peripheral melting of a snowpack on an east-facing claystone slope initiates dislodgment of aggregates along the side of a rill (February 18, 1982). Metre stick for scale.

movement occurred on middle and upper slope regions of claystone slopes, but with less frequency and intensity than on lower slopes influenced by basal snowpacks. Steep, aggregate-mantled upper slopes retaining melting snowpacks were often subject to particle sloughing and downslope tumbling of aggregates, as regolith materials weakened and yielded to the effects of gravity (Figure 4.72).

Large-scale slumping and collapse of massive, coherent slope portions generally did not occur during the field season. Deflation of snow produces a lack of sufficient meltwater on most slope faces. Even though meltwater normally penetrates subsurface materials to greater depths than rainwater, the preferential redistribution of snow into lowland areas and slope bases limits the amount of water available to the total slope surface, and hence decreases the probability of major failure, especially rotational slumping. However, the smaller-scale undermining and removal of basal slope materials by peripheral snowpack melting during winter thaws increases the likelihood of massive slope collapse during spring and summer rainstorms.

An exception to the general absence of significant mass movement during winter is noted in areas covered in vegetation, such as slopes adjacent to stream channels, or on the upper side slopes of terraces and prairie flats, where vegetation serves as a "cap rock" for underlying materials. In these latter areas particularly, prolonged snowmelt infiltration often triggered overburden collapse, resulting in the removal of the protective lip of vegetation (Figure 4.73) along a failure plane conforming to the surface slope profile. Because of the great infiltrating capacity of vegetated surfaces, this type of mass wasting is common under both snowmelt and rainfall.

Of the three sub-basins, sb-Z showed more evidence of snowmelt-induced mass movement than either of the others. In fact, very little mass movement was recognized in sub-basins X and Y. This is mainly due to the fact that sb-Z possesses more claystone slopes per unit surface area than sb-X or sb-Y, as well as more total claystone surfaces, due to its larger area. In addition, the relationship between slope aspect and snow distribution seems to be an important factor in determining which claystone slopes are most susceptible to mass movement. Similar to the findings of Beaty (1972), there appeared to be a higher percentage of mass movement activity occurring on claystone units facing north, northeast, east, and southeast. Beaty found that the highest percentage

Figure 4.72. Mid- and upper-slope snowpacks on an east-facing claystone slope near sb-Z generate moisture-weakened aggregates which, aided by strong winds, tumble downslope into a basal snowpack (February 20, 1982). Footprints for scale.

Figure 4.73. Snowmelt infiltration into a north-facing vegetation-mantled claystone slope results in the collapse of a section of the moisture-weakened overhang. Depth of material removed is 30 cm.

of relict slump scars examined (34%) were located on northeast-oriented slopes, with the second highest occurrence (23%) on east slopes. Although no quantitative tally was made in the badlands, it is certain that the highest percentage of material sloughing and caving observed during 1981-1982 occurred on east-facing slopes.

As explained earlier (and illustrated previously in Figure 4.27), east slopes received more snow than others (except south) due to the joint actions of chinook and Arctic winds. Receiving more snow than radiation-protected north slopes, and receiving less radiation than the snow-abundant south slopes, east slopes were subjected to the optimum erosional conditions of slower melt of larger snow reserves, resulting in longer infiltration of more meltwater, and thus a higher magnitude of erosion during mid-winter chinook thaws. Furthermore, the northerly component of snow-redistributing Arctic winds serves to alter the erosionally effective moisture regime from predominantly northeast slopes (southwestern Alberta - Beaty's results), to predominantly east slopes (southeastern Alberta - these findings). This explanation is likely the reason for the increased mass movement activity seen in sub-basin Z, which displays far more east- and northeast-facing claystone slopes than the other sub-basins.

Sloughing and small-scale slumping on east and north claystone slopes was recognized in the watershed during the later stages of the mid-February and mid-March chinook intervals. South- and west-facing slopes, on which very little snow remained, experienced micro-scale clay aggregate slumping and partial surface sealing under daytime radiation melt and chinook activity. However, the magnitude of sloughing and surface creep occurring during chinooks was greatly lessened by continuous mid-winter radiation melt, which decreased the supply of snow available on these slope faces, for rapid, chinook-induced melt and ensuing mass movement. Additionally, chinook winds probably generated quicker evaporation and material desiccation on windward-facing south and southwest slopes, also resulting in reduced meltwater infiltration depths and decreased erosion.

These observations suggest that aspect-related differential snowmelt plays an active role in differential slope denudation during winter. Although short-term observations point to a less intense degree of geomorphic activity during winter than summer, its concentration on slopes of particular aspects may show more clearly through

examination of the long-term effects of erosion. This line of reasoning was therefore pursued further through the analysis of slope angle measurements taken subsequent to the winter field season (previously described in detail in Chapter 2).

Mean angle data for the 110 paired, north- and south-facing claystone and sandstone slopes examined is shown in Appendix G, and yields results which support a spatially-differentiated erosion regime. As structural and compositonal differences of both lithologies produce a wide range of slope angles, comparison of the overall mean slope angle among unpaired north- and south-facing claystones, sandstones, or between lithologies, is meaningless to the investigation of aspect-related slope variations. The key element of comparison lies in the examination of angles on opposite-facing slopes of the same topographic feature, thus assuring uniformity of structure and composition. Table 4.10 shows tabulations of the numbers and percentages of paired claystone and sandstone slopes showing steeper (or equal) north- or south-facing slope angles. Of the 55 paired claystone slopes sampled, 33, or, 60% display a steeper south-facing slope. Steeper north faces were encountered on 15 occasions, and 7 paired slopes display equal or near-equal slope angles. For sandstones, north and south slope distribution is extremely close, with 22 showing a steeper north face, and 23 exhibiting a steeper south face. Just over 18% of the paired slopes sampled maintain equal angles.

To ascertain whether there is a significant difference in the frequency of slopes of a given lithology which possess a steeper slope aspect, the chi-square (X^2) statistical test was employed separately for claystones and sandstones, using the values appearing in rows 4 and 5 (Table 4.10). For the test, the null hypothesis is given that there is no significant difference in the frequency with which south-facing slopes of topographic features are steeper than the north-facing slopes of the same feature. For claystone slopes, the calculated chi square, with one degree of freedom is 6.75. As this value is greater than the tabled X^2 value (6.64) at the 0.01 significance level, there is less than a 1% probability that the sampled distribution is random. On this basis, the null hypothesis must be rejected for the case of claystone slopes. For sandstones, the calculated X^2 value (0.022) is far less than the tabled figure (6.64) at the 0.01 significance level, indicating acceptance of the null hypothesis.

TABLE 4.10. RESULTS OF SLOPE ANGLE DATA ANALYSIS.

Row		Claystone	Sandstone	Claystone and Sandstone
1	Number of North-facing Slopes Examined	55	55	100
2	Number of Opposite, South-facing Slopes Examined	55	55	110
3	Total Number of Slopes Examined	110	110	220
4	Number of Paired Slopes Showing a Steeper North Face	15	22	
5	Number of Paired Slopes Showing a Steeper South Face	33	23	
6	Number of Paired Slopes Maintaining Equal Angles*	7	10	
7	Total Number of Paired Slopes	55	55	
8	Percentage of Paired Slopes Showing a Steeper North Face	27.3	40.0	
9	Percentage of Paired Slopes Showing a Steeper South Face	60.0	41.8	
10	Percentage of Paired Slopes Maintaining Equal Angles*	12.7	18.2	
11	Total Percentage	100	100	

* Opposite-facing slopes displaying mean angles + or - 2° of one another are considered equal..

These results show that claystone features show a significant difference in the frequency with which the mean angles of south-facing slopes exceed those of their north-facing counterparts. Further analysis reveals that the average difference between north- and south-facing mean slope angle is 10.4°, when the south-facing slope gradient is the steeper of the two. As the value is fairly low, it serves to obscure the numerically-evaluated slope relationship from detection by visual field observations. Nonetheless, there is an existing difference, which cannot be attributed to either lithologic changes or structural alterations. It is therefore concluded that differential solar radiation receipt and its effect on moisture availability is the primary cause of preferential slope steepness on claystone slopes.

These findings are in general agreement with aridland south slope steepening recognized by Von Engeln (1948); Spence (1972); Toy (1977); and Churchill (1981), and are probably indicative of a higher susceptibility of north-facing slopes to gradient reduction by slumping and aggregate sliding, or creep. However, it is clear that the degree of slope variation is not as great as that found in the South Dakota badlands, where it is maintained that steeper south slopes erode primarily by rockfalls initiated by desiccation or freeze-drying, and north slopes by slumping, mudflows, and creep (Churchill, 1981). Similar to observations of Churchill, a high degree of small rockfalls of clay aggregates occurs on steep, south-facing claystone slopes. However, north, east, and west slopes are also subject to such activity upon dehydration and shrinkage of aggregates, and a possible dominance of this mode of erosion on a particular slope aspect was not investigated.

Contrary to Churchill's observations in South Dakota, there is no conspicuous difference in the degree of rill dissection on varying slope aspects in the Alberta badlands. This implies that denudation by rill wash on the Oldman claystones is effective on both north- and south-facing slopes, and that there may not be a great variation (though there is likely some difference) in the infiltration characteristics of these slope aspects. There has been virtually no examination of infiltration variations according to slope orientation in the Alberta badlands, as there has been in the Israeli badlands (Yair *et al*., 1980; Yair and Lavee, 1982) and in South Dakota (Churchill, 1984).

Nevertheless, numerical data on slope form suggests that long-term weathering regimes on north- and south-facing claystones differ to some degree. On the basis of winter field observations, it appears that slope form is affected by moisture retention variations caused by differential radiation receipt. The best documentation of this is seen in the pattern of snowmelt disappearance and slope degradation. The longer duration of snowpacks on north and east slopes, and the quick-drying, mid-winter melt and evaporation on south and west slopes, indicates a differential moisture penetration regime whereby enhanced gradient reduction by sloughing and micro-slumping occurs on north and east slopes, and, a reduction in geomorphic activity on south and west slopes.

The overall decrease in the frequency and magnitude of geomorphic events occurring in winter, however, suggests that differential solar radiation must also function effectively during summer. It is fairly certain that increased radiation receipt on south-facing claystone slopes during summer leads to quicker dehydration by evaporation, as it does in winter, and may also limit the extent of infiltration and water penetration, favouring the development of steeper south slopes. Further research is needed on this.

This study suggests that winter snow distribution and snowmelt does cause aspect-induced south slope steepness on claystone slopes in the Alberta badlands. And, in answer to the three possible roles of snow distribution and melt in contributing to preferential slope steepness (posed at the end of Chapter 3), clause number 3, "...snow distribution and melt is such that it enhances the effects of differential insolation", is likely the adequate explanation of the effects of snow on slope development.

The implied correlation between differential solar radiation receipt and slope form cannot be extended to include the weathering regime of sandstone slopes. The denser and more indurated sandstones limit deep water penetration on all slope aspects. The combination of compactness and grain size inhibits the formation of surface aggregates, resulting in runoff and weathering characteristics which are very different from those recognized on claystones. In effect, sandstones are not susceptible to mass movement except where removal of large portions of basal support material facilitates slope collapse. The sloughing and sliding occurring on claystones is replaced on sandstones by sheetwash and concentrated degradation in rills. Hence, sandstone slope form is negligibly influenced by differential radiation receipt, but is determined rather, by inherent

structural and lithological controls.

The ineffectiveness with which solar radiation invokes differential slope gradient reduction on sandstones is clearly evident from numerical slope data given in Table 4.10. The near-identical frequency with which north and south slope faces exceed one another in steepness (rows 4 and 5, and rows 8 and 9) attests to this, with significance confirmed by the X^2 statistical analysis and adoption of the null hypothesis.

4.5.4 Sediment Erosion and Transport

There is some similarity between the relative amounts of sediment transported through the main channel of the watershed during individual rainstorms and snowmelt runoff episodes. This observation is drawn from comparisons of suspended sediment data of rainstorms *versus* snowmelt, and from measurements of sediment deposition and accumulation within the channel upon termination of runoff events.

Table 4.11 gives suspended sediment concentrations sampled during a long-duration rainstorm of 1983, as well as seven samples taken during the chinook runoff period of February, 1982. Although the data reflects the known variability in sediment concentrations during individual runoff events (c.f., concentration values at 10:42 *versus* 16:18 for the June 18 rainstorm at a 14 cm stage height), and variations are also recognized from one runoff period to the next, the two sets of data show complimentary concentrations for like stage heights. Additionally, both sets generally show the expected increase in material concentration levels with increase in water flow. Furthermore, sediment concentrations during snowmelt runoff remain at "normal" levels despite the fact that the snowmelt runoff period lasted almost six days, as opposed to a few hours for most rainstorms.

The depth of sediment deposited in the main channel outlet after rainstorms and snowmelt runoff episodes is also similar. Waning flow during the early morning hours of March 12 permitted measurement of material derived from bedload transport and suspension settling, which became deposited atop a pre-formed layer of channel ice. Sediment thickness varied, expecially in meander stream sections (Figure 4.74). On relatively straight reaches, sediment deposition averaged about 7 cm (Figure 4.75) atop the ice layer. This is similar to rainstorms, as sediment aggradation observed in the flume

TABLE 4.11. COMPARISON OF SUSPENDED SEDIMENT SAMPLES FROM A SPRING RAINSTORM VERSES SNOWMELT RUNOFF.

Date	Time	Flume Stage Height (cm)	Suspended Sediment ($gr.l^{-1}$)
	Rainstorm of June 18, 1983		
	9:17	16	14.57
	9:23	18	11.03
	10:10	14	13.21
	10:42	14	12.04
	10:56	15	9.85
	11:05	15	10.71
June 18	13:55	9	12.17
	14:11	8	8.90
	14:19	8	10.85
	14:35	8	11.71
	15:03	20	27.84
	15:06	22	27.36
	15:20	25	35.61
	15:44	19	33.91
	16:18	14	23.93
	Snowmelt Runoff of the February, 1982 Chinook		
Feb. 19	10:00	8.3 *	14.45
	16:00	12.0 *	15.66
Feb. 20	10:00	13.5	19.84
	16:00	20.0	21.04
	19:00	16.8	12.89
Feb. 21	10:00	4.2	3.56
	15:00	3.6	3.13

* Depth of channel ice subtracted

Figure 4.74. Sediment deposition beneath a slip-off slope near the main channel outlet is exposed during an early morning period of waning diurnal flow (March 12, 1982).

Figure 4.75. Sediment accumulation and ripple formation in a straight reach of the main channel (March 12, 1982). Alluvium obtains a thickness of 7.0 cm at ripple crests, and is underlain by 2.0 cm of solid ice, formed by refreeze of waning runoff upon cessation of the late February chinook. Note the surface ice-crystal marks formed nocturnally, under a minimum temperature of −5.5°C.

after cessation of rainstorms frequently measures 5 to 10 cm.

These observations support the statement made earlier that chinook-induced snowmelt runoff events may be likened to individual rainstorms, in the absence of one large, spring thaw period. This idea seems to hold for sediment removal too, but the gross simplification of suspended sediment and depth comparisons between rainfall and snowmelt may obscure some important differences between the relative amounts of sediment removed under the seasonally-varying erosion regime. For example, sediment loads appear to be approximately the same under rainfall and snowmelt, despite the fact that snowmelt suspended sediment samples contained little alluvium derived secondarily, from the channel bottom, as normally occurs under rainfall runoff. This is due to the ubiquitous 2-5 cm ice cover, which, throughout both the February and March chinook periods, protected underlying channel sediments from re-entrainment and transport by suspension or traction. Thus, per unit volume, snowmelt runoff likely contains more "newly derived" material than rainfall runoff.

This interpretation implies an expected decrease in the content of sediment carried through the main channel under conditions of early-winter ice formation. Also pointing to an eminent reduction in the amount of material channeled through the watershed during snowmelt runoff, is the seasonal variability of the surface area contributing sediment to the system. That is, preferential snow accumulation in rills and gullies greatly reduces the potential for flow-induced entrainment and transport from snow-barren slopes and interfluves, circumstances not occurring under rainfall.

The question remaining, therefore, concerns the lack of reduction or tapering off of per unit volume sediment concentrations during chinook runoff periods. As already mentioned, the previously expected high spring sediment yields postulated for the badlands (Hogg, 1978), and realized in Colorado (Schumm and Lusby, 1963; Schumm, 1964), did not occur in the winter of 1982-83 because of the constant removal of material by repeated mid-winter runoff events; there was no end-of-season culmination of geomorphic activity. The apparent equality of sediment concentrations during rainstorms and snowmelt may be attributed to the greater efficiency with which sediment is produced in rill zones between chinook thaws. Due to winter processes of freeze-thaw desiccation and frost heaving, more sediment is produced in these areas than during summer

rainstorms. Thus, heightened rill degradation in winter probably yields more sediment during chinook runoff, but this realization becomes obscured by the smaller, total surface area from which it generated, and by the decreased contribution of transient, main channel alluvium.

5. SUMMARY OF RESULTS AND CONCLUSIONS

5.1 Summary of Results

This investigation of the role of snow and snowmelt has provided a first understanding of geomorphic processes operating in the Alberta badlands during the winter season. Field examinations of the behaviour of snow accumulation, distribution, melt, infiltration, and runoff have yielded greater insight on the relationship between snow and badland erosional response, and have generated many questions. Results of these examinations are summarized below.

5.1.1 Snow Accumulation

1. Past meteorological records and field measurements of snow accumulation show that close to one-third of the total mean annual precipitation normally received in the badlands fell as snow during the winter of 1981-1982.
2. Snow surveys revealed that the amount of snow present prior to mid-winter runoff episodes was similar in snow / water equivalent to low-intensity summer rainstorms.

5.1.2 Wind and Snow Distribution

1. Short-term observations and long-term wind records show high-velocity Arctic northwest winds and southwest chinooks characterically dominate during winter, and that alternations of these winds in winter are typical and seasonally repetitious.
2. The bimodal nature of these effective, snow-moving winds is realized in zones of southern Alberta which lie on the outskirts of the "heavy chinook belt" as defined by Beaty (1975).
3. The redistribution of snow, during and after storms results in a snowcover characterized by bare areas, and areas of heavy drifting and snow deposition. Areas which experience snow removal include slope crests, faces, and expansive, relatively flat areas, especially those covered by pediments and fans with low surface roughness characteristics. Grass-covered regions are also subject to deflation, but less so on terraced flats in low-elevation areas of the watershed than

on upper prairie surfaces.

4. Areas characterized by heavy snow accumulation and drifting include wind-sheltered surface depressions, such as gullies and rills. Large snow deposits are also located on lee slope bases oriented clockwise from north to south. On slopes, greatest deposition is permitted on those facing east, due to the joint, westerly component of the bimodally-influencing winds.

5.1.3 Snowmelt

1. Chinook activity strongly influences badland hydrology by initiating a number of snowmelt episodes throughout the winter season.
2. Differential solar radiation melt is evident, and contributes to both south slope snowmelt under air temperatures below 0°C, and rapid melt on south and west slopes during chinooks.
3. Differential radiation receipt is the most important factor governing the rate and sequence of snowmelt on badland slopes, overshadowing the influence of snow distribution.

5.1.4 Infiltration

1. Snowmelt penetration into the subsurface generally exceeds that of rainfall on all lithologies except those covered by vegetation, where it is usually dependent on the amount of water available.
2. Deeper snowmelt penetration is primarily attributed to the longer duration and slower rate with which melting snowpacks provide a source of moisture for prolonged sorption and infiltration processes.
3. Due to preferential snow redistribution, the deeper penetration realized under snowmelt is spatially limited on many slopes, to rills and rill sides, the latter of which experience relatively extensive lateral infiltration.

5.1.5 Runoff

1. Observed patterns of snow distribution indicate a seasonally-varying runoff source area, concentrated in rills, gullies and other drainageways of the watershed.
2. Many slopes remain largely dehydrated during winter runoff periods, a condition not recognized during rainstorms.
3. Concentration of moisture in rills is also indicative of a higher runoff efficiency in winter, due in part to a reduced loss of water to absorbent interfluves, steep slope faces, and slope crests.
4. The early formation and widespread coverage of rill ice and frozen, solid ground beneath lowland areas also favours a higher runoff efficiency in winter.
5. Spot monitoring of main channel runoff during the February, 1982 chinook reveals that total discharge exceeded the volumetric outflow recorded for all individually-monitored rainstorms of 1981 and 1982.

5.1.6 Geomorphology

1. The partial area concept, whereby rills, gullies, and other lowland areas in the badlands are major contributors to overland flow, is extended to include partial area sediment generation and accelerated winter erosion in rill zones. Loosening of rill material by frost heave, permitted by repeated thaw and refreeze of moisture in areas of high snow accumulation ensures focussed, and preferential production and removal of sediment in rills during winter.
2. Agglomeration of rill materials, and obliteration of rills in winter is not recognized in the Alberta badlands as it is in the Mancos shales of Colorado, due to continuous removal of sediment by chinook-induced flow. Restricted meltwater penetration and high clay content of Oldman lithologies also reduces intense frost disaggregation by subsurface free ice formation. Most ice-related material detachment is achieved through differential frost heave around rills, associated with the volumetric expansion obtained by frozen water.
3. Mass movement activity on claystone slopes is not as common or as widespread in winter as in summer due to limited meltwater availability on slope face interfluves.

4. Preferential snow accumulation at slope bases permits differential erosion in these areas in winter. Basal and mid-slope break sapping primarily operates through micro-slumping, aggregate sloughing, and liquifaction, during rapid, chinook-induced meltwater production.
5. East-facing slopes and slope bases show the highest magnitude of mass wasting than other slopes, primarily as a result of receiving more redistributed snow.
6. Differential solar radiation receipt is a critical factor controlling snowmelt and evaporation rates, and plays an integrated role with snow accumulation and distribution in determining the relative intensity of geomorphic action on varying slope aspects.
7. Slope aspect measurements and statistical analysis reveals a significant difference in the frequency with which south-facing claystone slopes retain higher mean slope angles than their uniformly-composed and structured, north-facing counterparts. This indicates the presence of an established spatially-varying weathering regime which is most likely related to year-round differential solar radiation receipt. Winter observations of differential snowmelt and erosional intensity support the observed diversity in long-term slope form evolution.
8. Suspended sediment samples show that near-equal amounts of materials are removed during rainfall and snowmelt runoff episodes, per unit volume of water leaving the watershed. Due to the partial area contribution of runoff and sediment during chinook runoff, however, it would be expected that sediment yields should decrease during winter runoff. As the data does not reflect this assumption, it is likely that a higher percentage of material is entrained from rill zones in winter, to "compensate" for the expected reduction. This view is indirectly supported by the widespread presence of frost and frozen materials in and around rills, which probably increases normal sediment production through frost heave loosening.
9. Large spring sediment yields were not recognized during the 1981-1982 field season, due to the lack of final, substantial melt episode of the total season accumulation of snow. Instead, chinook interference provoked a number of smaller, yet effective mid-winter runoff and sediment transport events. This is likely a seasonal characteristic in the badlands, as evidenced by long-term meteorological

records that show a repetitive occurrence of southwest chinook winds during winter.

5.2 Conclusions

The results of this research yield a number of conclusions concerning the interrelationships among snow accumulation, distribution, melt, infiltration, runoff, and badland geomorphology. Because this study represents an initial appraisal of the role of snow and snowmelt, the results raise questions which merit further attention.

Regarding the relationship between snow accumulation and geomorphology, it is concluded that sufficient quantities of snow are typically available in the badlands to maintain a year-round continuity in moisture input and geomorphic activity. This is evident despite the larger than average amount of snow received during the 1981-1982 field season, and is indicative from the 27-year snow accumulation records of the AHRC weather station. As acknowledged earlier, however, the overall geomorphic impact of snow is reduced in comparison to rain, due to the smaller frequency of melt episodes relative to the number of summer rainstorms, and, because normally three-quarters of the mean annual precipitation falls as rain.

The primary effect of snow distribution in the badlands in terms of geomorphology, is the establishment of preferential snow accumulation and redistribution areas, which ultimately results in the creation of spatially non-uniform zones of effective moisture input and erosion. Variations in snowmelt rate, caused by differential solar radiation receipt also alter the spatial homogeneity of these two regimes. However, the badlands are under the influence of differential radiation receipt all year round, and winter observations of snow depletion generally adhere to the expected summer-time moisture variations (e.g., quicker desiccation of south slopes, slower melt and infiltration of north slopes). Therefore, although differential radiation causes spatial variations in badland moisture and erosion regimes (as evidenced by slope angle measurements, and differential mass movement on claystone slopes in winter), it does not cause a significant change of the established alteration from one season to the next (warm season to cold season).

It is therefore concluded that the major difference in erosion and moisture characteristics of badland materials between winter and summer seasons lies in moisture variations caused by snow redistribution. Specifically, the unbalanced distribution of the snowcover whereby rills, gullies, and slope bases retain significantly larger snow reserves and deeper infiltration depths than slope faces, is the key *seasonal* difference in badland moisture input and geomorphic development. During winter, the "normal" rate of interfluve denudation lags behind the "normal" rate of rill and slope base erosion, resulting in a year-round degradation in these latter areas, but a retarded rate, or, what may be termed 'partial-season' slope denudation.

A major question arising from this conclusion concerns the amount of variability, or, the extent to which retarded slope erosion is present in winter. The question remains unanswered, and may thus serve as a focus of continued winter research in the badlands. Recommended methods of investigating this diversity in seasonal-spatial erosion rates include intensive suspended sediment sampling of runoff emanating from plot-size slopes under rainfall and snowmelt. Additionally, a means of monitoring and correlating the average depth of rill and interfluve erosion on a given slope or slopes under rainstorm conditions should be established, with results compared to average depth reductions measured under a number of snowmelt episodes.

Suspended sediment sampling of plot sites may additionally aid in determining the degree of influence of preferential frost heave in rill zones, but physical measurements, and close-up, sequential photography of selected rills would also improve this investigation. These suggestions may help quantify winter-time erosion estimates according to source areas, and should be used in conjunction with a more intense suspended sediment sampling scheme at the main channel outlet during chinook runoff periods.

References

Adams, W.P. 1976. Areal differentiation of snowcover in east-central Ontario. *Water Resources Research*, **12** (6) 1226-1234.

American Geological Institute. 1976. *Dictionary of Geological Terms.* Revised Edition, Anchor Press/Doubleday, Garden City, New York.

American Geological Institute. 1980. *Glossary of Geology* (2nd Ed.), R.L. Bates and J.A. Jackson (eds.), Falls Church, Virginia.

Anderson C.H. and Bisal, F. 1969. Snow cover effect on the erodible soil fraction. *Canadian Journal of Soil Science*, **49**, 287-296.

Anderson, E.A. 1972. Techniques for predicting snow cover runoff. WMO-2: *Forecasting Runoff*, International Symposia on the Role of Snow and Ice in Hydrology, 30 p.

Anderson, E.A. 1978. Streamflow simulation models for use on snow covered watersheds. In *Modeling of Snow Cover Runoff*, S. Colbeck and M. Ray (eds.), U.S. Army Cold Regions Research and Engineering Laboratory, Hanover, New Hampshire, September 26-28, pp. 336-350.

Ashwell, I.Y. 1968. Studies of the chinook at Calgary: a progress report. *The Albertan Geographer*, **4**, 45-47.

Atkinson, T.C. 1978. Techniques for measuring subsurface flow on hillslopes. Chapter 3 in: *Hillslope Hydrology*, M.J. Kirkby (ed.), John Wiley Interscience, Chichester, 73-120.

Bagnold R.A. 1941. *The Physics of Blown Sand and Desert Dunes.* Methuen, London, 265 p.

Barendregt, R.W. and Ongley, E.D. 1979. Slope recession in the Onefour Badlands, Alberta, Canada: an initial appraisal of contrasted moisture regimes. *Canadian Journal of Earth Sciences*, **16** (2), 224-229.

Baver, L.D. 1956. *Soil Physics*, (3rd Ed.), John Wiley and Sons, New York, 489 p.

Baver, L.D., Gardner, W.H., and Gardner, W.R. 1972. *Soil Physics*, (4th Ed.), John Wiley and Sons, New York, 498 p.

Beaty, C.B. 1972. Geographical distribution of post-glacial slumping in southern Alberta. *Canadian Geotechnical Journal*, **9**, 219-224.

Beaty, C.B. 1975. Coulee alignment and the wind in southern Alberta, Canada. *Geological Society of America Bulletin*, **86**, 119-128.

Beaty, C.B. 1976. *Landscapes of Southern Alberta - A Regional Geomorphology.* University of Lethbridge Production Services, 95 p.

Benedict, J.B. 1970. (in Thorn, 1979). Downslope soil movement in a Colorado alpine region: rates, processes, and climatic significance. *Arctic and Alpine Research*, **2**, 165-226.

Bengtsson, L. 1982. Groundwater and meltwater in the snowmelt induced runoff. *Hydrological Sciences Journal*, **27** (2), 147-158.

Beskow, G. 1935. (in Williams, 1957 and Schumm, 1964). Tjalbildningen och tjallyftningen med sarskild hansyn till vagar och jernvagar. (Soil freezing and frost heaving with special application to roads and railroads). *Sveriges Geologiska Undersokning*, Meddelande, **48** (375), 142 p.

Betson, R.P. 1964. What is watershed runoff? *Journal of Geophysical Research*, **69** (8), 1541-1552.

Betson, R.P. and Marius, J.B. 1969. Source areas of storm runoff. *Water Resources Research*, **5**, 574-582.

Beven, K.J. and Dunne, T. 1982. Modeling the effect of runoff processes on snowmelt hydrographs. In: *Rainfall/Runoff Relationships*, V.P. Singh (ed.), Proceedings of the International Symposium on Rainfall-Runoff Modeling, Mississippi State University, May, 1981. Water Resources Publications, Littleton, Colorado, 277-284.

Beven, K.J. and Kirkby, M.J. 1979. A physically based, variable contributing area model of basin hydrology. *Hydrological Sciences Bulletin*, **24** (1), 43-69.

Bird, J.B. 1967. (in French, 1976). *The Physiography of Arctic Canada*. The Johns Hopkins Press, Baltimore, 336 p.

Blackwelder, E. 1940. The hardness of ice. *American Journal of Science*, **238**, 61-62.

Brinkmann, W. 1969. The definition of the chinook in the Calgary area. Unpublished M.Sc. Thesis, University of Calgary.

Brinkmann, W. and Ashwell, I.Y. 1970. The structure and movement of the chinook in Alberta. In: *Weather and Climate*, J.G. Nelson, M.J. Chambers, and R.E. Chambers (eds.), Methuen, Toronto, 241-250.

Brown, G.W. 1962. Piping erosion in Colorado. *Journal of Soil and Water Conservation*, **17**, 220-222.

Bruce, J.P. 1962. Snowmelt contributions to maximum floods. *Eastern Snow Conference, Proceedings* of the 1961-1962 Meeting, February 9-10, 85-103.

Bruce, J.P. and Clark, R.H. 1966. *Introduction to Hydrometeorology*, Pergamon Press, Oxford, 319 p.

Bryan, R.B. 1979. The influence of slope angle on soil entrainment by sheetwash and rainsplash. *Earth Surface Processes*, **4**, 43-58.

Bryan, R.B. and Campbell, I.A. 1980. Sediment entrainment and transport during local rainstorms in the Steveville Badlands, Alberta. *Catena*, **7** (1), 51-65.

Bryan, R.B. and Campbell, I.A. 1982. Surface flow and erosional processes in semi-arid mesoscale channels and drainage basins. Recent Development in the Explanation and Prediction of Erosion and Sediment Yield, *IASH Publication*, **137**, Proceedings of the Exeter Symposium, July, 1982, 123-133.

Bryan, R.B. and Campbell, I.A. 1984. Runoff generation and sediment transport in a semiarid ephemeral drainage basin. Manuscript submitted to *Zeitschrift fur geomorphologie*.

Bryan, R.B., Yair, A., and Hodges, W.K. 1978. Factors controlling the initiation of runoff and piping in Dinosaur Provincial Park badlands, Alberta, Canada. *Zeitschrift fur Geomorphologie Supplement Band*, **29**, 151-168.

Buckham, A.F. and Cockfield, W.E. 1950. Gullies formed by sinking of the ground. *American Journal of Science*, **248**, 137-141.

Budel, J. 1953. Die "periglazial" morphologischen Wirkungen des Eiszeitklimas auf der ganzen Erde. *Erdkunde*, bd., **7**, 249-266.

Buffo, J., Fritschen, L.J., and Murphy, J.L. 1972. Direct solar radiation on various slopes from 0 to 60 degrees north latitude. *U.S.D.A. Forest Service Research Paper*, **PNW-142**, Portland, Oregon, 74 p.

Byrne, P.J.S. and Farvolden, R.N. 1959. The clay mineralogy and chemistry of the Bearpaw Formation of southern Alberta. *Research Council of Alberta Bulletin*, **4**, 44 p

Campbell, I.A. 1970. Erosion rates in the Steveville Badlands, Alberta. *The Canadian Geographer*, **14**, 202-216.

Campbell, I.A. 1974. Measurements of erosion on badland surfaces. *Zeitshrift fur Geomorphologie Supplement Band*, **21**, 122-137.

Campbell, I.A. 1978. Local storms and sediment yields in the Steveville Badlands, Alberta. In: *Essays on Meteorology and Climatology: In Honour of Richmond W. Longley*, Studies in Geography, Monograph 3, Department of Geography, University of Alberta, 27-39.

Campbell, I.A. 1981. Spatial and temporal variations in erosion measurements. Erosion and Sediment Transport Measurement, *IASH Publication*, **133**, Proceedings of the Florence Symposium, June 1981, 447-456.

Campbell, I.A. 1984. The partial area concept and its application to the problem of sediment source areas. Proceedings of the International Conference on Soil Erosion and Conservation, Honolulu, Hawaii. (manuscript).

Campbell, I.A. and Honsaker, J.L. 1982. Variability in badlands erosion; problems of scale and threshold identification. In: *Space and Time in Geomorphology*, C.E. Thorn (ed.), The Binghamton Symposia in Geomorphology, International Series **12**, 59-79.

Chebotarev, N.P. 1962. *Theory of Stream Runoff*. Izdatel'stvo Moskovskogo Universiteta, Israel Program for Scientific Translations, Jerusalem, 46-51.

Churchill, R.R. 1981. Aspect-related differences in badlands slope morphology. *Annals of the Association of American Geographers*, **71** (3) 374-388.

Colbeck, S.C. 1974. Water flow through snow overlying an impermeable boundary. *Water Resources Research*, **10**, 119-123.

Collins, E.H. 1934. Relationship of degree-days above freezing to runoff. *Transactions of the American Geophysical Union*, **15**, 624-629.

Connell, D.C. and Tombs, J.M.C. 1971. The crystallization pressure of ice - a simple experiment. *Journal of Glaciology* **10**, 312-315.

Davar, K.S. 1970. Peak flow-snowmelt events. Chapter 9 in: *Handbook on the Principles of Hydrology*, D.M. Gray (ed.), Research Council of Canada, 9.1-9.25.

Diamond, M. 1953. Evaporation or melt of snowcover. *U.S. Snow, Ice and Permafrost Research Establishment*, Research paper, **6**, November, 1953.

Dickinson, W.T. and Whiteley, H.R. 1972. A sampling scheme for shallow snowpacks. *IASH Bulletin*, **17**, (3), 247-258.

Dickison, R.B.B. and Daugharty, D.A. 1978. A square grid system for modeling snow cover in small watersheds. In: Proceedings, *Modeling of Snow Cover Runoff*, S. Colbeck and M. Ray (eds.), U.S. Army Cold Regions Research and Engineering

Laboratory, Hanover, New Hampshire, September 26-28, pp. 71-76.

Dirksen, C. and Miller, R.D. 1966. Closed-system freezing of unsaturated soil. *Soil Science Society of America Proceedings*, **30**, 168-173.

Dodson, P. 1970. Sedimentology and taphonomy of the Oldman Formation (Carpaiean) Dinosaur Provincial Park, Alberta. Unpublished M.Sc. Thesis, University of Alberta.

Dreibelbis, F.R. 1949. Some influences of frost penetration on the hydrology of small watersheds. *Transactions of the American Geophysical Union*, **30** (2), 279-282.

Dunne, T. 1978. Field studies of hillslope flow processes. In: *Hillslope Hydrology*, M.J. Kirkby (ed.), Wiley and Sons, Chichester, 227-294.

Dunne, T. and Black, R.D. 1970a. An experimental investigation of runoff processes in permeable soils. *Water Resources Research*, **6**, 478-490.

Dunne, T. and Black, R.D. 1970b. Partial area contributions to storm runoff in a small New England watershed. *Water Resources Research*, **6**, 1296-1311.

Dunne, T. and Black, R.D. 1971. Runoff processes during snowmelt. *Water Resources Research*, **7**, 11601172.

Dunne, T., Price, A.G., and Colbeck, S.C. 1976. The generation of runoff from subarctic snowpacks. *Water Resources Research*, **12**, 677-685.

Dyunin, A.K. 1967. Fundamentals of the mechanics of snow storms. In: *Physics of Snow and Ice*, H. Oura (ed.), Proceedings of the International Conference on Low Temperature Science, I (2), Hokkaido University, Sapporo, 1065-1073.

Embleton, C. and King, C.A.M. 1975. *Periglacial Geomorphology*. Edward Arnold, London, 203 p.

Emery, K.O. 1947. Asymmetrical valleys of San Diego County, California. *Bulletin of the Southern California Academy of Science*, **46**, 61-71.

Engelen, G.B. 1973. Runoff processes and slope development in Badlands National Monument, South Dakota. *Journal of Hydrology*, **18**, 55-79.

Environment Canada. *Monthly Record: Meterological Observations in Western Canada*, Downsview, Ontario, Volumes Covering Years 1969 to 1981.

Environment Canada. 1973. *Snow Surveying*. (2nd Ed.), Manual of Standards / Snow Surveying Procedures. Toronto, Ontario, 20 p.

Environment Canada. 1975. *Canadian Normals: Wind 1955-1972.*, **Vol. 3**, Downsview, Ontario.

Environment Canada. 1982. *Canadian Climate Normals: 1951-1980. Temperature and Precipitation - Prairie Provinces*, Downsview, Ontario.

Environment Canada. 1982. *Canadian Climate Normals: Temperature 1951-1980.*, **Vol. 2**, Downsview, Ontario.

Environment Canada. 1982. *Canadian Climate Normals: Precipitation 1951-1980*, **Vol. 3**, Downsivew, Ontario.

Environment Canada. 1982. *Canadian Climate Normals: Wind 1951-1980*, **Vol. 5**, Downsview, Ontario.

Faulkner, P.H. 1970. Aspects of channel and basin morphology in the Steveville Badlands, Alberta. Unpublished M.Sc. Thesis, University of Alberta.

Ffolliott, P.F. and Hansen, E.A. 1968. Observations of snowpack accumulation, melt, and runoff on a small Arizona watershed. *U.S.D.A. Forest Service Research Note*, **RM-124**, 7 p.

Fitzgibbon, J.E. and Dunne, T. 1979. Characteristics of subarctic snowcover. *Hydrological Sciences Bulletin*, **24** (4), 465-476.

Fletcher, J.E., Harris, K., Peterson, H.B., and Chandler, V.N. 1954. Piping. *Transactions of the American Geophysical Union*, **35**, 258-262.

French, H.M. 1976. *The Periglacial Environment*. Longman Group, London, 309 p.

Gardner, J.S. 1969. Snowpatches: their influence on mountain wall temperatures and the geomorphic implications. *Geografiska Annaler*, **51A**, 114-120.

Gary, H.L. and Coltharp, G.B. 1967. Snow accumulation and disappearance by aspect and vegetation type in the Santa Fe Basin, New Mexico. *U.S.D.A. Forest Service Research Note*, **RM-93**, 11 p.

Gerson, R. 1971. Geomorphic processes in Mt. Sdom. Unpublished Ph.D. Thesis, The Hebrew University, Jerusalem.

Golding, D.L. 1978. Calculated snowpack evaporation during chinooks along the eastern slopes of the Rocky Mountains in Alberta. *Journal of Applied Meteorology*, **17**, 1647-1651.

Goodison, B.E. 1978. Comparability of snowfall and snow cover data in a southern Ontario basin. In: Proceedings, *Modeling of Snow Cover Runoff*, S. Colbeck and M. Ray (eds.), U.S. Army Cold Regions Research and Engineering Laboratory, Hanover, New Hampshire, September 26-28, pp. 34-43.

Goodison, B.E. and McKay, D.J. 1978. Canadian snowfall measurements: some implications for the collection and analysis of data from runoff stations. *Western Snow Conference, Proceedings* of the 46th Annual Meeting, April 18-20, Otter Rock, Oregon, 48-57.

Granger, R.J., Chanasyk, D.S., Male, D.H., and Norum, D.I. 1977. Thermal regime of a prairie snowcover. *Soil Science of America Journal*, **41**, 839-842.

Gray, D.M. 1970. Snow hydrology of the prairie environment. *Proceedings, Workshop Seminar on Snow Hydrology*, February 28-29, 1968, Queen's Printer of Canada, Ottawa, 21-33.

Gray, D.M. and Others. 1978. Snow accumulation and distribution. In: Proceedings, *Modeling of Snow Cover Runoff*, S. Colbeck and M. Ray (eds.), U.S. Army Cold Regions Research and Engineering Laboratory, Hanover, New Hampshire, September 26-28, pp. 3-33.

Gray, D.M., Steppuhn, H.W., and Abbey, F.L. 1979. Estimating the areal snow water equivalent in the prairie environment. Paper Presented at the Canadian Hydrology Symposium 79, Cold Climate Hydrology, May 10-11, 1979, Vancouver, 19 p.

Hack, J.T. and Goodlett, J.C. 1960. Geomorphology and forest ecology of a mountain region in the central Appalachians. *U.S. Geological Survey Professional Paper*, **347**, 66 p.

Hadley, R.F. 1961. Some effects of microclimate on slope morphology and drainage basin development. *U.S. Geological Survey Professional Paper*, **424-B**, B32-34.

Hasholt, B. 1972. Random sampling techniques applied in measuring snow water equivalent in a drainage basin. WMO-1: *Measurement in Space and Time*,,

International Symposium on Measurement and Forecasting, 6 p.

Heede, B.H. 1971. Characteristics and processes of soil piping in gullies. *U.S.D.A. forest Service Research Paper*, **RM-68,** 13 p.

Heim, A. 1885. (in Teichert, 1939). *Handbuch der Gletscherkunde*. Stuttgart, 286 p.

Hendrick, R.L., Filgate, B.D., and Adams, W.M. 1971. Application of environmental analysis to watershed snowmelt. *Journal of Applied Meteorology*, **10** (3), 418-429.

Hendrie, L.K. and Price, A.G. 1978. Energy balance and snowmelt in a deciduous forest. In: Proceedings, *Modeling of Snow Cover Runoff*, S. Colbeck and M. Ray (eds.), U.S. Army Cold Regions Research and Engineering Laboratory, Hanover, New Hampshire, September 26-28, pp. 211-221.

Hewlett, J.D. and Hibbert, A.R. 1967. Factors affecting the response of small watersheds to precipitation in humid areas. In: *Forest Hydrology*, W.E. Sopper and H.W. Lull (eds.), Pergamon, Oxford, 275-290.

Hillel, D. 1980. *Fundamentals of Soil Physics*. Academic Press, New York, 413 p.

Hinman, W.C. and Bisal, F. 1968. Alterations of soil structure upon freezing and thawing and subsequent drying. *Canadian Journal of Soil Science*, **48,** 193-197.

Hodges, W.K. 1982. Hydraulic characteristics of a badland pseudo-pediment slope system during simulated rainstorm experiments. In: *Badland Geomorphology and Piping*, R. Bryan and A. Yair (eds.), Geo Books, Norwich, 127-151.

Hodges, W.K. and Bryan, R.B. 1982. The influence of material behaviour on runoff in the Dinosaur Badlands, Canada. In: *Badland Geomorphology and Piping*, R. Bryan and A.Yair (eds.), Geo Books, Norwich, 13-46.

Hogg, S. 1978. Near surface hydrology of the Steveville Badlands. Unpublished M.Sc. Thesis, University of Alberta.

Hoover, O.H. 1948. Effects of chinook (foehn) winds on snow cover and runoff. International Union of Geodesy and Geophysics, General Assembly at Oslo, *IASH Publication*, **2,** 86-100.

Horton, R.E. 1945. Erosional development of streams and their drainage basins: hydrophysical approach to quantitative morphology. *Geological Society of America Bulletin*, **56,** 275-370.

Hudec, P.P. 1973. Weathering of rocks in Arctic and Sub-arctic Environment. In: *Proceedings of the Symposium on the Canadian Arctic*, J.D. Aitken annd D.J. Glass (eds.), University of Waterloo, Waterloo, Ontario, 313-335.

Hutchinson, B.A. 1966. A comparison of evaporation from snow and soil surfaces. *IASH Bulletin*, **11** (1), 34-42.

Ives, R.L. 1950. Frequency and physical effects of chinook winds in the Colorado High Plains region. *Annals of the Association of American Geographers*, **40** (4), 293-327.

Jones, A. 1971. Soil piping and stream channel initiation. *Water Resources Research*, **7** (3), 602-610.

J-Tec Associates, Inc. 1978. *Wind Speed and Direction Sensor: Instruction Manual for the Model VA - 320-2-1 Anemometer*, J-Tec Associates, Inc., Cedar Rapids, Iowa.

Justus, C.G. 1978. *Winds and Wind System Performance*. The Franklin Institute Press, Philadelphia, 120 p.

Kennedy, B.A. and Melton, M.A. 1972. Valley asymmetry and slope forms in a permafrost area in the Northwest Territories, Canada. In: *Polar Geomorphology*, Institute of British Geographers Special Publication, **4**, 107-121.

Kind, R.J. 1976. A critical examination of the requirements for model simulation of wind-induced erosion/deposition phenomena such as snow drifting. *Atmospheric Environment*, **10**, 219-227.

Kind, R.J. 1981. Snow drifting. Chapter 8 in: *Handbook of Snow - Principles, Processes, Management and Use*, D.M. Gray and D.H. Male (eds.), Pergamon Press, Toronto, 338-359.

Kirkby, M.J. (ed.) 1978. *Hillslope Hydrology* Wiley Interscience, Chichester, 389 p.

Kirkby, M.J. and Chorley, R.J. 1967. Throughflow, overland flow and erosion. *IASH Bulletin*, **12** (3), 5-21.

Kobayashi, D. 1973. Studies of snow transport in low-level drifting snow. *Institute of Low Temperature Science, Report*, **231**, Sapporo, 58 p.

Koch, J.P. and Wegener, A. 1930. (in Teichert, 1939). Wissenschaftliche Ergebnisse der danischen Expedition nach Dronning Luise-Land und quer uber das Inlandeis von Nordgronland 1912-1913. *Meddelelser om Gronland*, **75**, Copenhagen, 302 p.

Kotlyakov, V.M. 1961. Results of study of the ice sheet in eastern Antarctica. Internation Union of Geodesy and Geophysics, General Assembly at Helsinki, *IASH Publication*, **55**, 88-99.

Kung, E.C., Bryson, R.A., and Lenschow, D.J. 1964. Study of a continental surface albedo on the basis of flight measurements and structure of the earth's surface cover over North America. *Monthly Weather Review* **92**, 543-564.

Kungertsev, A.A. 1956. The transfer and deposit of snow. *Geographical Institute, Academy of Science*, U.S.S.R., English Translation by: University of Colorado, Engineering Science Research Division, Boulder Colorado.

Kuz'min, P.P. 1960. Snowcover and Snow Reserves. *Gidrometeorologischeskoe, Izdatelsko*, Leningrad. Translation by: U.S. National Science Foundation, Washington, D.C., 1963, 140 p.

Landals, A.L. and Gill, D. 1972. Differences in the volume of surface runoff during the snowmelt period: Yellowknife Northwest Territories. WMO-2: *Forecasting Runoff*, International Symposia on the Role of Snow and Ice in Hydrology, 14 p.

Larson, L.W. and Peck, E.L. 1974. Accuracy of precipitation measurements for hydrologic modeling. *Water Resources Research* **10**, 857-863.

Leaf, C.F. 1971. Areal snow cover and disposition of snowmelt runoff in central Colorado. *U.S.D.A. Forest Service Research Paper*, **RM-66**, 19 p.

Lester, P.F. 1976. *A Quantitative Definition of the Chinook in Southern Alberta.* Environmental Sciences Centre (Kananaskis), The University of Calgary, Calgary, Alberta. 52 p.

Lewis, W.V. 1939. Snow-patch erosion in Iceland. *Geographical Journal*, **94**, 153-161.

Linsley, R.K., Kohler, M.A., and Paulhus, J.L.H. 1958. *Hydrology for Engineers*, McGraw-Hill, New York, 482 p.

Longley, R.W. 1967. The frequency of chinooks in Alberta. *The Albertan Geographer*, **3**, 20-22.

Longley, R.W. 1968. *Climatic Maps for Alberta.* Department of Geography, University of Alberta, 8 p.

Longley, R.W. 1972. *The Climate of the Prairie Provinces.* Climatological Study 13, Environment Canada, Toronto, 79 p.

Louie, P.Y.T. 1977. Potential evaporative loss from snow in southwestern Alberta. *Proceedings, Canadian Hydrology Symposium* **77,** Edmonton, August 29-31, Associate Committee on Hydrology, National Research Council of Alberta, 25-30.

Male, D.H. 1980. The seasonal snowcover. Chapter 6 in: *Dynamics of Snow and Ice Masses,* S.C. Colbeck (ed.), U.S. Army Cold Regions Research and Engineering Laboratory, Hanover, New Hampshire. Academic Press, New York, 305-395.

Male, D.H. and Granger, R.J. 1978. Energy mass fluxes at the snow surface in a prairie environment. In: Proceedings, *Modeling of Snow Cover Runoff,* S. Colbeck and M. Ray (eds.), U.S. Army Cold Regions Research and Engineering Laboratory, Hanover, New Hampshire, September 26-28, pp. 101-124.

Male, D.H. and Gray, D.M. 1981. Snowcover ablation and runoff. Chapter 9 in: *Handbook of Snow - Principles, Processes, Management and Use,* D.M. Gray and D.H. Male (eds.), Pergamon, Toronto, 360-436.

Marsh, J.S. 1965. The chinook and its geographic significance in southern Alberta. Unpublished M.Sc. Thesis, University of Calgary.

Martini, R.J., III. 1972. (in Thorn, 1979, and Thorn and Hall, 1980). Time-dependent crack growth in quartz and its application to the creep of rocks. *Journal of Geophysical Research,* **77,** 1406-1419.

McKay, G.A. 1964. Relationships between snow survey and climatological measurements for the Canadian Great Plains. *Western Snow Conference, Proceedings* of the April 21-22, 1964 Meeting, Nelson, B.C., pp. 9-18, and Discussion (p. 19).

McKay, G.A. 1970a. Problems of measuring and evaluating snowcover. *Proceedings of the Workshop Seminar on Snow Hydrology,* Queen's Printer of Canada, Ottawa, February 28-29, 1968. 42-62.

McKay, G.A. 1970b. Precipitation. Chapter 2 in: *Handbook on the Principles of Hydrology,* D.M. Gray (ed.), Research Council of Canada; 2.1-2.111.

McKay, G.A. and Findlay, B.F. 1971. Variation of snow resources with climate and vegetation in Canada. *Western Snow Conference, Proceedings* of the April 20-22, 1971 Meeting, (#39), Billings, Montana, 17-25.

McKay, G.A. and Gray, D.M. 1981. The distribution of snowcover. Chapter 5 in: *Handbook of Snow - Principles, Processes, Management and Use,* D.M. Gray and D.H. Male (eds.) Pergamon, Toronto, 153-190.

McKay, G.A. and Thompson, H.A. 1968. Snowcover in the prairie provinces of Canada. *Transactions of the American Society of Agricultural Engineers,* **11** (6), 812-815.

Mears, B. 1963. Karst-like features in badlands of the Arizona Petrified Forest. *Contributions to Geology,* University of Wyoming, **2** (1), 101-104.

Meentemeyer, V. and Zippin, I. 1981. Soil moisture and texture controls of selected parameters of needle ice growth. *Earth Surface Processes,* **6,** 113-125.

Meiman, J.R. 1970. Snow accumulation related to elevation, aspect, and forest canopy. *Proccedings of the Workshop on Snow Hydrology,* Queen's Printer of Canada, Ottawa, February 28-29, 1968, 35-47.

Melton, M.A. 1960. (in Spence, 1972). Intravalley variation in slope angles related to microclimate and erosional environment. *Geological Society of America Bulletin*, **71**, 133-144.

Mellor, M. 1965. Blowing snow. In: *Cold Regions Science and Engineering*, F.J. Sanger (ed.), Part 3, Section A3C, U.S. Army Cold Regions Research and Engineering Laboratory, Hanover, New Hampshire, November, 1965, 78 p.

Miller, R.D. 1980. Freezing phenomena in soils. Chapter 11 in: *Application of Soil Physics*, D.Hillel (ed.), Academic Press, New York, 254-298.

Nkemdirim, L.C. and Benoit, P.W. 1975. Heavy snowfall expectation for Alberta. *The Canadian Geographer*, **19**, (1), 60-72.

Norrish, K. 1954a. Manner of swelling of montmorillonite. *Nature*, **173**, 256-257.

Norrish, K. 1954b. The swelling of montmorillonite. *Discussions of the Faraday Society*, **18**, 120-134.

North, M. 1976. *A Plant Geography of Alberta*. Studies in in Geography, Monograph 2, Department of Geography, University of Alberta, 147 p.

Obled, C. and Harder, H. 1978. A review of snow melt in the mountain environment. Proceedings, *Modeling of Snow Cover Runoff*, S. Colbeck and M. Ray (eds.), U.S. Army Cold Regions Research and Engineering Laboratory, Hanover, New Hampshire, September 26-28, pp. 179-204.

Obolenskii, V.N. 1929. (in Chebotarev, 1962). Klimat Lesnogo po dannym Meteorologicheskoi observatorii Leningradskogo Lesnogo Instituta 1890-1925. *Izvestiya Leningradskogo Instituta*, **37**.

Odynsky, W. 1958. U-shaped dunes and effective wind directions in Alberta. *Canadian Journal of Soil Science*, **38**, 56-62.

O'Neill, A.D.J. and Gray, D.M. 1971. Energy balance and melt theories. In: *Runoff From Snow and Ice*, Eighth Canadian Hydrology Symposium, Inland Waters Branch, Department of Energy, Mines, and Resources, 31-58.

O'Neill, A.D.J. and Gray, D.M. 1972. Solar radiation penetration through snow. UNESCO-2: *Conditioning, Ripening, and Melting of Snowcover*, International Symposium on Properties and Processes, 16 p.

Osborn, H.B. and Renard, K.G. 1969. Analysis of two major runoff-producing southwest thunderstorms. *Journal of Hydrology*, **8**, 282-302.

Osborn, H.B. and Renard, K.G. 1970. Thunderstorm runoff on the Walnut Gulch experimental watershed, Arizona, U.S.A. In: *Results of Research on Representatie and Experimental Basins*, Proceedings of the Wellington Symposium, December, 1970, *IASH Publication*, **96**, 455-464.

Østrem, G. 1964. Glacio-hydrological investigations in Norway. *Journal of Hydrology*, **2**, 101-115.

Oura, H.T., Ishida, D., Kobayashi, S., and Yamada, T. 1967. Studies on blowing snow. In: *Physics of Snow and Ice*, H. Oura (ed.), Proceedings of the International Conference on Low Temperature Science, 1 (2), Hokkaido University, Sapporo, 1098-1117.

Packer, P.E. 1962. Elevation, aspect, and cover effects on maximum snowpack water content in a western white pine forest. *Forest Science*, **8**, 225-235.

Parker, G.G. 1964. Piping, a geomorphic agent in landform development of the drylands.

IASH Bulletin, **65**, 103-113.

Paulhus, J.C. 1971. The March-April 1969 snowmelt floods in the Red River of the North, Upper Mississippi, and Missouri Basins. *National Oceanic and Atmospheric Administration Technical Report*, **NWS-13**, Silver Spring, Maryland.

Peck, E.L. 1972. Review of methods of measuring snow cover, snowmelt, and streamflow under winter conditions. WMO-I: *Measurements in Space and Time*, International Symposium on Measurement and Forecasting, 18 p.

Popov, E.G. 1972. Snowmelt runoff forecasts - theoretical problems. WMO-2: *Forecasting Runoff*, International Symposium on the Role of Snow and Ice in Hydrology, 14 p.

Potter, J.G. 1965. *Snow Cover*. Climatological Studies #3 Canada Department of Transport, Meteorological Branch, Toronto, 69 p.

Potts, A.S 1970. (in Thorn, 1979, and Thorn and Hall, 1980). Frost action in rocks: some experimental data. *Transactions of the Institute of British Geographers*, **49** 109-124.

Powers, D.L. 1931. Subsurface study of Pale beds and Foremost Formation in Lethbridge-Brooks are of southern Alberta. In: *Stratigraphy of Plains of Southern Alberta*, American Association of Petroleum Geologists, 69-85.

Price, A.G. and Dunne, T. 1976. Energy balance computations of snowmelt runoff in a subarctic area. *Water Resources Research*, **12** (14), 686-694.

Price, A.G., Hendrie, L.K., and Dunne, T. 1978. Controls on the production of snowmelt runoff. In: Proceedings, *Modeling of Snow Cover Runoff*, S. Colbeck and M. Ray (eds.), U.S. Army Cold Regions Research and Engineering Laboratory, Hanover, New Hampshire, September 26-28, pp. 257-268.

Putnam, W.C. and Sharp, R.P. 1940. (in Spence, 1972). Landslides and earth flows near Ventura southern California. *Geographical Review*, **30**, 591-600.

Radok, U. 1977. Snow drift. *Journal of Glaciology*, **19** (181), 123-139.

Ragan, R.M. 1967. An experimental investigation of partial area contributions. General Assembly of the Bern Symposium, *IASH Publication*, **76**, 241-249.

Research Council for Agriculture, Forestry, and Fisheries, 1970. *Revised Standard Soil Color Chart*.

Rikhter, G.D. 1945. *Snow cover - Its Formation and Properties*. Translation by U.S. Army Snow, Ice and Permafrost Research Establishment, Translation, **6**.

Rubey, W.W. 1928. Gullies in the Great Plains formed by sinking of the ground. *American Journal of Science* **15**, 417-422.

Russell, J.R. 1931. Geomorphological evidence of a climatic boundary. *Science*, **74** (1924), 484-485.

Russell, L.S. and Landes, R.W. 1940. Geology of the southern Alberta plains. *Geological Survey of Canada Memoir* **221**, Canada Department of Mines and Resources, 223 p.

Schiff, L. and Dreibelbis, F.R. 1949. Infiltration, soil moisture, and land use relationships with reference to surface runoff. *Transactions of the American Geophysical Union*, **30**, 75-88.

Schmidt, R.A., Jr. 1972. Sublimation of wind-transported snow - a model. *U.S.D.A. Forest Service Research Paper*, **RM-90**, 24 p.

Schumm, S.A 1956. The role of creep and rainwash on the retreat of badland slopes. *American Journal of Science*, **254**, 693-706.

Schumm, S.A. 1964. Seasonal variations of erosion rates and processes on hillslopes in western Colorado. *Zeitschrift fur Geomorphologie Supplement Band*, **5**, 215-238.

Schumm, S.A. and Lusby, G.C. 1963. Seasonal variation of infiltration capacity and runoff on hillslopes in western Colorado. *Journal of Geophysical Research*, **68** (12), 3655-3666.

Smith, J.L. 1974. Hydrology of warm snowpacks and their effects upon water delivery: some new concepts. In: *Advanced Concepts and Techniques in the Study of Snow and Ice Resources*, U.S. National Academy of Sciences, Washington, D.C., 76-89.

Smith, D.D. and Wischmeier, W.H. 1957. Factors affecting sheet and rill erosion. *Transactions of the American Geophysical Union*, **38**, 889-896.

Solomon, R.M., Ffolliot, P.F., and Thorud, D.B. 1975. Characterization of snowmelt runoff efficiencies. In: *Watershed Management*, Proceedings of a Symposium Conducted by the Irrigation and Drainage Division of the American Society of Civil Engineers, Logan, Utah, August 11-13, 1975, 306-327.

Spence, D.H. 1972. Relationships between slope and aspect in an area of hummocky moraine, south central Alberta. Unpublished M.Sc. Thesis, University of Alberta.

Steppuhn, H.W. 1976. Areal water equivalents for prairie snowcover. *Western Snow Conference, Proceedings* of the April 20-22 Meeting, (#44), Calgary, Alberta, 63-68.

Steppuhn, H.W. and Dyck, G.E. 1974. Estimating true basin snowcover. In: *Advanced Concepts and Techniques in the Study of Snow and Ice Resources*, U.S. National Academy of Sciences, Washington, D.C., 304-313.

Storr, D. 1973. Wind-snow relations at Marmot Creek, Alberta. *Canadian Journal of Forest Research*, **3**, 479-485.

Storr, D. and Golding, D.L. 1974. A preliminary water balance evaluation of an intensive snow survey in a mountainous watershed. In: *Advanced Concepts and Techniques in the Study of Snow and Ice Resources*, U.S. National Academy of Sciences, Washington, D.C., 294-303.

Strahler, A.N. 1950. Equilibrium theory of erosional slopes approaoched by frequency distribution analysis. *American Journal of Science*, **248**, 673-696.

Taber, S. 1929. Frost heaving. *Journal of Geology*, **37**, 428-461.

Tabler, R.D. 1975. Estimating the transport of blowing snow. In: *Snow Management on the Great Plains*, Great Plains Agricultural Committee, and University of Nebraska Agricultural Experiment Station, Lincoln. Publications, **73**, 85-117.

Teichert, C. 1939. Corrasion by wind-blown snow in polar regions. *American Jounal of Science*, **237**, 146-148.

Tennessee Valley Authority, 1964. A pilot study in areastream factor correlation. *Office of Tributary Area Development, Research Paper*, **4**, 64 p.

Thorn, C.E. 1979. Bedrock freeze-thaw weathering regime in an alpine environment, Colorado Front Range. *Earth Surface Processes*, **4**, 221-228.

Thorn, C.E. 1982. Bedrock microclimatology and the freeze-thaw cycle: a brief illustration. *Annals of the Association of American Geographers*, **72** (1), 131-137.

Thorn, C.E. and Hall, K. 1980. Nivation: an arctic-alpine comparison and reappraisal. *Journal of Glaciology*, **25** (91), 109-124.

Toy, T.J. 1977. Hillslope form and climate. *Geological Society of America Bulletin*, **88**, 16-22.

Tricart, J. 1956 (in Thorn, 1979, and Thorn and Hall, 1980). Etudes experimentale due probleme de la gelivation. *Biuletyn Peryglajalny*, **4**, 285-318.

Underhill, A.G. 1962. *Report on the Effect of a Change in the Vegetation on Run-off and Erosion Characteristics of Alberta Streams.* Water Resources Division, Alberta Department of Agriculture, 57 p.

UNESCO, IASH, and WMO, 1970. *Seasonal Snowcover: A Contribution to the International Hydrological Decade.* Technical Papers in Hydrology, UNESCO, IASH, WMO, 38 p.

U.S. Army Corps of Engineers, 1956. *Snow Hydrology.* U.S. Department of Commerce, Office of Technical Services, Portland, 437 p.

Van Haveren, B.P. and Striffler, W.D. 1976. Snowmelt recharge on a shortgrass prairie site. *Western Snow Conference, Proceedings* of the April 20-22, 1970 Meeting, Calgary, Alberta 52-62.

Verschuren, J.P. and Wojtiw, L. 1980. *Estimate of the Maximum Probable Precipitation for Alberta River Basins.* Alberta Environment, Hydrology Branch, **RMD 80/1**, 307 p.

Volkovitskaya, Z.I. and Maskova, G.B. 1965. The wind profiles and the turbulence characteristics in the bottom 300-meter layer of the atmosphere. In: *Investigation of the Bottom 300-Meter Layer of the Atmosphere*, Academy of Sciences of the USSR, Institute for Applied Geophysics, Moscow, 1963. Translation, 13-25.

Von Engeln, O.D. 1942. *Geomorphology.* MacMillan, NewYork, 655 p.

Walker, E.H. 1948. (in Spence, 1972). Differential erosion of slopes of north and south exposure in Wyoming. Abstract, *Geological Society of America Bulletin*, **59**, p. 1360.

Ward, R.C. 1975. *Principles of Hydrology.* (2nd Ed.), McGraw-Hill, London, 367 p.

Webb, R., Johnston, A., and Soper, J.Dd. 1967. The prairie world. Chapter 5 in: *Alberta, A Natural History*, W.G. Hardy (ed.) Hurtig, Edmonton, 93-133.

Weiss, L.L. and Wilson, W.T. 1957. Precipitation gauge shields. IASH General Assembly of Toronto, 1, *IASH Publication*, **43**, Gentbrugge. 462-484.

White, S.E. 1976. Is frost action really only hydration shattering? *Arctic and Alpine Research*, **8** (1), 1-6.

Williams, P.J. 1957. Some investigations into solifluction features in Norway. *The Geographical Journal*, **123**, 42-58.

Wiman, S. 1963. (in Thorn, 1979, and Thorn and Hall, 1980). A preliminary study of experimental frost weathering. *Geografiska Annaler*, **45A**, 113-121.

Wisler, C.O. and Brater, E.F. 1959. *Hydrology.* (2nd Ed.), Wiley, New York, 408 p.

Yair, A. and Lavee, H. 1982. Application of the concept of partial area contribution to small arid watersheds. In: *Rainfall/Runoff Relationships*, V.P. Singh (ed.), Proceedings of the International Symposium on Rainfall-Runoff Modeling, Mississippi

State University, May, 1981. Water Resources Publications, Littleton, Colorado, 335-350.

Yair, A., Lavee, H., Bryan, R.B., and Adar, E. 1980. Runoff and erosion processes and rates in the Zin Valley badlands, northern Negev, Israel. *Earth Surface Processes*, **5**, 205-225.

Yoon, Y.N. and Wenzel, H.G. 1971. Mechanics of sheet flow under simulated rainfall. *Proceedings of the American Society of Civil Engineers*, Journal of the Hydraulic Division, **HY9**, 1367-1386.

Appendix A1. MEAN MONTHLY WIND FREQUENCY PERCENTAGE AT BROOKS AHRC: 1955-1966.

Station: Brooks AHRC

Wind Direction	Jan.	Feb.	Mar.	Apr.	May	Jun.	Jul.	Aug.	Sep.	Oct.	Nov.	Dec.	Year
N	(20)	(19)	(19)	(20)	17	15	13	16	14	10	15	[17]	16
NE	6	6	9	8	12	10	9	9	6	4	4	6	8
E	5	6	6	6	7	6	5	4	5	3	3	4	5
SE	14	14	[17]	[19]	20	16	17	18	19	(19)	17	14	17
S	[19]	[18]	16	16	13	14	14	12	15	(19)	(18)	(20)	16
SW	14	12	12	11	10	13	13	14	13	(19)	(18)	[17]	14
W	9	10	7	7	7	9	9	7	8	9	9	9	8
NW	13	14	14	13	14	17	20	20	20	16	16	13	16
Calm	-	1	-	-	-	-	-	-	-	1	-	-	-

( ) = Highest Mean Monthly Percentage Frequency

[ ] = Second Highest Mean Monthly Percentage Frequency

Data Source: Canadian Normals: Wind 1955-1972. Vol. 3, Environment Canada, 1975.

Appendix A2. MEAN MONTHLY WIND FREQUENCY PERCENTAGE AT BROOKS: 1966-1980.

Station: Brooks

Wind Direction	Jan.	Feb.	Mar.	Apr.	May	Jun.	Jul.	Aug.	Sep.	Oct.	Nov.	Dec.	Year
N	15.4	14.9	13.8	12.5	8.9	7.6	8.1	8.7	8.6	8.3	9.6	14.1	11
NE	6.6	6.5	7.5	11.0	9.9	11.3	12.0	12.2	10.7	5.6	5.0	5.6	9
E	4.0	5.3	5.6	6.5	6.4	5.4	5.7	5.1	3.9	2.6	3.5	2.8	5
SE	8.0	8.6	9.8	11.5	14.2	11.7	12.6	12.1	10.3	7.5	8.7	7.0	10
S	14.5	[17.0]	15.5	13.7	16.0	12.7	13.4	16.0	18.5	[20.0]	(20.4)	17.3	16
SW	[16.5]	16.7	[17.7]	[16.4]	15.1	15.6	15.9	14.2	14.8	(23.0)	[20.2]	(19.7)	17
W	14.2	12.9	10.1	8.9	9.3	11.7	11.5	9.9	10.8	12.8	12.7	13.0	12
NW	(19.7)	(17.2)	(19.5)	(19.4)	20.0	23.9	20.4	21.7	22.2	[20.0]	19.4	[19.4]	20
Calm	1.1	0.9	0.5	0.1	0.2	0.1	0.4	0.1	0.2	0.2	0.5	1.1	-

( )= Highest Mean Monthly Percentage Frequency

[ ]= Second Highest Mean Monthly Percentage Frequency

Data Source: Canadian Climate Normals: Wind 1951-1980. Vol. 5, Environment Canada, 1982.

APPENDIX A3. MEAN MONTHLY WIND SPEEDS ($km \cdot hr^{-1}$) AT BROOKS AHRC: 1955-1966.

Station: Brooks AHRC

Wind Direction	Jan.	Feb.	Mar.	Apr.	May	Jun.	Jul.	Aug.	Sep.	Oct.	Nov.	Dec.	Year
N	14.6	16.6	17.4	[20.3]	18.8	15.9	12.1	11.4	14.8	13.5	16.1	15.3	15.6
NE	11.6	11.6	12.6	14.3	14.3	14.3	11.1	10.6	13.7	10.3	11.3	10.6	12.2
E	10.5	12.4	12.7	15.4	15.8	14.2	11.9	9.3	12.7	10.0	8.7	11.1	12.1
SE	12.6	12.4	14.5	15.0	13.5	13.0	11.4	10.6	11.1	13.0	12.7	12.2	12.7
S	10.3	12.2	12.9	13.8	14.8	12.9	11.7	9.8	11.4	12.6	11.7	11.6	12.1
SW	(19.0)	[18.5]	(19.0)	[20.3]	21.1	20.3	16.9	15.5	17.2	(21.1)	(20.0)	(21.1)	(19.2)
W	14.2	15.1	15.1	18.5	17.2	16.7	14.8	13.0	14.0	16.3	13.5	14.8	15.3
NW	[18.2]	(20.3)	[18.8]	(21.6)	21.6	18.3	15.8	15.5	19.3	[18.5]	[19.8]	[18.3]	[18.8]
All Directions	14.1	15.1	15.6	17.4	16.9	15.8	13.4	12.4	14.5	15.3	15.3	15.0	15.1

( ) = Highest Mean Monthly Wind Speed

[ ] = Second Highest Mean Monthly Wind Speed

Data Source: Canadian Normals: Wind 1955-1972. Vol. 3, Environment Canada, 1975.

Appendix A4. MEAN MONTHLY WIND SPEEDS ($km \cdot hr^{-1}$) AT BROOKS: 1966-1980.

Station: Brooks

Wind Direction	Jan.	Feb.	Mar.	Apr.	May	Jun.	Jul.	Aug.	Sep.	Oct.	Nov.	Dec.	Year
N	12.5	11.9	12.6	15.7	14.3	11.1	9.2	9.1	10.0	11.3	11.7	13.9	11.9
NE	11.5	11.2	12.9	16.2	14.8	14.7	12.3	12.3	13.3	13.5	10.7	11.1	12.9
E	10.4	10.5	12.4	14.2	13.6	11.3	10.4	9.6	9.4	9.5	10.7	9.1	10.9
SE	13.3	12.3	13.4	14.3	16.0	13.2	12.5	12.3	12.1	12.7	12.1	12.4	13.1
S	11.6	11.9	12.7	13.7	13.7	13.3	11.5	11.1	11.2	13.0	13.1	12.4	12.4
SW	(17.4)	(16.3)	(15.8)	(18.4)	16.8	16.7	14.9	14.9	15.0	(17.5)	(18.2)	(17.6)	16.6
W	11.9	11.3	10.6	14.2	12.7	12.1	11.3	10.9	10.4	11.6	11.5	11.8	11.7
NW	[14.3]	[13.1]	[14.5]	[18.0]	15.9	14.7	13.4	13.1	14.2	[15.5]	[14.0]	[14.2]	14.6
All Directions	13.2	12.6	13.4	16.0	14.9	13.9	12.3	12.1	12.5	14.1	13.6	13.6	13.5

( )= Highest Mean Monthly Wind Speed

[ ]= Second Highest Mean Monthly Wind Speed

Data Source: Canadian Climate Normals: Wind 1951-1980. Vol. 5, Environment Canada, 1982.

APPENDIX B. Slope Angle Values Surveyed in the Sub-basins.

Sb-X		Sb-Y		Sb-Z	
8.5°	31.5°	18°	19°	0°	7°
19°	39°	32°	12.5°	3.5°	28°
26°	11°	16°	24°	32°	12°
4.5°	14.5°	4°	28°	21°	1°
31°	42.5°	8°	17°	1°	6.5°
47°	7°	21.5°	43°	17.5°	44°
21°	10.5°	19°	47°	24.5°	25.5°
12°	3°	4°	30°	25°	52°
4°	26°	42°	34°	1°	6°
50°	23.5°	6°	22°	5°	4°
18°	12.5°	75°	5.5°	2.5°	1.5°
47°	21°	28°	56°	25°	17°
31°	13°	55°	21°	8°	2.5°
30.5°	18.5°	42°	40°	15.5°	11°
33.5°	7°	31°	20°	9.5°	6.5°
29°	11.5°	43°	13°	48.5°	15°
3°	11°	45°	24°	37°	25°
30°	14°	15°	24°	29°	25.5°
7°	28.5°	45°	31°	38.5°	4.5°
10°	3°	42°	44°	24.5°	4°
13°	0°	11°	6°	14.5°	29.5°
12°	23°	34°	36°	23.5°	0.5°
14°	13°	21.5°	22°	6°	0.5°
11°	21°	28°	21°	1°	10.5°
Mean Angle 19.1°		27.6°		15.7°	

APPENDIX C. Station Names Corresponding to Letter Denotations and Water Equivalent Values of Figure 4.5.

Station Letter	Station Name	Number of Years on Which Data is Based
A	Carbon	5-19
B	Drumheller Andrew	25-29
C	Craigmyle	20-24
D	Hanna	20-24
E	Scotfield	5-19
F	Naco	5-19
G	Sibbald	25-29
H	Oyen Cappon	5-19
I	Empress	5-19
J	Vulcan	5-19
K	Majorville	5-19
L	Armada Exp. Sta.	5-19
M	Rainier	5-19
N	Duchess	5-19
O	Brooks North	5-19
P	Brooks AHRC	27
Q	Pollockville	25-29
R	Jenner	5-19
S	Picture Butte	5-19
T	Lethbridge CDA	30
U	Coaldale	5-19
V	Vauxhall CDA	5-19
W	Taber	30
X	Hays	5-19
Y	Bow Is. R.D.	5-19
Z	Suffield A	30
AA	Ralston	20-24
BB	Medicine Hat A	30

APPENDIX D1. Snow Survey Data for January 17, 1982.

(Weighing - in - Field Method)

column		1	2	3	4
Basin	Point #	Snow Depth (cm)	Other Sampled Snow Depths (cm)	Snow Density (gr. cm^{-3})	Snow/Water Equivalent (cm)
Sb-X	1	21.6	21.6	0.14	2.5
	2	2.5	23.3	0.19	4.5
	3	1.4	14.5	0.17	2.5
	4	1.0	30.8	0.27	8.5
	5	5.1			
Average	-	6.3	-	0.19	-
Sb-Y	1	11.1	22.0	0.07	1.5
	2	1.8	25.0	0.08	2.0
	3	11.0	22.2	0.09	2.0
	4	19.0	23.3	0.09	2.0
	5	2.0			
	6	4.1			
Average	-	8.2	-	0.08	-
Sb-Z	1	4.3	8.0	0.18	1.5
	2	3.4	6.2	0.24	1.5
	3	2.9	9.3	0.14	1.3
	4	2.7	11.0	0.14	1.5
	5	8.1	13.7	0.15	2.0
	6	11.2	24.2	0.12	3.0
	7	8.8	24.7	0.20	5.0
	8	6.3			
	9	2.3			
Average	-	5.5	-	0.17	-

Total Average Snow Density = 0.15 gr. cm^{-3}

APPENDIX D2. Snow Survey Data for February 5, 1982.

(Bulk Sampling Method)

Column		1	2	3	4
Basin	Survey Point	Snow Depth (cm)	Snow Core Weight (gr)	Snow Density ($gr.cm^{-3}$)	Snow/Water Equivalent (cm)
Sb-X	1	16.0	36.9	0.21	3.36
	2	3.0	5.1	0.15	0.45
	3	3.4	4.5	0.12	0.41
	4	2.8	5.7	0.18	0.50
	5	2.0	2.5	0.11	0.22
Average	-	5.4	-	0.15	-
Sb-Y	1	13.0	35.5	0.24	3.12
	2	14.3	45.4	0.28	4.00
	3	12.4	20.8	0.15	1.86
	4	14.5	36.3	0.22	3.19
	5	0.3	0.04	0.12	0.04
	6	5.2	9.8	0.17	0.88
Average	-	10.0	-	0.19	-
Sb-Z	1	1.5	2.0	0.12	0.18
	2	5.0	10.6	0.19	0.95
	3	9.8	20.9	0.19	1.86
	4	7.5	13.0	0.16	1.20
	5	15.0	31.8	0.19	2.85
	6	2.8	4.8	0.15	0.42
	7	3.0	5.1	0.15	0.45
	8	6.5	11.6	0.16	1.04
	9	2.2	3.1	0.13	0.29
Average	-		-	0.16	-

APPENDIX D3. Snow Survey Data for March 15, 1982.

(Bulk Sampling Method)

Column		1	2	3	4
Basin	Survey Point	Snow Depth (cm)	Snow Core Weight (gr)	Snow Density ($gr.cm^{-3}$)	Snow/Water Equivalent (cm)
Sb-X	1	7.5	9.0	0.11	0.83
	2	9.0	8.5	0.08	0.72
	3	5.0	3.6	0.06	0.30
	4	10.0	7.3	0.07	0.70
	5	8.5	5.9	0.06	0.51
Average	-	8.0	-	0.08	-
Sb-Y	1	6.5	8.0	0.11	0.72
	2	7.0	7.5	0.10	0.70
	3	6.0	7.1	0.11	0.66
	4	7.5	9.0	0.11	0.83
	5	7.0	8.0	0.10	0.70
	6	7.0	7.9	0.10	0.70
Average	-	6.8	-	0.105	-
Sb-Z	1	4.0	4.6	0.10	0.40
	2	6.5	7.0	0.10	0.65
	3	8.0	9.2	0.10	0.80
	4	5.5	6.4	0.10	0.55
	5	3.5	4.1	0.10	0.35
	6	2.5	2.5	0.09	0.23
	7	6.5	6.7	0.09	0.59
	8	8.5	9.3	0.10	0.85
	9	7.5	9.1	0.11	0.83
Average	-	5.8	-	0.10	-

APPENDIX E. Wind Data for Brooks AHRC: 1981-1982 Winter Season.

(Use in conjunction with Figure 4.26 (a-c))

(a)

Frequency Percentage of Dominant Wind Direction for 404 Six-hour Intervals: December 1 to March 31

N	NE	E	SE	S	SW	W	NW	calm
14.4	13.9	5.2	17.3	9.7	18.6	4.5	16.6	-

(b)

Direction of Mean Highest Wind Speed during 97 24-hour Intervals ($km \cdot hr^{-1}$): December 1 to March 31

N	NE	E	SE	S	SW	W	NW	calm
22.7	19.9	11.3	18.4	11.3	32.7	13.7	28.6	-

(c)

Frequency Percentage of Prevailing Wind Direction during 1981-1982 Snowfalls: November 17 to March 31

N	NE	E	SE	S	SW	W	NW	calm
16.9	30.5	3.4	13.6	1.7	0	3.4	23.7	6.8

Appendix F: Weather Map for March 15, 1982.

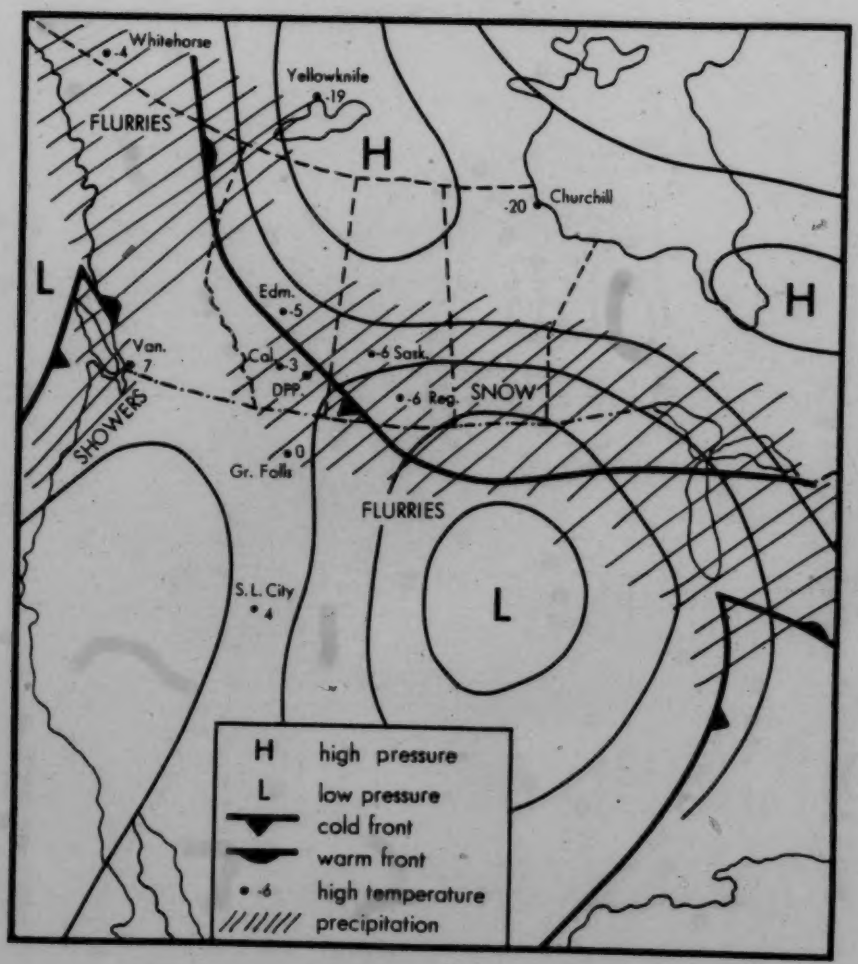

Source: Environment Canada

APPENDIX G. Paired Slope Angle Measurements.

(a) Claystone Slope Measurements

Paired Slope Number	Angle of North-facing Slope (Degrees)	Angle of South-facing Slope (Degrees)	Difference Between North and South Slope Angles (Degrees)	Direction of Steeper Slope Component
1	27	47.5	20.5	S
2	20	11	9	N
3	26	35.5	9.5	S
4	19	12	7	N
5	10	18	8	S
6	15	11	4	N
7	13.5	22	8.5	S
8	28	27	1	N
9	41	41.5	0.5	S
10	23.5	29	5.5	S
11	15	20	5	S
12	16	8.5	7.5	N
13	30.5	31.5	1.5	S
14	20	40	20	S
15	13.5	14	0.5	S
16	27	34	7	S
17	11	21	10	S
18	19	30.5	11.5	S
19	46	49	3	S
20	42	52.5	10.5	S
21	35	55	20	S
22	5.5	21	15.5	S
23	41	38.5	2.5	N
24	29	47	18	S
25	43	28	15	N
26	32.5	20	12.5	N
27	20	12	8	N
28	12	11.5	0.5	N
29	27	32	5	S
30	25	34	9	S

Con't ...

Con't claystone slopes

Paired Slope Number	Angle of North-facing Slope (Degrees)	Angle of South-facing Slope (Degrees)	Difference Between North and South Slope Angles (Degrees)	Direction of Steeper Slope Component
31	21	21	0	-
32	42	39	3	N
33	31	41	10	S
34	69	46	23	N
35	14	27	13	S
36	23	30	7	S
37	32	38	6	S
38	9	22	13	S
39	32	27	5	N
40	26	29	3	S
41	21.5	30	8.5	S
42	40	37	3	N
43	29	37	8	S
44	25	42	17	S
45	27	43	16	S
46	26	32	6	S
47	24	49	25	S
48	27	38	11	S
49	24	21	3	N
50	25	33	8	S
51	39	39	0	-
52	43	64.5	21.5	S
53	34	48	14	S
54	34.5	31	3.5	N
55	57	55	2	N

(b) Sandstone Slope Measurements

Paired Slope Number	Angle of North-facing Slope (Degrees)	Angle of South-facing Slope (Degrees)	Difference Between North and South Slope Angles (Degrees)	Direction of Steeper Slope Component
1	49	29	20	N
2	18.5	39	20.5	S
3	72.5	36	36.5	N
4	21	23	2	S
5	51	38.5	12.5	N
6	28	20.5	7.5	N
7	42	37	5	N
8	39	45	6	S
9	75.5	67.5	8	N
10	22	39.5	17.5	S
11	41.5	36.5	5	N
12	32	35	3	S
13	42	25	17	N
14	16	13.5	2.5	N
15	35	12	23	N
16	17	15	2	N
17	26	37	11	S
18	26	25	1	N
19	53	45	8	N
20	28	32	4	S
21	54	31.5	22.5	N
22	14.5	38	23.5	S
23	31	43.5	12.5	S
24	21.5	26	4.5	S
25	14	65	51	S
26	49.5	39	10.5	N
27	31.5	47	15.5	S
28	19	24	5	S
29	36	29	7	N
30	31.5	35	3.5	S

Con't ...

Con't sandstone slopes

Paired Slope Number	Angle of North-facing Slope (Degrees)	Angle of South-facing Slope (Degrees)	Difference Between North and South Slope Angles (Degrees)	Direction of Steeper Slope Component
31	33	31	2	N
32	21	14	7	N
33	28	11	17	N
34	21.5	26	4.5	S
35	11	11	0	-
36	23	17	6	N
37	49	56	7	S
38	25	5	20	N
39	24	12.5	11.5	N
40	29	33	4	S
41	21	34	13	S
42	24	31	7	S
43	29	29	0	-
44	23	23	0	-
45	21	31	10	S
46	37	22	15	N
47	32	40.5	8.5	S
48	25	19	6	N
49	26	48.5	22.5	S
50	61	52	9	N
51	16	22	6	S
52	27	27	0	-
53	30.5	29	1.5	N
54	18.5	30.5	12	S
55	35	35	0	-